UNIVERSITE DE NANTES

FACULTE DE MEDECINE

Nouvelles approches thérapeutiques de l'infarctus du myocarde : Cellules souches mésenchymateuses et Ingénierie tissulaire et cellulaire

THESE DE DOCTORAT

Ecole doctorale BIOLOGIE-SANTE de NANTES

Discipline : Sciences de la vie et de la santé

Spécialité : Recherche clinique

Présentée et soutenue publiquement par

Eva MATHIEU

Le 02 Novembre 2011, devant le jury ci dessous

Rapporteurs	**Dr. Didier Letourneur**, *Directeur de recherche CNRS, Paris*
	Dr. Denis Angoulvant, *Praticien hospitalier, CHRU de Tours*
Examinateurs	**Pr. Daniel Cussac,** *Professeur des Universités, Toulouse*
	Pr. Patrice Guérin, *PU-PH, Nantes*
	Dr. Jérôme Guicheux, *Directeur de recherche INSERM, Nantes*
Membre invité	**Pr. Pierre Weiss,** *PU-PH, Nantes*
Directeur de thèse	**Pr. Patricia Lemarchand,** *PU-PH, Nantes*

TABLES DES MATIERES

TABLE DES FIGURES

LISTE DES TABLEAUX

LISTE DES PRINCIPALES ABREVIATIONS

2D: deux dimensions

3D: trois dimensions

CE : cellules endothéliales

CMLV : cellules musculaires lisses vasculaires

CSC : cellules souches cardiaques

CSE: cellules souches embryonnaires

CSM : cellules souches mésenchymateuses

FT : facteur de transcription

HPMC-Si: hydroxylpropyl methylcellulose silanisé

IDM : infarctus du myocarde

iPS : induced pluripotent stem cells

IVA : interventriculaire ascendante

MEC: matrice extracellulaire

VG: ventricule gauche

AVANT – PROPOS

L'infarctus du myocarde (IDM) est une nécrose ischémique systématisée du muscle cardiaque le plus souvent due à une thrombose occlusive brutale d'une artère coronaire. Cette occlusion coronaire aiguë par un thrombus survient le plus souvent sur une plaque d'athérome devenue instable à la suite d'une érosion, d'une ulcération, d'une fissuration ou d'une rupture. L'IDM constitue une urgence cardiologique absolue dont l'incidence reste encore élevée avec 120 000 cas par an en France. Selon des données de l'organisation mondiale de la santé (OMS), sur 50 millions de décès annuels dans le monde, les cardiopathies ischémiques sont la première cause de décès avec 7.2 millions de décès d'origine coronaire. En France, son pronostic reste grave puisque l'IDM est responsable de 10 à 12% de la mortalité totale annuelle chez l'adulte. A cette mortalité, il faut ajouter une morbidité importante et le retentissement socio-économique qu'elle représente. L'IDM est une maladie avec un risque fatal important à court et à moyen terme mais sa morbi-mortalité a toutefois été réduite de façon significative depuis 20 ans grâce aux progrès réalisés à plusieurs niveaux d'intervention.

La prise en charge hospitalière à la phase aigüe en unité de soins intensifs cardiologiques (USIC) a permis de diminuer considérablement les décès. La stratégie actuelle a pour objectif la reperfusion rapide de l'artère responsable de l'IDM. Il s'agit de rétablir complètement et le plus précocement possible le flux dans l'artère responsable de l'IDM, soit par thrombolyse intraveineuse soit par angioplastie coronaire primaire (Commeau, 2011). En effet, une reperfusion précoce diminue la mortalité et les risques de complications comme l'insuffisance cardiaque (Morrison and Sacks, 2003; Neuman *et al.*, 2011). Plusieurs paramètres peuvent influencer le choix d'une technique de reperfusion: l'âge, les conditions hémodynamiques, les pathologies associées et la logistique de transfert du patient. Les résultats d'essais cliniques randomisés montrent une diminution des récidives ischémiques et de la mortalité chez des patients traités efficacement et précocement par angioplastie primaire

par rapport à ceux traités par thrombolyse (lorsque les deux options sont disponibles rapidement). L'intérêt des endoprothèses (stents) implantées au cours de l'angioplastie primaire dans le traitement de l'IDM est maintenant privilégié de même que l'utilisation d'antiplaquettaires puissants (thienopyridines (ticlopidine/clopidogrel) et inhibiteurs de la glycoprotéine membranaire GP IIb/IIIa) (Calverley and Roth, 1998; Mukherjee, 2011; Parikh and Juergens, 2011). Les mesures de prévention secondaire par une prise en charge active des facteurs de risque cardiovasculaires; développement des campagnes anti-tabac, programmes d'éducation pour une meilleure hygiène alimentaire, dépistage et prise en charge du diabète et de l'hypertension artérielle. Enfin une meilleure pénétration de la prescription de bêta-bloquants et d'aspirine et plus récemment de statines et d'inhibiteurs de l'enzyme de conversion, permet de limiter les effets délétères liés au remodelage du ventricule gauche.

Néanmoins, dans les cas les plus sévères, seule une greffe cardiaque permet la survie, mais ces transplantations restent aujourd'hui limitées. Ainsi en France, en 2010, sur plus de 900 malades en attente, seulement 356 ont pu être greffés (données de l'Agence de la biomédecine). Pour ces malades, la seule réponse est le cœur artificiel ou l'assistance mécanique de la circulation. Le cœur artificiel présente encore de nombreuses limites. La taille excessive de la prothèse, trop inconfortable, le risque de compression des organes voisins, d'infections, d'embolies et de décès prématurés ont considérablement freiné les programmes de recherche. Aujourd'hui, après la déception d'un nouvel espoir avec l'AbioCor au début des années 2000, rares sont les sociétés dans le monde, comme Carmat en France, à poursuivre dans cette voie. Il s'agit donc désormais de rechercher des solutions thérapeutiques qui pourraient permettre d'accélérer et amplifier le processus de réparation du muscle cardiaque. La médecine régénératrice cardiaque actuelle vise à remplacer non plus l'organe entier mais la partie du tissu cardiaque atteinte en apportant de nouvelles cellules. L'étude et la compréhension de ces cellules et plus particulièrement des cellules souches a permis de

développer considérablement les approches de thérapie cellulaire cardiaque. Cependant, la régénération « *ad integrum* » du myocarde est complexe et l'utilisation des cellules souches seules ne semble pas suffisante. Dans ce contexte, notre travail de recherche est de développer de nouvelles approches visant à optimiser les effets bénéfiques des cellules souches par des concepts d'ingénierie tissulaire et cellulaire. Notre objectif a été dans un premier travail d'améliorer l'implantation des cellules souches mésenchymateuses dans le myocarde ischémique afin d'augmenter leur survie et leur efficacité en utilisant un hydrogel. Puis dans l'objectif de mieux comprendre à plus long-terme les mécanismes moléculaires physiopathologiques cardiaques, nous avons développé un modèle d'étude de culture tridimensionnelle de cardiomyocytes au sein d'une matrice. Enfin, dans la perspective de créer de nouvelles cellules contractiles fonctionnelles, nous nous sommes penchés sur la reprogrammation directe des cellules souches mésenchymateuses en cellules cardiaques.

INTRODUCTION BIBLIOGRAPHIQUE

La thérapie cellulaire constitue, pour un grand nombre de pathologie, une des stratégies thérapeutiques avec un développement majeur ces dernières années. Elle a émergé comme une nouvelle approche attractive permettant de prévenir l'extension de dommages tissulaires et de stimuler la régénération d'un organe endommagé. La thérapie cellulaire cardiaque a été conçue initialement pour régénérer des zones infarcies du myocarde en y implantant des cellules susceptibles d'en restaurer la fonctionnalité. A ce jour, les essais cliniques de thérapie cellulaire en cardiologie ont été basés sur l'utilisation des myoblastes squelettiques et des cellules issues de la moelle osseuse, ils ont concerné trois pathologies distinctes : l'insuffisance cardiaque chronique, l'angor réfractaire et l'infarctus du myocarde (IDM). Dans le cas de l'IDM, les cellules utilisées sont les cellules médullaires mononucléées (Flynn and O'Brien, 2011; Roncalli *et al.*, 2010) et les cellules souches mésenchymateuses (CSM) issues de la moelle osseuse. Grâce à leurs propriétés uniques, les CSM apparaissent aujourd'hui comme des cellules prometteuses pour la réparation myocardique. De plus en plus d'expériences précliniques chez l'animal, mais également d'essais cliniques utilisant les CSM, démontrent le potentiel thérapeutique de ces cellules et encouragent les recherches afin d'optimiser l'utilisation des CSM comme traitement de l'IDM.

Partie 1 : Les cellules souches mésenchymateuses.

1. Description.

Découvertes dans les années 1960 par Friedenstein (Friedenstein *et al.*, 1976), et initialement appelées colony-forming unit-fibroblasts, les cellules souches mésenchymateuses (CSM) sont principalement localisées dans la moelle osseuse où elles servent de soutien aux cellules souches hématopoïétiques (Perl *et al.*, 2010). Elles ne représentent qu'une faible proportion (0,01%) des cellules mononucléées issues de la moelle. Ce sont des cellules

multipotentes capables de se différencier en plusieurs types de cellules : cellules musculaires squelettiques, ostéoblastes, chondrocytes ou adipocytes (Charbord, 2010; Pittenger et al., 1999). Elles ne possèdent pas à leur surface de marqueurs de cellules sanguines comme CD45, CD34, CD11 ou le CD14. En revanche, il est convenu qu'elles expriment des marqueurs tels que CD105, CD44, CD90, STRO-1 ou des molécules d'adhésion telles que VCAM-1 ou ICAM-1. Récemment, le comité de l'ISCT (*International Society for Cellular Therapy*) a proposé des standards de caractérisation des CSM (Dominici *et al.*, 2006). Cette définition des CSM comprend:

- l'adhérence cellulaire au plastique dans des conditions de culture standards.
- un phénotype cellulaire défini en cytométrie de flux par la présence ou l'absence d'antigènes de surface (Tableau 1)
- un potentiel de différenciation multipotent *in vitro* dans des conditions standards et vers au minimum les trois voies mésenchymateuses majeures: ostéoblastes, chondrocytes et adipocytes.

Si ces CSM sont habituellement extraites de la moelle osseuse, il a été montré que des cellules avec des propriétés similaires, pouvaient provenir d'autres tissus, plus facilement accessibles, comme le cordon ombilical ou les tissus adipeux sous-cutanés (Henning *et al.*, 2007; Merceron *et al.*, 2008; van der Bogt *et al.*, 2009).

Antigènes	Moelle osseuse	Tissu adipeux	Cordon ombilical
CD10 (CALLA: common acute lymphocytic antigen, neutral endopeptidase	+	+	+
CD13 (ANP: Aminopeptidase N)	++	?	++
CD29 (intégrine sous-unité VLA-b1)	++	?	++
CD44 (HCAM: homing-associated cell adhesion molecule, hyaluronic acid receptor)	++	++	++
CD54 (ICAM-1: intracellular adhesion molecul 1)	+	+	-/+
CD73 (ecto5' nucleotidase, SH2 et SH3)	++	?	++
CD90 (Thy-1)	++	++	++
CD105 (SH4, endogline)	++	++	++
CD106 (VCAM: vascular cell adhesion molecule 1)	++	+	+
CD147	++	++	
CD166 (activated leucocyte cell adhesion molecule)	++	+	+
CD271 (LNGFR: low-affinity nerve growth factor receptor	+	++	?
HLA classe I	++	?	+
STRO-1	++	+	-
ASMA (alpha smooth muscle actine)	++	?	?
CD34	-/+	-/+	-
CD49d (intégrine sous-unité VLA-a4)	-	?	+
CD49e (intégrine sosu-unité VLA-a5)	++	?	+
CD71 (récepteur à la transferrine)	++	?	?
CD14 (récepteur aux lipopolysaccharides)	-	-	-
CD31 (PECAM-1: platelet endothelial cell adhesion molecule)	-	?	+
CD45 (antigène commun aux leucocytes)	-	-	-
CD117 (Aka c-kit, stem cell factor receptor)	-	-	-/+
VEGFR2	-	-	?
HLA classe II	-	?	-

Tableau 1: Expression des marqueurs de surface de CSM humaines isolées à partir de différents tissus. *D'après (Can and Karahuseyinoglu, 2007; Madonna et al., 2009; Peroni et al., 2008; Pittenger et al., 1999).*

2. Les mécanismes d'action des cellules souches mésenchymateuses.

De nombreuses études *in vivo* ont démontré les effets fonctionnels bénéfiques de la transplantation des CSM dans les modèles d'IDM petits et grands animaux (Boyle *et al.*, 2010; Herrmann *et al.*, 2011). Pour contribuer à la réparation cardiaque, les CSM participent à

la régénération du tissu cardiaque ainsi qu'à la vasculogenèse et secrètent de nombreuses molécules qui vont stimuler les cellules endogènes (Figure 1).

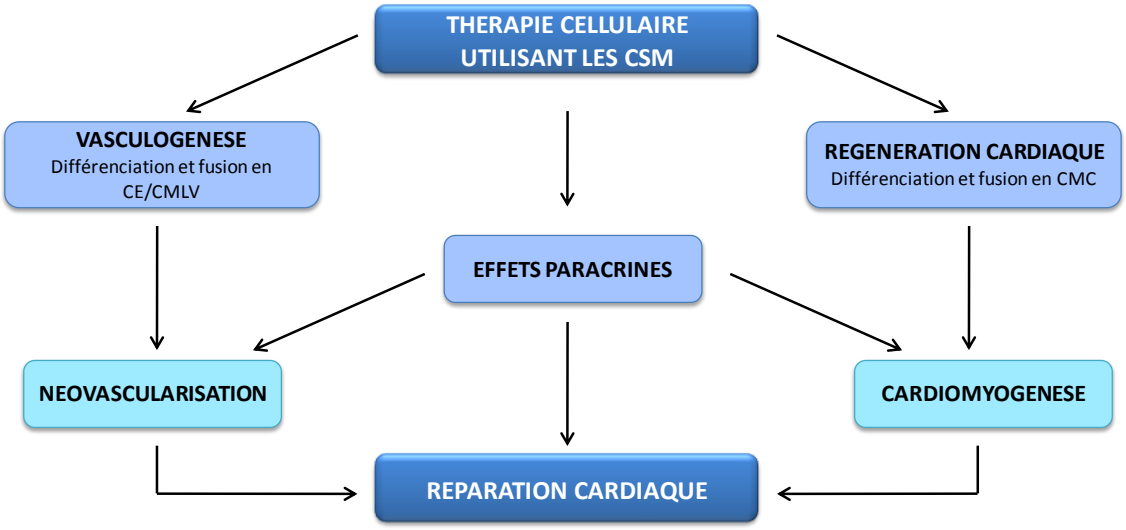

Figure 1: Mécanismes d'action des cellules souches mésenchymateuses (CSM) dans la réparation cardiaque. *D'après (Gnecchi et al., 2008).*

2.1. La régénération cardiaque.

Tout comme les cardiomyocytes, les CSM dérivent du mésoderme, de ce fait il est apparu intéressant d'étudier la capacité des CSM à se différencier en cellule de phénotype cardiaque. La validation du concept de différenciation des CSM en cardiomyocyte exige une approche globale de l'évaluation de la morphologie et de la fonction des cardiomyocytes. Les cardiomyocytes possèdent un appareil contractile, des battements spontanés, un potentiel membranaire d'excitation spécifique avec des courants ioniques et des structures permettant la communication intracellulaire. La différenciation morphologique et fonctionnelle des CSM en cardiomyocytes *in vitro* a été décrite pour la première fois en 1999 (Makino *et al.*, 1999). Ce phénomène a été obtenu grâce à la modulation épigénétique du profil transcriptionnel des CSM par déméthylation de leur ADN avec le 5-azacytidine. La population cellulaire obtenue montrait d'importantes caractéristiques de cellules musculaires cardiaques avec une

expression de la troponine T et des chaines lourdes de myosine. Les cellules adoptaient alors un automatisme de type nodal avec des potentiels d'action de type ventriculaire et présentaient entre elles des interactions spécifiques de type gap junction (Hakuno *et al.*, 2002). L'acétylation des histones contrôle le profil transcriptionnel cardiomyogénique des CSM, et s'avère être plus efficace que la déméthylation de l'ADN seul pour induire la différenciation des CSM en cardiomyocytes (Feng *et al.*, 2009). Cependant, les effets délétères pouvant être induits par la déméthylation de l'ADN et/ou l'acétylation des histones sur le comportement cellulaire à long terme ne sont pas connus, rendant l'utilisant de ces cellules impossible en clinique. La reproduction d'un micro environnement *ex vivo* pourrait induire la transformation des CSM en cardiomyocytes (Furlani *et al.*, 2009). En effet, des facteurs de croissance, tels que les protéines morphogénétiques osseuses (BMP-2), les facteurs de croissance hépatocytes (HGF), les facteurs de croissance transformants (TGF-β1) et la protéine exogène Jagged 1 (ligand du récepteur Notch) induisent l'expression de plusieurs marqueurs cardiomyogéniques. D'autres stratégies visant à promouvoir la différenciation cardiomyocytaire des CSM ont été décrites, notamment la co-culture avec des cardiomyocytes matures (He et al., 2010; Okamoto et al., 2007; Ventura et al., 2007; Yang et al., 2010a) ou avec des extraits de cardiomyocytes (Labovsky *et al.*, 2010; Peran *et al.*, 2010). Cependant, beaucoup de ces concepts restent controversés. Ainsi les résultats obtenus de différenciation n'ont pu être reproduits par d'autres groupes (Koninckx *et al.*, 2009; Roura *et al.*, 2010). L'ensemble de ces études suggère que la différenciation des CSM en cardiomyocytes semble possible à condition que les CSM soient soumises à d'importantes manipulations *in vitro*. Il est peu probable que l'environnement physiologique cardiaque soit suffisamment puissant pour orienter les CSM en une lignée myogénique sans une stimulation exogène (Airey et al., 2004; Hattan et al., 2005; Toma et al., 2002).

2.2. La vasculogenèse : différenciation en cellules endothéliales et cellules musculaires lisses vasculaires.

Le faible approvisionnement en sang étant l'une des conséquences majeures des cardiomyopathies ischémiques, les processus angiogéniques apparaissent primordiaux pour la réparation myocardique. Sous l'influence de divers facteurs de croissance endothéliaux les CSM sont capables de se différencier *in vitro* en cellules endothéliales (CE), cellules musculaires lisses vasculaires (CMLV) et péricytes (Jiang et al., 2006; Silva et al., 2005). Cultivées en 3D dans des matrices, ces cellules peuvent générer par la suite des tubules similaires aux vaisseaux de petits calibres. L'implantation directe de CSM dans les modèles animaux d'IDM, tels que le chien (Silva et al., 2005), la souris (Li *et al.*, 2010a), le porc (Zhou *et al.*, 2009) et le rat (Tang *et al.*, 2006), permet d'augmenter la densité vasculaire. Aujourd'hui il n'est pas encore bien défini si ce phénomène est dû à une réelle différenciation des CSM en CE et/ou CMLV ou à une incorporation des CSM dans les nouveaux vaisseaux formés. Cependant il a été estimé qu'environ 3% des CSM implantées avec succès acquièrent un phénotype endothéliale (Zeng *et al.*, 2007).

2.3. Les effets paracrines des cellules souches mésenchymateuses.

2.3.1. Généralités.

Les effets thérapeutiques des CSM sont principalement paracrines, en amplifiant les phénomènes naturels de réparation des tissus lésés (Figure 2) Les CSM sécrètent différents facteurs pro-angiogéniques comme le SDF-1 (Tang *et al.*, 2010), le HGF (Deuse et al., 2009; Tang et al., 2010), l'IGF-1 (Enoki *et al.*, 2010), bFGF (Yoon *et al.*, 2005), le VEGF (Matsumoto *et al.*, 2005; Zisa *et al.*, 2009), l'Ang-1 (Sun *et al.*, 2007), le PlGF, le MCP-1, mais aussi des interleukines, IL-1, IL-6 (Westrich *et al.*, 2010) ou le TNF-α (Kim *et al.*, 2009). Enfin, les CSM sont capables d'exprimer HIF-1α, facteur de transcription régulé par

l'hypoxie, à l'origine de l'expression notamment du VEGF (Okuyama *et al.*, 2006) (Tableau 2). Outre l'apparition de néo-vaisseaux (Tang *et al.*, 2009), ces phénomènes peuvent protéger les tissus existants, voire amplifier les phénomènes d'auto-régénération de l'organe en stimulant les cellules souches cardiaques endogènes ainsi que le recrutement et la différenciation des cellules progénitrices endothéliales (Urbanek *et al.*, 2005). Par ailleurs, les CSM ont la faculté de se localiser préférentiellement dans les zones tissulaires ischémiques ou inflammatoires (Chamberlain *et al.*, 2007; Psaltis *et al.*, 2008). Chez différents animaux, l'injection intracardiaque de CSM après un IDM diminue la taille de la cicatrice, améliore la densité capillaire et la fonction cardiaque (Angoulvant *et al.*, 2011; Gnecchi *et al.*, 2009; Mias *et al.*, 2009; Schuleri *et al.*, 2009). Les mécanismes paracrines des CSM sont également impliqué dans le remodelage de la matrice extracellulaire ainsi que la digestion des tissus cicatriciels (Mias et al., 2009).

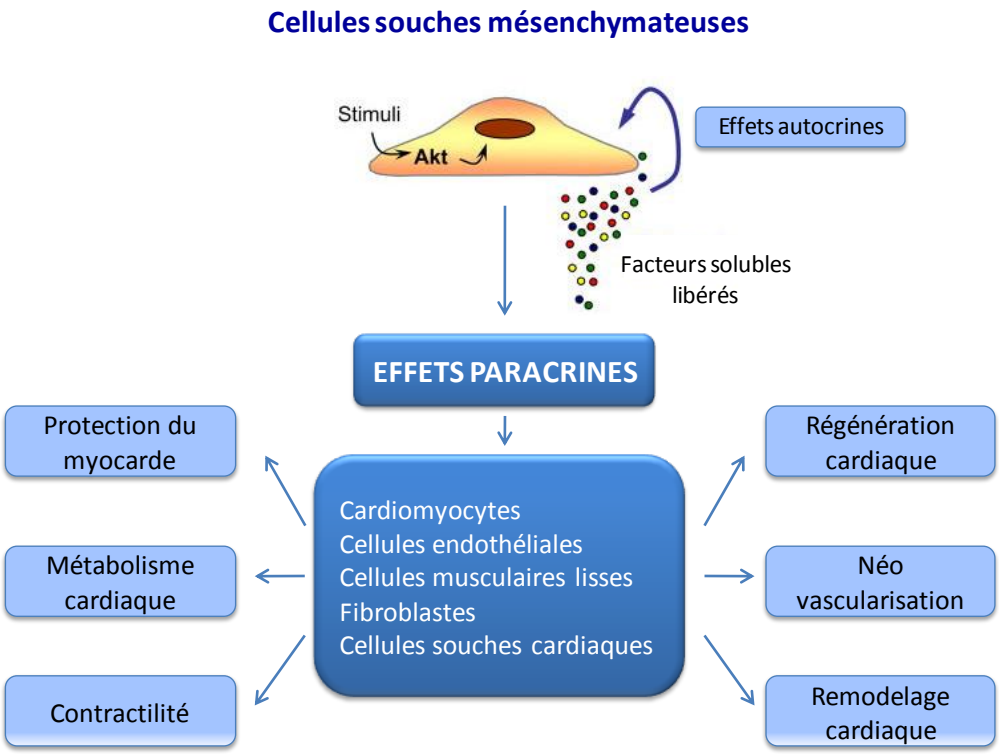

Figure 2 : Mécanismes paracrines et autocrines des cellules souches mésenchymateuses.

D'après (Gnecchi et al., 2008).

Facteurs sécrétés	Abréviations	Fonctions proposées
Adrenomedullin	ADM	cytoprotection
Angio-associated migratory protein	AAMP	angiogenèse
Angiogenin	ANG	angiogenèse; prolifération
Angiopoetin-1	AGPT61	migration; stabilisation vasculaire
Bone morphogenetic protein-2	BMP-2	développement
Bone morphogenetic protein-6	BMP-6	différenciation; croissance
Connective tissue growth factor	CTGF	angiogenèse; croissance cellulaire
Endothelin-1	EDN-1	cytoprotection; prolifération
Fibroblast growth factor-2	FGF-2	prolifération et migration
Fibroblast growth factor-7	FGF-6	stabilisation et prolifération
Hepatocyte growth factor	HGF	cytoprotection; angiogenèse; migration
Insulin-like growth factor-1	IGF-1	cytoprotection; migration; contractilité
Interleukin-1	IL-1	VEGF induction
Interleukin-6	IL-6	VEGF induction
Interleukin-11	IL-11	cytoprotection
Kit ligand/stem cell factor	KITLG (SCF)	proliferation et migration
Leukemia inhibitory factor	LIF	prolifération; cytoprotection
Macrophage migration inhibitory factor	MIF	prolifération; réponse inflammatoire
Matrix metalloproteinase-1	MMP-1	destruction matrice, formation des tubules
Matrix metalloproteinase-2	MMP-2	destruction matrice, formation des tubules
Matrix metalloproteinase-9	MMP-9	destruction matrice
Monocyte chemoattractant protein-1	MCP-1	migration des monocytes
Macrophage-specific colony-stimulating factor	M-CSF	prolifération et migration des monocyte
Placental growth factor	PGF	prolifération cellulaire
Plasminogen activator	PA	dégradation molecules matricielles
Platelet-derived growth factor	PDGF	prolifération et migration cellulaire
Pleiotrophin	PTN	prolifération cellulaire
Secreted frizzled-related protein-1	SFRP-1	développement
Secreted frizzled-related protein-2	SFRP-2	développement
Stem cell–derived factor-1	SDF-1	recrutement des cellules progénitrices "homing"
Thrombospondin-1	THBS-1	migration cellulaire
Thymosin-beta 4	TMS-β4	migration cellulaire; cytoprotection
Tissue inhibitor of metalloproteinase-1	TIMP-1	migration cellulaire
Tissue inhibitor of metalloproteinase-2	TIMP-2	migration cellulaire
Transforming growth factor-beta	TGF-β	maturation des vaisseaux; prolifération cellulaire
Tumor necrosis factor-alpha	TNF-α	dégradation molecules matricielles; prolifération
Vascular endothelial growth factor	VEGF	cytoprotection; prolifération; migration; angiogenèse

Tableau 2: Facteurs paracrines sécrétés par les CSM. *D'après (Gnecchi et al., 2008).*

2.3.2. La néovascularisation.

La néovascularisation est un processus biologique important influencé par les CSM dans la réparation cardiaque après un IDM. Les processus moléculaires menant à la vasculogenèse, l'angiogenèse et l'arteriogenèse impliquent des médiateurs tels que l'oxyde nitric (NO), le VEGF, le bFGF, l'HGF, le SDF-1, l'angiopoïétine, et d'autres. Ces molécules stimulent la migration et la prolifération des cellules endothéliales et des cellules musculaires lisses vasculaires, le bourgeonnement endothélial ou « sprouting » entraînant la formation de nouvelles ramifications « branching » et la synthèse de matrice extracellulaire (Figure 3) Comme décrit précédemment, les CSM peuvent exprimer ces molécules pro-angiogéniques (Kinnaird *et al.*, 2004). L'implantation de CSM permet d'augmenter la densité capillaire et de développer des artères collatérales dans le tissu ischémique. De plus les CSM expriment des facteurs, tels que le bFGF, le VEGF, et l'angiopoïétine-1, l'IL-1β et le TNF-α, connus pour avoir une activité angiogénique (Kamihata *et al.*, 2001). Les différentes études menées depuis plus de 10 ans ont permis de mettre en évidence que les facteurs pro-angiogéniques, libérés par les CSM, jouent un rôle dans la néovascularisation lorsque ces dernières sont implantées dans un cœur ischémique favorisant ainsi la régénération myocardique (Halkos *et al.*, 2008; Wang *et al.*, 2008).

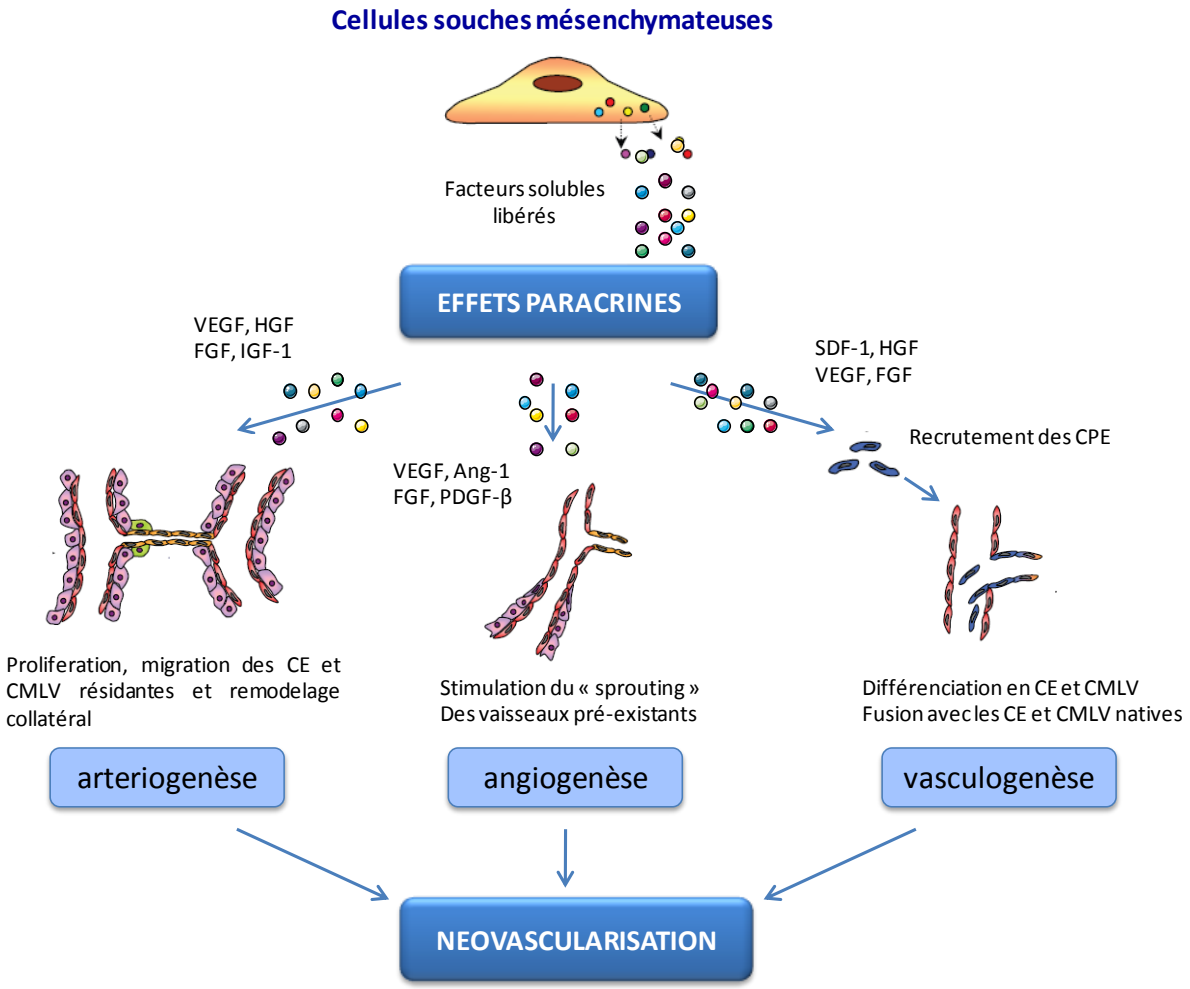

Figure 3: Mécanismes impliqués dans la néovascularisation.

D'après (Gnecchi et al., 2008)

CE : cellule endothéliale ; CMLV : cellule musculaire lisse vasculaire

2.3.3. Effets des cellules souches mésenchymateuses sur la régénération cardiaque.

Le cœur était considéré, jusqu'à récemment, comme un organe possédant des cellules post-mitotiques dépourvu de capacités de régénération ou de réparation. Ce principe a été bousculé par la découverte de niches de cellules souches cardiaques (CSC) endogènes. Ces cellules présentent des caractéristiques de cellules souches capables de se différencier dans tous les types cellulaires composant le cœur, à savoir des cardiomyocytes, des cellules musculaires et des cellules endothéliales. Il a été identifié des cellules souches exprimant à

leur surface, le marqueur c-kit (cellules c-kit$^+$), le marqueur Sca-1 (cellules Sca-1$^+$ ou *side population*) ainsi que des cardioblastes ou cellules progénitrices, telles que les cellules exprimant le marqueur Isl1 (Evans et al., 2007). Ces cellules sont particulièrement sensibles aux facteurs de croissance, tels que le VEGF, le HGF et IGF-1 (Padin-Iruegas et al., 2009; Tang et al., 2011; Urbanek et al., 2005). Suite à un IDM, ces CSC sont naturellement recrutées et mobilisées sur le site lésé, ces phénomènes sont amplifiés par l'implantation de CSM (Fazel *et al.*, 2005). En effet, les CSM stimulent la migration des CSC vers la zone ischémique du myocarde grâce au VEGF (Zisa et al., 2009). Elles jouent également un rôle dans la mobilisation et la différenciation des cellules progénitrices, par la sécrétion du SDF-1α et du TGF-β (Zhao *et al.*, 2009). Ainsi les CSM implantées peuvent augmenter les capacités régénératrices de ces CSC *via* leurs effets paracrines. Cependant, il faut noter que la stimulation des CSC par les CSM peut également être due à un effet de contact entre les cellules (Loffredo *et al.*, 2011).

2.3.4. Les effets des cellules souches mésenchymateuses sur la protection du myocarde.

Quelles soient exogènes ou endogènes, directement mobilisées de la moelle osseuse après un IDM, les CSM s'intègrent aux sites lésionnels le long des gradients chimiotactiques, médiés spécifiquement par le SDF-1 (Toma *et al.*, 2002). Une fois localisées dans ces sites hypoxiques, les CSM libèrent des molécules cytoprotectrices augmentant la survie des cardiomyocytes (Gnecchi *et al.*, 2005). Ces données ont été corroborées par les effets cardioprotecteurs durant un IDM d'injections de milieux conditionnés provenant de CSM (Gnecchi *et al.*, 2006). L'effet cytoprotecteur sur les cardiomyocytes est augmenté lorsque les CSM sur-expriment le gène Akt (Akt-CSM). En présence d'Akt-CSM ou de milieu conditionné par ces cellules (Akt-CSM-MC) les CSM libèrent des facteurs, tels que VEGF, bFGF, HGF et IGF-1, diminuant l'apoptose et la nécrose des cardiomyocytes (Angoulvant et al., 2011; Gnecchi et al., 2009; Lim et al., 2006). Ces facteurs améliorent également la

contractilité des cardiomyocytes (Freestone *et al.*, 1996) ainsi que leur métabolisme (Feygin *et al.*, 2007).

2.3.5. Les effets des cellules souches mésenchymateuses sur le remodelage de la matrice extracellulaire du myocarde.

En plus de la néovascularisation et de la cytoprotection, les facteurs paracrines, libérés par les CSM transplantées dans le myocarde ischémique, peuvent modifier la MEC, agissant directement sur la cicatrisation de la zone infarcie. Les CSM transplantées libèrent des molécules, telles que des métalloprotéinases (MMPs) et des sérines protéases. Ces molécules atténuent la prolifération des fibroblastes, l'expression du collagène de type I et III, l'inhibiteur tissulaire de la MMP-1 (TIMP-1) et le TGFβ, diminuant ainsi la fibrose et limitant l'amincissement de la paroi cicatricielle, l'ensemble préservant la fonction systolique et diastolique cardiaque (Ohnishi et al., 2007; Xu et al., 2005).

2.4. Les cellules souches mésenchymateuses et l'immunologie dans le cœur.

L'infarctus du myocarde est associé à de nombreux processus immunologiques qui peuvent à la fois être bénéfiques et nuisibles à la réparation cardiaque. Les CSM sont particulièrement sensibles à l'inflammation et migrent préférentiellement vers les zones lésées où elles peuvent réprimer activement les processus immunologiques et réduire l'inflammation en inhibant de façon dose-dépendante la prolifération des lymphocytes T induite par les cellules dendritiques (Di Nicola *et al.*, 2002). Les CSM modifient le profil d'expression des cytokines produites par les cellules dendritiques, les cellules Natural Killer (NK) et les lymphocytes T en favorisant un phénotype anti-inflammatoire (Figure 4). En effet, les CSM diminuent la sécrétion de molécules pro-inflammatoires telles que IL-12, IL-6, TNF-α et INF-γ et stimulent la production de cytokines anti-inflammatoires telles que IL-10 et le TGF-β par les cellules dendritiques (Aggarwal and Pittenger, 2005; Du et al., 2008). En plus d'influencer

l'inflammation cardiaque, les CSM réagissent également aux cytokines présentes dans le cœur ischémique (Abarbanell *et al.*, 2009). La production accrue des cytokines pro-inflammatoires au cours d'un IDM, tel que le TNF-α par exemple, stimule les récepteurs du TNF-α (TNFR)-1 et/ou -2 des CSM, modifiant leur profil d'expression pour le VEGF, TNF-α, IL-6 et IL-1 (Bao *et al.*, 2008; Markel *et al.*, 2008). Les effets immuno-modulateurs des CSM semblent transitoires, dose-dépendants et variables selon le degré de la réponse inflammatoire (Renner *et al.*, 2009). L'interaction complexe entre les CSM, l'inflammation et la régénération du myocarde est un domaine de la recherche qui est encore loin d'être complètement compris.

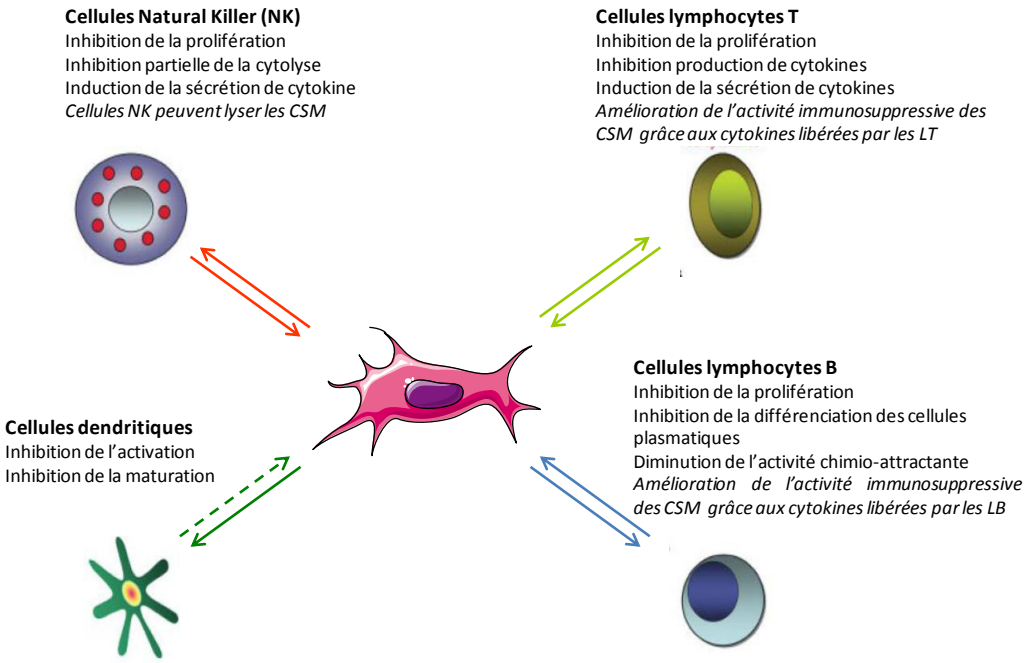

Figure 4: Rôle immunomodulateur des cellules souches mésenchymateuses.

Modifiée d'après *(Uccelli et al., 2006).*

Interaction bidirectionnelle entre les CSM, les cellules T, les cellules B et les cellules *natural killeur* (NK)

3. Les essais cliniques.

3.1. Les cellules souches allogéniques *versus* autologues.

Aujourd'hui l'utilisation des CSM autologues apparait comme la thérapie la plus sûre, puisque elle n'induit pas de réaction inflammatoire, de rejet des cellules après transplantation et permet de s'affranchir des traitements immunosuppresseurs. Cependant, d'un point de vue clinique, l'utilisation de ces cellules autologues présente quelques inconvénients. Le prélèvement de moelle osseuse est un acte douloureux et invasif pour le patient. De plus les cellules prélevées chez des patients, qui présentent des maladies et des facteurs de risque, pourraient s'avérer moins efficace. Enfin avant d'obtenir une population homogène de CSM à partir d'un prélèvement de moelle osseuse, un délai de culture d'environ 3 semaines est indispensable, limitant l'accès de ces cellules aux traitements d'IDM en phase aigüe. De manière très intéressante, les CSM peuvent échapper à la détection et l'élimination par le système immunitaire de l'hôte car elles n'expriment pas de molécules de classe II du complexe majeur d'histo-compatibilité (CMH II) et expriment très faiblement les molécules de classe I (CMH I) (Amado et al., 2005; Grinnemo et al., 2004). Cette donnée est fondamentale puisqu'elle permet d'envisager une transplantation allogénique sans traitement immunosuppresseur préalable. Cependant, une question se pose sur le potentiel immunogène de ces cellules allogéniques si la thérapie vise à utiliser les CSM pour leur capacité de différenciation et d'intégration sous forme de cardiomyocytes et/ou de cellules endothéliales. En effet la différenciation des précurseurs endothéliaux allogéniques en cellules endothéliales aortiques dans une allogreffe chez le rat induit une réexpression du CMH I et du CMH II, entrainant une réaction inflammatoire et finalement un rejet des cellules *in vivo (Ladhoff et al., 2010)*. L'utilisation d'un traitement immunosuppresseur peut cependant améliorer considérablement la thérapie à base de CSM allogéniques (Min *et al.*, 2006; Poncelet *et al.*, 2010). Le prétraitement des CSM avec des cytokines anti-inflammatoires, notamment l'IL-10

et le HGF, afin de moduler les propriétés immunomodulatrices des CSM, leur différenciation et leur immunotolérance, peut être une option pour augmenter l'efficacité de la thérapie. Les différents essais cliniques actuellement en cours devraient permettre d'apporter plus d'informations sur l'utilisation des CSM autologues *versus* allogéniques comme traitement de l'IDM.

3.2. Les études cliniques de thérapie cellulaire de l'infarctus du myocarde.

3.2.1. Les essais cliniques publiés.

Actuellement, l'expérience clinique de la thérapie cellulaire cardiaque utilisant des CSM est limitée (Tableau 3) en raison du temps de production des CSM dans des conditions cliniques de qualité en accord avec les bonnes pratiques de production (conditions GMP, Good Manufacturing Practice) qui est d'environ trois semaines. Ce délai a un coût prohibitif et limite leur utilisation en phase aigüe d'IDM. Le premier essai clinique randomisé a été réalisé chez 69 patients et publié en 2004 par Chen et son équipe (Chen et al., 2004). Le protocole consistait à injecter en par voie percutanée et en intracoronaire des CSM autologues issues de sang autologue de moelle osseuse 3 semaines après l'IDM. Il n'a pas été observé d'effets indésirables graves liés aux CSM et 3 mois après l'implantation, le groupe de patients traités avec les CSM présentait une meilleure fraction d'éjection du ventricule gauche *(left ventricular ejection fraction, LVEF)* par rapport au groupe contrôle. Le même groupe a ensuite réalisé un essai randomisé chez des patients souffrant de cardiomyopathie ischémique chronique, à l'aide d'un protocolaire similaire. Là encore, les patients traités avec des CSM autologues avaient une amélioration significative de leur fonction cardiaque (Chen et al., 2006). Par la suite 3 autres essais cliniques utilisant des CSM autologues ont été réalisés et publiés. Les résultats ont montré une amélioration de la fonction cardiaque (Katritsis et al., 2005), une diminution des troubles du rythme chez des patients présentant des arythmies

(Katritsis et al., 2007) et ont finalement permis de s'affranchir des risques potentiels liés à l'injection de CSM autologues en intracoronaire au cours d'un cathétérisme cardiaque (Yang et al., 2010b). Hare et son équipe ont été les premiers à réaliser et à publier en 2009 un essai clinique randomisé, en double aveugle utilisant des CSM allogéniques administrées en intraveineux chez 53 patients en phase aigüe d'IDM (Hare et al., 2009). Cette étude a permis de valider la faisabilité et la sûreté de cette thérapie et de mettre en évidence son efficacité sur l'amélioration de la fonction cardiaque. La perspective d'utiliser un produit de thérapie cellulaire cardiaque allogénique est particulièrement attractive. Cependant, les problèmes mentionnés précédemment concernant la tolérance immunologique de ces cellules doivent être étudiés plus en détails, afin de pouvoir écarter les éventuels effets indésirables.

Trial design phase	Cell type	design	No. Of enrolled patient	Contions treated	Delivery method	Primary cinical outcome	Institution	Référence
I	Autologous MSC	RSBPC	69	Acute MI	Intracoronary	LVEF	Nanjing First hopital, China	(Chen *et al.*, 2004)
I	Autologous MSC	C	46	Chronic MI (LAD)	Intracoronary	LVEF	Nanjing First Hospital, China	(Chen *et al.*, 2006)
I	Autologous MSC + EPC	RSBPC	22	Acute MI	Intracoronary	LVEF, SPECT	Athens Euroclinic, Greece	(Katritsis *et al.*, 2005; Tongers *et al.*, 2011)
I	Autologous MSC + EPC	CR	5	Chronic MI arrhythmia	Intracoronary	LVEF, arrhytmies	Athens Euroclinic, Greece	(Katritsis *et al.*, 2007)
I	Allogeneic MSC	RDBPC	53	Acute MI	Intravenous	LVEF, MACE	Osiris therapeutic, USA	(Hare *et al.*, 2009)
I	Allogeneic MSC	RDBPC	16	Acute MI	Intracoronary	LVEF, SPECT	Nanjing First Hospital, China	(Yang et al., 2010b)
I	Autologous MSC	RDBPC	31	Refractory angina with CAD	Intramyocardial	LVEF, SPECT	Hearth Centre, Rigshospitalet Copenhagen University Hospital, Denmark	(Friis *et al.*, 2011)

Tableau 3: Essais cliniques publiés de thérapie cellulaire de l'infarctus du myocarde utilisant des cellules souches mésenchymateuses.

C, controlled; CAD; coronary artery diseases; CR, case report; EPC, endothelial progenitor cell; LAD, left anterior descending artery; LVEF, left ventricular ejection fraction; MACE, major adverse cardiac event; MI, myocardial infarction; MSC, mesenchymal stem cell; RDBPC, randomized, double blinded, placebo controlled; RSBPC, randomized, single blinded, placebo controlled; SPECT, single-photon emission computed tomography.

3.2.2. Les essais cliniques en cours.

Les premiers essais cliniques publiés ont apporté un réel intérêt à l'utilisation des CSM comme produit de thérapie cellulaire cardiaque. Cependant il apparait primordial aujourd'hui de réaliser des essais cliniques multicentriques à plus grande échelle et d'évaluer à long terme le gain de cette thérapie sur la survie des patients ainsi que l'incidence d'éventuels effets secondaires indésirables. Au moment de la rédaction de ce manuscrit, ClinicalTrials.gov (http://www.clinicaltrials.gov) a répertorié 14 essais cliniques dans lesquels

sont utilisés des CSM autologues et/ou allogéniques comme traitement de l'IDM (Tableau 4). Une nouvelle source de cellules reçoit actuellement une attention particulière : les cellules souches dérivées du tissu adipeux (*adipose-derived stem cell, ADSC* ou *adipose-derived regenerative cell, ADRC*). Après prélèvement par lipo-aspiration ces cellules sont rapidement disponibles et utilisables contrairement aux cellules issues de la moelle osseuse qui nécessitent un temps de culture et d'amplification d'environ 3 semaines, le temps d'éliminer les cellules hématopoïétiques. Ces cellules sont donc facilement accessibles pour une thérapie d'IDM en phase aigüe. Actuellement 2 essais cliniques, réalisés en Espagne et aux Pays-Bas utilisent ces cellules (Principale investigateur : Patrick Serruys). Elles ne présentent pas strictement les mêmes propriétés que les CSM issues de la moelle osseuse, mais les premières données sont encourageantes.

Parallèlement aux essais cliniques en cours officialisés et répertoriés, de nombreux patients souffrant de cardiopathies ischémiques peuvent avoir facilement accès aux produits de thérapie cellulaire dans le monde, à base de CSM en dehors d'études cliniques *via* un vaste marché développé sur internet (Taylor *et al.*, 2010). Dans de nombreux pays, le cadre juridique autorise la réalisation de thérapies cellulaires cardiaques à des fins purement médicales. Par exemple en Extrême-Orient, l'utilisation de cellules souches dérivées du tissu adipeux est un marché en plein essor. Le nombre de patients ainsi traité dépasserait de loin celui des patients recrutés pour des essais cliniques. Malheureusement, tant que la préparation des cellules et les conditions de traitements ne seront pas soumises à une réglementation internationale, ces pratiques perdureront.

Finalement, la faisabilité technique de la thérapie cellulaire cardiaque est aujourd'hui bien établie et, globalement, l'expérience clinique montre une bonne tolérance aux transferts intra-myocardiques des CSM même si une accélération des lésions coronaires ne peut encore être formellement éliminée, et exige d'être mieux caractérisée. L'efficacité, en revanche,

paraît marginale, ce qui n'est pas surprenant compte tenu du caractère encore balbutiant de ces nouvelles approches thérapeutiques. Ces essais cliniques initiaux sont cependant riches d'enseignements et permettent de mieux identifier le choix entre produits autologues et allogéniques, les doses optimales, l'amélioration des techniques de transfert cellulaire et le développement parallèle de l'imagerie pour suivre le devenir des cellules greffées. Enfin, ces essais permettent d'identifier des problèmes qu'il convient désormais de résoudre afin de rendre plus efficace la thérapie cellulaire cardiaque.

Trial design phase	Cell type	design	No. Of enrolled patient	Contions treated	Delivery method	Primary cinical outcome	Institution	Référence
I/II	Autologous MSC		10	CHF	Transendocardial	Safety, feasibility	Université de Toulouse, France	NCT01076920
I	Allogeneic MSC	RDBPC	48	AMI	Intraveinous	safety	Osiris Therapeutics, USA	NCT00114452
I/II	Autologous MSC Allogeneic MSC (phase II)	RDBPC	30	CHF	Transendocardial	TE-SAE	Natiomal Heart Lung and Blood Institute, USA	NCT01087996
I/II	Allogeneic MSC	RDBPC	20	AMI	Intraveinous	Safety, efficacy	Stempeutics research Pvt Ltd, India	NCT00883727
II	Allogeneic MSC	RDBPC	220	AMI	Intraveinous	LVEF	Osiris Therapeutics, USA	NCT00877903
I/II	Autologous MSC	RDBPC	45	CHF	Intraveinous	SAE	Natiomal Heart Lung and Blood Institute, USA	NCT00587990
I/II	Autologous MSC	NCR	40	CHF	Intramyocardial	Safety, efficacy	Rigshospitalet, Denmark	NCT00260338
I/II	Autologous MSC / BMC	RDBPC	60	CHF	Intramyocardial	Safety, efficacy	University of Miami, USA	NCT00768066
II	Autologous MSC	RDBPC	60	CHF	Transendocardial	LVEF	Helsinki University, Finland	NCT00418418
I/II	Autologous MSC	RDBPC	60	CHF	Intramyocardial	LVEF	Rigshospitalet, Denmark	NCT00644410
II	Autologous MSC	RC	60	CHF	Transendocardial	safety	TCA Cellular Therapy, USA	NCT00790764
II	Allogeneic MSC	RDBPC	80	CHF	intracoronary ou transendocardial	safety	Natiomal Heart Lung and Blood Institute, USA	NCT00927784
I	Autologous ADRC	RDBPC	48	AMI	Transendocardial	safety	Cytori Therapeutics, USA	NCT00442806
I	Autologous ADRC	RDBPC	36	CHF	Transendocardial	safety	Cytori Therapeutics, USA	NCT00426868

Tableau 4: Essais cliniques en cours de thérapie cellulaire de l'infarctus du myocarde aigu ou d'insuffisance cardiaque chronique utilisant des cellules souches mésenchymateuses.

(**ClinicalTrials.gov).** ADRC, adipose-derived regenerative cell; AMI, acute myocardial infarction; BMC, bone marrow mononuclear cell; CHF, chronic heart failure; DCM, dilative cardiomyopathy; LVAD, left ventricular assist device; LVEF, left ventricular ejection fraction; MSC, mesenchymal stem cell; NRC, nonrandomized controlled; R, randomized; RDBPC, randomized, double blinded, placebo controlled; SAE, sustained ventricular arrhythmias, ectopic tissue formation, or sudden unexpected death; TE-SAE, death, nonfatal myocardial infarction, stroke, hospitalization for worsening heart failure, cardiac perforation, pericardial tamponade, ventricular arrhythmias >15 sec or with hemodynamic compromise or atrial fibrillation.

4. Les limites de la thérapie cellulaire de l'infarctus du myocarde utilisant les cellules souches mésenchymateuses.

4.1. Les limites liées à la culture *in vitro*.

L'utilisation des CSM s'inscrit dans la vague d'enthousiasme dans laquelle les cellules souches adultes sont utilisées pour réparer les tissus, cependant, plusieurs précautions essentielles ne sont pas pleinement prises en compte, notamment dans les essais cliniques (Prockop and Olson, 2007). Un des risques majeurs, est que les CSM qui se multiplient largement en culture pourraient produire des cellules tumorales une fois implantées chez les patients (Tolar *et al.*, 2007). En parallèle avec le développement de leur utilisation en clinique, des préoccupations sur le fait que les CSM peuvent être sujettes à une transformation maligne ont récemment été soulevées par plusieurs groupes de recherche. Il a été montré que des CSM issues de la moelle osseuse pouvaient subir une transformation spontanée après une longue période de culture *in vitro* (Rosland *et al.*, 2009). En 2005, Rubio et son équipe, montrait des résultats similaires avec des CSM dérivées du tissu adipeux (Rubio *et al.*, 2005). L'analyse du caryotype de ces CSM montrait des trisomies, des tétraploïdies et/ou des réarrangements chromosomiques. Cependant, de la Fuente et ses collègues démentent ces résultats et soupçonnent les phénomènes de transformations spontanées d'être dus à des artefacts de contamination. En 2010, Rubio et les auteurs de l'article sont contraints de rétracter leur publication (de la Fuente *et al.*, 2010). En 2007, l'agence française de sécurité sanitaire des produits de santé (Afssaps) avait décidé de stopper tous les essais cliniques utilisant l'administration de CSM, à cause de ces altérations génétiques observées dans les cultures de CSM. Grâce à des recherches de la communauté scientifique sur ce problème (Hatzistergos *et al.*, 2011; Tarte *et al.*, 2010), l'Afssaps a de nouveau donné l'autorisation, en août 2009, d'utiliser les CSM comme produit de thérapie cellulaire dans des essais cliniques,

mais ces essais sont limités à des patients avec des atteintes très sévères et un pronostic vital engagé à court terme.

4.2. Les limites de l'efficacité des cellules souches mésenchymateuses *in vivo*.

4.2.1. La fonctionnalité des cellules.

L'une des limites majeures des CSM utilisées en clinique à ce jour, serait leur incapacité à donner naissance à de véritables cardiomyocytes pouvant se coupler électriquement et mécaniquement avec ceux du receveur. Il s'agit pourtant là d'un pré-requis évident pour que le greffon se contracte de façon synchrone avec le cœur natif et contribue à en améliorer la fonction. Le pré-requis à l'utilisation des CSM est leur spécification préalable afin de les orienter vers une différenciation cardiomyogénique, tant pour optimiser leur fonction *in vivo* que pour prévenir la survenue d'un tératome (observé que lorsque les cellules sont laissées à l'état complètement indifférencié). Les problèmes à résoudre (amplification, spécification, sélection) restent nombreux, mais la rapidité de la recherche dans ce domaine ne rend pas impossible que ces cellules puissent, à relativement brève échéance, donner des cardiomyocytes capables de régénérer le myocarde.

4.2.2. La rétention intracardiaque des cellules.

Que les injections se fassent par voie épicardique, sous contrôle visuel, au cours d'une intervention de chirurgie cardiaque, ou par cathéter, elles ne permettent qu'à une petite fraction des cellules de rester présentes dans le cœur. L'administration de cellules mâles à des rates a bien montré que le chromosome Y pouvait être identifié dans de multiples organes, traduisant ainsi la dissémination systémique majeure (Dow *et al.*, 2005). De même, chez le porc, ce n'est que 3% des cellules mésenchymateuses injectées par voie intra-coronaire qui sont retrouvées dans le cœur (chiffre très proche de celui rapporté dans une étude clinique), et ce pourcentage est encore réduit de moitié lorsque l'administration se fait par la voie endo-

ventriculaire gauche (Freyman *et al.*, 2006). Il y a donc un besoin réel d'améliorer les techniques d'injection par des systèmes permettant des transferts cellulaires précis, reproductibles et efficaces. Ces améliorations ne pourront venir que d'une étroite collaboration entre les biologistes et les industriels impliqués dans les dispositifs médicaux et le développement des biomatériaux. Il est également important, dans une perspective sécuritaire, de mieux préciser le devenir des cellules ayant migré dans des localisations ectopiques.

4.2.3. La survie des cellules.

L'efficacité thérapeutique potentielle des transplantations cellulaires est encore obérée par le fait que, parmi les cellules qui ont pu être retenues dans le tissu cardiaque cible, la majorité d'entre elles (jusqu'à 90%) meurt dans les jours qui suivent l'injection (Maurel et al., 2005; Toma et al., 2002). Cette mort cellulaire est un phénomène multifactoriel, dans lequel interviennent, la réponse inflammatoire aux injections elles-mêmes, l'apoptose, l'ischémie consécutive à la faible vascularisation des zones infarcies fibreuses greffées et la perte des rapports normaux des cellules avec la matrice extracellulaire. L'amélioration de la survie des cellules souches permettrait de réduire de façon significative le nombre de cellules à injecter, d'empêcher la répétition des injections, de diminuer les temps d'amplification des cellules et finalement de réduire l'inflammation tissulaire conséquente à l'élimination des débris cellulaires.

5. L'optimisation de la thérapie cellulaire utilisant les cellules souches mésenchymateuses.

Les premiers essais cliniques obtenus utilisant les CSM comme produit de thérapie cellulaire de l'IDM sont extrêmement prometteurs, cependant comme nous venons de le décrire plusieurs contraintes, telles que la fonctionnalité, la rétention et la survie des cellules,

limitent considérablement les bénéfices thérapeutiques. Face à ces limites, plusieurs stratégies ont récemment émergé afin d'optimiser les CSM avant leur implantation, favorisant ainsi par exemple leur recrutement, leurs fonctions paracrines et leur survie. Les méthodes spécifiques utilisées pour améliorer les capacités régénératrices des CSM incluent au cours de l'expansion *ex vivo*, le pré-conditionnement hypoxique, les manipulations génétiques ciblées et les prétraitements pharmacologiques (Herrmann et al., 2011).

5.1. Le Pré-conditionnement hypoxique.

Les premières études réalisées sur le pré-conditionnement à l'ischémie ont permis de mettre en évidence que l'hypoxie *via* une régulation positive de la voie de signalisation impliquant HIF-1α diminue l'apoptose des cardiomyocytes, limite la taille de l'infarctus et favorise la néovascularisation (Cai *et al.*, 2003; Cai *et al.*, 2008). La caractérisation de ce phénomène *in vitro* a révélé que les CSM cultivées dans des conditions hypoxiques expriment des facteurs de survie, tels que HIF-1α, Bcl-2 et Bcl-xL, et diminuent l'expression des caspases 3 (Hu *et al.*, 2008). Au travers de ces différents facteurs, l'hypoxie régule les voies PI3K/Akt et ERK, connues pour leur implication dans la survie cellulaire et leurs mécanismes anti-apoptotiques (Rosova *et al.*, 2008). Le pré-conditionnement hypoxique des CSM favorise également la production du VEGF *via* le facteur de transcription STAT-3 (*signal transducer and activator of transcription 3*) et l'expression du récepteur de HGF, favorisant respectivement la néovascularisation et la migration cellulaire. Cette stratégie de pré-conditionnement des CSM avant implantation a pour avantage d'être facilement applicable à de grandes quantités de cellules.

5.2. Les manipulations génétiques des cellules souches mésenchymateuses.

La capacité à cibler l'expression spécifique des gènes impliqués dans les mécanismes de cardioprotection médiés par les CSM a permis d'optimiser l'efficacité thérapeutique des

CSM. De plus, la manipulation génique de ces cellules peut offrir un changement phénotypique plus durable qu'un pré-conditionnement hypoxique ou qu'un traitement pharmacologique. Ces manipulations impliquent généralement de modifier le génome afin de permettre la régulation de l'expression de gènes impliqués dans le recrutement des cellules ou « homing », les fonctions paracrines ou la survie (Tableau 5).

Homing	Fonctions paracrines	survie
SDF-1	VEGF	Akt
CXCR4	Angiogenin	Bcl-2
	Ang-1	Hsp20
	HGF	HO-1
	IL-18bp	FGF-2
	TNFR1, 2	

Tableau 5: Cibles moléculaires des manipulations géniques dans les CSM.

SDF-1: stromal cell-derived factor 1; VEGF: vascular endothelial growth factor, Ang-1: angiopoietin 1; HGF:hepatocyte growth factor; IL-18BP: interleukine 18 binding protein; TNFR: tumor necrosis factor receptor; Hsp20: heat-shock protein 20; HO-1: heme oxygenase-1; FGF-2: fibroblast growth factor-2.

Grâce à l'expression membranaire du récepteur CXCR4, les cellules souches endogènes sont immédiatement recrutées vers les zones lésées du myocarde par un gradient de SDF-1 qui est considérablement augmenté après un IDM (Askari *et al.*, 2003). La surexpression du CXCR4 et/ou du SDF-1 dans les CSM favorise leur « homing » vers le myocarde, mais également la mobilisation et la survie des CSC et des cellules progénitrices (Cheng *et al.*, 2008; Zhang *et al.*, 2007b). Comme décrit précédemment le VEGF secrété par les CSM possède des rôles majeurs dans la réparation cardiaque. Les CSM modifiées pour sur-exprimer le VEGF stimule l'angiogenèse et la myogenèse (Yang *et al.*, 2007) et celles sur-exprimant le gène anti-apoptotique Akt sont plus résistantes à l'apoptose *in vitro* et *in vivo*

(Gnecchi et al., 2006; Lim et al., 2006). Les Akt-CSM augmentent la surexpression de différentes cytokines protectrices, telles que le VEGF, HGF, b-FGF et IGF-1, limitant ainsi le remodelage ventriculaire et améliorant de façon significative la fonction cardiaque en réduisant l'inflammation au sein du tissu lésé (Noiseux *et al.*, 2006). Enfin la survie des CSM peut également être améliorée grâce à la surexpression du gène codant l'Heme Oxygénase-1 (HO-1, enzyme ayant des propriétés antioxydantes). De plus, ces cellules semblent avoir un effet cardioprotecteur en diminuant de façon importante l'apoptose des cellules résidentes (Tsubokawa *et al.*, 2010).

La modification génique des CSM avant leur greffe est bénéfique et optimise considérablement leur efficacité thérapeutique. Cependant, cette approche de thérapie génique peut poser des problèmes pour un transfert de ces protocoles chez l'Homme. De ce fait, d'autres études ont visé à obtenir des effets semblables sans manipulation des cellules mais en les pré-conditionnant avec divers agents pharmacologiques.

5.3. Les prétraitements pharmacologiques.

Il est maintenant communément admis que de nombreux facteurs de croissance et cytokines améliorent l'efficacité des CSM. Le prétraitement des CSM avec le FGF-2, l'IGF-1et/ou la BMP-2 stimule les voies de signalisation anti-apoptotique ainsi que la différenciation en cellules myogéniques ou endothéliales. Le FGF-2 et l'IGF-1 favorisent le contact entre les cellules *via* l'augmentation de l'expression de connexine-43 (Aberg *et al.*, 2003). Ces données suggèrent que le prétraitement des CSM avec un cocktail de facteurs de croissance et de cytokines pourrait améliorer l'efficacité thérapeutique de la transplantation des CSM pour la réparation du myocarde (Hahn *et al.*, 2008). Les facteurs de croissance ne sont pas les seules molécules capables d'optimiser les effets thérapeutiques des CSM. Céline Mias et *al.* ont récemment montré que le prétraitement *ex vivo* des CSM avec une hormone

connue pour réduire les atteintes tissulaires, la mélatonine, augmentait significativement la survie des CSM après leur greffe dans le myocarde ischémique, favorisant ainsi leurs activités paracrine, vasculotrope et mitogénique (Mias *et al.*, 2008).

Le prétraitement pharmacologique des cellules souches représente une approche innovante et facilement réalisable afin d'optimiser considérablement l'effet thérapeutique de la greffe.

Nous venons de décrire trois aspects, visant à optimiser les effets thérapeutiques des CSM dans l'IDM : le pré-contionnement hypoxique, la manipulation génétique et le prétraitement pharmacologique. Cependant ces techniques ne permettent toujours pas, à ce jour, aux CSM de donner naissance à de nouveaux cardiomyocytes capables de régénérer un tissu cardiaque fonctionnel. Il apparait donc nécessaire de poursuivre la quête de cellules capables d'assurer une véritable régénération myocardique.

6. L'ingénierie cellulaire : La reprogrammation des cellules adultes.

6.1. Généralités.

Le 25 Août 2006, la parution dans le journal « *Cell »* des travaux d'une équipe de chercheurs de l'université de Kyoto révolutionne le monde scientifique. Takahashi et Yamanaka présentaient leur technique de reprogrammation de cellules adultes murines en cellules ayant des capacités de cellules souches embryonnaires (Takahashi and Yamanaka, 2006). La reprogrammation était obtenue par la transduction, dans des cellules adultes, de quatre gènes codant pour des facteurs de transcription, Oct4, sox2, klf4 et c-myc, choisis parmi 24 gènes jouant un rôle dans la pluripotence des cellules souches embryonnaires. Les cellules ainsi reprogrammées et dénommées *induced pluripotent stem cells* (*iPS cells*) étaient

obtenues sans utiliser d'embryons ni d'ovocytes, et donc réglementairement et éthiquement plus faciles à utiliser. Dès l'année suivante, l'équipe de Yamanaka (Takahashi *et al.*, 2007), ainsi que celle de James Thomson, aux États-Unis (Yu *et al.*, 2007), obtiennent des cellules pluripotentes induites par reprogrammation de cellules cutanées humaines. Des recherches de plus en plus nombreuses ont par la suite été consacrées à ces cellules pour en améliorer la qualité et pour explorer les possibilités qu'elles apportent à l'étude et au traitement de maladies humaines.

6.2. La reprogrammation directe.

Dans la vague de ces nouveaux résultats des équipes se sont penchées sur la reprogrammation directe d'une cellule somatique en une autre sans passer par le stade de cellule pluripotente induite. Ieda et ses collègues ont exprimé dans des cardio-fibroblastes murins, 14 gènes de régulation cardiaque, dont la plupart codent des facteurs de transcription. Après criblage, 3 facteurs de transcription, Mef2C, Gata-4 et Tbx5, se sont révélés nécessaires et suffisants pour induire la différenciation d'environ 20% des fibroblastes en cardiomyocytes (Ieda *et al.*, 2010). Si l'on suit le mouvement de cette théorie de reprogrammation des cellules adultes en un autre phénotype, il apparait alors possible d'envisager une reprogrammation directe des CSM en cardiomyocytes. De par leur caractère « souche », les CSM ne sont pas à un stade terminal de différenciation et possède une plasticité plus importante que des cellules somatiques. Suivant cette idée, des études ont proposé de co-transduire des CSM avec deux facteurs de transcriptions, Nkx2.5 et Gata-4, connus pour jouer un rôle déterminant au cours de la cardiogenèse (Arminan *et al.*, 2009; Yamada *et al.*, 2007). Les cellules obtenues expriment plusieurs marqueurs cardiogéniques, tels que la troponine I, les peptides natriurétiques, l'actine sarcomérique, cependant ces cellules ne possèdent pas toutes les caractéristiques fonctionnelles des cardiomyocytes.

Comme la reprogrammation des cellules somatiques en cellules pluripotentes induites, le criblage des gènes pouvant induire la différenciation des CSM en cardiomyocytes est primordiale, il convient donc de trouver le bon cocktail capable d'induire cette différenciation. En plus de cette manipulation génique, le microenvironnement apparait une fois de plus comme une condition nécessaire pour orienter la différenciation des CSM en cardiomyocytes.

L'optimisation de la thérapie cellulaire utilisant les CSM n'est pas dépendante d'un seul traitement ou d'une seule manipulation de ces cellules. Le bénéfice attendu semble être possible grâce à la combinaison de plusieurs conditions de pré-conditionnement des CSM avant leur implantation. Malgré toutes ces études prometteuses visant à optimiser la thérapie cellulaire, pour régénérer le myocarde, l'efficacité de cette thérapie ne donne toujours pas entière satisfaction pour les patients. La thérapie cellulaire rejoint ici l'ingénierie tissulaire. Il apparaît que, pour améliorer l'efficacité thérapeutique des greffes cellulaires, il convient d'élargir le paradigme de la thérapie cellulaire, en ne raisonnant plus uniquement en termes de cellules, mais en y incluant un support matriciel afin d'optimiser la rétention, la survie et finalement la fonctionnalité des CSM.

Partie 2 : L'ingénierie tissulaire de l'infarctus du myocarde.

1. Généralités.

Le concept d'ingénierie tissulaire peut se définir comme l'ensemble des techniques et des méthodes s'inspirant des principes de l'ingénierie et des sciences de la vie pour développer des substituts biologiques pouvant restaurer, maintenir ou améliorer les fonctions des tissus (Griffith and Naughton, 2002; Merceron *et al.*, 2010; Vinatier *et al.*, 2009). Cette approche associe une composante artificielle d'origine synthétique ou naturelle (élaborée à

partir d'un ou plusieurs biomatériaux) et une composante cellulaire ou tissulaire (Figure 5). La Sociéte Européenne des Biomatériaux (ESB) a défini lors de la conférence de Chester (UK) en 1991, un biomatériau comme « un matériau conçu pour interagir avec des systèmes biologiques, qu'il participe à la constitution d'un dispositif à visée diagnostique ou à celle d'un substitut de tissu ou d'organe ou encore à celle d'un dispositif de suppléance (ou d'assistance) fonctionnelle ». Les biomatériaux doivent diriger l'organisation, la croissance et la différenciation des cellules, en apportant un support physique. Dans le cas idéal, il doit se résorber au rythme de la réparation des tissus environnant la lésion. Parmi les biomatériaux en cours de développement les polymères et hydrogels occupent une place prépondérante en raison de leurs propriétés de biocompatibilité, d'injectabilité et de réticulation. Le domaine de l'ingénierie tissulaire peut être principalement découpé en deux champs d'investigations complémentaires. Le premier concerne le développement de matrices capables de répondre biologiquement et physiquement aux attentes de l'ingénierie du tissu cardiaque. Le deuxième champ d'investigation s'intéresse à l'étude physiologique de cellules, telles que des cardiomyocytes ou des cellules souches, cultivées en 3D dans ces matrices et les conditions de culture permettant de stimuler la cardiogénèse.

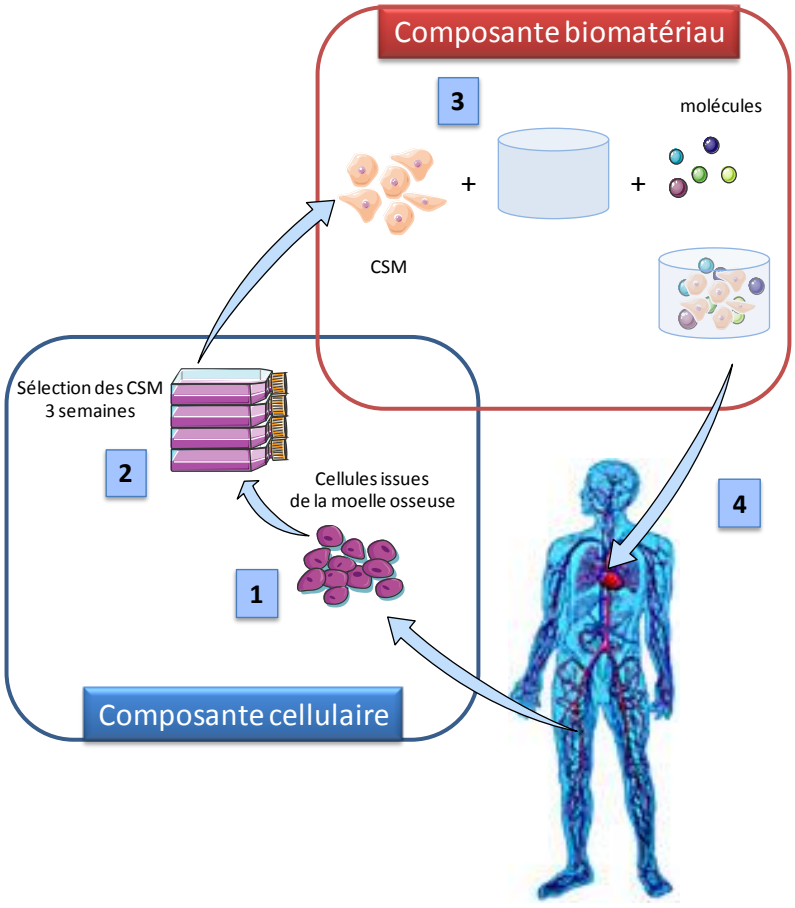

Figure 5: Principe de l'ingénierie tissulaire de l'infarctus du myocarde.

(1) La moelle osseuse est prélevée à partir du patient (autologue) ou d'un donneur (allogénique). (2) Culture, expansion et purification afin d'obtenir une population homogène de CSM. (3) Association des CSM à un biomatériau. Des molécules peuvent être associées seules ou avec des cellules dans le biomatériau. (4) Implantation du produit d'ingénierie tissulaire chez le patient.

2. Les biomatériaux dans le traitement de l'infarctus du myocarde.

Actuellement il existe trois sortes de biomatériaux pour le traitement de l'IDM (Figure 6) (Christman and Lee, 2006). La première stratégie utilisant des biomatériaux consiste à appliquer une matrice sur la surface du ventricule gauche afin de prévenir la dilatation associée à un IDM. La seconde vise à développer *in vitro* des substituts tissulaires puis de les implanter *in vivo,* tels que les patchs épicardiques (Tableau 6) La troisième approche est d'injecter un biomatériau seul, avec des cellules ou des molécules pharmacologiques, afin de régénérer *in situ* un tissu cardiaque.

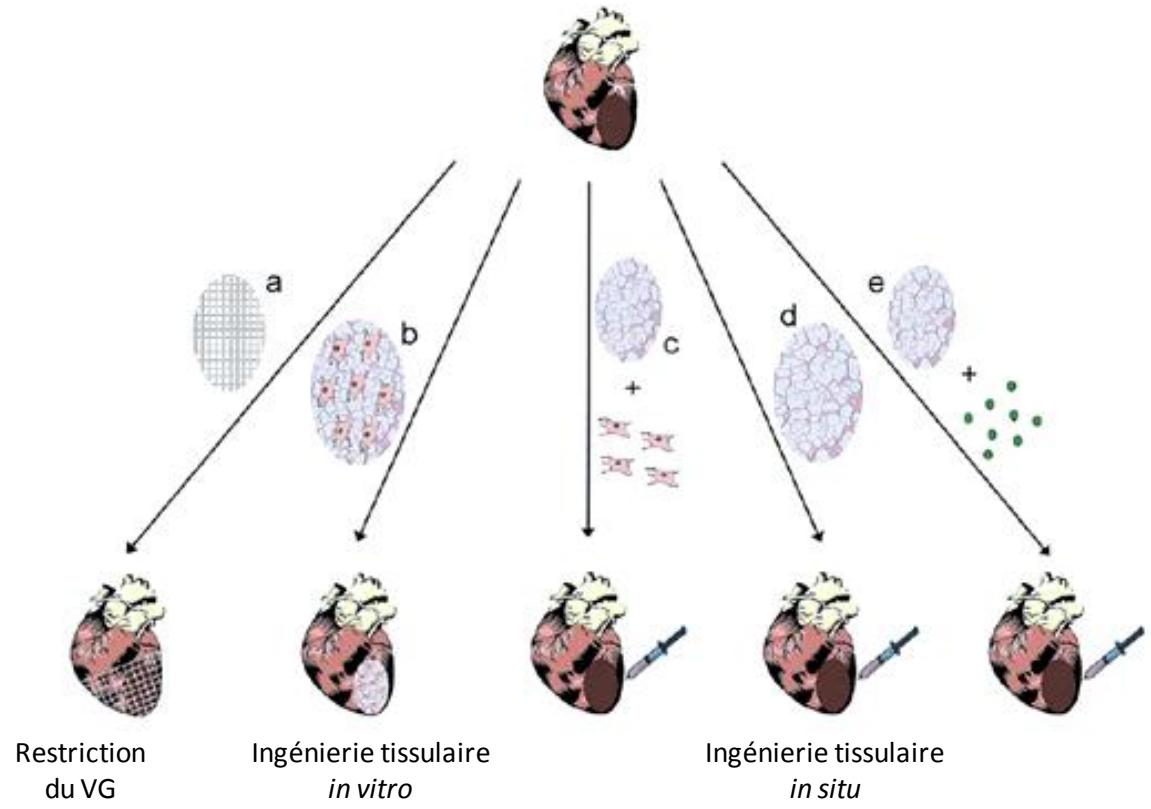

Figure 6: Stratégies pour le traitement de l'IDM utilisant des biomatériaux.

(a) Application de matrice pour restreindre et préserver la géométrie du ventricule gauche (VG). (b) L'ingénierie tissulaire *in vitro* consiste à cultiver des cellules sur ou dans des matrices puis de les appliquer par la suite sur la surface de l'épicarde (patch épicardique). (c) et (d) et (e) constituent l'ingénierie tissulaire *in situ*. Elle consiste à injecter un biomatériau avec des cellules (c), seul (d), ou avec des molécules thérapeutiques (e) (cytokines, facteurs de croissances, gènes). *D'après (Christman and Lee, 2006)*

	Materiaux	Transplantation	Références
Restriction du VG	Polypropyléne	Seul	(Kelley *et al.*, 1999; Ruvinov *et al.*, 2010) (Enomoto *et al.*, 2005; Zhang *et al.*, 2010b) (Gorman *et al.*, 2011; Zhang et al., 2010b)
	Polyester	Seul	(Chaudhry *et al.*, 2000) (Olsson *et al.*, 2005)
Ingénierie tissulaire ***in vitro***	Gélatine	Seul ou avec des cardiomyocytes fœtaux	(Leor *et al.*, 2000)
	Alginate	Cardiomyocytes fœtaux	(Kellar *et al.*, 2005)
	Poly(glycolide)/(poly(lactide)	Fibroblastes de la peau	(Zimmermann *et al.*, 2002a)
	collagène type I, matrigel	Cardiomyocytes néonataux	(Zimmermann and Eschenhagen, 2003) (Zimmermann *et al.*, 2006)
	PTFE, PLA, collagène type I, matrigel	Seul ou avec des cellules progénitrices de la moelle osseuse	(Krupnick *et al.*, 2002)
	Collagène type I	Seul ou avec des CSE	(Kofidis *et al.*, 2005)
	PNIPAAM	Feuillets cellulaires de cardiomyocytes néonataux ou ADSC	(Shimizu *et al.*, 2002) (Miyahara *et al.*, 2006)

Tableau 6: Biomatériaux utilisés pour le traitement de l'IDM : restriction du ventricule gauche (VG) et ingénierie tissulaire *in vitro*.

PLA : poly(L-lactic) acide; PNIPAAM: poly(N-isopropylacrylamide); PTFE: poly(tetrafluoroethylène) ; CSE : cellule souche embryonaire ; ADSC : adipose derived stem cell.

Aujourd'hui la médecine s'oriente vers des procédures chirurgicales moins invasives pour diminuer le temps d'hospitalisation et favoriser un retour rapide des patients à une activité normale. Dans cette optique, l'ingénierie tissulaire cherche à développer des matériaux injectables, c'est-à dire capables de passer par l'aiguille d'une seringue, d'un cathéter ou par des dispositifs d'angioplasties (Leor *et al.*, 2009). Dans ce contexte, les hydrogels représentent des matériaux attractifs en ingénierie tissulaire. Les hydrogels forment un réseau de chaînes de polymères hautement hydratées pouvant avoir une élasticité similaire au tissu naturel (Baroli, 2007). Une solution visqueuse réalisée à partir d'un polymère hydrophile peut contenir des cellules ainsi que des principes actifs (facteurs de croissances,

cytokines, ADN). Une fois injectée, cette solution aura la capacité de durcir *in situ* sous l'influence de différents facteurs (physique, chimique, ionique) pour former un réseau tridimensionnel encapsulant cellules et principes actifs (Bourges *et al.*, 2002a; Yan and Pochan, 2010) (Figure 7).

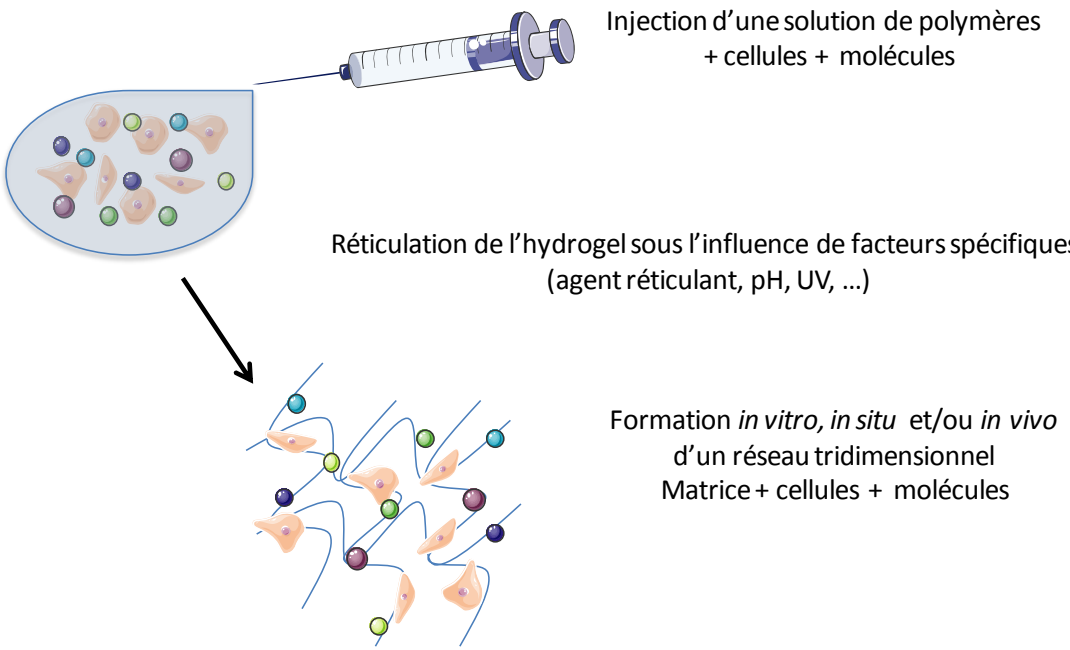

Figure 7: Principe de formation des hydrogels in vitro, in situ et/ou in vivo associés à des cellules et diverses molécules.

3. Les hydrogels en ingénierie tissulaire cardiaque.

3.1. Les critères requis pour les hydrogels.

De nombreux matériaux injectables ont déjà été explorés en ingénierie tissulaire cardiaque, cependant il est important de définir des critères, indispensables à la formation et l'utilisation d'un hydrogel injectable idéal. Une des fonctions que l'on attribue de façon intuitive aux hydrogels est celle de vecteur et de support des cellules au niveau du tissu à remplacer. L'objectif est de recréer artificiellement un microenvironnement présent *in vivo*.

Un hydrogel idéal en ingénierie tissulaire cardiaque doit mimer le tissu cardiaque natif de façon structurale, mécanique et bio-fonctionnelle et être techniquement applicable (Jawad *et al.*, 2007).

L'hydrogel doit fournir un environnement poreux tridimensionnel, biocompatible, permettant de retenir les cellules dans la matrice (Yu *et al.*, 2009). Les pores doivent être interconnectés avec un diamètre supérieur à 10 µm afin de permettre l'infiltration cellulaire et vasculaire ainsi que la diffusion des nutriments (Lutolf and Hubbell, 2005). L'environnement fourni par l'hydrogel doit favoriser la prolifération et la différenciation cellulaire (Leor *et al.*, 2005). Pour cela, des molécules bioactives (facteurs de croissance, cytokines…) peuvent être additionnées à la matrice (Kretlow *et al.*, 2007). L'hydrogel doit également adhérer au tissu environnant et posséder une résistance mécanique. Il doit supporter la fonction du tissu endommagé et ce durant toute la durée de la nouvelle croissance tissulaire. L'hydrogel doit être capable de se dégrader dans le temps pour être peu à peu remplacé par le tissu néoformé. Un des critères importants pour une utilisation de l'hydrogel en médecine est sa capacité à être stérilisé afin d'éviter des sources de contaminations par des agents pathogènes et cela sans subir de modification de ses propriétés physiques, chimiques et biologiques. Pour finir, il doit être injectable de préférence par chirurgie mini-invasive. Les progrès de la technologie des cathéters permettent aujourd'hui d'accéder au tissu cardiaque par des voies percutanées, intracoronaires et transendocardiales éliminant la nécessité d'une intervention chirurgicale invasive, telle que la sternotomie (Janssens, 2010; Perin *et al.*, 2003; Zhang *et al.*, 2010a). L'hydrogel doit avoir des propriétés de cinétique de gélification adaptées. Il doit être suffisamment liquide au moment de l'injection pour pouvoir diffuser dans le cathéter tout en permettant la formation d'un gel solide au sein du myocarde.

3.2. Les hydrogels synthétiques *versus* naturels.

3.2.1. Les hydrogels synthétiques.

Les matériaux synthétiques pour l'ingénierie tissulaire ont l'avantage d'être modulables, permettant la conception d'hydrogels avec une porosité adaptée, une stabilité mécanique et des propriétés de dégradation (Lutolf and Hubbell, 2005). Récemment des dérivés de poly (N-isopropyl) (PNIPAAM) et de poly (éthylène glycol) (PEG) ont été synthétisés et adaptés pour être injectables (Tableau 7) L'hydrogel de PNIPAAM a pour avantage d'être thermosensible. Alors qu'il est liquide à température ambiante, sa réticulation est déclenchée aux alentours de 32°C (Liu *et al.*, 2004). Des dérivés de PNIPAAM ont la capacité d'être biodégradables (Li et al., 2010b; Wang et al., 2009d), d'autres ont montré qu'ils pouvaient préserver ou améliorer la fonction cardiaque dans des modèles d'IDM chez de petits animaux (Fujimoto *et al.*, 2009). Les PEG sont des matériaux bio-inertes et non dégradables capables d'augmenter l'épaisseur de la paroi du ventricule gauche (VG) après un IDM (Dobner *et al.*, 2009). Wang *et al.* ont montré que l'injection de CSM avec un hydrogel d'alpha-cyclodextrin/MPEG-PCL-MPEG améliore les effets de la transplantation des cellules dans un modèle d'IDM chez le lapin. Cependant une étude récemment publiée, montre que l'injection de PEG directement dans le myocarde en post-infarctus n'est pas suffisante pour empêcher la progression des effets délétères à long terme liés à l'ischémie (Rane *et al.*, 2011). Ainsi alors que les biomatériaux synthétiques offrent l'avantage d'être modulables, ils ne sont pas bioactifs et de ce fait ne permettent pas l'adhésion cellulaire, la prolifération et la croissance des cellules, qui peuvent jouer des rôles clés dans la régénération cardiaque.

Hydrogels	Abréviations	Caractéristiques	Modèles	Transplantation	Références
dextran- poly(E-caprolactone)-2-hydroxylethyl methacrylate/poly (N-isopropylacrylamide)	Dex-PCL-HEMA/PNIPAAm	Thermosensible Gelation rapide *in situ*	IDM lapin	Seul BMMNC	(Li *et al.*, 2010b; Wang *et al.*, 2009d)
copolymerisation NIPAAm avec acide acrylic et hydroxylethyl methracrylate-poly(trimethylene carbonate)	poly(NIPAAm-co-Aac-co-HEMAPTMC	Thermosensible, Biodégradable	IDM rat	Seul	(Fujimoto *et al.*, 2009)
assemblage entre alpha-cyclodextrin et methoxy polyethylene glycol-poly (caprolactone)-(dodecanedioic acid)-poly (caprolactone)-methoxypolyethylene glycol	MPM/alpha-CD	Biocompatible Biodégradable	IDM lapin	Seul	(Wang *et al.*, 2009a)
polyethylene glycol	PEG	Non-dégradable Biocompatible	IDM rat	Seul	(Dobner *et al.*, 2009)
alpha-cyclodextrin/poly(ethylene glycol)-b-polycaprolactone-(dodecanedioic acid)-polycaprolactone-poly(ethylene glycol)	α-cyclodextrin/MPEG-PCL-MPEG	Biocompatible Gelation rapide in situ	IDM lapin	Seul CSM	(Jiang *et al.*, 2009; Wang et al., 2009c)
poly(N-isopropylacrylamide-co-propylacrylic acid-co-butyl acrylate	p[NIPAAm-co-PAA-co-BA]	pH- et temperature-sensible	IDM rat	b FGF	(Garbern *et al.*, 2010)

Tableau 7: Hydrogels synthétiques en ingénierie tissulaire cardiaque.

BMMNC : *bone marrow-derived mononuclear cell* ; b FGF : *basic fibroblast growth factor* ; CSM : cellule souche mésenchymateuse; IDM: infarctus du myocarde.

3.2.2. Les hydrogels naturels.

Les polymères naturels utilisés pour l'ingénierie tissulaire cardiaque incluent principalement deux catégories de molécule : les protéines, telles que le collagène et la fibrine ainsi que les polysaccharides comme l'alginate et le chitosane (Tableau 8).

3.2.2.1. Les hydrogels naturels à base de protéines et de polypeptides.

Le collagène et la fibrine ont été les premiers matériaux naturels à être explorés dans le domaine de l'ingénierie tissulaire cardiaque.

3.2.2.1.1. Le collagène.

Le collagène est une glycoprotéine fibrillaire présente dans la plupart des tissus humains, elle est le principal composant de la matrice extracellulaire. La porosité des gels de collagène est un paramètre très favorable à la prolifération cellulaire et à la synthèse des protéoglycanes de la MEC (Schussler *et al.*, 2010). Le collagène injecté, seul dans le myocarde en post-infarctus (Dai et al., 2005), avec des cellules souches ou des cardiomyocytes (Cortes-Morichetti *et al.*, 2007; Kutschka *et al.*, 2006), limite le remodelage du ventricule. Cependant, le collagène est un dérivé protéique d'origine animal qui peut provoquer des réactions immunologiques et être rapidement dégradé une fois implanté *in vivo* (Lee *et al.*, 2001). La matrice perd alors rapidement ses fonctions de soutien mécanique. La combinaison des collagènes avec des matrices à base d'élastine ou de glycosaminoglycanes permet de ralentir sa dégradation (Deng *et al.*, 2010).

3.2.2.1.2. La fibrine.

La fibrine est une protéine présente dans le sang au moment de la coagulation sous l'action de la thrombine (Naito *et al.*, 2000; Thompson *et al.*, 1992). Il s'agit d'une protéine impliquée dans la cicatrisation et la réparation tissulaire (Sierra, 1993). La fibrine est préparée à partir du plasma du patient et peut être disponible sous la forme de gel (colle de fibrine) ou de microparticules. La colle de fibrine, non-toxique et non-immunogène est biodégradable, ne requérant aucun agent stabilisant. Ces caractéristiques permettent l'utilisation de cette protéine sous sa forme native pour la réalisation de matrices et la culture de cellules en 3 dimensions (Christman *et al.*, 2004a). La colle de fibrine augmente la survie de greffe de cellules, diminue la taille de l'infarctus, et augmente le flux sanguin vers le myocarde ischémique (Christman *et al.*, 2004b). Cependant, l'utilisation de fibrine comme unique composé pour la réalisation de matrices est délicate. En effet la matrice est rapidement dégradée par les mécanismes de fibrinolyse une fois introduite dans le tissu cardiaque.

3.2.2.1.3. L'auto-assemblage de peptides.

Certains peptides sont capables de s'auto-assembler en hydrogels stables à basse concentration de peptides (0.1% à 1%) dans des conditions osmotiques et de pH physiologiques. L'injection puis l'auto-assemblage des peptides RAD16-II seuls dans le myocarde sain favorise le recrutement des cellules endothéliales, ainsi que la différenciation des cellules souches embryonnaires (CSE) en cardiomyocytes (Davis *et al.*, 2005). Dans le myocarde ischémique, les peptides assemblés ou nanofibres doivent être combinés avec des facteurs de croissance pour induire un effet bénéfique. L'ajout de l'IGF-1 aux nanofibres, permet de créer un microenvironnement protecteur pour les cellules transplantées (Davis *et al.*, 2006; Padin-Iruegas et al., 2009). L'injection de nanofibres associées avec le facteur de croissance plaquettaire (PDGF) permet d'améliorer la fraction de raccourcissement du ventricule gauche, alors que l'injection du PDGF seul n'a pas d'effet (Hsieh *et al.*, 2006a; Hsieh *et al.*, 2006b). Enfin ces nanofibres favorisent également le recrutement des cellules souches cardiaques endogènes, lorsqu'elles sont associées au SDF-1 (Segers *et al.*, 2007). Cependant, l'injection de nanofibres avec des myoblastes en présence ou en absence de PDGF n'a aucun effet sur la survie des myoblastes ainsi que la fonction cardiaque (Dubois *et al.*, 2008).

3.2.2.2. Les hydrogels naturels à base de polysaccharides.

L'alginate et le chitosane sont deux polymères qui forment des gels physiques par interaction ionique. Cette méthode de préparation d'hydrogels physiques est extrêmement douce et simple, la formation d'hydrogels chimiques nécessitant l'utilisation d'agents de réticulation souvent toxiques ou de longues étapes de purification.

3.2.2.2.1. Le chitosane.

Le chitosane est un amino-polysaccharide cationique biodégradable dérivé de la chitine avec de nombreuses applications en ingénierie tissulaire (Khor and Lim, 2003). Il possède une surface hydrophile qui permet l'adhésion, la prolifération et la différenciation cellulaire. Il est également doté d'une activité antimicrobienne et d'un faible pouvoir antigénique. Il est thermosensible et réticule *in situ* après son injection dans le myocarde (Lu *et al.*, 2009). Plusieurs études montrent que le chitosane augmente la rétention des cellules greffées dans le myocarde en post-infarctus, favorise la néovascularisation et finalement améliore la fonction cardiaque (Wang *et al.*, 2010). Cependant ces propriétés dépendent fortement du pH, le rendant soluble particulièrement dans des milieux acides.

3.2.2.2.2. Les alginates.

Les alginates commerciaux proviennent de trois souches d'algues brunes différentes (Laminaria hyperbora, Ascophyllum nodosum et Macrocystis pyrifera) (d'Ayala *et al.*, 2008). Les alginates forment des gels en présence de cation divalents. Il s'agit d'une gélification ionotropique. Dans les hydrogels d'alginate de calcium, la formation du gel est due à la chélation de l'ion calcium dans les cavités éléctronégatives formées par les groupements carboxylates des résidus guluronates. Cette propriété unique de gélification permet à ces hydrogels de réticuler *in situ* en chélatant le calcium endogène du myocarde. L'injection d'alginate dans des modèles d'IDM aigu et chronique chez le rat améliore significativement la fonction cardiaque et limite le remodelage ventriculaire. Les alginates permettent de véhiculer et de libérer des facteurs de croissance, tel que le VEGF et le PDFG (Hao *et al.*, 2007) et l'HGF (Ruvinov *et al.*, 2010), mais également des cellules et notamment des CSM (Trouche *et al.*, 2010). Ils peuvent également être modifiés par l'attachement de séquences arginine-glycine-asparagine (RGD) (Shachar *et al.*, 2011; Tsur-Gang *et al.*, 2009). Récemment, l'équipe de Leor en Israël a montré dans un modèle porcin d'IDM reperfusé, que l'hydrogel

d'alginate pouvait être injecté par la voie intracoronaire et avoir un effet bénéfique sur la fonction cardiaque (Leor *et al.*, 2009). Cependant l'alginate possède un faible pouvoir d'adhérence et d'infiltration pour les cellules.

3.2.2.2.3. Le dextrane et le pullulane.

D'autres polymères, tels que le dextrane et le pullulane, sont utilisés pour former des matrices poreuses polysaccharidiques (Cadee *et al.*, 2000). Ces hydrogels chimiques sont obtenus par polymérisation radicalaire. La porosité élevée de ces hydrogels permet la diffusion de l'oxygène, des nutriments et des cellules. Ces hydrogels ont été utilisés pour véhiculer les CSM en phase aigüe d'IDM chez le rat (Le Visage et al., 2011). L'injection des CSM avec cet hydrogel polysaccharidique augmente la rétention et la survie des cellules dans le myocarde par rapport à une injection classique des cellules dans l'endocarde. La prise de greffe des CSM est favorisée par la dégradation complète de l'hydrogel un mois après l'injection. Les phosphatases acides et les lysozymes sont plus actifs en phase aigüe d'IDM et peuvent contribuer à la dégradation *in vivo* de la matrice (Chavan *et al.*, 2007).

3.2.2.2.4. L'acide hyaluronique.

L'acide hyaluronique est un glycosaminoglycane, constitué de la répétition d'un disaccharide composé d'un acide D-glucuronique et d'une D-glucosamine N-acétylée. L'acide hyaluronique est un composant majeur de la MEC, qui possède un rôle fonctionnel important pendant la morphogenèse embryonnaire, la régénération cellulaire et la cicatrisation (Itano, 2008; Toole, 2001). L'acide hyaluronique est un polysaccharide hautement hydrophile qui possède une viscosité élevée. Récemment, un hydrogel composé de deux macromères d'acide hyaluronique methacrylés (MeHA) a été synthétisé, puis injecté dans un myocarde ovin en post-infarctus (Ifkovits *et al.*, 2010). Cet hydrogel atténue le remodelage ventriculaire qui suit l'infarctus en augmentant l'épaisseur de la paroi ventriculaire et en limitant

l'extension de la zone cicatricielle. De même, Yoon et son équipe ont montré dans un modèle d'IDM chez le rat que l'hydrogel d'acide hyaluronique atténuait la formation de tissu fibreux dans la cicatrice et finalement améliorait la fonction cardiaque (Yoon et al., 2009).

4. L'utilisation des hydrogels en ingénierie tissulaire cardiaque.

4.1. L'injection d'hydrogel seul.

Le remodelage ventriculaire gauche définit l'ensemble des modifications géométriques et structurales que subit le ventricule gauche (VG) après un IDM. Il associe schématiquement une expansion de la zone infarcie avec un amincissement pariétal, une dilatation et une modification en forme de sphère du ventricule gauche, ces modifications induisant à terme une réduction des performances cardiaques. Les hydrogels seuls ont la capacité de fournir naturellement un soutien mécanique au myocarde infarci et d'atténuer le remodelage ventriculaire. Injectés dans le myocarde en phase aigüe d'infarctus, ils augmentent l'épaisseur de la paroi ventriculaire et limitent l'extension de la cicatrice. Ils diminuent les contraintes pariétales (Loi de Laplace) exercées sur la paroi ventriculaire et de ce fait, limite la dilatation des zones saines, bordant la zone ischémique. Les hydrogels naturels, tels que le collagène, les colles de fibrine et les alginates, possèdent de part leur composition une activité biologique intrinsèque. Ils peuvent favoriser le recrutement des cellules endogènes sur le site lésé, moduler le microenvironnement inflammatoire et stimuler la néovascularisation. Les hydrogels bio-inertes, tels que les hydrogels à base de PEG, utilisés seuls ne semblent pas être suffisants pour atténuer à long terme le remodelage ventriculaire (Rane et al., 2011). Cette donnée suggère que les hydrogels dépourvus d'activité biologique ont un effet protecteur transitoire sur le myocarde et qu'une composante cellulaire et/ou moléculaire semble nécessaire pour assurer un effet sur le long terme.

	Hydrogel	Caractéristiques	Inconvénients	Modèles	Transplantation	Références
Protéines ou polypeptides	Collagène	Composant principal de la MEC Porosité élevée	Immunogène Rapidement dégradé *in vivo*	IDM rat	Cardiomyocytes HUCBC	(Cortes-Morichetti *et al.*, 2007; Dai *et al.*, 2005; Kutschka *et al.*, 2006)
	Colle de fibrine	Non-toxique Non-immunogène biodégradables	Rapidement dégradée (fibrinolyse)	IDM rat	Seule Myoblastes ADSC	(Christman *et al.*, 2004a; Christman *et al.*, 2004b; Zhang *et al.*, 2010b)
	Auto-assemblage de peptides	Protection des cellules transplantées Recrutements des cellules endogènes	Dépend des facteurs de croissance	IDM rat	IGF-1 PDGF SDF-1	(Davis *et al.*, 2006; Hsieh *et al.*, 2006b; Padin-Iruegas *et al.*, 2009; Roncalli *et al.*, 2010; Segers *et al.*, 2007)
Polysaccharides	Chitosane	Thermosensible Activité antimicrobienne Peu immunogène Adhésion, prolifération et différenciation des cellules	Soluble Dépend des variations de pH	IDM rat	CSE bFGF	(Lu *et al.*, 2009; Wang *et al.*, 2010)
	Alginate	Gélification ionotropique	Peu adhérent pour les cellules	IDM rat IDM porc	Seul VEGF, PDGF, HGF CSM RGD	(Hao *et al.*, 2007; Leor *et al.*, 2009; Ruvinov et al., 2010; Shachar *et al.*, 2011; Trouche *et al.*, 2010; Tsur-Gang *et al.*, 2009)
	Dextrane et Pullulane	Porosité élevée Dégradable par les enzymes endogènes Hémocompatible	Peut diffuser dans la circulation systémique	IDM rat	CSM	(Le Visage *et al.*, 2011)
	Acide hyaluronique	Régénération cellulaire cicatrisation	Rapide résorption après implantation	IDM rat mouton	Seul	(Yoon *et al.*, 2009) (Ifkovits *et al.*, 2010)

Tableau 8: Hydrogels naturels en ingénierie tissulaire cardiaque.

ADSC : *adipose-derived stem cell* ; b FGF : *basic fibroblast growth factor* ; CSM : cellule souche mésenchymateuse ; CSE: cellule souche embryonnaire; IDM : infarctus du myocrade ; IGF-1: *insulin growth factor-1*; HGF: *Hepatocyte growth factor*; HUCBC : *human umbilical cord blood cell*; MEC : matrice extracellulaire ; PDGF : *Platelet-derived growth factor*; RGD: arginine-glycine-asparagine peptide ; SDF-1: *stromal-derived factor-1*; VEGF : *vascular endothelium growth factor.*

4.2. L'injection d'hydrogel avec des cellules souches mésenchymateuses.

L'un des avantages des hydrogels injectables est qu'ils peuvent véhiculer des cellules dans le myocarde sous leur forme liquide, puis polymériser *in situ*, et ainsi retenir les cellules sur le site d'injection (Ye *et al.*, 2011). Dans le tissu cardiaque natif, la MEC contient des protéines, telles que les collagènes, mais également des polysaccharides et de l'eau (Spinale, 2007). La composition privilégiée des hydrogels permet d'imiter la MEC native (Vunjak-Novakovic *et al.*, 2010). Ils apportent un support tridimensionnel sur lequel les cellules peuvent adhérer, recréant un microenvironnement semblable à « une niche », nécessaire au maintien des mécanismes intrinsèques des cellules souches (Morrison and Spradling, 2008). En plus d'augmenter la rétention des cellules sur le site d'injection, les hydrogels protègent les cellules greffées en leur apportant un support physique, le temps qu'elles secrètent, à leur tour, leur propre MEC pour s'intégrer au tissu cardiaque.

L'injection d'hydrogels avec des CSM dans des modèles animaux d'IDM a fait l'objet de quelques études ces trois dernières années (Tableau 9) Ces études mettent en évidence le bénéfice de l'utilisation des hydrogels comme véhicule des CSM dans le myocarde. Les hydrogels protègent les CSM pendant l'injection et favorisent la prise de greffe des cellules dans le tissu cardiaque. En augmentant la rétention et la survie des CSM dans le myocarde ischémique, les hydrogels optimisent les effets des CSM pour la réparation cardiaque après un IDM.

Equipe, année	Cellules	Hydrogels	Modèles	Injection	Effets	Références
Wang T., 2009	BM-MSC	alpha-cyclodextrin/MPEG-PCL-MPEG	IDM lapin	Intramyocardique	Augmentation rétention et survie des cellules, FC.	(Wang *et al.*, 2009c)
Zhang X., 2010	ADSC	Colle de fibrine	IDM rat	Intramyocardique	Augmentation FC, densité des capillaires.	(Flynn and O'Brien, 2011; Zhang et al., 2010b)
Yu, 2010	hMSC	Microsphères d'alginate modifiées avec des séquences RGD	IDM aigu rat	Intramyocardique	Augmentation survie des cellules, angiogenèse. Diminution taille de l'IDM.	(Yu *et al.*, 2010)
LeVisage, 2011	MSC	Polysaccharide poreux : mélange de pullulane et de dextrane	IDM rat	Intramyocardique	Augmentation survie et rétention des cellules. Diminution des la fibrose	(Le Visage et al., 2011)

Tableau 9: Co-injection d'hydrogels et de cellules souches mésenchymateuses dans le myocarde en post-infarctus.

BM-MSC: *bone morrow-derived mesenchymal stem cell*; ADSC: *adipose-derived stem cell*; hMSC: *human mesenchymal stem cell.*

4.3. L'injection d'hydrogel avec des molécules actives.

Il est admis que les effets bénéfiques des CSM sont majoritairement dus à leurs effets paracrines. La sécrétion de nombreux facteurs de croissance et cytokines contribuent à la réparation du myocarde en post-infarctus. Ces données suggèrent, que l'utilisation de ces facteurs de croissance et cytokines avec des hydrogels pourrait, d'une part mimer les effets des CSM en s'affranchissant de celles-ci, et d'autre part potentialiser la bio-activité des hydrogels. Des études ont ciblé des facteurs de croissance précis afin de stimuler l'angiogenèse, le recrutement ou « homing » des cellules progénitrices et des cellules souches cardiaques endogènes, la croissance des cellules ainsi que leur différenciation (Tableau 10).

Equipe, année	Molécules actives	Hydrogels	Modèles	Injection	Effets	Références
Lopez JJ, 1997	bFGF	Microsphères d'alginate hépariné	IDM chronique porc	Périvasculaire	Stimule l'angiogenèse.	(Lopez *et al.*, 1997)
Laham RJ, 1999	bFGF	Microsphères d'alginate hépariné	Essai clinique phase I, randomisé en double aveugle	Périvasculaire	Sureté et faisabilité Améliore la FC.	(Flynn and O'Brien, 2011; Laham *et al.*, 1999)
Iwakura A., 2003	bFGF	Gélatine	IDM rat	Intra myocardiaque	Angiogenèse Augmente la FC.	(Iwakura *et al.*, 2003)
Sakakibara Y., 2003	bFGF	Microsphères de gélatine	IDM rat et porc	Intra myocardique	Maintien le bFGF dans le myocarde. Augmente la FC et atténue le remodelage ventriculaire.	(Sakakibara *et al.*, 2003)
Liu Y., 2003	bFGF	Gélatine	IDM chien	Intra myocardique	Augmentation de la densité des microvaisseaux. Amélioration de la FC.	(Liu *et al.*, 2004)
Shao ZG, 2006	bFGF	Gélatine	IDM rat	Intra myocardique	Stimule l'arteriogenèse. Augmente FC et atténue remodelage.	(Shao *et al.*, 2006)
Hao X., 2007	VEGF, PDGF	Alginate	IDM rat	Intra myocardique	Livraison des facteurs dans le myocarde. Maturation des vaisseaux.	(Hao et al., 2007)
Christman KL., 2005	Pleiotrophin	Colle de fibrine	IDM rat	Intra myocardique	Néovascularisation	(Christman *et al.*, 2005)
Zhang G., 2007	SDF-1	PEG/fibrine patch	IDM aigu souris	Patch déposé sur la surface de la zone ischémique	Recrutement des cellules c-kit+ vers la zone ischémique	(Zhang *et al.*, 2007a)
Wang T., 2009	EPO	alpha-cyclodextrin/MPEG-PCL-MPEG	IDM aigu souris	Intra myocardique	Diminue l'apoptose des cellules. Néovascularisation Augmentaion FC, diminution taille de l'infarctus	(Wang *et al.*, 2009b)

Tableau 10: Co-injection d'hydrogels et de molécules actives dans l'infarctus du myocarde.

EPO : erythropoiétine ; FC : fonction cardiaque.

La Figure 8 résume les applications des hydrogels en ingénierie tissulaire cardiaque.

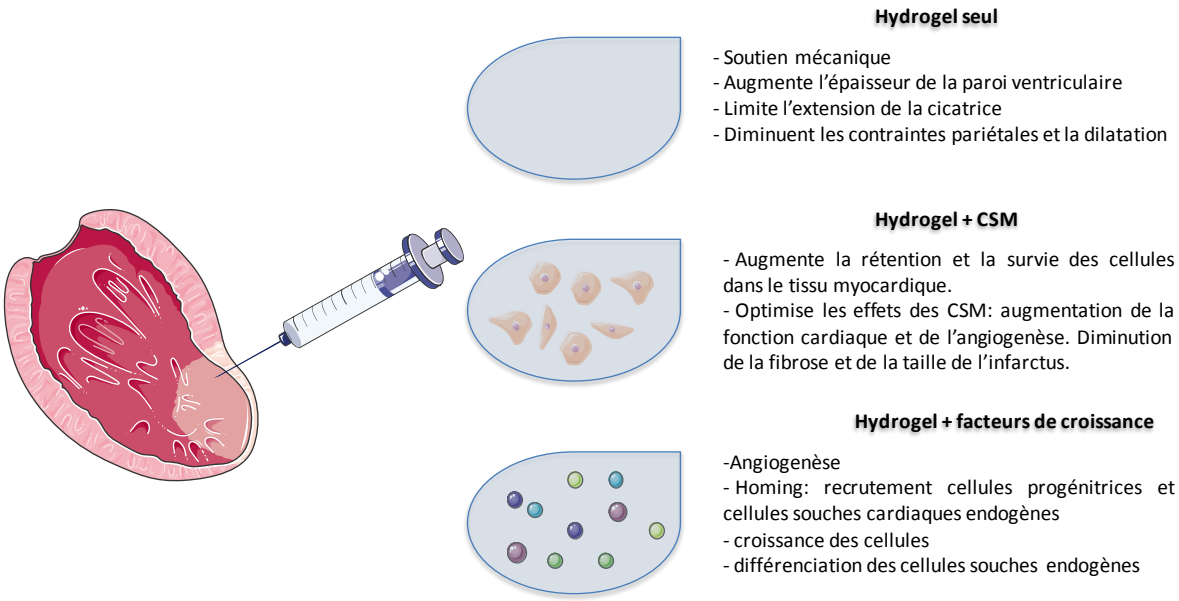

Figure 8: Utilisation des hydrogels en ingénierie tissulaire cardiaque.

5. L'utilisation des hydrogels pour la culture cellulaire en trois dimensions.

5.1. L'utilisation des hydrogels pour la culture des cardiomyocytes en trois dimensions.

Dans le passé, le modèle d'étude *in vitro* des cellules était la culture en monocouche. Bien que ce modèle en deux dimensions (2D) ait longtemps contribué à la compréhension des mécanismes cellulaires, il présente certaines limites intrinsèques qui ont entrainées le développement des matrices tridimensionnelles (3D) (Curtis and Russell, 2009). Ces matrices 3D offrent la possibilité d'imiter *in vitro* le microenvironnement cardiaque et ainsi de mieux appréhender l'étude et le comportement physiologiques des cardiomyocytes. Bursac et *al.* ont montré notamment que les propriétés électrophysiologiques de cardiomyocytes cultivés en 3D sont plus proches de celles du tissu cardiaque (Bursac *et al.*, 1999). Les matrices tridimensionnelles favorisent le contact entre les cardiomyocytes, le couplage

électromécanique et l'activité contractile (Eschenhagen *et al.*, 1997). La formation de tissus cardiaques artificiels, composés de matrice et de cardiomyocytes, présente des activités contractiles continues et synchronisées, possédant des propriétés mécaniques et biologiques proches de celles du tissu cardiaque natif (Kofidis *et al.*, 2002). Enfin, ces modèles de culture 3D permettent de tester et d'évaluer les effets physiologiques de différentes substances et drogues pouvant être administrées dans le cas de maladies cardiaques (Bartholoma *et al.*, 2005).

Ces modèles apparaissent aujourd'hui comme de véritables outils d'études physiologiques et pharmacologiques indispensables à l'optimisation des futures thérapeutiques cardiaques.

5.2. Les matrices tridimensionnelles pour la différenciation des cellules souches mésenchymateuses.

Un des nouveaux concepts de la biologie cellulaire est que les cellules souches peuvent commencer à se différencier lorsqu'elles sont exposées à des propriétés intrinsèques de la MEC, telles que sa structure, sa composition et son élasticité. Ces paramètres sont déjà bien connus pour moduler les forces physiques et mécaniques exercées sur la matrice d'une cellule. Les voies de signalisation mécano-sensibles convertissent ces forces en signaux biochimiques qui engagent la cellule dans une lignée spécifique. Tout comme les mécanismes d'action des facteurs de croissance, les paramètres de la MEC sont extrêmement dynamiques et sont spatialement et temporellement contrôlés pendant le développement, ce qui suggère qu'ils jouent un rôle morphogénique dans l'orientation de la différenciation des cellules. Classiquement des cocktails de différents facteurs de croissance sont utilisés pour induire la différenciation des cellules souches, mais ce phénomène est devenu de plus en plus lié à l'application de forces mécaniques et physiques sur les cellules (Engler *et al.*, 2006). Il a récemment été montré que la différenciation des CSM était régulée en partie par la rigidité des

tissus (Tse and Engler, 2011). Les CSM se heurtent souvent à des gradients de rigidité dans les tissus pathologiques et notamment dans le cas de l'IDM. Dans un tissu myocardique sain le gradient de rigidité est d'environ 1 kPa/mm, alors que dans le tissu ischémique il est d'environ 10 kPa/mm. Des CSM cultivées pendant 21 jours sur un hydrogel contenant un gradient de rigidité physiologique de 1 kPa/mm migrent dans l'hydrogel en suivant ce gradient de rigidité (durotaxis) plutôt que de rester immobiles. L'évaluation des marqueurs de différenciation, indique que les CSM migrent, puis se différencient en un phénotype contractile myogénique. Ces données indiquent que les gradients de rigidité et pas seulement la rigidité en elle-même peuvent être des régulateurs important du comportement des CSM.

Les matrices tridimensionnelles sont un outil indispensable à la compréhension des mécanismes cellulaires. A l'avenir ces matrices vont permettre de mieux appréhender la complexité et le dynamisme des « niches » ainsi que la différenciation des cellules souches en cardiomyocytes afin de régénérer un tissu contractile fonctionnel.

<u>Partie 3</u> : Objectif de la thèse.

Même si les CSM ont un effet bénéfique sur le myocarde en post-infarctus, elles n'ont pas la capacité, à elles seules, de le régénérer. La compréhension des mécanismes de réparation endogène du myocarde a permis de mieux appréhender la complexité de ce phénomène et d'en élucider les principaux acteurs. L'optimisation de la thérapie cellulaire de l'IM utilisant les CSM ne peut se résumer à la seule manipulation ou modification des cellules.

Dans ce contexte, l'objectif de cette thèse a été de développer de nouvelles approches thérapeutiques de l'IDM en utilisant les CSM, l'ingénierie tissulaire et cellulaire cardiaque.

Dans un premier temps, nous avons utilisé un hydrogel injectable à base de cellulose, auto-réticulant en fonction du pH. Notre stratégie était de co-injecter cet hydrogel avec des CSM issues de la moelle osseuse dans un modèle d'infarctus du myocarde chez le rat, afin de préserver la fonction cardiaque et d'atténuer le remodelage ventriculaire. Dans la perspective de créer *in vitro* un microenvironnement cardiaque, nous avons développé un modèle d'étude cardiaque à partir de culture en trois dimensions de cardiomyocytes néonataux murins dans l'hydrogel. Finalement, afin d'obtenir des cardiomyocytes fonctionnels, nous nous sommes intéressés à la reprogrammation directe des CSM en cardiomyocytes.

RESULTATS EXPERIMENTAUX

ETUDE 1

Injection intramyocardique de cellules souches mésenchymateuses avec un hydrogel pour préserver la fonction cardiaque et atténuer le remodelage ventriculaire après un infarctus du myocarde

- **Publication N°1**

Intramyocardial delivery of mesenchymal stem cell-seeded hydrogel preserves cardiac function and attenuates ventricular remodeling after myocardial infarction

Eva Mathieu*,* Guillaume Lamirault, Claire Toquet, Emilie Rederstorff, Kévin Biteau, Virginie Forest, Philippe Hulin, Pierre Weiss, Jérôme Guicheux et Patricia Lemarchand

Journal : *Biomaterials*
Soumis le 29 Juillet 2011

- **Brevet**

Silylated biomolecule-based hydrogel for culturing cardiomyocytes and stem cells, and use of the hydrogel thereof for treating heart failure.

Eva Mathieu, Pierre Weiss, Jérôme Guicheux et Patricia Lemarchand

Numéro de référence : EP n° 11 305 683.2
Déposants : INSERM, Université de Nantes, CHU de Nantes
Année : 2011

ETUDE 1 : Injection intramyocardique de cellules souches mésenchymateuses avec un hydrogel, pour préserver la fonction cardiaque et atténuer le remodelage ventriculaire après un infarctus du myocarde.

1. Contexte de l'étude.

Plusieurs études ont montré qu'un des problèmes majeurs liés aux protocoles de thérapie cellulaire cardiaque est la faible rétention ainsi que la survie très limitée des cellules implantées dans le tissu ischémique (Maurel *et al.*, 2005; Toma *et al.*, 2002). Or, le nombre de cellules injectées et survivant dans le tissu hôte est directement proportionnel à l'amélioration de la fonction cardiaque. Dans ce contexte, notre hypothèse de travail était que l'utilisation d'un biomatériau injectable comme support aux cellules permettrait d'améliorer l'implantation et la survie des cellules souches mésenchymateuses (CSM) dans un modèle d'infarctus du myocarde (IDM) chez le rat. Dans le cadre d'une collaboration avec l'unité Inserm U791 (Jérôme Guicheux et Pierre Weiss, LIOAD), nous disposions d'un hydrogel constitué d'un dérivé de la cellulose, l'hydroxylpropyl méthylcellulose silanisée (HPMC-Si) (Bourges *et al.*, 2002b; Fatimi *et al.*, 2008). L'hydrogel d'HPMC-Si est obtenu par l'association de deux solutions : une solution basique visqueuse contenant l'HPMC-Si, avec une solution tampon acide. Le mélange des deux solutions permet d'obtenir une solution injectable qui gélifie après implantation *in situ* (Merceron *et al.*, 2011; Vinatier *et al.*, 2007).

Après avoir vérifié que les propriétés mécaniques et rhéologiques de l'hydrogel d'HPMC-si étaient compatibles avec celles du tissu cardiaque, nous avons testé sa compatibilité avec les CSM issues de la moelle osseuse de rat Lewis. La viabilité des CSM cultivées en trois dimensions (3D) au sein de l'hydrogel a été validée par des tests de cytotoxicité.

L'étude *in vivo* a été réalisée à partir d'un modèle d'IDM par ligature de l'artère inter-ventriculaire antérieure (IVA) chez des rats femelles de souche Lewis, déjà utilisé dans le laboratoire (Fernandes 2006). Grâce à leur protection hormonale, les femelles sont plus résistantes à l'IDM que les mâles (Piro *et al.*, 2010). La souche Lewis est syngénique ce qui permet de s'affranchir du rejet de greffe allogénique des CSM. Le modèle de ligature de l'artère coronaire a été décrit dès les années 1950 (Johns and Olson, 1954). L'occlusion complète et définitive de l'artère IVA conduit à un infarctus transmural qui détruit la totalité du territoire ischémique sur toute l'épaisseur de la paroi, de l'endocarde vers l'épicarde et induit une hypertrophie cardiaque excentrique (Pfeffer and Braunwald, 1990). La Figure 9 décrit le protocole expérimental que nous avons utilisé pour réaliser cette étude.

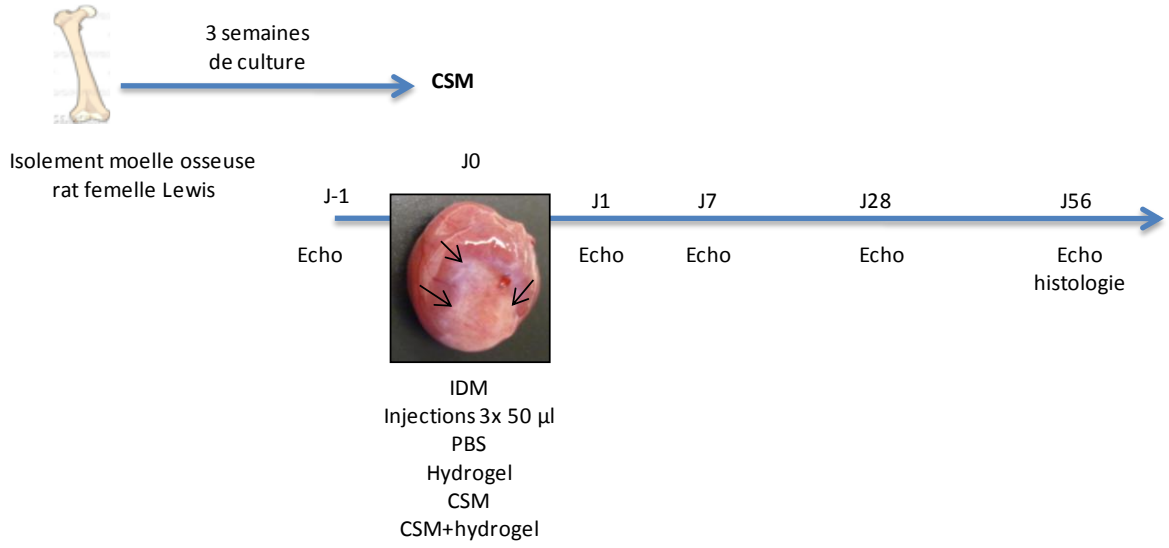

Figure 9: Protocole expérimental utilisé.

Les cellules souches mésenchymateuses (CSM) sont isolées à partir de la moelle osseuse de rats femelles Lewis. Une échocardiographie (Echo) est réalisée en contrôle 1 jour (J-1) avant l'intervention chirurgicale (J0). Immédiatement après l'induction de l'infarctus du myocarde (IDM) par la ligature de l'artère IVA, 3 injections intramyocardiques de 50 µl, de PBS (contrôle), hydrogel seul, CSM seules ou CSM+hydrogel sont réalisées. Des échocardiographies sont ensuite réalisées à 1, 7, 28 et 56 jours suivant l'injection. Les animaux sont sacrifiés à 56 jours, les cœurs sont prélevés et inclus en paraffine pour l'étude histologique.

2. Résultats et discussion de l'étude.

Dans cette étude, notre objectif a été de déterminer si un hydrogel constitué d'un dérivé de la cellulose, l'hydroxylpropyl méthylcellulose silanisée (HPMC-Si), injecté dans en intramyocardique avec des cellules souches mésenchymateuses (CSM) issues de la moelle osseuse était capable de préserver la fonction cardiaque et de prévenir les effets délétères liés au remodelage du ventricule gauche (VG) dans un modèle d'infarctus du myocarde chez le rat.

Les paramètres physicochimiques de l'hydrogel d'HPMC-si, tels que son auto-réticulation ait lieu à un pH physiologique et son temps de gélation soit d'environ 30 min, permettaient de le manipuler et de l'injecter facilement sous forme liquide avec des cellules dans le tissu cardiaque. L'élasticité de l'hydrogel d'HPMC-si était inférieure à celle du tissu cardiaque, de ce fait, l'hydrogel n'avait pas d'effets néfastes sur les propriétés mécaniques du cœur après son injection dans le tissu myocardique (Engler *et al.*, 2006). La biocompatibilité est un autre paramètre clé dans le développement préclinique d'un biomatériau innovant pour la médecine régénératrice. L'hydrogel d'HPMC-si a déjà bien été décrit pour être cytocompatible avec des chondrocytes (Vinatier *et al.*, 2005) et des ostéoblastes (Trojani *et al.*, 2005). Dans cette étude, les données obtenues indiquaient que l'hydrogel d'HPMC-si était également cytocompatible avec les CSM et qu'il permettait leur culture en 3D.

Nous avons ensuite évalué les effets de l'injection de l'hydrogel seul, des CSM seules ou avec l'hydrogel sur la fonction cardiaque et le remodelage du VG. Les résultats ont montré que l'injection de l'hydrogel seul préservait à court-terme la fonction cardiaque et que l'hydrogel seul n'était probablement pas suffisant pour prévenir une progression vers l'insuffisance cardiaque (Rane *et al.*, 2011). L'effet transitoire de l'hydrogel injecté *in situ* dans le myocarde peut-être lié à la capacité des hydrogels à augmenter l'épaisseur de la paroi cicatricielle et à stabiliser la taille de l'infarctus en apportant un support physique dans la

paroi du VG (Vunjak-Novakovic *et al.*, 2010). Contrairement aux effets de l'hydrogel seul, il est bien connu que chez le rat, l'injection intramyocardique de CSM a un effet optimal à partir de 4 semaines après l'IDM (Hu *et al.*, 2007; Mazo *et al.*, 2010). En accord avec ces données, nos résultats ont montré que les CSM injectées dans le myocarde avaient un effet bénéfique sur la fonction cardiaque et le remodelage du VG principalement 4 semaines après l'injection. L'absence d'effet à court-terme des CSM peut-être dû à l'hypoxie, l'inflammation et à la dégradation de la matrice extracellulaire dans le tissu cardiaque infarci, limitant ainsi la greffe et la survie des cellules dans le myocarde (Zhang *et al.*, 2001). Compte tenu de l'effet à court terme de l'hydrogel d'HPMC-si et de l'effet retardé des CSM, nous avons associé l'hydrogel d'HPMC-si avec les CSM afin de déterminer si cette association pouvait être bénéfique, non seulement à court-terme mais également à moyen-terme (8 semaines), et ainsi prévenir les conséquences néfastes générées par l'IDM. Comme prévu, nos résultats ont montré que la co-injection de l'hydrogel d'HPMC-Si avec les CSM avait un effet à court et moyen terme sur la fonction ventriculaire gauche et le remodelage. Normalement les cellules souches, telles que les CSM, résident dans des « niches » et sont régulées par des interactions physiques et des facteurs solubles (Morrison and Spradling, 2008). L'hydrogel d'HPMC-si pourrait être capable de simuler cet environnement tridimensionnel et ainsi protéger les cellules pendant et après leur implantation dans le tissu cardiaque. À l'appui de cette hypothèse, plusieurs études ont indiqué que les hydrogels à base de fibrine, de polyéthylène glycol ou de polysaccharides étaient capables d'augmenter la survie et la rétention des cellules dans le myocarde et ainsi améliorer la fonction cardiaque et limiter les phénomènes de remodelage ventriculaire par rapport à l'injection de CSM seules (Le Visage et al., 2011; Wang et al., 2009c; Zhang et al., 2010b). Cependant, la capacité de l'hydrogel d'HPMC-si à améliorer la survie et la greffe des cellules dans le tissu cardiaque nécessite une étude plus approfondie. En plus des paramètres échocardiographiques utilisés pour évaluer la fonction cardiaque et le remodelage

ventriculaire après l'IDM, des analyses histologiques ont été réalisées sur des coupes 2 mois après les injections. Il est connu que la présence de métaplasies au niveau de l'endocarde reflète la gravité de l'infarctus (Boor and Ferrans, 1985; Lehoczky-Mona and McCandless, 1964). L'analyse histologique des coupes a montré que l'injection des CSM avec l'hydrogel limitait l'étendue de l'infarctus et préservait les myocytes au niveau de l'endocarde, réduisant significativement la formation de métaplasie. Ces données renforçaient notre hypothèse selon laquelle l'injection intramyocardique de CSM avec l'hydrogel d'HPMC-Si pouvait être une stratégie pertinente pour prévenir les effets délétères de l'infarctus sur le remodelage ventriculaire.

Pour résumer, nous avons montré dans cette étude que l'injection intramyocardique d'un hydrogel dérivé de la cellulose associé à des CSM est capable d'améliorer la fonction cardiaque à court terme et atténuer le remodelage ventriculaire à plus long terme dans un modèle de rat d'IDM. Ces effets bénéfiques peuvent être liés aux propriétés intrinsèques de l'hydrogel d'HPMC-Si, qui en apportant un soutien physique aux cellules, améliore la survie et la greffe des cellules dans le tissu cardiaque.

Malgré son effet bénéfique sur la fonction cardiaque et le remodelage ventriculaire, l'injection de l'hydrogel d'HPMC-Si avec les CSM ne semble pas suffisante pour induire une réelle régénération d'un tissu cardiaque contractile et fonctionnel. Avant que cette stratégie thérapeutique prometteuse puisse aboutir à un essai clinique chez l'homme, il convient d'améliorer nos connaissances de base concernant les événements moléculaires physiopathologiques de l'infarctus du myocarde. Le développement de modèles *in vitro* apparait aujourd'hui indispensable, si nous voulons dans un futur proche mieux appréhender les mécanismes nécessaires pour induire la régénération cardiaque.

3. Résumé de l'article.

Afin d'améliorer l'efficacité de la thérapie cellulaire de l'infarctus du myocarde (IDM) basée sur l'utilisation de cellules souches mésenchymateuses (CSM) issues de la moelle osseuse, nous avons étudié la capacité d'un hydrogel autoréticulant, l'hydroxylpropyl méthylcellulose silanisée (HPMC-Si), à véhiculer des CSM dans le myocarde afin de préserver la fonction cardiaque et atténuer le remodelage du ventricule gauche (VG) durant 8 semaines après un IDM. L'étude consistait à injecter immédiatement dans le myocarde après la ligature de l'artère coronaire interventriculaire antérieure (IVA) chez des rats femelles de souche Lewis, l'hydrogel seul, les CSM seules ou avec l'hydrogel (CSM+ hydrogel). Le suivi des animaux par échocardiographie a montré une récupération de la fonction cardiaque 28 jours après l'IDM dans le groupe CSM+hydrogel et une préservation de la fonction cardiaque ainsi qu'une atténuation du remodelage ventriculaire 56 jours après l'IDM. Les analyses histologiques ont montré que l'injection de CSM+hydrogel diminuait significativement la taille de l'IDM, augmentait l'épaisseur de la paroi du VG et finalement limitait la transmuralité de l'IDM. L'ensemble de ces résultats montre que l'injection intramyocardique de CSM+hydrogel induit une récupération à court terme de la fonction cardiaque et une atténuation à moyen terme des effets délétères liés à l'ischémie sur la fonction cardiaque et le remodelage ventriculaire chez le rat. Les effets bénéfiques de l'hydrogel pourraient être liés à sa capacité à améliorer la rétention et la survie des CSM injectées dans le myocarde en post-infarctus.

*Title Page

Intramyocardial delivery of mesenchymal stem cell-seeded hydrogel preserves cardiac function and attenuates ventricular remodeling after myocardial infarction

Mathieu E [1, 2], Lamirault G [1, 2, 3], Toquet C [3, 4], Rederstorff E [2, 5], Biteau K [1, 2], Hulin P [2, 6], Forest V [1, 2], Weiss P [2, 3, 5], Guicheux J [2, 5 $] and Lemarchand P [1, 2, 3 *, $].

[$]Both authors contributed equally.

[1] INSERM, U915, l'institut du thorax, Nantes, F-44007, France.

[2] Université de Nantes, Institut Fédératif de Recherche thérapeutique 26 (IFR26), Nantes, F-44000 France.

[3] CHU de Nantes, Nantes, F-44000, France.

[4] Service d'Anatomie Pathologique, E.A. Biometadys, CHU de Nantes, Nantes, F-44000, France.

[5] INSERM, U791, Laboratory of Osteo-Articular and Dental Tissue Engineering, Group STEP "Skeletal tissue Engineering and Physiopathology", Nantes, F-44042, France.

[6] Cellular and Tissular Imaging Core Facility of Nantes University (MicroPICell), Nantes, F-44007, France

[*]Corresponding author: P. Lemarchand

INSERM UMR915, IRT-Université de Nantes, 8 quai Moncousu, BP 70721, 44007 Nantes cedex 1, France

Phone: +33 2 28 08 01 33 Fax: +33 2 28 08 01 30,

E-mail address: patricia.lemarchand@univ-nantes.fr

E-mails:

Eva Mathieu: eva.mathieu@inserm.fr

Guillaume Lamirault : guillaume.lamirault@univ-nantes.fr

Claire Toquet: claire.toquet@chu-nantes.fr

Emilie Rederstorff: rederstorff.emilie@gmail.com

Kévin Biteau : kevin.biteau@etu.univ-nantes.fr

Virginie Forest : virginie.forest@univ-nantes.fr

Philippe Hulin : philippe.hulin@univ-nantes.fr

Pierre Weiss : pierre.weiss@univ-nantes.fr

Jérôme Guicheux : jerome.guicheux@inserm.fr

Patricia Lemarchand : patricia.lemarchand@univ-nantes.fr

Abstract

To improve the efficacy of bone marrow-derived mesenchymal stem cell (MSC) therapy targeted to infarcted myocardium, we investigated whether a self-setting silanized hydroxypropyl methylcellulose (Si-HPMC) hydrogel seeded with MSC (MSC+hydrogel) could preserve cardiac function and attenuate left ventricular (LV) remodeling during an 8-week follow-up study in a rat model of myocardial infarction (MI). Si-HPMC hydrogel alone, MSC alone or MSC+hydrogel were injected into the myocardium immediately after coronary artery ligation in female Lewis rats. Animals in the MSC+hydrogel group showed an increase in cardiac function up to 28 days after MI and a mid-term prevention of cardiac function alteration at day 56. Histological analyses indicated that the injection of MSC+hydrogel induced a decrease in MI size and an increase in scar thickness and ultimately limited the transmural extent of MI. These findings show that intramyocardial injection of MSC+hydrogel induced short-term recovery of ventricular function and mid-term attenuation of remodeling after MI. These beneficial effects may be related to the specific scaffolding properties of the Si-HPMC hydrogel that may provide the ability to support MSC injection, engraftment and viability within myocardium.

1. Introduction

After myocardial infarction (MI), left ventricular (LV) remodeling occurs with early and progressive extracellular matrix (ECM) degradation, infarct zone expansion, scar thinning, LV enlargement and eventually, transition to heart failure [1, 2]. Current anti-remodeling therapies are limited as they fail to prevent ventricle enlargement [3, 4] and morbidity-mortality remains high [5]. Mesenchymal stem cell (MSC) injection into the infarcted myocardium is a newly developed strategy for cardiac tissue repair and regeneration after MI [6]. The beneficial effects of MSC injection have been partly related to their paracrine activity. MSC secrete angiogenic, anti-apoptotic, and anti-inflammatory cytokines that may contribute to the recovery of cardiac function [7, 8] and significantly decrease fibrosis of the myocardium [9, 10]. Most MSC administration strategies use intramyocardial injections of cells suspended in culture medium. However, this technique is limited by low cell retention and survival rates. For example, several studies have shown that more than 80%–90% of grafted cells die within 72 hours after injection into the myocardium [11, 12]. Multiple mechanisms may contribute to the premature death of grafted cells, including oxidative stress, hypoxia, and inflammation [13, 14]. Recently, cardiac tissue engineering, combining cells and scaffolding biomaterials, has emerged as a promising approach to provide support for tissue repair after MI [15, 16]. Among the various types of biomaterials currently available, hydrogels comprising hydrophilic, biocompatible polymers and peptides may represent excellent cell delivery systems due to their unique property of permitting *in situ* gel formation [17]. There are two major types of hydrogels: natural hydrogels, such as fibrin glue [18] and alginate [19], and synthetic hydrogels, such as polyethylene glycol (PEG) [20]. Natural hydrogels are used as scaffolds because they exhibit several critical biological functions that synthetic polymers lack, such as cell adhesion and biodegradation. We previously designed a

water-rich hydrogel consisting of silanized hydroxypropyl methylcellulose (Si-HPMC) that can be steam sterilized [21] and supports the diffusion of signaling molecules and nutrients [22]. Interestingly, this Si-HPMC hydrogel can be injected together with MSC *in vivo* and is able to self-crosslink to form a scaffolding matrix [23].

In this context, and to develop a novel cardiac tissue engineering strategy, we questioned whether a hydrogel-assisted intramyocardial injection of bone marrow-derived MSC could attenuate post-MI cardiac disorders. To address this issue, we used a rat model to evaluate the effects of injecting Si-HPMC hydrogel seeded with MSC on cardiac function and LV remodeling in a rat model of MI.

2. Materials and Methods

2.1. Isolation and culture of Bone Marrow Mesenchymal Stem Cells.

Bone marrow (BM) was obtained from female Lewis rats weighing 180–200 g (Janvier, France). BM from the femur cavity was flushed with α-MEM medium (Invitrogen corporation, Paisley, U.K.) containing 10% FCS (Hyclone Perbio, Thermo Fisher Scientific), 1% L-Glutamine, 1% penicillin/streptomycin (Invitrogen) and 2 ng/mL of human basic FGF2 (AbCys, Paris, France). The cell suspension was centrifuged (1,200 rpm, 7 min) and cells were plated in culture flasks (200,000 cells/cm^2). Non adherent cells were removed after 72 h. MSC were recovered by their capacity to strongly adhere to plastic culture dishes. MSC were then routinely cultured and used for experiments after phenotype analysis by fluorescence-activated cell-sorting (FACS) (FACS Calibur instrument with CellQuestPro software; BD

Biosciences, San Jose, CA) after incubation with anti-CD45–phycoerythrin (PE), anti-CD90–PE, anti-CD29–CyChrome and anti-Sca1–PE (BD Biosciences) at passage 3.

2.2. Silanized hydroxypropyl methylcellulose-based hydrogel preparation.

Synthesis of Si-HPMC hydrogel.

Hydroxypropyl methylcellulose (HPMC E4M®) was purchased from Colorcon-Down chemical (Bougival, France). Si-HPMC was synthesized by mixing silicium 0.5% (w/v) with HPMC to form a heterogeneous medium, as previously described [21]. Si-HPMC was solubilized in 0.2M NaOH (3%) under constant stirring for 48h at room temperature. The solution was dialyzed against 0.09 M NaOH using 6–8 kDa dialysis tubes (SpectraPor 1, Thermo Fisher Scientific, France). The resulting viscous solution (pH 12.6) was sterilized by autoclaving and then mixed using luer-lock syringes with sterile 4-(2-hydroxyethyl)-1-piperazineethanesulfonic acid buffer (HEPES, pH 3.6; Sigma-Aldrich, St Louis, USA) at a volume ratio of 1:1 as previously described [21]. The final product was a hydrogel (pH 7.4) containing 1.5% Si-HPMC.

Rheological and mechanical measurements.

Cross-linking of 1 ml Si-HPMC hydrogel was induced in 12-well plates. Dynamic rheological measurements were performed with a rotational rheometer (Rheostress 300, ThermoHaake®, Germany) using a coni-cylindrical geometry with a diameter of 60 mm and a cone angle of 1°. A multi-wave procedure was performed with 3 frequencies of 1, 3.2 and 10 Hz, with an imposed stress of 1 Pa. Oscillation tests measuring storage modulus (G') and loss modulus (G'') were performed to study the self-setting process and gel point. Gel points, given as the time taken for the liquid (G''>G') to turn into a solid (G'>G''), were evaluated according to the derived percolation theory [24]. Shear strain measurements were performed

on 9 samples with a Haake mars. Frequencies were applied at a fixed total shear stress (1Pa) and 0.21N. Oscillation tests were performed to measure G' and G'' after 3 weeks of gelation. The Si-HPMC hydrogel compressive modulus was measured using a TA HD-Plus (Stable Micro Systems). Six samples were tested after three weeks of cross-linking and the compressive modulus was calculated on the basis of strain change from 0 to 5%.

2.3. Cell viability in three dimensional culture.

Three-dimensional MSC viability was quantitatively assessed by Live & Dead assays (Invitrogen, France) followed by confocal imaging. MSC viability was assessed by measurement of fluorescence intensity using ImageJ (NIH) software. Briefly, MSC were trypsinized and immediately mixed with Si-HPMC hydrogel at a final concentration of 10^6 cells/mL. They were then molded into ultra-low attachment 24-well plates and incubated at 37°C for 1 h to allow for the hydrogel to crosslink. Culture medium was then added and the MSC were cultured within the hydrogel for 24 h, 48 h and 7 days. Live & Dead assays were performed according to the manufacturer instructions (Invitrogen). Briefly, culture medium was replaced by fresh culture medium supplemented with 5 mM calcein-AM and 2 mM ethidium homodimer-1. After 10 min, the dye mixture was removed and the hydrogel was thoroughly rinsed with PBS, before being analyzed with a Nikon A1R confocal laser-scanning microscope (Nikon France) equipped with an argon laser (488 nm) and a laser diode (561 nm).

Images were recorded in 512 x 512 pixels with an objective CFI Plan Fluor ELWD 40X objective. For each sample, 6 random positions were chosen within the hydrogel, and a stack of 100 planes were taken from these 6 positions along the z axis using a 10 μm step size. Images obtained per sample were analyzed using ImageJ (NIH) software with the "3D object

counter" plug-in. Each condition was tested in triplicate, and each experiment was repeated three times.

2.4. Induction of myocardial infarction in rats and implantation.

Animal studies were performed the agreement of the regional Animal Ethics Committee (CREEA, Comité régional d'éthique en matière d'expérimentation animale). Myocardial infarction was obtained by coronary artery ligation and intramyocardial injections were performed as previously described [25]. In brief, Female Lewis congenic rats (180-190g, Janvier) were anesthetized with a mix of isoflurane/oxygen inhalation (3%/97%), intubated and ventilated (Harvard Rodent Ventilator, Harvard Apparatus). A left lateral thoracotomy in the fourth intercostal space was performed to expose the anterior surface of the heart. The proximal left anterior descending (LAD) coronary artery was ligated with a 6.0 polypropylene snare (Ethicon). The area displaying tissue blanching and wall motion akinesis was identified as the infarct. Immediately after coronary artery ligation, 150 µl of a solution containing Si-HPMC hydrogel alone (hydrogel), MSC alone (3.10^6 cells) in PBS, a combination of MSC and Si-HPMC hydrogel (MSC+hydrogel), or PBS (used as the control) were injected into the myocardium using a 26-gauge needle. A final volume of 150 µl was delivered to 3 injection sites surrounding the infarcted area.

2.5. Echocardiography measurements.

Echocardiography measurements were performed 1 day before MI induction (baseline), and 1, 7, 28, and 56 days after MI, in anesthetized rats (2% isoflurane inhalation) using a General Electric Vivid 7VR (GE Medical System; Milwaukee, WI, USA) equipped with a 13-

MHz transducer. Left ventricular end-diastolic diameter (LVEDD), LV end-systolic diameter (LVESD), and LV fractional shortening (LVFS) were recorded from the parasternal long-axis M-mode images using averaged measurements from 3 to 5 consecutive cardiac cycles in accordance with the American Society of Echocardiography guidelines [26]. Left ventricular end-diastolic and end-systolic volumes (LVEDV and LVESV) were calculated from bidimensional long-axis parasternal views taken through the infarcted area by means of the single-plane area-length method [27]. The LV ejection fraction (LVEF) was calculated as follows: LVEF = (LVEDV-LVESV)/LVEDV) x 100.

2.6. Histopathology.

Rat hearts were recovered, washed in PBS and fixed in 10% formalin. Hearts were then embedded in paraffin and 6 μm sections were cut from the apex to the level just below the ligation site. Three evenly spaced sections were stained with Masson trichrome and observed with a Nikon TE2000-E inverted microscope.

The circumferential extent of the scar to total LV tissue [28], relative scar thickness, and infarct expansion index [29] were quantified as previously described using ImageJ software (NIH). The average epicardial and endocardial infarct ratios were calculated for each section based on the measurement of epicardial and endocardial infarct lengths and epicardial and endocardial LV circumferences. For each heart, the infarct size was calculated as the mean value for the 3 analyzed sections.

Scar and septum thickness were measured at 3 different random sites and relative scar thickness was calculated as the mean scar thickness/septum thickness. The infarct expansion index was calculated as the LV cavity area / (whole LV area/relative scar thickness). The percentage area of fibrosis in the remote left ventricle was quantified using in-house image

analysis software based on the equation: %fibrosis=fibrotic area / (fibrotic area + non-fibrotic area) [28].

2.7. Statistical Analysis.

All values are shown as mean±SEM. Comparison of means was performed using one-way ANOVA followed by a post-hoc test when appropriate (Fisher's projected least significant difference). Frequency comparisons were performed using the Fisher exact test. Echocardiography parameters measured during the 8-week follow-up period were compared between groups using one-way ANOVA and within groups using one-way repeated measures ANOVA. Comparisons were followed by post hoc tests when appropriate. $p<0.05$ was selected as the threshold for statistical significance. All tests were carried out using SigmaStat 3.5 software for Windows.

3. Results

3.1. Rheological characteristics of Si-HPMC hydrogel.

Rheological properties of Si-HPMC solution mixed with acidic buffer (1:1) were measured. The final product (Si-HPMC hydrogel) was a reticulated hydrogel with a pH value of 7.4 after 27.2±3.4 min. Dynamic rheological measurements were performed to characterize the Si-HPMC hydrogel, including shear strain measurements to evaluate the storage modulus (G', which characterizes the hard component), and the loss modulus (G'', which characterizes the liquid component). After three weeks of cross-linking and completion of the self-setting process, the G' value was 343.2±106.5 Pa and the G'' was 44.5±15.4 Pa. The compressive

modulus (which reflects the stiffness of the material in a compressive experiment) at a 5% strain was 328.6±97.0 Pa.

3.2. MSC viability in three-dimensional culture within the Si-HPMC hydrogel.

To evaluate whether the Si-HPMC hydrogel was cytotoxic, MSC viability was monitored in Si-HPMC 3D-culture by confocal fluorescent microscopy (Fig. 1A). MSC viability was assessed by measurement of green fluorescence intensity, as a consequence of incorporation of the calcein fluorescent probe into the cytoplasm (Fig. 1B). The results showed that MSC viability was maintained throughout the experiment.

3.3. Comparative effects of hydrogel, MSC, and MSC+hydrogel on cardiac function and LV remodeling.

MI was induced by ligation of the LAD coronary artery in 62 rats. After MI induction, rats were randomized into 4 treatment groups to receive intramyocardial injections of (1) PBS as the control, (2) hydrogel, (3) MSC and (4) MSC+hydrogel. In our study, the overall mortality 24 hours after surgery was 30.7±7.7% (19/62 rats) with no significant differences between treatment groups (Table 1A). Echocardiography was performed 1 day after coronary artery ligation to exclude rats without a significant MI (defined as animals with a LVEF > 70%; Table 1B). Importantly, the number of excluded rats was not significantly different between treatment groups (Table 1B), nor were the parameters of LV dimensions and function measured at Day 1 of the echocardiography follow-up analysis (Table 2).

As expected, MI induced an increase in LV remodeling, characterized by an increase in LV chamber dimensions, (LVESD and LVEDD) leading to a decrease in LVFS and LVEF (Fig.

2, PBS conditions). As compared to the PBS group, injections of hydrogel, MSC or MSC+hydrogel, significantly attenuated the MI-induced increase in LV end-systolic diameter (LVESD) over the time period analyzed (Fig. 2A). These injections also preserved the LV end-diastolic diameter (LVEDD) as compared to the PBS group, but did not improve the LVEDD (Fig. 2B). The injection of hydrogel alone induced a transient but a significant increase in LVEF at Day 28, but not at Day 7 and Day 56 as compared to the PBS group. In contrast, MSC injection induced a significant increase in LVEF at Days 28 and 56 but not at Day 7, suggesting a delayed effect (Fig. 2C). In addition, the LVEF did not significantly differ between the two groups throughout the study follow-up, as compared to Day 1. The injection of MSC+hydrogel during the acute phase of MI induced a significant increase in LVEF from Day 7 at Day 56 after injection, as compared to the PBS group, and a significant increase in LVEF as compared to Day 1 post MI. Interestingly, the LVEF in the MSC+hydrogel group was higher as compared to that in the MSC group at Day 7 and as compared to that in the hydrogel group at Day 56.

3.4. Comparative effects of hydrogel, MSC or MSC+hydrogel on infarct expansion and ventricular fibrosis.

Morphometric analyses of heart sections were performed at Day 56 to analyze LV remodeling. For all animals, the infarct area was located in the anterior region of the left ventricle (Fig. 3A). The MI size was significantly reduced in the hydrogel group, the MSC group and the MSC+hydrogel group as compared to the PBS group (Fig. 3B). In addition, the size of the MI was also reduced in the MSC and MSC+hydrogel groups as compared to the hydrogel group. The percentage of ventricular fibrosis (Fig. 3C) was also significantly reduced in the hydrogel group, the MSC group, and the MSC+hydrogel group as compared to

the PBS group. Next, the effects of different treatments on the LV wall were assessed by measuring the relative scar thickness (Fig. 4A-4B). The results showed a significant increase in the relative scar thickness in the hydrogel, MSC and MSC+hydrogel groups as compared to the PBS group. The infarct expansion index was calculated using both MI size and relative scar thickness parameters (Fig. 4C). This index was significantly reduced with the injections of hydrogel, MSC and MSC+hydrogel as compared to the injection of PBS. Interestingly, chondroid metaplasia of the endocardium (indicated by arrows in Fig. 4A) was often observed in the PBS group (83% of rats) whereas this feature was visible in only 14% ($p<0.05$ *vs.* PBS) of rats in the MSC+hydrogel group, 67% of rats in the hydrogel group and 60% of rats in the MSC group (p=NS).

4. Discussion

There has been growing interest in the use of scaffolding biomaterials as a vehicle for delivery of reparative cells to improve the efficacy of targeted stem cell therapy for myocardial infarction. Among the biomaterials that have been considered for tissue engineering and regenerative medicine, hydrogels are probably the most appropriate synthetic matrices since they exhibit injectability and cross-linking properties. When considering stem cell-based cardiac tissue engineering, the ideal hydrogel should be biocompatible with respect to MSC and cardiac tissue and should also be injectable into the myocardium to provide the advantage of minimally invasive delivery [30]. In the present study, our objective was to investigate whether a self-setting cellulosic hydrogel seeded with MSC could preserve cardiac function and prevent LV remodeling during an 8-week follow-up period in a rat model of MI.

Among the various hydrogels used in cardiac tissue engineering, we focused our attention on a cellulose derivative hydrogel (Si-HPMC) that exhibits rheological properties compatible

with its implantation by mini-invasive surgery [31]. The grafting of silanol groups along the HPMC chains confers this hydrogel with a self-setting property. The pH-dependent condensation between the silanol groups allows the Si-HPMC viscous solution to rapidly transform into Si-HPMC solid gel, leading to the formation of a 3D network. The gelation time is a physicochemical parameter that has to be finely tuned, to enable successful manipulation and injection of the Si-HPMC hydrogel/cells mixture *in situ* [24]. Of interest and as previously suggested by our group, the gelation time of Si-HPMC (about 30 min) is sufficient to enable cell-hydrogel mixing [32] as well as its injection *in vivo* [33]. The need for optimizing hydrogel elasticity has also been recognized as a physicochemical parameter that governs the regenerative potential of biomaterials, supporting adequate stem cell differentiation [34] as well as the mechanical function of the targeted tissue [35]. Engler *et al.* defined a range of rigidity for various tissues measured by the elastic modulus (E). For cardiac muscle tissue, the E value ranges between 8 and 17 kPa [34]. Of note, our mechanical data showed that Si-HPMC hydrogel exhibits an E value of about 0.3 kPa, which is quite lower than that of cardiac tissue and as such, is unlikely to adversely affect the mechanical properties of the myocardium. Other key parameters in the preclinical development of innovative biomaterial-based regenerative strategies include the biological properties of biomaterials, such as cytocompatibility. Along these lines, whereas Si-HPMC has been largely described as being cytocompatible with both osteogenic [36] and chondrogenic cells [32], the data reported in the current study additionally indicate that Si-HPMC supports the 3D viability of bone marrow-derived MSC.

In light of these data, we logically embarked on *in vivo* experiments to determine the beneficial effects of injecting either hydrogel alone, MSC alone or MSC-seeded hydrogel, on the cardiac parameters of infarcted rat hearts. LV dysfunction and remodeling after MI are major determinants of transition to heart failure and cardiac mortality [4, 37]. We thus

evaluated LV dysfunction by determining the LV ejection fraction (LVEF). The LV diameters, infarct size, LV fibrosis and scar thickness were then assessed to determine LV remodeling. Over the past decade, several studies have documented the cardioprotective effects of injecting hydrogels alone. For instance, the intramyocardial injection of alginate hydrogel [38] or fibrin glue [39] has been proposed as an effective acellular strategy to prevent adverse cardiac remodeling and dysfunction after MI in rats. Interestingly, in our study, the injection of Si-HPMC hydrogel alone affected the LV function mainly during the first 4 weeks after MI, with a progressive decrease thereafter. Taken together, these data suggest that the injection of hydrogel primarily preserves short-term cardiac function but is probably insufficient to prevent long-term heart failure [40]. The mechanism underlying the transient effect of hydrogel injected *in situ* may be related to the capability of hydrogels to increase scar thickness and stabilize the early infarct, by providing scaffolding and critical physical support to the LV wall [16].

Contrary to the effects of hydrogels alone, it is well known that in rats, intramyocardial injection of MSC gives an optimal therapeutic benefit starting 4 weeks after MI [41, 42]. Accordingly, our data indicate that bone marrow-derived MSC exert a significant beneficial effect on both the functional and remodeling parameters, mainly after a 4 week interval. The absence of a short-term effect of MSC after implantation may be due to the hypoxia, inflammation and loss of ECM support in infarcted cardiac tissue that probably leads to a poor engraftment, survival and persistence of transplanted cells [43]. Given the short-term effect of Si-HPMC and the delayed effect of MSC, we associated our hydrogel with MSC in order to determine whether this association may be beneficial, not only in the short-term but also in the mid-term, to prevent the detrimental consequences of MI. As expected, our results showed that the co-injection of Si-HPMC hydrogel and MSC has a marked short and mid-term effect on LV function and remodeling. Of particular interest, the co-injection of Si-HPMC and MSC

had a more prominent effect during the first 7 day-acute phase period as compared to the injection of hydrogel alone. Considering that stem cells, such as MSC, normally reside in "niches", complex 3D environments regulated by physical interactions and soluble factors [44], one can assume that hydrogel may be able to simulate this microenvironment, thereby providing cells with a protective "niche". In support of this hypothesis, several reports have indicated that hydrogels made of fibrin or polyethylene glycol may be able to increase the survival and retention of intramyocardial transplanted cells and further improve the impaired cardiac function compared to MSC alone [45, 46]. Whether our cellulose derivative Si-HPMC hydrogel can provide cells with such a favorable environment with appropriate mechanical and biological stimuli requires further investigation. In addition to the echocardiography parameters used to assess LV function and remodeling after MI, such as LVEF and LVFS, histological analyses may also provide further insight into the tissue changes that occur. It is recognized for a long time that the presence of focal endocardial metaplasia, consisting of chondroid tissue in areas of transmural scarring, reflects the severity of MI [47, 48]. Accordingly, the intramyocardial administration of Si-HPMC hydrogel seeded with MSC was found to limit the extent of transmural MI, preserve endocardial myocytes and reduce metaplasia. These data strengthen our hypothesis that the intramyocardial injection of hydrogel and MSC may be a relevant strategy to prevent the mid-term deleterious effects of MI on ventricular remodeling.

5. Conclusion

In summary, we have demonstrated that intramyocardial injection of a self-setting cellulose derivative hydrogel seeded with MSC induced short-term recovery of ventricular function and mid-term prevention of remodeling in a rat model of coronary artery ligation-induced MI.

These beneficial effects may be related to the specific scaffolding properties of the Si-HPMC hydrogel that provide it with the ability to support MSC injection, engraftment and viability within the cardiac tissue. Together with a catheter-based cell delivery system [49], the use of an injectable scaffolding hydrogel offers the possibility to prevent the damaging consequences of MI.

Acknowledgements

This work was supported by grants from INSERM (Institut National de la Santé et la Recherche Médicale) and « Fondation de l'Avenir ». Eva Mathieu received a fellowship from the French Ministry of Research and Technology. The authors gratefully thank the "Unité Thérapeutique Expérimentale", Cardiex platform and the "Photologie" Department for their help. The authors also gratefully acknowledge Sophie Sourice for assistance in tissue embedding and processing. We also thank Paul Pilet, Claire Vinatier and members of STEP group "Skeletal Tissue Engineering and Physiopathology" for helpful suggestions, Laurent Beck and Joanna Ashton-Chess for critically reading the manuscript and Béatrice Delasalle for her help with statistical analyses.

References

[1] Cohn JN, Ferrari R, Sharpe N. Cardiac remodeling--concepts and clinical implications: a consensus paper from an international forum on cardiac remodeling. Behalf of an International Forum on Cardiac Remodeling. J Am Coll Cardiol. 2000;35:569-82.
[2] Jugdutt BI. Ventricular remodeling after infarction and the extracellular collagen matrix: when is enough enough? Circulation. 2003;108:1395-403.
[3] Bolognese L, Neskovic AN, Parodi G, Cerisano G, Buonamici P, Santoro GM, et al. Left ventricular remodeling after primary coronary angioplasty: patterns of left ventricular dilation and long-term prognostic implications. Circulation. 2002;106:2351-7.
[4] Savoye C, Equine O, Tricot O, Nugue O, Segrestin B, Sautiere K, et al. Left ventricular remodeling after anterior wall acute myocardial infarction in modern clinical practice (from the REmodelage VEntriculaire [REVE] study group). Am J Cardiol. 2006;98:1144-9.
[5] Verma A, Meris A, Skali H, Ghali JK, Arnold JM, Bourgoun M, et al. Prognostic implications of left ventricular mass and geometry following myocardial infarction: the VALIANT (VALsartan In Acute myocardial iNfarcTion) Echocardiographic Study. JACC Cardiovasc Imaging. 2008;1:582-91.
[6] Segers VF, Lee RT. Stem-cell therapy for cardiac disease. Nature. 2008;451:937-42.
[7] Aggarwal S, Pittenger MF. Human mesenchymal stem cells modulate allogeneic immune cell responses. Blood. 2005;105:1815-22.
[8] Tse WT, Pendleton JD, Beyer WM, Egalka MC, Guinan EC. Suppression of allogeneic T-cell proliferation by human marrow stromal cells: implications in transplantation. Transplantation. 2003;75:389-97.
[9] Nagaya N, Kangawa K, Itoh T, Iwase T, Murakami S, Miyahara Y, et al. Transplantation of mesenchymal stem cells improves cardiac function in a rat model of dilated cardiomyopathy. Circulation. 2005;112:1128-35.
[10] Li L, Zhang Y, Li Y, Yu B, Xu Y, Zhao S, et al. Mesenchymal stem cell transplantation attenuates cardiac fibrosis associated with isoproterenol-induced global heart failure. Transpl Int. 2008;21:1181-9.
[11] Maurel A, Azarnoush K, Sabbah L, Vignier N, Le Lorc'h M, Mandet C, et al. Can cold or heat shock improve skeletal myoblast engraftment in infarcted myocardium? Transplantation. 2005;80:660-5.
[12] Toma C, Pittenger MF, Cahill KS, Byrne BJ, Kessler PD. Human mesenchymal stem cells differentiate to a cardiomyocyte phenotype in the adult murine heart. Circulation. 2002;105:93-8.
[13] Niagara MI, Haider H, Jiang S, Ashraf M. Pharmacologically preconditioned skeletal myoblasts are resistant to oxidative stress and promote angiomyogenesis via release of paracrine factors in the infarcted heart. Circ Res. 2007;100:545-55.
[14] Tang YL, Tang Y, Zhang YC, Qian K, Shen L, Phillips MI. Improved graft mesenchymal stem cell survival in ischemic heart with a hypoxia-regulated heme oxygenase-1 vector. J Am Coll Cardiol. 2005;46:1339-50.
[15] Christman KL, Lee RJ. Biomaterials for the treatment of myocardial infarction. J Am Coll Cardiol. 2006;48:907-13.
[16] Vunjak-Novakovic G, Tandon N, Godier A, Maidhof R, Marsano A, Martens TP, et al. Challenges in cardiac tissue engineering. Tissue Eng Part B Rev. 2010;16:169-87.
[17] Ye Z, Zhou Y, Cai H, Tan W. Myocardial regeneration: Roles of stem cells and hydrogels. Adv Drug Deliv Rev. 2011.

[18] Christman KL, Vardanian AJ, Fang Q, Sievers RE, Fok HH, Lee RJ. Injectable fibrin scaffold improves cell transplant survival, reduces infarct expansion, and induces neovasculature formation in ischemic myocardium. J Am Coll Cardiol. 2004;44:654-60.
[19] Leor J, Tuvia S, Guetta V, Manczur F, Castel D, Willenz U, et al. Intracoronary injection of in situ forming alginate hydrogel reverses left ventricular remodeling after myocardial infarction in Swine. J Am Coll Cardiol. 2009;54:1014-23.
[20] Jiang XJ, Wang T, Li XY, Wu DQ, Zheng ZB, Zhang JF, et al. Injection of a novel synthetic hydrogel preserves left ventricle function after myocardial infarction. J Biomed Mater Res A. 2009;90:472-7.
[21] Bourges X, Weiss P, Daculsi G, Legeay G. Synthesis and general properties of silated-hydroxypropyl methylcellulose in prospect of biomedical use. Adv Colloid Interface Sci. 2002;99:215-28.
[22] Bourges X, Weiss P, Coudreuse A, Daculsi G, Legeay G. General properties of silated hydroxyethylcellulose for potential biomedical applications. Biopolymers. 2002;63:232-8.
[23] Merceron C, Portron S, Masson M, Lesoeur J, Fellah BH, Gauthier O, et al. The effect of two and three dimensional cell culture on the chondrogenic potential of human adipose-derived mesenchymal stem cells after subcutaneous transplantation with an injectable hydrogel. Cell Transplant. 2011.
[24] Fatimi A, Tassin JF, Turczyn R, Axelos MA, Weiss P. Gelation studies of a cellulose-based biohydrogel: the influence of pH, temperature and sterilization. Acta Biomater. 2009;5:3423-32.
[25] Fernandes S, Amirault JC, Lande G, Nguyen JM, Forest V, Bignolais O, et al. Autologous myoblast transplantation after myocardial infarction increases the inducibility of ventricular arrhythmias. Cardiovasc Res. 2006;69:348-58.
[26] Lang RM, Bierig M, Devereux RB, Flachskampf FA, Foster E, Pellikka PA, et al. Recommendations for chamber quantification: a report from the American Society of Echocardiography's Guidelines and Standards Committee and the Chamber Quantification Writing Group, developed in conjunction with the European Association of Echocardiography, a branch of the European Society of Cardiology. J Am Soc Echocardiogr. 2005;18:1440-63.
[27] Folland ED, Parisi AF, Moynihan PF, Jones DR, Feldman CL, Tow DE. Assessment of left ventricular ejection fraction and volumes by real-time, two-dimensional echocardiography. A comparison of cineangiographic and radionuclide techniques. Circulation. 1979;60:760-6.
[28] Kanashiro-Takeuchi RM, Tziomalos K, Takeuchi LM, Treuer AV, Lamirault G, Dulce R, et al. Cardioprotective effects of growth hormone-releasing hormone agonist after myocardial infarction. Proc Natl Acad Sci U S A. 2010;107:2604-9.
[29] Takagawa J, Zhang Y, Wong ML, Sievers RE, Kapasi NK, Wang Y, et al. Myocardial infarct size measurement in the mouse chronic infarction model: comparison of area- and length-based approaches. J Appl Physiol. 2007;102:2104-11.
[30] Singelyn JM, Christman KL. Injectable materials for the treatment of myocardial infarction and heart failure: the promise of decellularized matrices. J Cardiovasc Transl Res. 2010;3:478-86.
[31] Fatimi A, Tassin JF, Quillard S, Axelos MA, Weiss P. The rheological properties of silated hydroxypropylmethylcellulose tissue engineering matrices. Biomaterials. 2008;29:533-43.
[32] Vinatier C, Magne D, Weiss P, Trojani C, Rochet N, Carle GF, et al. A silanized hydroxypropyl methylcellulose hydrogel for the three-dimensional culture of chondrocytes. Biomaterials. 2005;26:6643-51.

[33] Vinatier C, Magne D, Moreau A, Gauthier O, Malard O, Vignes-Colombeix C, et al. Engineering cartilage with human nasal chondrocytes and a silanized hydroxypropyl methylcellulose hydrogel. J Biomed Mater Res A. 2007;80:66-74.
[34] Engler AJ, Sen S, Sweeney HL, Discher DE. Matrix elasticity directs stem cell lineage specification. Cell. 2006;126:677-89.
[35] Engler AJ, Carag-Krieger C, Johnson CP, Raab M, Tang HY, Speicher DW, et al. Embryonic cardiomyocytes beat best on a matrix with heart-like elasticity: scar-like rigidity inhibits beating. J Cell Sci. 2008;121:3794-802.
[36] Trojani C, Weiss P, Michiels JF, Vinatier C, Guicheux J, Daculsi G, et al. Three-dimensional culture and differentiation of human osteogenic cells in an injectable hydroxypropylmethylcellulose hydrogel. Biomaterials. 2005;26:5509-17.
[37] Poulsen SH. Clinical aspects of left ventricular diastolic function assessed by Doppler echocardiography following acute myocardial infarction. Dan Med Bull. 2001;48:199-210.
[38] Landa N, Miller L, Feinberg MS, Holbova R, Shachar M, Freeman I, et al. Effect of injectable alginate implant on cardiac remodeling and function after recent and old infarcts in rat. Circulation. 2008;117:1388-96.
[39] Christman KL, Fok HH, Sievers RE, Fang Q, Lee RJ. Fibrin glue alone and skeletal myoblasts in a fibrin scaffold preserve cardiac function after myocardial infarction. Tissue Eng. 2004;10:403-9.
[40] Rane AA, Chuang JS, Shah A, Hu DP, Dalton ND, Gu Y, et al. Increased infarct wall thickness by a bio-inert material is insufficient to prevent negative left ventricular remodeling after myocardial infarction. PLoS One. 2011;6:e21571.
[41] Hu X, Wang J, Chen J, Luo R, He A, Xie X, et al. Optimal temporal delivery of bone marrow mesenchymal stem cells in rats with myocardial infarction. Eur J Cardiothorac Surg. 2007;31:438-43.
[42] Mazo M, Gavira JJ, Abizanda G, Moreno C, Ecay M, Soriano M, et al. Transplantation of mesenchymal stem cells exerts a greater long-term effect than bone marrow mononuclear cells in a chronic myocardial infarction model in rat. Cell Transplant. 2010;19:313-28.
[43] Zhang M, Methot D, Poppa V, Fujio Y, Walsh K, Murry CE. Cardiomyocyte grafting for cardiac repair: graft cell death and anti-death strategies. J Mol Cell Cardiol. 2001;33:907-21.
[44] Morrison SJ, Spradling AC. Stem cells and niches: mechanisms that promote stem cell maintenance throughout life. Cell. 2008;132:598-611.
[45] Zhang X, Wang H, Ma X, Adila A, Wang B, Liu F, et al. Preservation of the cardiac function in infarcted rat hearts by the transplantation of adipose-derived stem cells with injectable fibrin scaffolds. Exp Biol Med (Maywood). 2010;235:1505-15.
[46] Wang T, Jiang XJ, Tang QZ, Li XY, Lin T, Wu DQ, et al. Bone marrow stem cells implantation with alpha-cyclodextrin/MPEG-PCL-MPEG hydrogel improves cardiac function after myocardial infarction. Acta Biomater. 2009;5:2939-44.
[47] Boor PJ, Ferrans VJ. Ultrastructural alterations in allylamine cardiovascular toxicity. Late myocardial and vascular lesions. Am J Pathol. 1985;121:39-54.
[48] Lehoczky-Mona J, McCandless EL. Ischemic Induction of Chondrogenesis in Myocardium. Arch Pathol. 1964;78:37-42.
[49] Sherman W, Martens TP, Viles-Gonzalez JF, Siminiak T. Catheter-based delivery of cells to the heart. Nat Clin Pract Cardiovasc Med. 2006;3 Suppl 1:S57-64.

Captions

Fig.1. MSC viability in 3D culture within the Si-HPMC hydrogel. MSC were cultured in 3D Si-HPMC hydrogel for the indicated times. (A) Labeling cells with calcein-AM (green color) and with EthD-1 (red color) revealed living and dead cells, respectively. Representative samples of MSC cultures visualized by confocal microscopy. **(B)** As described in the Materials section, the percentages of living and dead MSCs cultured in 3D within hydrogel over 7 days (p= NS as compared between time points, one-way ANOVA). All values represent mean ± SEM. Scale bar = 100µm.

Fig.2. Evaluation of cardiac function by echocardiography in rats after myocardial infarction (MI). Measurements were performed at baseline before MI and 1, 7, 28 and 56 days after MI as indicated. (A) Left ventricular end-diastolic diameter (LVEDD). (B) Left ventricular end-systolic diameter (LVESD). (C) Left ventricular fractional shortening (LVFS). (D) Left ventricular ejection fraction (LVEF). $^{¥}p<0.05$ compared to day 1 post-MI in the same group, one-way repeated measures ANOVA. $^{*}p<0.001$ *vs.* the PBS group at the same time-point, $^{\$}p<0.05$ *vs.* the hydrogel group at the same time-point and $^{+}p<0.05$ *vs.* the MSC group at the same time-point, one-way ANOVA. All values represent mean ± SEM.

Fig.3. Evaluation of myocardial infarction size and left ventricular fibrosis. (A) Representative transversal histology sections of heart and Masson trichrome staining for infarct size measurement at day 56 after MI. Collagen-rich areas (scar tissue) are colored in blue and healthy myocardium in red. Scale bar = 1.5 mm. (B) Percentage of circumferential infarct size (MI size) divided by total LV tissue, and (C) percentage of fibrosis in total LV tissue. For (B) and (C): $^{*}p<0.05$ and $^{**}p<0.001$ *vs.* the PBS group, $^{\$}p<0.05$ and $^{\$\$}p<0.001$ *vs.* the hydrogel group, one-way ANOVA. *LV, left ventricle; RV, right ventricle.* All values represent mean ± SEM.

Fig.4. Evaluation of scar thickness and infarct expansion. (A) Representative photomicrographs of Masson trichrome staining of the scar area (collagen-rich areas in blue and healthy myocardium in red). The double arrow depicts the LV wall (*epi*, epicardium; *endo*, endocardium). The arrows show chondroid metaplasia of the endocardium. Scale bar = 0.5 mm. (B) Relative scar thickness (scar thickness/wall thickness). (C) Infarct expansion index ([LV cavity area/whole LV area]/relative scar thickness). For (B) and (C): *p<0.05 and **p<0.001, one-way ANOVA. All values represent mean ± SEM.

Tables

Table 1: Number of animals included in the study.

A

	Animals number at baseline	Living animals at day 1
PBS	11	10
hydrogel	14	11
MSC	15	9
MSC+hydrogel	22	13
Total	62	43

B

	Animals number with LVEF>70% at day 1	Animals number with LVEF≤70% at day 1
PBS	4	6
hydrogel	4	7
MSC	1	8
MSC+hydrogel	4	9
Total	13	30

(A) Number of animals surviving 1 day post-MI. p=0.21 (Fisher exact test). (B) Number of animals in the follow-up study with an EF≤70% 1 day after MI. p=0.26 (Fisher exact test).

Table 2: Echocardiography measurements at baseline (Bsl) and at 1 day (d1), 7 days (d7), 28 days (d28) and 56 days (d56) after MI.

Parameters	PBS (n = 6)	hydrogel (n = 7)	MSCs (n = 8)	MSC+hydrogel (n = 9)
LVEDD (mm)				
Bsl	5.4 ± 0.2	5.2 ± 0.2	5.6 ± 0.1	5.6 ± 0.2
d1	5.9 ± 0.1	5.8 ± 0.3	6.2 ± 0.2	6.0 ± 0.1
d7	6.6 ± 0.1	6.1 ± 0.3	6.3 ± 0.1	6.1 ± 0.2
d28	7.2 ± 0.2 ¥	6.9 ± 0.3 ¥	7.0 ± 0.3	6.6 ± 0.3
d56	7.4 ± 0.3 ¥	7.3 ± 0.5 ¥	7.0 ± 0.4	6.8 ± 0.2
LVESD (mm)				
Bsl	2.4 ± 0.1	2.6 ± 0.2	2.8 ± 0.1	3.0 ± 0.2
d1	4.0 ± 0.1	4.1 ± 0.3	4.3 ± 0.1	4.3 ± 0.2
d7	5.0 ± 0.1 ¥	4.0 ± 0.3 *	4.3 ± 0.2 *	3.9 ± 0.2 *
d28	5.7 ± 0.3 ¥	5.0 ± 0.3 *	5.2 ± 0.4 *	4.3 ± 0.3 *
d56	6.0 ± 0.3 ¥	5.5 ± 0.5 *	4.9 ± 0.3 *	4.8 ± 0.1 * $
LVFS (%)				
Bsl	56.6 ± 1.7	49.4 ± 2.0	49.5 ± 1.0	47.1 ± 2.2
d1	29.0 ± 2.4	29.9 ± 2.8	30.4 ± 1.8	27.9 ± 1.9
d7	24.1 ± 0.9	34.1 ± 2.0 *	31.2 ± 2.5	36.9 ± 1.7 ¥ * +
d28	20.2 ± 2.3 ¥	28.0 ± 1.2*	26.7 ± 3.3 *	34.4 ± 1.9 ¥ * + $
d56	19.6 ± 1.5 ¥	25.6 ± 2.9 *	30.8 ± 2.4 *	29.4 ± 1.5 * $
LVEF (%)				
Bsl	87.4 ± 1.5	86.0 ± 1.2	86.8 ± 1.9	88.2 ± 1.5
d1	61.3 ± 4.0	64.6 ± 2.6	64.6 ± 1.8	61.2 ± 2.9
d7	55.7 ± 2.4	68.0 ± 2.3	63.5 ± 3.2	76.0 ± 1.6 ¥ * +
d28	49.0 ± 2.5 ¥	71.7 ± 2.6 *	72.4 ± 1.5 *	76.4 ± 1.5 ¥ *
d56	47.4 ± 2.4 ¥	56.9 ± 4.6	65.4 ± 3.3 *	68.5 ± 2.0 * $

LVESD, left ventricular end-systolic diameter; LVEDD, left ventricular end-diastolic diameter; LVEF, ejection fraction; LVFS, fraction shortening. $^{¥}p<0.05$ compared to Day 1 post-infarction in the same group, one-way repeated measures ANOVA. $*p<0.001$ *vs.* the PBS group, $^{\$}p<0.05$ vs. the hydrogel group and $^{+}p<0.05$ *vs.* the MSC, one-way ANOVA. All values represent mean ± SEM.

Figure
Click here to download high resolution image

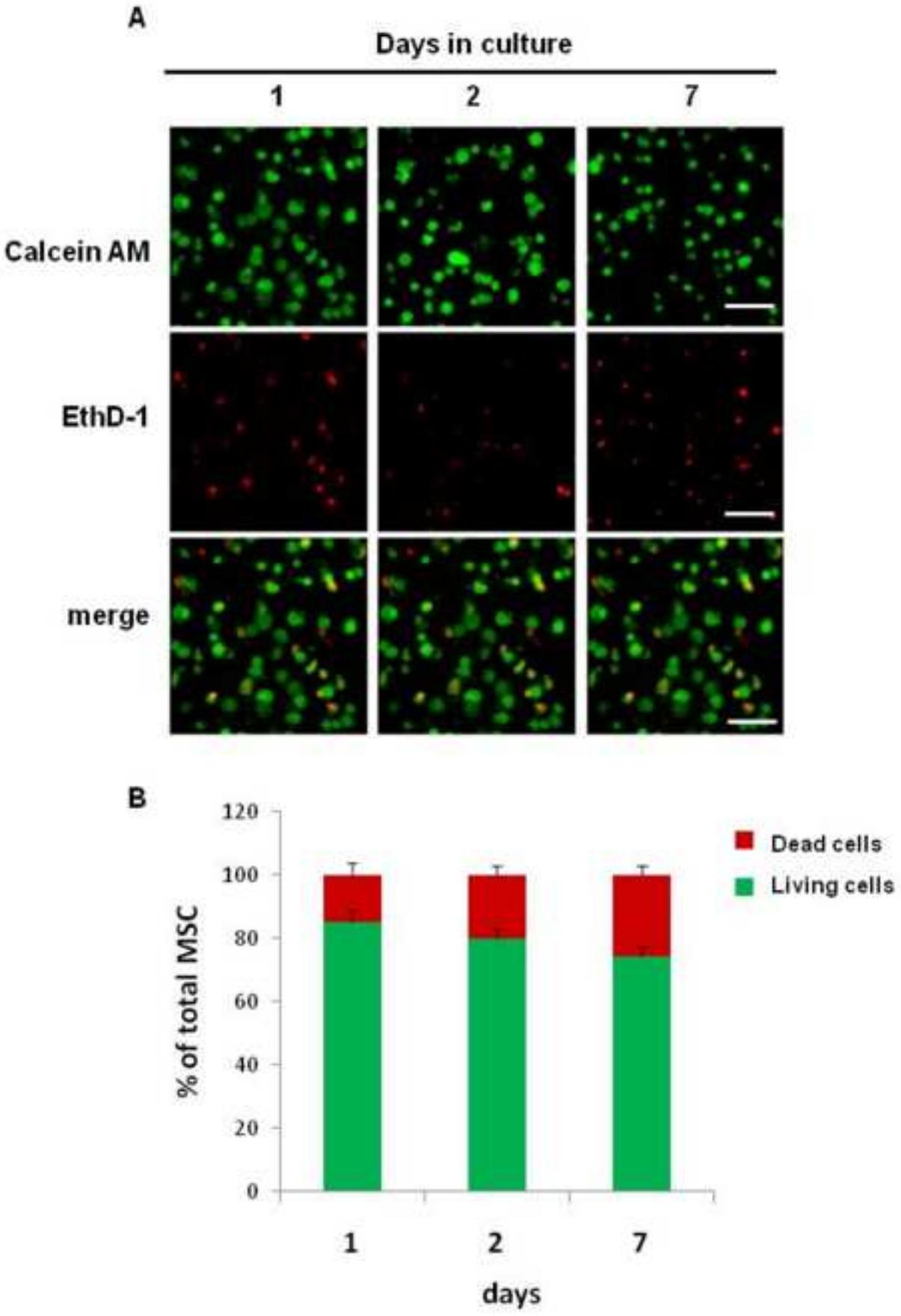

Figure 1

Figure
Click here to download high resolution image

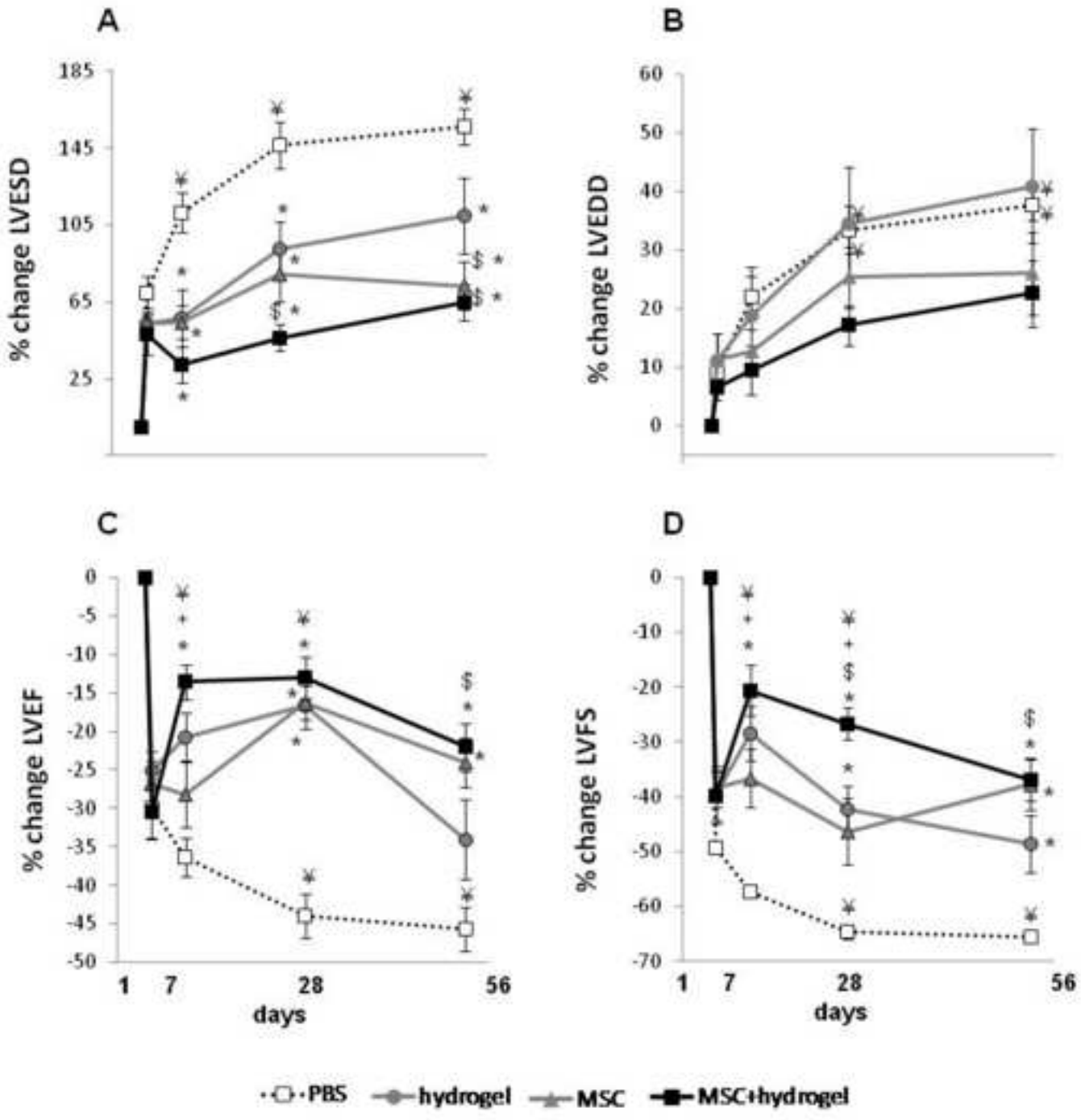

Figure 2

Figure
Click here to download high resolution image

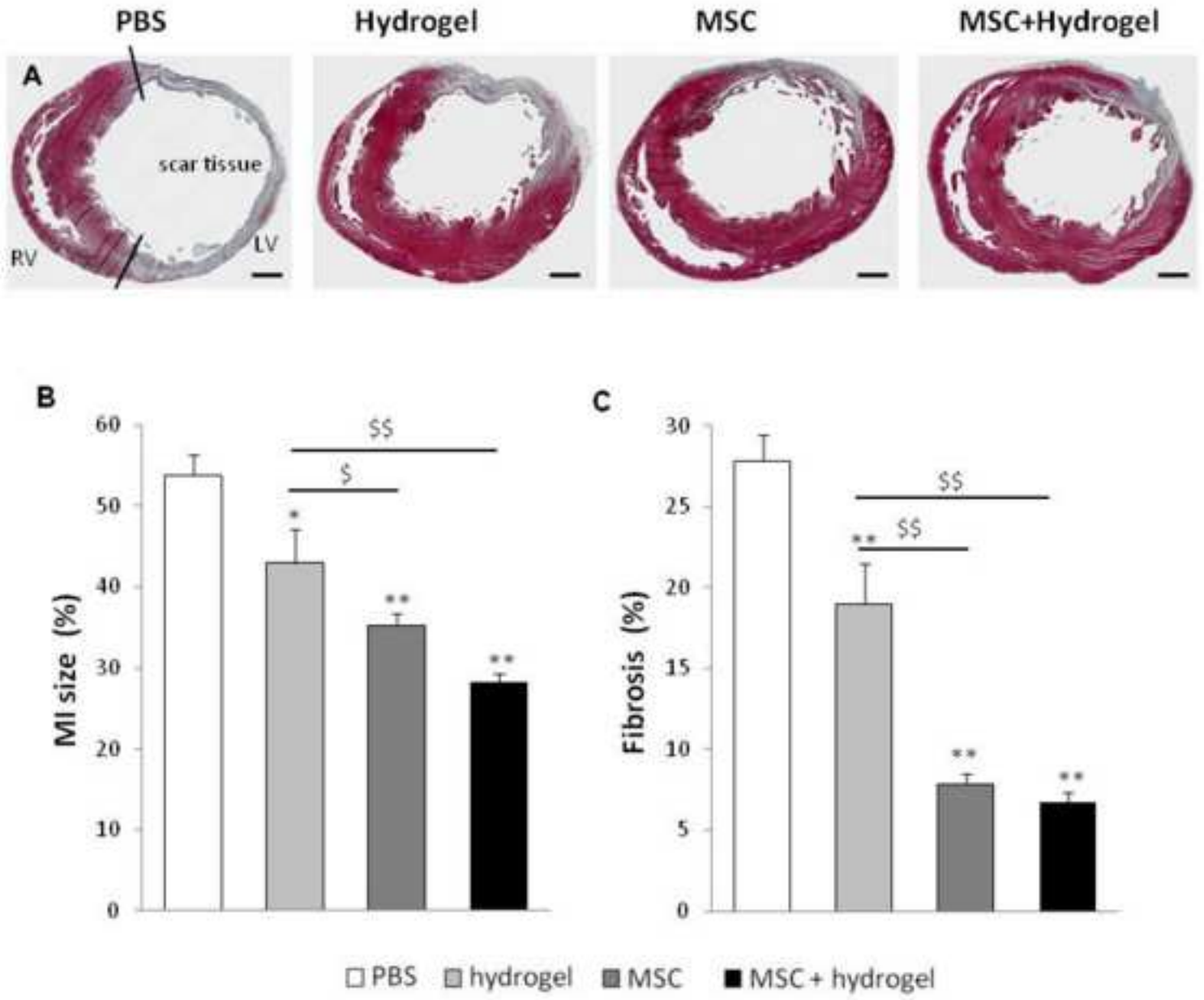

Figure 3

Figure
Click here to download high resolution image

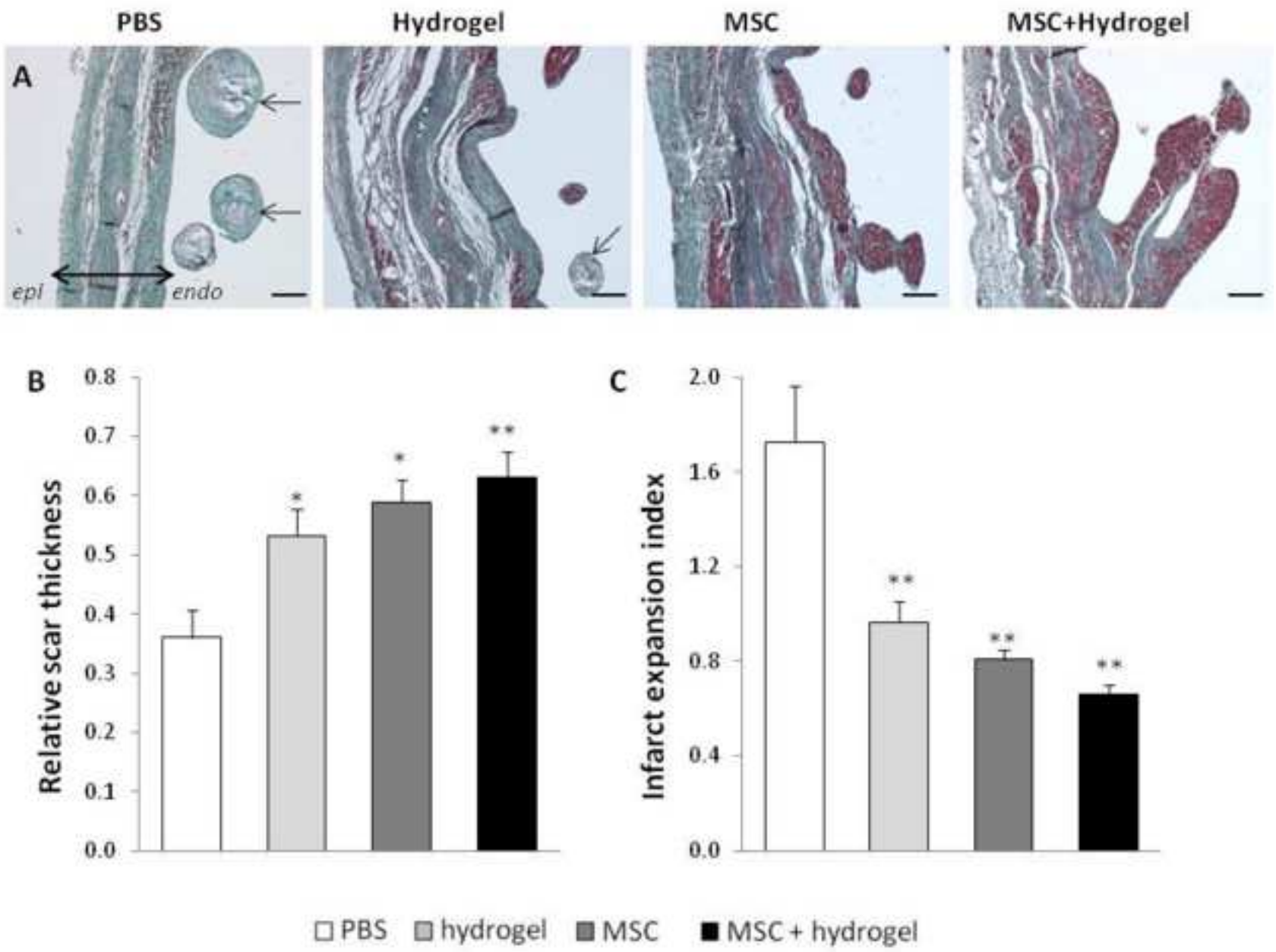

Figure 4

ETUDE 2

Culture en trois dimensions de cardiomyocytes fonctionnels dans un hydrogel dérivé de la cellulose : un outil pour la bio-ingénierie cellulaire et tissulaire cardiaque

- **Publication N°2**

Three-dimensional culture of functional cardiomyocytes in a cellulose derived-hydrogel: A tool for cardiac cell and tissue bioengineering

Eva Mathieu*,* Emilie Rederstorff, Guillaume Lamirault, Philippe Hulin, Virginie Forest, Pierre Weiss, Jérôme Guicheux et Patricia Lemarchand

En cours de soumission dans: *Journal of Molecular and Cellular Cardiology*

- **Brevet**

Silylated biomolecule-based hydrogel for culturing cardiomyocytes and stem cells, and use of the hydrogel thereof for treating heart failure

Eva Mathieu, Pierre Weiss, Jérôme Guicheux et Patricia Lemarchand

Numéro de référence : EP n° 11 305 683.2
Déposants : INSERM, Université de Nantes, CHU de Nantes
Année: 2011

ETUDE 2: Culture en trois dimensions de cardiomyocytes fonctionnels dans un hydrogel dérivé de la cellulose : un outil pour la bio-ingénierie cellulaire et tissulaire cardiaque.

1. Contexte d'étude.

Plusieurs stratégies thérapeutiques pour régénérer le cœur après un infarctus du myocarde (IDM) en utilisant des cellules souches ainsi que l'ingénierie tissulaire se sont considérablement développées ces dix dernières années (Jawad *et al.*, 2007; Kuraitis *et al.*, 2010). Toutefois, avant que ces stratégies puissent remplacer l'arsenal thérapeutique actuel, il apparait nécessaire d'améliorer nos connaissances de base concernant les événements moléculaires physiopathologiques cardiaques. Dans ce contexte et afin de limiter l'utilisation de l'expérimentation animale, le développement de modèles *in vitro* de cardiomyocytes fonctionnels devrait nous permettre d'acquérir de nouvelles connaissances sur la biologie des cellules cardiaques (Athias *et al.*, 2006).

La culture des cardiomyocytes constitue un outil pour l'observation et la compréhension des aspects cellulaires myocardiques non seulement électrophysiologiques et contractiles mais également morphologiques, métaboliques et moléculaires (Athias et al., 2006; Chlopcikova *et al.*, 2001). Le modèle le plus couramment utilisé pour l'étude *in vitro* des cardiomyocytes est la culture en deux dimensions (2D) sur des boîtes de culture en plastique recouvertes d'une fine couche de protéines (collagène, fibronectine, la laminine, et la gélatine) (Sreejit et al. 2008). Bien que ces modèles 2D aient permis d'apporter de nombreuses connaissances concernant la biologie des cellules cardiaques, ils présentent certaines faiblesses intrinsèques, telles que les interactions limitées entre les cellules ainsi que leur morphologie aplatie. Ces limites ont incité le développement de cultures en trois dimensions (3D) basé sur l'utilisation de matrices tridimensionnelles capables de maintenir la viabilité et la fonctionnalité des cellules (Curtis and Russell, 2009).

Dans ce contexte, nous avons utilisé l'hydrogel d'hydroxylpropyl méthylcellulose silanisée (HPMC-Si) afin de mettre au point un modèle de culture 3D des cardiomyocytes. L'objectif de cette étude était d'évaluer la capacité de cet hydrogel à maintenir la viabilité, le phénotype et l'activité contractile des cardiomyocytes.

Pour cela, nous avons évalué la cytocompatibilité de l'hydrogel d'HPMC-Si avec des cardiomyocytes néonataux murins, puis la capacité de cet hydrogel à maintenir leur phénotype. Parmi les modèles de myocytes cardiaques, les cardiomyocytes néonataux restent le modèle de choix en raison de leur capacité de prolifération après dissociation et ensemencement permettant d'obtenir une population homogène de cardiomyocytes *in vitro*. A l'inverse, les cardiomyocytes adultes ne prolifèrent pas et subissent rapidement un processus de dédifférenciation en culture (Pignier *et al.*, 2002). Finalement, nous avons observé les cardiomyocytes battre au sein de l'hydrogel d'HPMC-Si par imagerie et enregistré leur potentiel membranaire à l'aide d'un colorant potentiométrique, le di-8-ANEPPS.

2. Résultats et discussion de l'étude.

Dans cette seconde étude, notre objectif était de développer un modèle d'étude *in vitro* à partir de cardiomyocytes néonataux murins cultivés en 3D dans un hydrogel constitué d'un dérivé de la cellulose, l'hydroxylpropyl méthylcellulose silanisée (HPMC-Si). La mise en place de ce modèle consistait à évaluer si l'hydrogel induisait une modification du comportement des cardiomyocytes. Pour cela, des cardiomyocytes néonataux murins ont été cultivés en 2D au contact de l'hydrogel d'HPMC-Si ou en 3D directement au sein de l'hydrogel. Les observations ont porté sur la viabilité et le phénotype des cardiomyocytes ainsi que sur la capacité de l'hydrogel à permettre l'activité contractile des cardiomyocytes.

Les paramètres physicochimiques de l'hydrogel d'HPMC-Si, tels que sa composition riche en eau, son auto-réticulation à un pH physiologique et sa capacité à permettre la diffusion des nutriments et des gaz, font de cet hydrogel un candidat idéal pour la culture tridimensionnelle de cellules. Plusieurs études montrent l'importance des propriétés élastiques du support de culture sur le comportement des cardiomyocytes cultivés en 2D sur ces matrices, et plus précisément sur la fonctionnalité de leur appareil contractile (Engler *et al.*, 2008; Jacot *et al.*, 2008). De même, d'autres études montrent que l'activité contractile des cardiomyocytes est dépendante de l'élasticité des matrices 3D (Curtis and Russell, 2011; Shapira-Schweitzer and Seliktar, 2007). Nos données sur l'étude mécanique de notre hydrogel d'HPMC-Si montrent que son élasticité est d'environ 300 Pa, suggérant que l'hydrogel d'HPMC-Si peut-être un support de culture 3D pertinent pour la culture de cardiomyocytes fonctionnels. L'hydrogel d'HPMC-Si a déjà été décrit pour être cytocompatible avec des chondrocytes (Vinatier et al., 2005) et des ostéoblastes (Trojani et al., 2005) et plus récemment avec des cellules souches mésenchymateuses (Merceron *et al.*, 2011). Nos données indiquent que l'hydrogel d'HPMC-Si maintient la viabilité des cardiomyocytes. De plus, lorsque les cardiomyocytes sont cultivés au contact de l'hydrogel, leur expression pour les deux facteurs de transcription, Nkx2.5 et Gata-4, requis pour la spécification du phénotype cardiomyogénique (Faustino *et al.*, 2008), n'est pas altérée. Nous avons également observé une expression cohérente de l'alpha actine sarcomérique, composant les structures sarcomériques de l'appareil contractile des cardiomyocytes, et de la connexine 43 qui participe à la formation des jonctions communicantes entre les cellules. En plus du maintien de la viabilité et de l'expression de gènes cardiaques, la capacité de l'hydrogel à permettre une activité contractile physiologique des cardiomyocytes est primordiale.

Eschenhagen et Zimmermann avaient créé une approche intéressante pour l'ingénierie du tissu cardiaque par la culture de cardiomyocytes néonataux de rat en suspension dans des

matrices à base de collagène et de Matrigel (Eschenhagen et al., 1997; Zimmermann *et al.*, 2002b). Dans ces conditions de culture, les cardiomyocytes présentaient une activité contractile et des propriétés éléctrophysiologiques. De la même façon, les cardiomyocytes néonataux murins cultivés en microgouttes suspendues dans l'hydrogel d'HPMC-Si présentent après 48 h de culture une activité contractile spontanée et synchronisée, sans stimulation électrique préalable à l'inverse des autres études.

Après avoir montré que l'hydrogel était cytocompatible avec les cardiomyocytes néonataux murins, qu'il maintenait leur phénotype et leur activité fonctionnelle contractile, il apparaissait intéressant d'évaluer si ce modèle de culture 3D permettait de réaliser des études éléctrophysiologiques des cardiomyocytes. Les méthodes classiques d'éléctrophysiologie, tel que le patch clamp, sont invasives pour la cellule et nécessitent des compétences techniques élaborées (Bursac *et al.*, 1999; Papadaki *et al.*, 2001). En utilisant l'un des colorants fluorescents potentiométriques, le di-8-ANEPPS, nous avons pu observer et enregistrer les variations de potentiels transmembranaires des cardiomyocytes. L'intensité de fluorescence émise par le di-8-ANEPSS est directement proportionnelle à la variation des potentiels membranaires (Hardy *et al.*, 2006; Tian *et al.*, 2011). Nos données indiquent que notre modèle de culture 3D est compatible avec l'utilisation de colorants sensibles au potentiel rendant ainsi possible l'évaluation des effets des agents pharmacologiques à travers un protocole d'imagerie fiable et facile à utiliser.

En résumé, nous avons démontré que l'hydrogel d'HPMC-Si permet la culture de cardiomyocytes fonctionnels battants. En plus de maintenir la viabilité et le phénotype des cardiomyocytes, ce modèle 3D permet également d'effectuer des études électrophysiologiques. Ce système de culture 3D des cardiomyocytes peut être utilisé comme un modèle de criblage pour tester les effets de différentes molécules (facteurs de croissance,

des cytokines, et / ou molécules pro-inflammatoires) ou d'agents pharmacologiques dans des conditions imitant l'environnement du tissu cardiaque. Ce système doit encore être optimisé pour la culture d'autres cellules cardiaques (fibroblastes, cellules endothéliales) ou de cellules souches et pourrait ainsi apporter de nombreuses opportunités d'expérimentation basées sur des stratégies d'ingénierie tissulaire pour la médecine régénérative cardiaque.

3. Résumé de l'article.

Afin d'améliorer nos connaissances de base concernant les événements moléculaires impliqués dans la physiopathologie cardiaque, il apparait essentiel de développer un modèle pertinent et fonctionnel de culture cellulaire cardiaque. De ce fait, nous avons cherché à identifier si un hydrogel constitué d'un dérivé de la cellulose, l'hydroxylpropyl méthylcellulose silanisée (HPMC-Si) pouvait être un outil pertinent pour la culture en trois dimensions (3D) de cardiomyocytes fonctionnels battants. Des cardiomyocytes néonataux murins ont été cultivés au contact de l'hydrogel d'HPMC-Si ou en 3D au sein de l'hydrogel. Après avoir définis les propriétés mécaniques et rhéologiques de l'hydrogel d'HPMC-Si, les observations ont porté sur la capacité de l'hydrogel d'HPMC-Si à maintenir la viabilité, le phénotype et la fonctionnalité des cardiomyocytes. Nos résultats montraient que l'hydrogel d'HPMC-si était cytocompatible avec les cardiomyocytes et qu'il n'altérait pas l'expression de marqueurs cardiogéniques. Les cardiomyocytes possédaient une activité contractile spontanée et synchronisée avec une fréquence de battement par minute de 60.3±5.2 bpm après 48 h de culture en 3D dans l'hydrogel. L'utilisation d'un colorant potentiométrique, le di-8-ANEPPS, a finalement permis d'enregistrer un potentiel membranaire de 408.8±8.6 ms. Ces données suggèrent que l'hydrogel d'HPMC-Si est un support pertinent pour la culture 3D de cardiomyocytes fonctionnels battants. Ce modèle de culture constitue un outil très utile pour l'observation et la compréhension des aspects cellulaires myocardiques non seulement éléctrophysiologiques et contractiles mais également morphologiques, métaboliques et moléculaires et pourrait apporter ainsi de nombreuses opportunités d'expérimentation basées sur des stratégies d'ingénierie tissulaire pour la médecine régénérative cardiaque.

Three-dimensional culture of functional cardiomyocytes in a cellulose derived-hydrogel: a tool for cardiac cells and tissue bioengineering

Mathieu E [1, 2], Rederstorff E [2, 3], Lamirault G [1, 2, 4], Hulin P [2, 5] , Forest V [1, 2], Weiss P [2, 3, 4] , Guicheux J [2, 3 *,$] and Lemarchand P [1, 2, 4 $].

[$]Both authors contributed equally.

[1] INSERM, U915, l'institut du thorax, Nantes, F-44007, France.

[2] Université de Nantes, Institut Fédératif de Recherche thérapeutique 26 (IFR26), Nantes, F-44000 France.

[3] INSERM, U791, Laboratory of Osteo-Articular and Dental Tissue Engineering, Group STEP "Skeletal tissue Engineering and Physiopathology", Nantes, F-44042, France.

[4] CHU de Nantes, Nantes, F-44000, France.

[5] Service d'Anatomie Pathologique, E.A. Biometadys, CHU de Nantes, Nantes, F-44000, France.

[6] Cellular and Tissular Imaging Core Facility of Nantes University (MicroPICell), Nantes, F-44007, France.

[*]Corresponding author: Jérôme Guicheux

INSERM UMR791, School of Dental Surgery, 1 Place Alexis Ricordeau, 44042 Nantes cedex 1, France.

Phone (office): +33-(0)2-40412919 Fax: +33-(0)2-40083712

E-mail address: Jerome.guicheux@inserm.fr

Abstract

To improve our understanding of the molecular events involved in cardiac physiopathology, the development of functionally relevant model of cardiac cell culture remains a crucial prerequisite. We therefore sought to decipher whether a hydrogel made of silanized hydroxypropyl methylcellulose (Si-HPMC) may be a useful tool for the *in vitro* three dimensions (3D) culture of functional beating cardiomyocytes. Neonatal murine cardiomyocytes were cultured in contact with Si-HPMC hydrogel or three dimensionally within the hydrogel. After having defined the mechanical and rheological properties of our Si-HPMC hydrogel, we evaluated the ability of Si-HPMC to maintain the viability, phenotype and functionality of cultured cardiomyocytes. Our results show that the Si-HPMC hydrogel was cytocompatible with cardiomyocytes and that it did not alter the expression of cardiogenic markers. Cardiomyocytes exhibited a spontaneous and synchronized contractile activity with frequency of 60.3 ± 5.2 bpm after 48 h of culture within the Si-HPMC hydrogel. Finally, using a potentiometric dye, di-8-ANEPPS, a membrane potential of 408.8 ± 8.6 ms was registered. These data strongly suggest that Si-HPMC hydrogel is a relevant support for the 3D culture of functional beating cardiomyocytes. This 3D culture of functional cardiomyocytes in a cellulose derived-hydrogel may be a very useful tool for the observation and the understanding of cellular aspects of the electrophysiological, contractile, morphological, metabolic and molecular properties of myocardium in a microenvironment that closely mimics cardiac tissue.

1. Introduction.

Cardiovascular disease remains the leading cause of death in the Western world and myocardial infarction is one of the primary facets of this disease [1, 2]. Several therapeutic strategies to regenerate injured heart using adult stem cells and pluripotent stem cells, cellular reprogramming and tissue engineering have recently been contemplated with a growing interest [3-5]. However, before these strategies may enter the therapeutic arsenal of cardiac surgeons, it remains necessary to improve our basic knowledge's regarding the molecular events involved in cardiac physiopathology. In this context and to limit the use of animal experiments, the development of *in vitro* models of functional cardiomyocytes may help gain new insights into the biology of cardiac cells [6, 7]. The cultures of cardiomyocytes thus represent a very useful tool for the observation and the understanding of the cellular aspects of the electrophysiological, contractile, morphological, metabolic and molecular properties of the myocardium [8, 9]. The most commonly used model for the *in vitro* study of cardiomyocytes is the two-dimensional (2D) culture of cells on plastic culture dishes coated with a thin layer of proteins (collagen, fibronectin, laminin, and gelatin) [10]. Although these 2D models have provided significant progress in the biology of cardiac cells, they exhibit certain intrinsic weaknesses. These 2D models indeed allow only limited cell-cell and cell-matrix interaction and confer a flattened morphology to cells. These limitations have prompted the development of three-dimensional (3D) models [11] based on the use of scaffolding matrices able to support cell viability, growth and functions. These 3D biomaterials-assisted cell culture systems are likely to be more relevant for mimicking *in vivo* situations through the control of concentration gradients of signaling molecules, composition and structure of extracellular matrix (ECM) around the cells, as well as morphology and arrangement of individual cells [12]. Different types of matrices have been used to create these 3D models including synthetic or natural hydrogels. Indeed, hydrogels, in addition to

being relevant cell carrier for in vivo transplantation [13-17], also exhibit physicochemical properties that are adapted to their use as scaffolding support for cell culture including their ability to cross-link, nutrient permeability and high water content [18, 19]. Recently, it has been described that hydrogel made of silanized hydroxypropyl methylcellulose (Si-HPMC) could be an adapted scaffolding matrix for the in vivo transplantation of chondrogenic cells in articular cartilage defects (Vinatier et al 2009, biotechnol bioeng). In the present work, we sought to decipher whether such a cellulose derivative hydrogel may be a useful tool for the *in vitro* 3D culture of functional beating cardiomyocytes.

To address this issue, we first assessed the cytocompatibility of Si-HPMC hydrogel with neonatal cardiomyocytes. Next, we cheked whether cardiomyocytes maintain their cardiogenic phenotype when cultured in contact with Si-HPMC. Finally, the physiological functions of 3 dimensionally cultured cardiomyocytes within Si-HPMC were assessed by imaging cell beating and recording membrane potential.

2. Materials and Methods.

2.1. Preparation of cultured neonatal mouse ventricular myocytes.

Primary ventricular myocytes were isolated from 1- to 2-day-old C57Bl/6j mice hearts (Janvier, France) by an established method [10], with minor modifications. Briefly, hearts were quickly excised, the atria were cut off, then the ventricles were minced and digested repeatedly (10min x 8) in HBSS solution (Invitrogen corporation, Paisley, U.K.) supplemented with collagenase II (100µg/ml) and pancreatin (1X) (Invitrogen) at 37°C.To reduce the contribution of nonmyocardial cells, cells are plated for 1 h. Myocytes were cultured in Dulbecco's modified Eagle's medium (Invitrogen) containing 10% horse serum (Invitrogen), 5% fetal bovine serum (Hyclone Perbio, Thermo Fisher Scientific), and 1% penicillin/streptomycin (Invitrogen).

2.2. Silanized hydroxypropyl methylcellulose-based hydrogel preparation.

Synthesis of Si-HPMC hydrogel.

Hydroxypropyl methylcellulose (HPMC E4M®) was purchased from Colorcon-Down chemical (Bougival, France). Si-HPMC was synthesized by mixing silicium 0.5% (w/v) with HPMC to form a heterogeneous medium, as previously described [20]. Si-HPMC was solubilized in 0.2M NaOH (3%) under constant stirring for 48h at room temperature. The solution was dialyzed against 0.09 M NaOH using 6–8 kDa dialysis tubes (SpectraPor 1, Thermo Fisher Scientific, France). The resulting viscous solution (pH 12.6) was sterilized by autoclaving and then mixed using luer-lock syringes with sterile 4-(2-hydroxyethyl)-1-piperazineethanesulfonic acid buffer (HEPES, pH 3.6; Sigma-Aldrich, St Louis, USA) at a volume ratio of 1:1 as previously described [20]. The final product was a hydrogel (pH 7.4) containing 1.5% Si-HPMC.

Rheological and mechanical measurements.

Cross-linking of 1 ml Si-HPMC hydrogel was induced in 12-well plates. Dynamic rheological measurements were performed with a rotational rheometer (Rheostress 300, ThermoHaake®, Germany) using a coni-cylindrical geometry with a diameter of 60 mm and a cone angle of 1°. A multi-wave procedure was performed with 3 frequencies of 1, 3.2 and 10 Hz, with an imposed stress of 1 Pa. Oscillation tests measuring storage modulus (G') and loss modulus (G'') were performed to study the self-setting process and gel point. Gel points, given as the time taken for the liquid (G''>G') to turn into a solid (G'>G''), were evaluated according to the derived percolation theory [21]. Shear strain measurements were performed on 9 samples with a Haake mars. Frequencies were applied at a fixed total shear stress (1Pa) and 0.21N. Oscillation tests were performed to measure G' and G'' after 3 weeks of gelation. The Si-HPMC hydrogel compressive modulus was measured using a TA HD-Plus (Stable Micro Systems). Six samples were tested after three weeks of cross-linking and the compressive modulus was calculated on the basis of strain change from 0 to 5%.

2.3. Two dimensional culture of cardiomyocytes in contact with Si-HPMC hydrogel.

The myocyte-enriched cells remaining in suspension were plated at a density of 55 000 cells/cm^2 in 24-well plates precoated with 10µg/ml laminin (Sigma-Aldrich, St-Louis, USA). After 48 h, culture medium was removed and 500 µl of Si-HPMC hydrogel were added in each well. Samples were incubated at 37 °C for 1 h before adding 500 µl of culture medium.

2.4. Cardiomyocyte viability.

To determine the cytotoxicity of Si-HPMC hydrogel, mitochondrial activity of primary cardiomyocytess was measured using the Methyl Tetrazolium Salt (MTS) test (Promega,

USA). After 24 h and 48 h, hydrogel and culture media were removed and the MTS solution was added in each well for 1 to 3 h according to the manufacturer's instructions. As a control, cells were also cultured in the absence of Si-HPMC hydrogel or in the presence of actinomycin-D (5 mg/ml) (Sigma-Aldrich), an inhibitor of RNA polymerase used as a potent inducer of cell death. Finally, colorimetric measurement was performed on a spectrophotometer at an optical density of 490 nm. Each condition was tested in quadruplicate and the results were expressed as relative MTS activities as compared to the positive control (cells cultured without hydrogel).

2.5. Gene expression analysis by real-time PCR.

To determine whether the Si-HPMC hydrogel may influence the gene expression of cardiomyocytes, total RNA of cardiomyocytes was isolated and treated with DNAse 1 (Qiagen S.A., France) after 1, 2 and 5 days, of culture without or in contact with hydrogel. First-strand cDNA was synthetized from 2 µg of total RNA using the High-capacity cDNA Archive kit (Applied Biosystems, life technologies corporation, USA). PCR reactions were then performed on TaqMan using the ABI 7900HT Sequence Detection System (Applied Biosystems). The following genes were selected for their cardiac expression and following TaqMan primers designed by Applied Biosystems: nkx2.5 (nkx2.5, Mm00657783_m1), gata4 (gata4, Mm00484689_m1), actin alpha cardiac muscle 1 (actc1, Mm01333821_m1), gap junction protein alpha 1 (gja1, Mm00439105_m1). Data were collected with instrument spectral compensation by the Applied Biosystems SDS 2.1 software and analyzed using the threshold cycle (Ct) relative-quantification method [22]. The hypoxanthine guanine phosphoribosyl transferase 1 (hprt1, Mm03024075_m1) was used as gene for data normalization. The relative expression of each gene *versus* hprt was calculated for each sample (ΔCt).

2.6. Fluorescent staining of cardiomyocytess.

After 48h of culture with or without hydrogel, cardiomyocytes were fixed in 4% formaldehyde for 30 min at room temperature and permeabilized with 0.2% Triton X-100 (Sigma) in BSA/PBS. Cells were labeled for 1h at room temperature with primary antibodies murine for polyclonal nkx2.5 (polyclonal, Santa Cruz Biotechnology, USA) dilued 1/500 in 1% BSA/PBS, gata4 (polyclonal, Santa Cruz Biotechnology) dilued 1/500 in 1% BSA/PBS, connexin 43 (monoclonal, Millipore) dilued 1/100 in 1% BSA/PBS and sarcomeric alpha actin (monoclonal, Millipore) dilued 1/1000 in 1% BSA/PBS. After 3 PBS washes, species compatible Alexa Fluor IgG secondary antibodies (Molecular Probes, Leiden, The Netherlands) diluted 1/1000 were added for 45 min. Cells were then rinsed with PBS and stored Vectaschield® medium with DAPI nuclear (vector laboratories, US. Headquaters). Fluorescence was captured using Zeiss Axioskop2 with equal exposure times.

2.7. Three-dimensional culture of cardiomyocytes within the Si-HPMC hydrogel.

After cross-linking of Si-HPMC hydrogel onto glass-bottom dishes (LabTekII) droplets of 10 µl containing 50 000 cardiomyocytess and culture medium were seeded in microdoplets within the hydrogel. The resulting samples were immersed in 2 ml complete medium and incubated at 37°C.

2.8. Record of cardiomyocytes beating in 3D culture.

The beating of cardiomyocytes cultivated in 3D within the Si-HPMC hydrogel were observed with the Nikon A1R confocal laser-scanning microscope (Nikon France) in resonant mode (30 frames/sec) using reflective protocol. Clusters beating cardiomyocytes are recorded using x20 and with 7 steps size of 5 µm (Nikon A1 Piezo drive). Four dimensional (4D) representation of beating cardiomyocytes is performed with NIS-element AR software.

2.9. Optical recordings of membrane potentials of cardiomyocytes in 3D culture.

Myocytes were loaded with the potentiometric dye di-8-ANEPPS at a concentration of 10 µM for 10 min at 37°C, prior to washing in normal Tyrode. The optical signal from a single cardiomyocyte is recorded by the Nikon A1R confocal laser-scanning microscope (Nikon France) in resonant mode (60 frames/sec). Myocytes were excited with Argon laser at 488nm. The emission was collected using à x60 oil immersion objective (NA=1.4, Nikon) between 650-700 nm with a photomultiplier. The variations in fluorescence intensity are observed using the NIS-element software.

2.10. Statistical analysis.

Results are expressed as mean ± SEM. Comparative studies of means were performed by using one-way ANOVA followed by post-hoc test (Fisher's projected least significant difference) with a statistical significances at $p<0.05$.

3. Results.

3.1. Rheological characteristics of Si-HPMC hydrogel.

The final product (Si-HPMC hydrogel) was a reticulated hydrogel with a pH value of 7.4 after 29.4±4.3 min. Dynamic rheological measurements were performed to characterize the Si-HPMC hydrogel, including shear strain measurements to evaluate the storage modulus (G', which characterizes the hard component), and the loss modulus (G'', which characterizes the liquid component). After three weeks of cross-linking and completion of the self-setting process, the G' value was 323.2±104.5 Pa and the G'' was 42.8±12.3 Pa. The compressive modulus (which reflects the stiffness of the material in a compressive experiment) at a 5% strain was 319.6±67.0 Pa.

3.2. Cytocompatibility of Si-HPMC hydrogel with cardiomyocytes.

To determine whether Si-HPMC hydrogel was not cytotoxic, the viability of cardiomyocytes cultured in contact with Si-HPMC was examined through a measurement of MTS activity after 24h and 48h of culture. Cardiomyocytes alone were used as positive controls. The results (Fig. 1) show that Si-HPMC did not affect MTS activity of cardiomyocytess after 24h and 48h of culture. On the contrary, actinomycin-D treatment reduced the MTS activity of cardiomyocytes by nearly 60% as early as 24h of treatment and by 90% after 48h of treatment. These results indicate that Si-HPMC hydrogel has no adverse effects on mitochondrial activity of cardiomyocytes.

3.3. Maintenance of cardiomyocyte phenotype in contact with the Si-HPMC hydrogel.

To assess whether Si-HPMC hydrogel allows the maintenance of a cardiomyocyte phenotype, cardiomyocytess were cultured for 5 days either in two dimensions (2D) without hydrogel or in contact with Si-HPMC hydrogel. The expressions of transcripts coding for two transcription factors, nkx2.5 and gata-4, the connexin 43 and the sarcomeric alpha actin were evaluated by real time PCR (Fig. 2). The results show that the presence of the Si-HPMC hydrogel did not alter the expression levels of these genes during the 5 days of culture.

To further analyse the expression and localization of proteins nkx2.5, gata4, Connexin 43 and sarcomeric alpha actin were observed by immunofluorescence staining after 48 hours of culture (Fig. 3). The expression of both transcription factors nkx2.5 (Fig. 3a) and gata-4 (Fig 3b) were maintained in the nuclei of cardiomyocytess cultured in the presence of hydrogel, as well as membrane expression of connexin 43. Staining for sarcomeric α-actin revealed typical sarcomeric striations in cardiomyocytess cultured in presence or absence of hydrogel.

Considered together, these results indicate that Si-HPMC hydrogel has no adverse effects on cardiomyocyte phenotype.

3.4. Sponteneous contraction of cardiomyocytes-seeded hydrogel.

Cardiomyocytes seeded in microdroplets within the Si-HPMC hydrogel were observed using live cell imaging. After 48 h of culture, most of cardiomyocytes in 3D had a round morphology (Fig.4). Few cells exhibited an elongated shape. Spontaneous and synchronized contractions of cardiomyocytes seeded within hydrogel were observed after 48 h of culture (see Supplementary video1) with a beating activity of 60.3±5.2 bpm at 37°C.

3.5. Optical recording of membrane potential in individual cardiomyocytes within the Si-HPMC hydrogel.

Cardiomyocytes were loaded with the potentiometric dye di-8-ANEPPS and observed by confocal image (Fig. 5A). This dye was mainly localized in the membrane of cells. The optical signal from a single cardiomyocyte was shown as the change in fluorescence intensity (Fig.5B). The sample recordings of the optical signals were recorded in response to an action potential in a single cardiomyocyte. We have recorded the optical action potentials of several cardiomyocytes with different morphologies (round or elongated). The result showed that the membrane potentials had a period of 408.8±8.6 ms at 37°C (n=17).

4. Discussion.

Understanding the molecular and cellular events occurring during and after cardiac injury is critical to improve the efficacy of future therapies [5, 23]. In this context, the development of *in vitro* models of functional cardiomyocytes is likely to be crucial and may help gain new insights into the biology of cardiac cells [7, 24]. In this study, we sought to

decipher whether a cellulose derivative hydrogel may be a useful tool for the *in vitro* tree-dimensional (3D) culture of functional beating cardiomyocytes.

The physicochemical parameters of Si-HPMC hydrogel such as, its high level of water content, its self-crosslinking at physiological pH and its ability to allow the diffusion of nutrients and gases, make it an ideal candidate for 3D cell culture. Several studies show the importance of the extracellular matrix stiffness on the behavior of cardiomyocytes cultured in 2D, especially on the functionality of their contractile apparatus [25, 26]. Similarly, the contraction amplitude of cultured cardiomyocyte strongly depends on the stiffness of the scaffolding 3D matrices [24, 27, 28]. Consistently, our mechanical data show that Si-HPMC hydrogel exhibits a stiffness value of about 300 Pa, thereby strongly suggesting that Si-HPMC may be an appropriate scaffolding support for the contractile activity of cardiomyocytes.

Among the models of cardiac myocytes, neonatal cardiomyocytes remains the model of choice because of their proliferation ability after dissociation and seeding that makes possible to obtain an *in vitro* homogenous population of cardiomyocytes. On the contrary, adult cardiomyocytes are widely recognized to be nonproliferative cells that undergo a rapid process of dedifferentiation in culture [29]. Along these lines, whereas Si-HPMC hydrogel has been largely described as being cytocompatible with both osteogenic [30] and chondrogenic cells [31], its cytocompatibility with respect to neonatal cardiomyocytes has not yet been documented. Our data have addressed this issue and convincingly indicate that Si-HPMC hydrogel supports the 3D viability of neonatal murine cardiomyocytes. In addition, when neonatal murine cardiomyocytes were cultured in contact with the hydrogel, their expression of two transcription factors, Nkx2.5 and Gata-4, required for the specification of cardiomyogenic phenotype [32] was not altered. We also observed a consistent expression of the sarcomeric alpha actin structures, one of the major components of the contractile apparatus of cardiomyocytes, and connexin 43, involved in the formation of gap junctions

between cells. In addition to maintaining the viability and the expression of cardiac genes, the ability of the hydrogel to allow a physiological contractile activity of cardiomyocytes is essential. Eschenhagen and Zimmermann established an effective approach to cardiac tissue engineering by the cultivation of neonatal rat heart cells in collagen gel and Matrigel. Under these conditions, cardiomyocytes exhibited an electrically-induced contractile activity [14, 15]. Interestingly, neonatal murine cardiomyocytes cultured in microdroplets within the Si-HPMC hydrogel exhibit a spontaneous and synchronized contractile activity without electrical stimulation.

After having demonstrated that Si-HPMC hydrogel is cytocompatible with neonatal murine cardiomyocytes, it maintains their phenotype and functional contractile activity, it appears interesting to evaluate whether our 3D model also allows the characterization of some electrophysiological parameters of cardiomyocytes. Conventional electrophysiological techniques, such as patch clamp, are invasive for the cell and require strong technical skills [6, 33]. The application of potential-sensitive dyes to isolated cardiomyocytes may prove useful in the study of electrical activity [34, 35]. In our study, we have used fluorescence microscopy to record the membrane potential from single isolated neonatal murine cardiomyoctes labeled with the potential sensitive dye di-8-ANEPPS. The optical signals obtained with di-8-ANEPPS are able to resolve the changes in voltage during a ventricular cardiac action potential, and the change in fluorescence intensity is linearly related to membrane potential over the full range of the cardiac action potential [34, 35]. Our data indicate that our 3D culture model is compatible with the use of potential sensitive dyes thereby making possible the evaluation of the effects of pharmacological agents through a reliable and easy-to-use imaging protocol.

In summary, we have demonstrated that Si-HPMC hydrogel makes possible the culture of functional beating cardiomyocytes. In addition to maintaining the viability and

phenotype of cardiomyocytes, this 3D model also allows to perform electrophysiological studies. This 3D culture system of cardiomyocytes can be used as a novel screening model to test the effects of various molecules (cytokines, growth factors and/or pro-inflammatory molecules) or pharmacological agents in conditions closely mimicking the cardiac tissue environment. Whilst this system still needs to be optimized for the culture of other cardiac cells (fibroblasts, endothelial cells) or stem cells, it could likely provide many experimental opportunities for the practical advancement of tissue engineered-based strategies for cardiac regenerative medicine.

Acknowledgements.

This work was supported by grants from INSERM (Institut National de la Santé et la Recherche Médicale) and « Fondation de l'Avenir ». Eva Mathieu received a fellowship from the French Ministry of Research and Technology. The authors gratefully thank the platform MicroPiCell and "Unité Thérapeutique Expérimentale". We also thank members of STEP group "Skeletal Tissue Engineering and Physiopathology" for helpful suggestions, Joanna Ashton-Chess for critically reading the manuscript and Béatrice Delasalle for her help with statistical analyses.

References.

[1] Fuster V, Kelly BB, Vedanthan R. Global cardiovascular health urgent need for an intersectoral approach. J Am Coll Cardiol. 2011 Sep 13; 58(12): 1208-10.

[2] Roger VL, Go AS, Lloyd-Jones DM, Adams RJ, Berry JD, Brown TM, et al. Heart disease and stroke statistics--2011 update: a report from the American Heart Association. Circulation. 2011 Feb 1; 123(4): e18-e209.

[3] Jawad H, Ali NN, Lyon AR, Chen QZ, Harding SE, Boccaccini AR. Myocardial tissue engineering: a review. J Tissue Eng Regen Med. 2007 Sep-Oct; 1(5): 327-42.

[4] Kuraitis D, Suuronen EJ, Sellke FW, Ruel M. The future of regenerating the myocardium. Curr Opin Cardiol. 2010 Nov; 25(6): 575-82.

[5] Vunjak-Novakovic G, Tandon N, Godier A, Maidhof R, Marsano A, Martens TP, et al. Challenges in cardiac tissue engineering. Tissue Eng Part B Rev. 2010 Apr; 16(2): 169-87.

[6] Bursac N, Papadaki M, Cohen RJ, Schoen FJ, Eisenberg SR, Carrier R, et al. Cardiac muscle tissue engineering: toward an in vitro model for electrophysiological studies. Am J Physiol. 1999 Aug; 277(2 Pt 2): H433-44.

[7] Athias P, Vandroux D, Tissier C, Rochette L. [Development of cardiac physiopathological models from cultured cardiomyocytes]. Ann Cardiol Angeiol (Paris). 2006 Apr; 55(2): 90-9.

[8] Akins RE, Jr., Rockwood D, Robinson KG, Sandusky D, Rabolt J, Pizarro C. Three-dimensional culture alters primary cardiac cell phenotype. Tissue Eng Part A. 2010 Feb; 16(2): 629-41.

[9] Chlopcikova S, Psotova J, Miketova P. Neonatal rat cardiomyocytes--a model for the study of morphological, biochemical and electrophysiological characteristics of the heart. Biomed Pap Med Fac Univ Palacky Olomouc Czech Repub. 2001 Dec; 145(2): 49-55.

[10] Sreejit P, Kumar S, Verma RS. An improved protocol for primary culture of cardiomyocyte from neonatal mice. In Vitro Cell Dev Biol Anim. 2008 Mar-Apr; 44(3-4): 45-50.

[11] Elliott NT, Yuan F. A review of three-dimensional in vitro tissue models for drug discovery and transport studies. J Pharm Sci. 2011 Jan; 100(1): 59-74.

[12] Yoshioka J, Prince RN, Huang H, Perkins SB, Cruz FU, MacGillivray C, et al. Cardiomyocyte hypertrophy and degradation of connexin43 through spatially restricted autocrine/paracrine heparin-binding EGF. Proc Natl Acad Sci U S A. 2005 Jul 26; 102(30): 10622-7.

[13] Zimmermann WH, Fink C, Kralisch D, Remmers U, Weil J, Eschenhagen T. Three-dimensional engineered heart tissue from neonatal rat cardiac myocytes. Biotechnol Bioeng. 2000 Apr 5; 68(1): 106-14.

[14] Zimmermann WH, Schneiderbanger K, Schubert P, Didie M, Munzel F, Heubach JF, et al. Tissue engineering of a differentiated cardiac muscle construct. Circ Res. 2002 Feb 8; 90(2): 223-30.

[15] Eschenhagen T, Fink C, Remmers U, Scholz H, Wattchow J, Weil J, et al. Three-dimensional reconstitution of embryonic cardiomyocytes in a collagen matrix: a new heart muscle model system. FASEB J. 1997 Jul; 11(8): 683-94.

[16] Kofidis T, Akhyari P, Boublik J, Theodorou P, Martin U, Ruhparwar A, et al. In vitro engineering of heart muscle: artificial myocardial tissue. J Thorac Cardiovasc Surg. 2002 Jul; 124(1): 63-9.

[17] Kelm JM, Ehler E, Nielsen LK, Schlatter S, Perriard JC, Fussenegger M. Design of artificial myocardial microtissues. Tissue Eng. 2004 Jan-Feb; 10(1-2): 201-14.

[18] Ye Z, Zhou Y, Cai H, Tan W. Myocardial regeneration: Roles of stem cells and hydrogels. Adv Drug Deliv Rev. 2011 Mar 1.
[19] Lutolf MP, Hubbell JA. Synthetic biomaterials as instructive extracellular microenvironments for morphogenesis in tissue engineering. Nat Biotechnol. 2005 Jan; 23(1): 47-55.
[20] Bourges X, Weiss P, Daculsi G, Legeay G. Synthesis and general properties of silated-hydroxypropyl methylcellulose in prospect of biomedical use. Adv Colloid Interface Sci. 2002 Dec 2; 99(3): 215-28.
[21] Fatimi A, Tassin JF, Turczyn R, Axelos MA, Weiss P. Gelation studies of a cellulose-based biohydrogel: the influence of pH, temperature and sterilization. Acta Biomater. 2009 Nov; 5(9): 3423-32.
[22] Livak KJ, Schmittgen TD. Analysis of relative gene expression data using real-time quantitative PCR and the 2(-Delta Delta C(T)) Method. Methods. 2001 Dec; 25(4): 402-8.
[23] Segers VF, Lee RT. Stem-cell therapy for cardiac disease. Nature. 2008 Feb 21; 451(7181): 937-42.
[24] Shapira-Schweitzer K, Habib M, Gepstein L, Seliktar D. A photopolymerizable hydrogel for 3-D culture of human embryonic stem cell-derived cardiomyocytes and rat neonatal cardiac cells. J Mol Cell Cardiol. 2009 Feb; 46(2): 213-24.
[25] Jacot JG, McCulloch AD, Omens JH. Substrate stiffness affects the functional maturation of neonatal rat ventricular myocytes. Biophys J. 2008 Oct; 95(7): 3479-87.
[26] Engler AJ, Carag-Krieger C, Johnson CP, Raab M, Tang HY, Speicher DW, et al. Embryonic cardiomyocytes beat best on a matrix with heart-like elasticity: scar-like rigidity inhibits beating. J Cell Sci. 2008 Nov 15; 121(Pt 22): 3794-802.
[27] Shapira-Schweitzer K, Seliktar D. Matrix stiffness affects spontaneous contraction of cardiomyocytes cultured within a PEGylated fibrinogen biomaterial. Acta Biomater. 2007 Jan; 3(1): 33-41.
[28] Curtis MW, Sharma S, Desai TA, Russell B. Hypertrophy, gene expression, and beating of neonatal cardiac myocytes are affected by microdomain heterogeneity in 3D. Biomed Microdevices. 2010 Dec; 12(6): 1073-85.
[29] Pignier C, Ancey C, Fares N, Bescond J, Potreau D. Reexpression of the nifedipine-resistant calcium channel during dedifferentiation of adult rat ventricular cardiomyocytes. J Cardiovasc Electrophysiol. 2002 Feb; 13(2): 178-83.
[30] Trojani C, Weiss P, Michiels JF, Vinatier C, Guicheux J, Daculsi G, et al. Three-dimensional culture and differentiation of human osteogenic cells in an injectable hydroxypropylmethylcellulose hydrogel. Biomaterials. 2005 Sep; 26(27): 5509-17.
[31] Vinatier C, Magne D, Weiss P, Trojani C, Rochet N, Carle GF, et al. A silanized hydroxypropyl methylcellulose hydrogel for the three-dimensional culture of chondrocytes. Biomaterials. 2005 Nov; 26(33): 6643-51.
[32] Faustino RS, Behfar A, Perez-Terzic C, Terzic A. Genomic chart guiding embryonic stem cell cardiopoiesis. Genome Biol. 2008; 9(1): R6.
[33] Papadaki M, Bursac N, Langer R, Merok J, Vunjak-Novakovic G, Freed LE. Tissue engineering of functional cardiac muscle: molecular, structural, and electrophysiological studies. Am J Physiol Heart Circ Physiol. 2001 Jan; 280(1): H168-78.
[34] Hardy ME, Lawrence CL, Standen NB, Rodrigo GC. Can optical recordings of membrane potential be used to screen for drug-induced action potential prolongation in single cardiac myocytes? J Pharmacol Toxicol Methods. 2006 Sep-Oct; 54(2): 173-82.
[35] Tian Q, Oberhofer M, Ruppenthal S, Scholz A, Buschmann V, Tsutsui H, et al. Optical action potential screening on adult ventricular myocytes as an alternative QT-screen. Cell Physiol Biochem. 2011; 27(3-4): 281-90.

Figure captions

Fig.1. Cardiomyocyte viability. Cardiomyocytess were cultured in 2-D without hydrogel (control), in contact with Si-HPMC hydrogel or in the presence of the actinomycin-D (5µg/ml) during 24h and 48h. Viability was assessed by MTS activity. Results were expressed as relative MTS activities as compared to the positive control (cells cultured without hydrogel).*P<0.001 as compared to control conditions.

Fig.2. Gene expression in cardiomyocytes cultivated in 2-D. Analysis of transcripts was harvested from cardiomyocytess after 1, 2 and 3 days of 2-D culture without Si-HPMC hydrogel (control) or in contact with hydrogel. Real-time PCR was performed by using Nkx2.5, Gata4, connexin 43 (Cx43) and sarcomeric alpha actin (α actin) corrected by HPRT gene expression levels. (p= NS as compared between time points, one-way ANOVA). All values represent mean ± SEM

Fig.3. Protein expression in cardiomyocytes cultivated in 2D. Representative immunofluorescence staining in cardiomyocytes after 48h of culture without Si-HPMC hydrogel (control) or with hydrogel for (a) Nkx2.5 (red fluorescence), (b) Gata-4 (red fluorescence), (c) Connexin43 (green fluorescence) and (d) sarcomeric alpha actin (red fluorescence). Nuclei labeled with DAPI (blue fluorescence). Scale bar = 20µm.

Fig.4. 3D representation of cardiomyocyte-seeded Si-HPMC hydrogel. Image was obtained after 48h of culture from video data. Microdroplets composed to cardiomyocytes have a height about 30 µm within hydrogel and cardiomyocytes exhibit principally a round shape.

Fig.5. Measure of membrane potential of cardiomyocytes in 3D culture.

(A) Confocal image of cardiomyocytes viewed under bright field illumination (a), di-8-ANEPPS fluorescence (b) and di-8-ANEPPS fluorescence signal with membrane potential in cardiomyocytes. **(B)** Record of membrane potential and fluorescence ratio from a single cardiomyocyte loaded with di-8-ANEPPS. Scale bar = 10 μm.

Figure 1

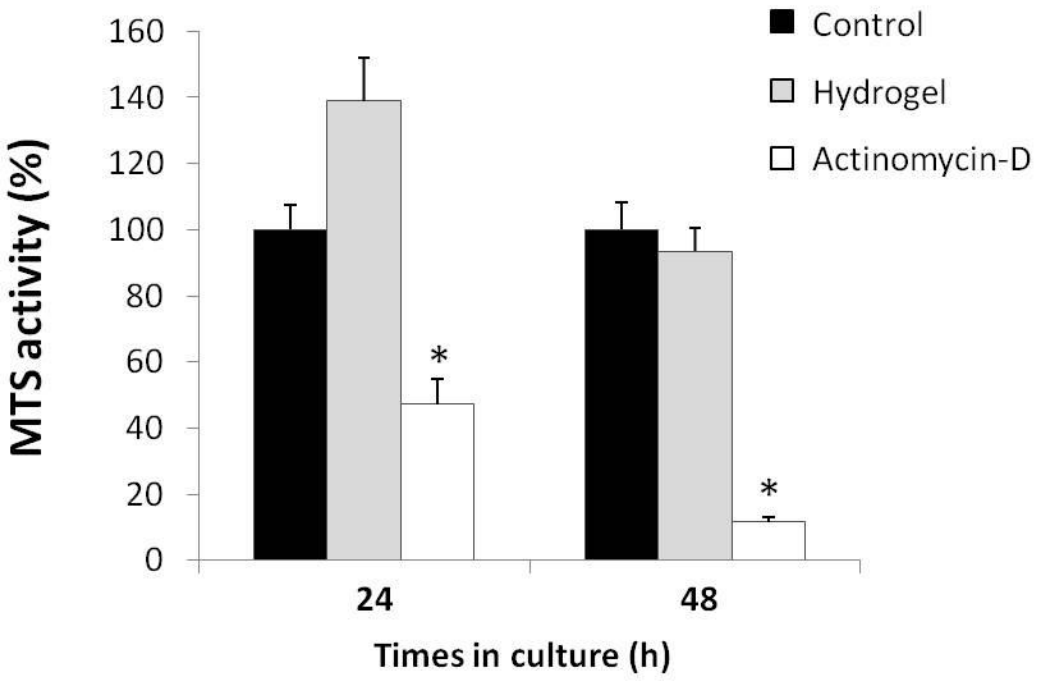
Control
Hydrogel
Actinomycin-D
MTS activity (%)
160
140
120
100
80
60
40
20
0
*
*
24
48
Times in culture (h)

Figure 2

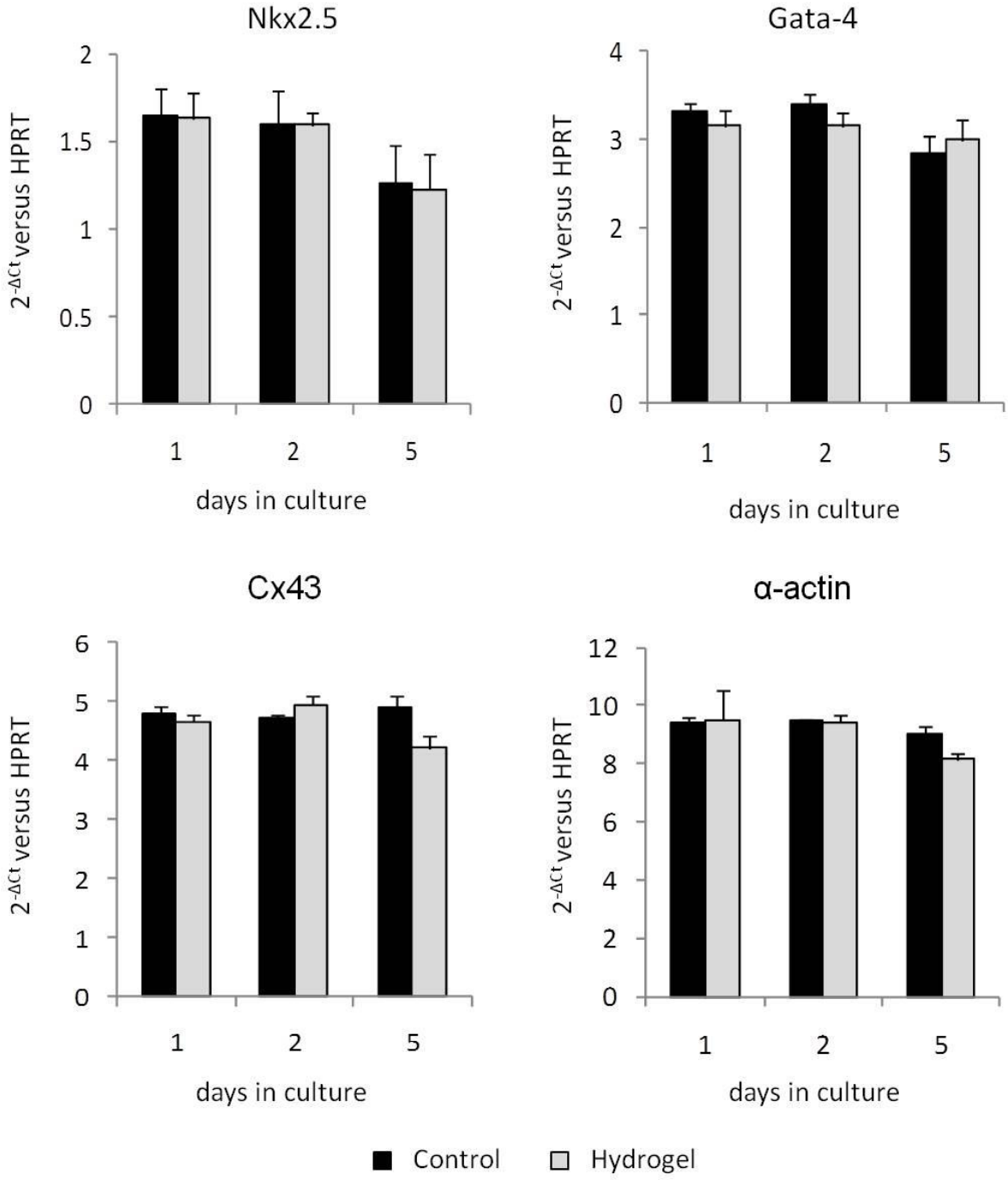
Nkx2.5
2
1.5
1
0.5
0
2-ΔCt versus HPRT
1
2
5
days in culture
Gata-4
4
3
2
1
0
2-ΔCt versus HPRT
1
2
5
days in culture
Cx43
6
5
4
3
2
1
0
2-ΔCt versus HPRT
1
2
5
days in culture
α-actin
12
10
8
6
4
2
0
2-ΔCt versus HPRT
1
2
5
days in culture
Control
Hydrogel

Figure 3

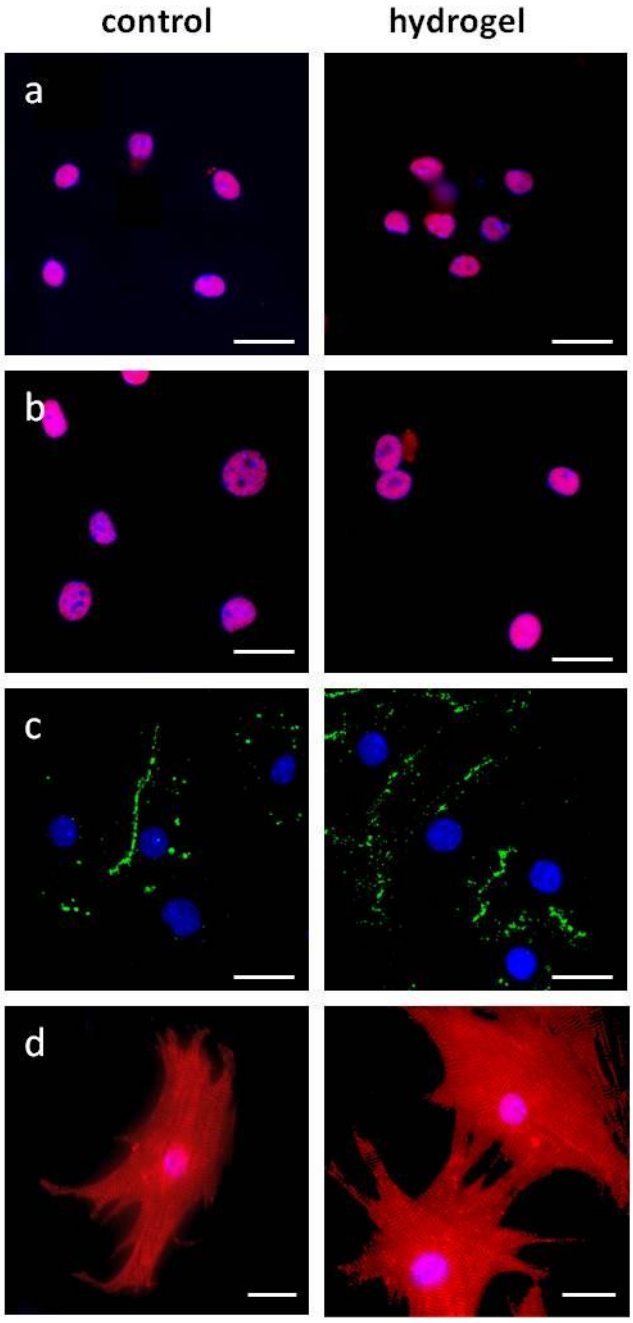

Figure 4

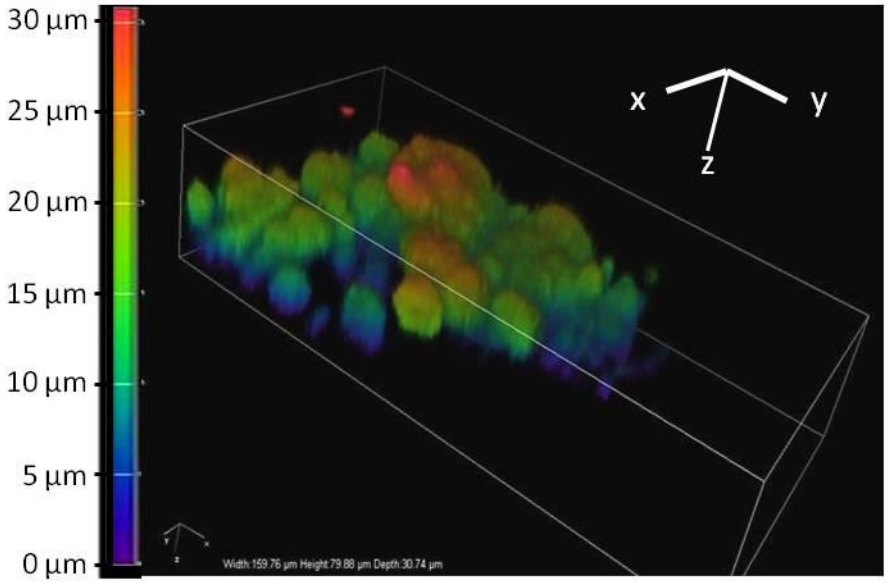

Figure 5

A

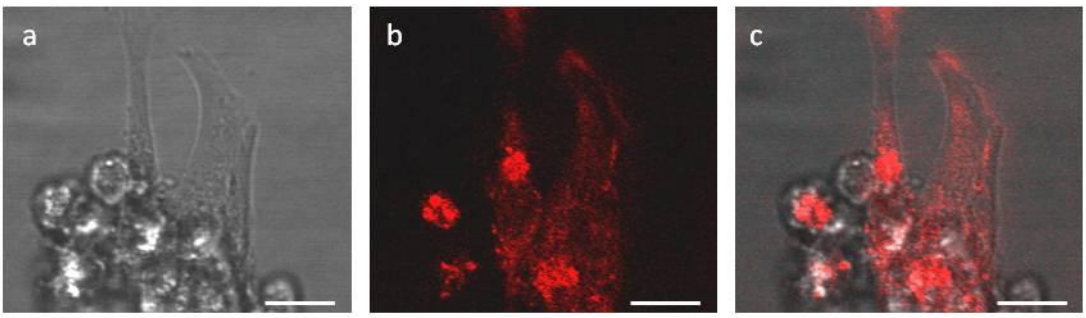

B

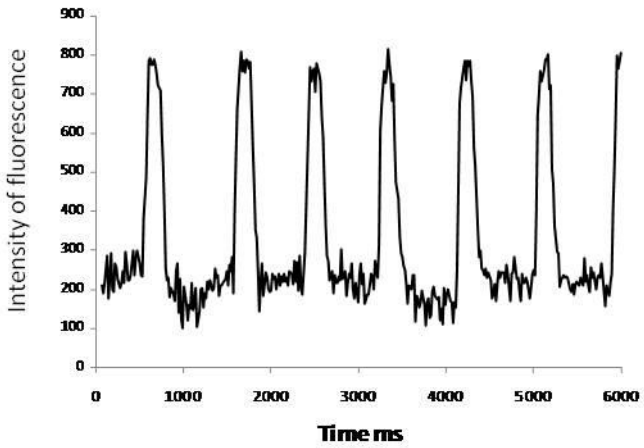

ETUDE 3

La reprogrammation directe de cellules souches mésenchymateuses murines en cardiomyocytes par l'expression de deux facteurs de transcription, Nkx2.5 et Gata-4, par transfert de gènes non viral.

ETUDE 3 : Reprogrammation directe de cellules souches mésenchymateuses murines en cardiomyocytes par l'expression de deux facteurs de transcription, Nkx2.5 et Gata-4, par transfert non viral de gènes.

1. Introduction.

La surexpression de certains facteurs de transcription est l'une des premières étapes indispensables à la cardiogenèse. Parmi ces facteurs de transcription, Nkx2.5 et Gata-4 sont requis pour la spécification du phénotype cardiomyogénique des cellules souches embryonnaires (Faustino *et al.*, 2008). Ces deux facteurs régulent la transcription de nombreux gènes cardiaques, tels que l'alpha-actine cardiaque et la chaine lourde de la myosine sarcomérique (Morkin, 2000). Au cours de la différenciation des CSM en cardiomyocytes induite par le 5-azacytidine, l'expression des deux facteurs de transcription, Nkx2.5 et Gata-4 est augmentée (Makino *et al.*, 1999). Cette expression est également augmentée lorsque les CSM sont cultivées en présence de cardiomyocytes (Arminan *et al.*, 2009). L'expression de ces deux facteurs de transcription *in vitro* dans les CSM pourrait permettre d'obtenir des cellules ayant des caractéristiques de cellules musculaires cardiaques en grand nombre. Pour générer des cellules pluripotentes induites, les cellules adultes sont infectées avec des rétrovirus ou des lentivirus, ce qui peut poser des problèmes de sécurité liés à l'insertion du génome viral dans un gène critique pour le bon fonctionnement de la cellule (gène suppresseur de tumeur par exemple). L'utilisation de structures non virales permet de s'affranchir de ces problèmes. Les éléments génétiques ne s'insèrent pas dans le génome de la cellule hôte, permettant une expression temporaire des deux facteurs de transcription.

Dans ce contexte, notre objectif a été d'étudier si l'expression des deux facteurs de transcription, Nkx2.5 et Gata-4, était capable de reprogrammer directement des CSM murines en cardiomyocytes sans passer par le stade embryonnaire, utilisant une méthode de transfert

de gène non viral. Dans une première étape, des CSM issues de la moelle osseuse de souris ont été isolées, puis transfectées avec deux plasmides codant Nkx2.5 et Gata-4. Dans une seconde étape, les mécanismes moléculaires induits par l'expression de ces deux facteurs ont été évalués par PCR quantitative en utilisant la technique *TaqMan* en cartes microfluidiques (Taqman Low Density Arrays, Applied Biosystems). Des algorithmes de classification ont ensuite été utilisés pour regrouper les gènes selon leurs profils d'expression (Gilbert *et al.*, 2000). Ces méthodes permettent d'identifier des groupes de gènes dont l'expression varie de façon similaire.

2. Matériels et méthodes.

2.1. Culture des cellules souches mésenchymateuses.

Des souris mâles sauvages de la souche SWISS, âgées de 8 semaines (Janvier, France) sont sacrifiées par une injection de nesdonal en intrapéritonéal (0.2ml). Après dissection des membres postérieurs, les fémurs et les tibias sont isolés, puis la moelle osseuse est récupérée par flush à l'aide du milieu de culture composé d'alpha- modified Eagle medium avec nucléotides (α-MEM) (Invitrogen corporation, Paisley, U.K.) auquel on ajoute 10 % de sérum fœtal de veau (Hyclone Perbio, Thermo Fisher Scientific, CNH0164), 1% de pénicilline/streptomycine, 1% de L-glutamine et 2 ng/mL of FGF2 basique humain (AbCys, Paris, France). Les cellules en suspension sont centrifugées (1200rpm, 7min), puis ensemencées dans des boites de pétri (500 000 cellules/cm^2). Le milieu de culture est changé après 72h pour enlever les cellules non adhérentes puis tous les 3 jours. Les cellules sont cultivées pendant 2 à 3 semaines jusqu'à confluence. Les cellules adhérentes sont détachées par l'utilisation de trypsine-EDTA à 0.5% puis réensemencées à une densité de 10 000 cellules/cm^2. Pour les passages suivants les cellules sont ensemencées à 5000 cellules/cm^2.

2.2. Caractérisation des cellules souches mésenchymateuses.

A chaque passage, les CSM sont caractérisées par cytométrie en flux (FACS Calibur instrument, CellQuestPro software; BD Biosciences, San Jose, CA) après incubation avec les anticorps anti-CD45, anti-CD90, anti-CD29 et anti-Sca1 (BD Biosciences). La culture de CSM est pure lorsque le nombre cellules CD29 positives est supérieur à 90% et celui des cellules CD45 positives inférieur à 1%.

2.2. Transfection des cellules souches mésenchymateuses.

Les vecteurs pcDNA3.1 (ampR) codant pour les facteurs de transcription, Nkx2.5 et Gata-4, ont été fabriqués et produits par la société GeneArt. Deux populations distinctes de CSM sont transfectées aux passages 7 avec 4µg de pcDNA3/Nkx2.5 et 4 µg de pcDNA3/Gata-4, soit 8µg de plasmide pour $1.5.10^6$ cellules, utilisant la méthode de nucléofection (Nucleofector Solution, Amaxa Biosystem). Huit microgrammes de plasmide vide (pcDNA3/vide) sont utilisés comme contrôle négatif. Une population de CSM correspond à un isolement de moelle osseuse provenant de deux souris.

2.3. Immunofluorescence.

L'expression des deux facteurs de transcription, Nkx2.5 et Gata-4, est observée en immunofluorescence dans des cardiomyocytes néonataux murins (contrôle positif), des CSM transfectées avec le pcDNA3/vide (contrôle négatif) et des CSM transfectées avec pcDNA3/Nkx2.5 et pcDNA3/Gata-4. L'immunomarquage est réalisé après 48h de culture pour les cardiomyocytes néonataux et 24h après la transfection des CSM. Brièvement, les cellules sont fixées dans une solution contenant 4% de paraformaldehyde. Après lavage au PBS, les cellules sont perméabilisées pendant 30 minutes avec 0.2% Triton X-100, puis incubées 1 heure à température ambiante soit avec l'anticorps primaire anti-Nkx2.5 (polyclonal, Santa Cruz Biotechnology, USA) dilué au 1/500 dans 1% BSA/PBS, soit avec

l'anticorps primaire anti-Gata-4 (polyclonal, Santa Cruz Biotechnology) dilué au 1/500 dans 1% BSA/PBS. Après 3 rinçages avec du PBS, les cellules sont incubées 45 min avec l'anticorps secondaire anti-IgG Alexa Fluor 488 (Molecular Probes, Leiden, The Netherlands) dilué au 1/1000. Les cellules sont rincées puis montées sur lame avec un milieu de montage contenant un marqueur fluorescent des noyaux (Vectaschield®, DAPI, vector laboratories, US. Headquaters). La fluorescence est observée au microscope (LEICA TCS- SP1) et analysée avec le logiciel Metamorph.

2.4. Préparation des ARN.

Les ARN totaux sont isolés et traités, 24h après la transfection avec un kit d'extraction (Qiagen S.A., France). La concentration d'ARN totaux est évaluée par mesure de l'absorbance à 260 nm (DO 260 nm, NanoDrop ND-1000, NanoDrop Technologies). La qualité des ARN totaux est contrôlée par une technique de microéléctrophorèse sur gel d'acrylamide en capillaire (Agilent 2100 Bioanalyser).

2.5. Analyse des transcrits à partir de cartes microfluidiques.

Les cartes microfluidiques ont été configurées pour analyser 192 facteurs de transcription cardiaques d'une part et 96 canaux ioniques cardiaques d'autre part. Les cartes microfluidiques sont composées de puits contenant chacun un couple d'amorces et une sonde TaqMan spécifique d'un gène.

Cent nanogrammes d'ADNc combinés aux réactifs *PCR TaqMan Universal Master Mix* (1X) sont déposés dans chaque réservoir puis distribués par centrifugation *via* les microcapillaires dans chacun des puits. Chaque puits contient 1 ng d'ADNc dans un volume réactionnel de 1 µl. Les amplifications sont réalisées dans un thermocycleur *ABI PRISM 7900HT Sequence Detection System*. Les données provenant des cartes microfluidiques sont analysées à l'aide du logiciel SDS 2.1. La méthode du $2^{-\Delta\Delta Ct}$ permet ensuite d'exprimer les

résultats (Livak and Schmittgen, 2001). Des algorithmes de classification ont ensuite été utilisés pour regrouper les gènes selon leurs profils d'expression.

3. Résultats.

3.1. Caractérisation phénotypique des cellules souches mésenchymateuses murines issues de la moelle osseuse.

Le phénotype des cellules est caractérisé à chaque passage par cytométrie en flux, jusqu'à l'élimination des cellules précurseurs hématopoïétiques CD45+ (<0.9%) (Figure 1). A partir du sixième passage nous obtenons une population homogène de CSM CD45-. Les CSM murines sont également caractérisées d'une part par l'absence d'expression de l'antigène CD90 et d'autre part par la présence des marqueurs CD29 et Sca1 (Figure 1).

3.2. Expression nucléaire de Nkx2.5 et Gata-4 dans les CSM transfectées.

L'efficacité de la transfection a été analysée par le marquage des protéines Nkx2.5 et Gata-4 (Figure 2). L'observation des cardiomyocytes en microscopie à fluorescence a montré une expression nucléaire des facteurs de transcription Nkx2.5 et Gata-4. Les CSM transfectées avec le plasmide vide n'exprimaient pas les deux facteurs de transcription, alors que celles transfectées avec les plasmides codant pour Nkx2.5 et Gata-4 exprimaient les deux protéines dans leur noyaux, 24h après la transfection.

Ces résultats valident la technique de transfert non viral des deux facteurs de transcription, Nkx2.5 et Gata-4, ainsi que leur expression nucléaire dans les CSM.

3.3. Profil d'expression des facteurs de transcription.

L'analyse globale des données révèle des différences d'expression entre les CSM transfectées avec le plasmide vide (-) et celles transfectées avec les plasmides codant pour Nkx2.5 et Gata-4 (+) (Figure 3). Les données confirment l'expression des deux facteurs de transcription Nkx2.5 et Gata-4 dans les CSM 24h après la transfection, alors qu'elles

n'expriment pas à la base ces deux facteurs. Deux clusters (1 et 2) sont mis en évidence suivant la similarité des profils d'expression des facteurs de transcription 24h après la transfection des CSM.

Le cluster 1 comprend des facteurs de transcription dont l'expression augmente 24h après la transfection des CSM avec Nkx2.5 et Gata-4 (Figure4). Les facteurs de transcription Tbx5, Tbx2, Tcf15 et le peptide natriurétique Nppb peuvent être cités à titre d'exemple. Le cluster 2 comprend des facteurs de transcription dont l'expression diminue 24h après la transfection des CSM avec Nkx2.5 et Gata-4 (Figure), tels que Id3, Tb18, Atf1 et Sox4.

3.4. Profil d'expression des canaux ioniques.

L'analyse globale des données 24h après la transfection révèle des différences d'expression des canaux ioniques entre les deux populations de CSM, mais pas entre les cellules transfectées avec le plasmide vide ou les deux plasmides codant pour Nk2.5 et Gata-4 (Figure5). Cependant il conviendrait de réaliser une analyse plus tardive à 7 jours pour analyser l'expression des canaux ioniques.

4. Discussion.

L'objectif de cette étude préliminaire était de définir si l'expression des deux facteurs de transcription, Nkx2.5 et Gata-4, pouvait induire la reprogrammation directe des CSM murines en cardiomyocytes, par transfert non viral de gène.

L'analyse du transcriptome des CSM, 24h après l'expression de Nk2.5 et Gata-4, a révélé une augmentation de quelques facteurs de transcription, tels que Tbx5 et le peptide précoce natriurétique b (Nppb). Tout comme, Nkx2.5 et Gata-4, le facteur de transcription Tbx5 joue un rôle clé dans la cardiogenèse (Bimber *et al.*, 2007). L'homéodomaine de Nkx2.5 interagit directement avec la boite Tbx de Tbx5 (Snyder *et al.*, 2010). De plus, Nkx2.5 et Gata-4 interagissent directement l'un avec l'autre *via* l'homéodomaine de Nkx2.5 et les doigts

zinc de Gata-4 (Sepulveda *et al.*, 1998; Shiojima *et al.*, 1999). Les interactions et co-régulations entre ces trois facteurs de transcription jouent un rôle déterminant au cours de la différenciation cardiaque (Nemer and Nemer, 2001; Snyder et al., 2010). Ces facteurs possèdent des actions synergiques et régulent l'expression de gènes cardiaques, comme le peptide précurseur natriurétique a (Nppa), l'alpha actine cardiaque et la chaine lourde de la myosine sarcomérique (Ghosh *et al.*, 2001; Hiroi *et al.*, 2001). L'expression de Nkx2.5 et Gata-4 induit également une diminution de l'expression de certains gènes, tel que l'inhibiteur de la différenciation (Id3) dans les CSM. Il a été montré qu'au cours de la différenciation des cellules musculaires, Id3 était diminué et qu'à l'inverse sa surexpression inhibait l'expression des gènes musculaires (Chen *et al.*, 1997; Melnikova and Christy, 1996). Cependant, sur les 192 facteurs de transcription cardiaques évalués, seule une dizaine de facteurs était augmentée dans les deux populations de CSM et une vingtaine diminuait. L'expression de Nkx2.5 et Gata-4 n'a pas eu d'effet à 24h sur l'expression des gènes codants pour les canaux ioniques. En 2010, Ieda et son équipe ont mis au point un système de sélection *in vitro* de facteurs de transcription induisant la reprogrammation directe des fibroblastes cardiaques en cardiomyocytes. Ce modèle leur a permis d'identifier trois facteurs de transcription, Gata-4, Mef2c et Tbx5, capables de générer en deux semaines des cellules battantes cardiaques (Ieda *et al.*, 2010). Nkx2.5 a été exclue de cette sélection à cause de son action répressive sur le promoteur de la tropinine C dans les fibroblastes cardiaques. Dans une autre étude, cette équipe a montré que la transdifférenciation directe du mésoderme du tissu cardiaque chez la souris était définie par la combinaison de deux facteurs de transcription, Gata-4 et Tbx5, ainsi qu'une sous-unité spécifique cardiaque des complexes BAF remodelant la chromatine, le Baf60c (Takeuchi and Bruneau, 2009). L'ajout d'un facteur agissant directement sur le remaniement de la chromatine facilite la fixation des facteurs de transcription et optimise ainsi leur action (Lickert *et al.*, 2004).

6. Conclusion.

Dans cette étude préliminaire, nous avons montré que l'expression de deux facteurs de transcription, Nkx2.5 et Gata-4, modifie l'expression de quelques facteurs de transcription cardiaques, mais n'est pas suffisante pour induire une réelle différenciation des CSM en cardiomyocytes. Le développement d'un système de sélection *in vitro* apparait indispensable pour identifier les facteurs induisant la reprogrammation des CSM en cardiomyocytes. Il convient également de définir les gènes régulant spécifiquement les complexes de la chromatine afin de potentialiser l'action des facteurs de transcription. Pour finir, l'expression des facteurs de transcription et des canaux ioniques cardiaques doit être analysée à plus long terme (48h, 7 jours et 14 jours) afin d'observer une éventuelle reprogrammation des CSM en cardiomyocytes.

Légendes des figures.

Fig.1. Caractérisation phénotypique des cellules issues de la moelle osseuse par cytométrie en flux. Evolution des marqueurs de surface CD45, CD90, CD29 et Sca1 au cours de la culture primaire du passage 2 au passage 6. La population de cellules souches mésenchymateuses est considérée homogène lorsque moins de 1.0% des cellules expriment le CD45 et le CD90 et que plus de 90.0% expriment le CD29 et le Sca1+.

Fig.2. Expression protéique des deux facteurs de transcription Nkx2.5 et Gata-4 par immunofluorescence. Les noyaux des cellules sont marqués en bleu au DAPI. (A) Cardiomyocytes néonataux murins. (B) CSM transfectées avec le plasmide pcDNA3/vide. (C) CSM transfectées avec les plasmides pcDNA3/Nkx2.5 et pcDNA3/Gata-4. Le marquage est réalisé 24h après la transfection des CSM et 48h de culture des cardiomyocytes.

Fig.3. Classification hiérarchique appliquée aux gènes codant les facteurs de transcription et cofacteurs (verticalement) en fonction des 4 échantillons (horizontalement). Chaque gène et chaque condition sont représentés par une ligne et une colonne respectivement. Chaque case colorée correspond au niveau d'expression relative du gène (ΔCt). La gamme de couleur s'étend du vert (moins exprimé) au rouge (plus exprimé). Les valeurs manquantes sont représentées en gris. Pop1 : population de CSM 1 ; Pop2 : population de CSM 2. (-) pcDNA3 vide ; (+) pcDNA3/Nkx2.5 + pcDNA3/Gata-4.

Fig.4. Détail des clusters 1 et 2. A. Le cluster 1 regroupe les gènes dont l'expression augmente. B. Le cluster 2 regroupe les gènes dont l'expression diminue. Pop1 : population de CSM 1 ; Pop2 : population de CSM 2. (-) pcDNA3 vide ; (+) pcDNA3/Nkx2.5 + pcDNA3/Gata-4.

Fig.5. Classification hiérarchique appliquée aux gènes codant les canaux ioniques (verticalement) en fonction des 4 échantillons (horizontalement). Chaque gène et chaque

condition sont représentés par une ligne et une colonne respectivement. Chaque case colorée correspond au niveau d'expression relative du gène (ΔCt). La gamme de couleur s'étend du vert (moins exprimé) au rouge (plus exprimé). Les valeurs manquantes sont représentées en gris. Pop1 : population de CSM 1 ; Pop2 : population de CSM 2. (-) pcDNA3 vide; (+) pcDNA3/Nkx2.5 + pcDNA3/Gata-4.

Figure 1

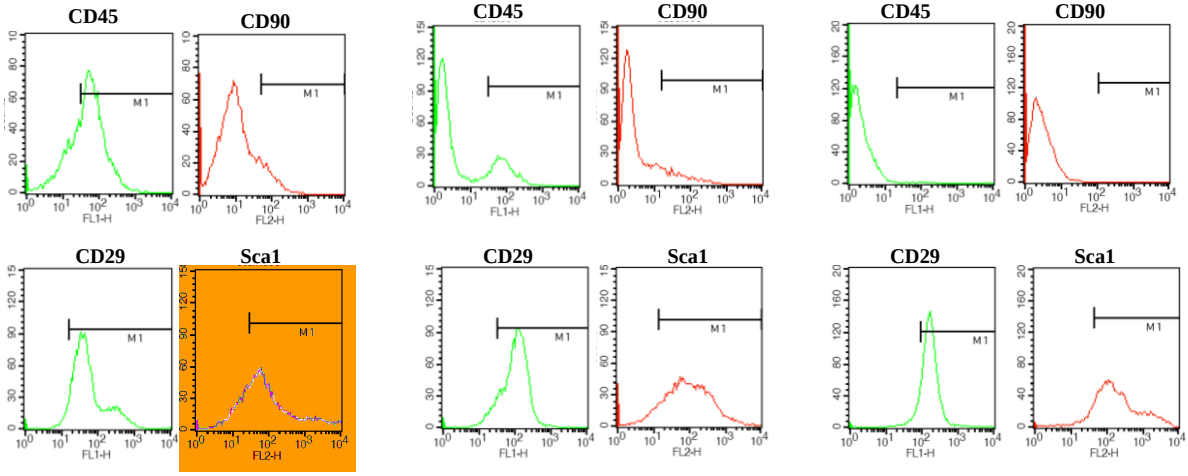

Figure 2

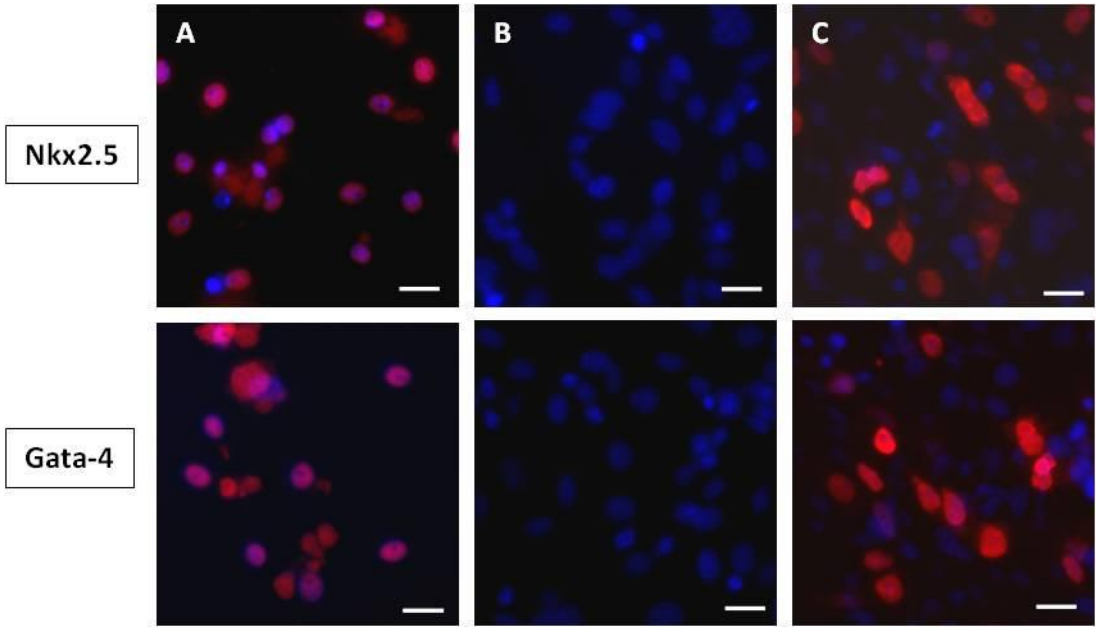

Figure 3

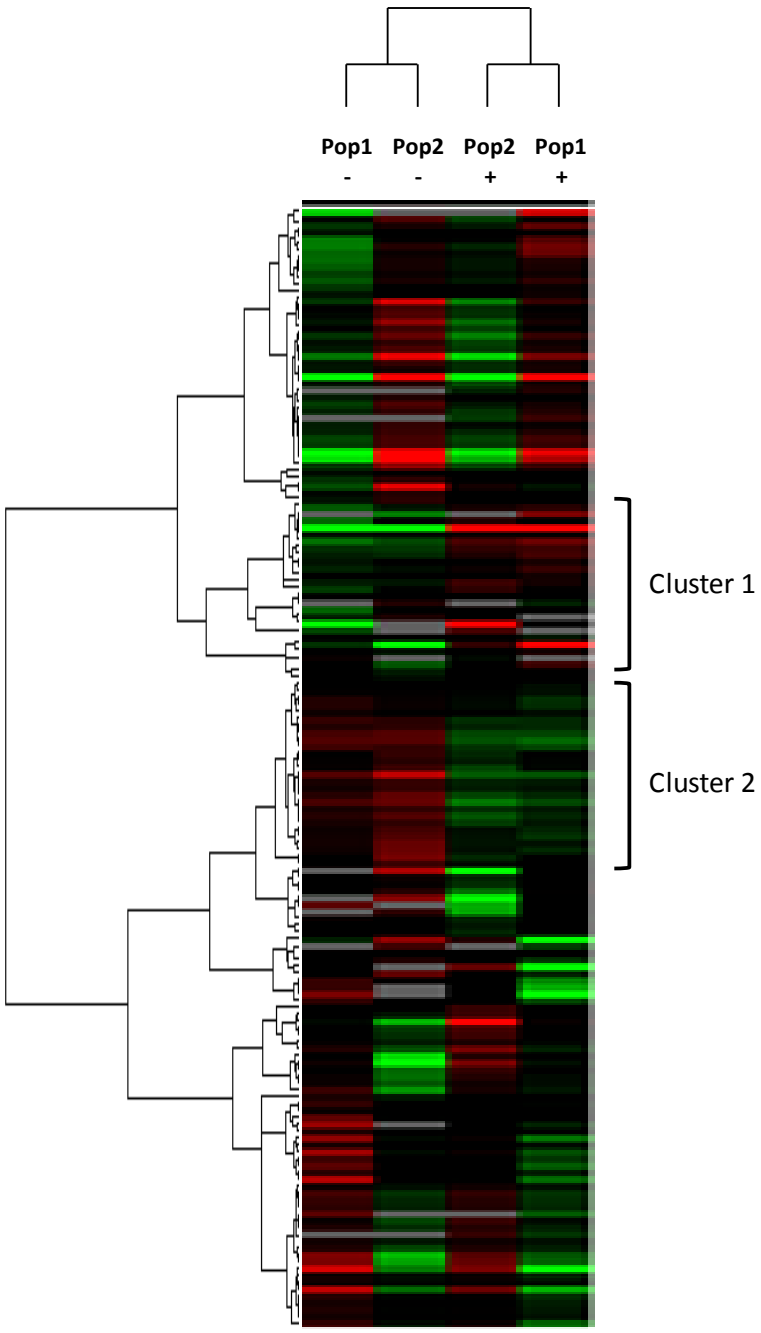

Figure 4

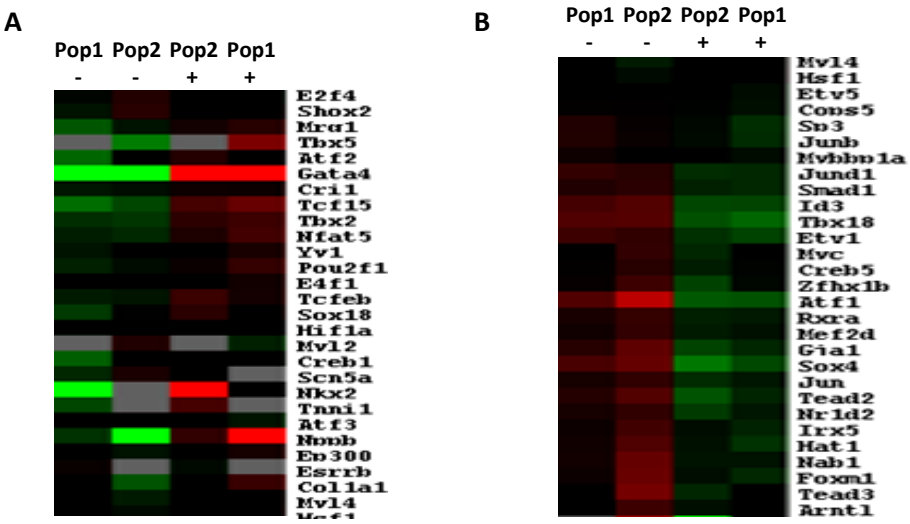

Figure 5

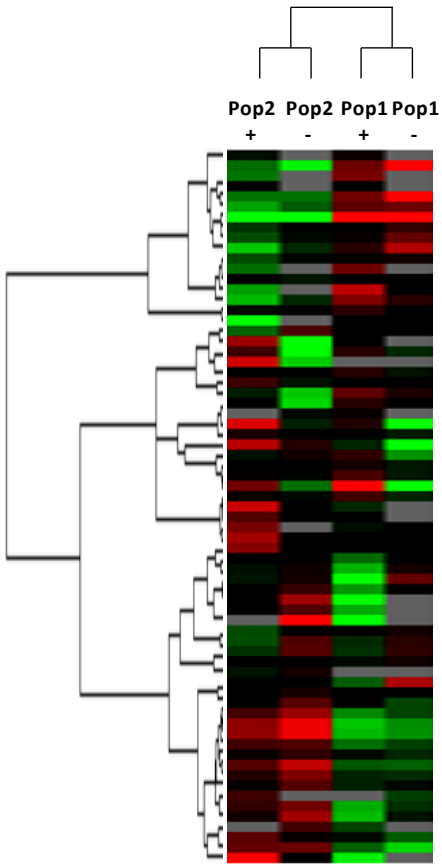

CONCLUSIONS ET FUTURES DIRECTIONS

1. Les nouvelles approches thérapeutiques de l'infarctus du myocarde.

Bien que les essais cliniques de thérapie cellulaire de l'infarctus du myocarde (IDM) utilisant les cellules souches mésenchymateuses (CSM) aient commencé en 2000, les bénéfices de cette approche sont encore largement débattus. L'idée que l'apport de cellules souches puisse remplacer physiquement les cellules cardiaques détruites après un infarctus a évolué vers l'exploitation des effets paracrines des cellules greffées sur diverses voies de signalisation cytoprotectrices, particulièrement celles impliquées dans l'angiogenèse, la limitation de l'apoptose et le recrutement de cellules endogènes capables d'acquérir un phénotype contractile. L'importance d'optimiser le transfert, l'implantation et la survie des cellules souches dans le tissu cardiaque est apparue indispensable pour permettre une amélioration des effets de ces cellules sur la réparation cardiaque. Finalement, les CSM ne semblant pas donner spontanément naissance à de nouveaux cardiomyocytes, il est important de poursuivre la quête de nouvelles cellules capables d'assurer une véritable régénération myocardique.

Dans ce contexte, notre travail a consisté à étudier et développer de nouvelles approches thérapeutiques de l'IDM utilisant les cellules souches mésenchymateuses et l'ingénierie tissulaire et cellulaire. Les deux premières études de ce travail de recherche ont concerné le domaine de l'ingénierie tissulaire cardiaque qui associe une composante artificielle d'origine synthétique ou naturelle, les biomatériaux, et une composante cellulaire. Ce domaine s'intéresse au développement des matrices capables de répondre biologiquement et physiquement aux attentes de l'ingénierie du tissu cardiaque ainsi que l'étude physiologique des cellules cultivées en trois dimensions (3D) dans ces matrices. Notre troisième étude a concerné quant à elle le domaine de l'ingénierie cellulaire cardiaque qui s'intéresse aux diverses techniques pouvant permettre d'obtenir des cellules compétentes pour la régénération du myocarde après un infarctus.

Au cours de notre première étude réalisée chez l'animal, nous avons montré l'importance d'utiliser un biomatériau et plus particulièrement un hydrogel pour optimiser les effets des CSM après un IDM. Cet hydrogel hémi-synthétique, constitué d'un dérivé de la cellulose, permet de véhiculer les CSM directement dans le tissu cardiaque et contribue grâce à ses propriétés mécaniques, rhéologiques et physiques à améliorer la fonction cardiaque en atténuant les effets délétères de l'ischémie sur le ventricule gauche. En effet, l'hydrogel est capable d'augmenter l'épaisseur de la paroi cicatricielle et de stabiliser l'expansion de l'infarctus en apportant un support physique à la paroi du ventricule gauche (Vunjak-Novakovic *et al.*, 2010). De plus en mimant les conditions d'une « niche » cellulaire, il protège les cellules des multiples agressions du tissu hôte ischémique, tels que le stress oxydatif, l'hypoxie et l'inflammation augmentant ainsi la survie des CSM dans le tissu cardiaque (Le Visage et al., 2011; Yu et al., 2010; Zhang et al., 2010b). Cependant, ces résultats ont été observés chez le rat, dans un modèle d'ischémie permanente et donc finalement assez éloigné de la situation clinique humaine d'ischémie puis reperfusion. En dehors de l'ischémie chronique du myocarde, telle que l'angine de poitrine, liée à une diminution du débit sanguin dans une artère coronaire, l'ischémie aigüe du myocarde est liée à l'occlusion brutale d'une artère coronaire. La prise en charge en urgence de ces patients permet dans la majorité des cas de reperfuser la zone ischémique. Afin d'améliorer notre modèle d'étude il conviendrait d'utiliser un modèle d'IDM reperfusé chez l'animal. Ce modèle est déjà utilisé chez le rat, mais cette technique reste très invasive puisqu'elle oblige à réaliser une thoracotomie (Fernandes *et al.*, 2010). Le modèle porcin permet de réaliser des techniques d'IDM reperfusées moins invasives par les voies percutanée et intracoronaire à l'aide de cathéters. Brièvement, l'accès aux artères coronaires se fait par l'introduction d'un cathéter *via* une artère fémorale. L'occlusion de l'artère coronaire est réalisée grâce à un ballonnet gonflé dans l'artère cible (Leor *et al.*, 2009). En plus de l'occlusion, un thrombus

peut être créé par l'injection dans l'artère coronaire de thrombine et de plasminogène (Forest *et al.*, 2010). Toujours par cathétérisme, le modèle porcin permet d'injecter des cellules directement dans l'endocarde du ventricule gauche grâce au système NOGA (Chan *et al.*, 2010). Avec l'aide des vétérinaires et cliniciens nantais, maitrisant déjà parfaitement ce modèle, il serait intéressant de poursuivre notre première étude afin d'observer si cette approche d'ingénierie tissulaire contribue réellement à l'amélioration de la fonction cardiaque et à la protection des effets délétères de l'ischémie sur le tissue cardiaque.

Notre stratégie de combiner les CSM avec un hydrogel est encourageante mais pour le moment insuffisante pour permettre une réelle régénération du myocarde après un infarctus. Face à ce problème, il apparait aujourd'hui nécessaire de développer des modèles cellulaires *in vitro* permettant d'étudier le comportement des cellules dans des microenvironnements simulant le tissu cardiaque natif ou ischémique. Nous avons orienté notre seconde étude dans ce contexte. Ce domaine d'étude étant très vaste de par le nombre de questions à résoudre, nous avons choisi de commencer par mettre en place un modèle de culture tridimensionnel (3D) à partir de cardiomyocytes néonataux murins au sein de notre hydrogel. Cette étude nous a permis de valider la cytocompatibilité de notre hydrogel avec les cardiomyocytes, mais également de montrer que cet hydrogel était capable de maintenir l'activité contractile des cardiomyocytes cultivés en 3D. Ce modèle reproductible et fonctionnel peut maintenant nous permettre d'étudier le comportement et le remodelage des cardiomyocytes vis-à-vis des différents facteurs de croissance et cytokines produits lors d'un IDM, mais également leurs interactions avec d'autres cellules, tels que les fibroblastes cardiaques, les cellules endothéliales et les CSM (Curtis and Russell, 2011). En modifiant les propriétés mécaniques de l'hydrogel, il est même possible d'augmenter sa rigidité et ainsi se rapprocher de celle d'un tissu ischémique fibreux qui est beaucoup plus élevée que celle du tissu cardiaque natif. Ce modèle permet également de tester les effets et la cytotoxicité de molécules pharmacologiques

sur les cardiomyocytes. La culture tridimensionnelle dans des matrices et la reconstitution d'un microenvironnement cardiaque est actuellement un vaste domaine de recherche. Engler et son équipe travaillent sur la capacité de ces matrices à orienter selon leur élasticité la différenciation des cellules souches vers les différents linéages cellulaires. Ils ont notamment montré que les cellules souches embryonnaires se différenciaient plus facilement en cardiomyocytes lorsqu'elles étaient cultivées dans des matrices possédant une élasticité proche de celle du tissu cardiaque natif (Engler *et al.*, 2008). De la même façon, ils montrent grâce à l'utilisation de ces matrices que la différenciation des CSM est orientée par la rigidité des tissus ou durotaxisme (Tse and Engler, 2011). En travaillant sur les propriétés mécaniques et rhéologiques de notre hydrogel d'HPMC-si, nous pourrons à l'avenir étudier le comportement des CSM cultivées en 3D, ainsi que leur éventuelle capacité de différenciation en cardiomyocytes.

L'utilisation des CSM a suscité un vif intérêt ces 15 dernières années, cependant aujourd'hui malgré leurs effets bénéfiques sur la fonction cardiaque, les CSM ne semblent pas capables de donner naissance *in vivo* à de nouvelles cellules cardiaques contractiles et fonctionnelles. Un espoir est né il y a quelques années avec la découverte des cellules pluripotentes induites (Takahashi and Yamanaka, 2006). Cette équipe japonaise a montré que la reprogrammation de cellules adultes par la transduction de quatre gènes codant pour des facteurs de transcription, oct4, sox2, klf4 et c-myc, permettait d'obtenir des cellules ayant toutes les capacités de cellules souches embryonnaires, les cellules pluripotentes induites ou iPS. Ces cellules pouvant par la suite être différenciées dans le type cellulaire désiré et notamment en cardiomyocytes. Cette technologie présente cependant un inconvénient majeur, de par l'utilisation de vecteurs viraux, tels que les rétrovirus et les lentivirus, entrainant une intégration non contrôlée des transgènes dans le génome. Dans ce contexte, nous nous sommes intéressés à une méthode de transfert de gènes transitoires n'utilisant pas de vecteurs

viraux. De plus, l'obtention de cardiomyocytes à partir de cellules adultes puis d'iPS nécessitent deux étapes de transformation. Partant du principe que les CSM possèdent une plus grande plasticité que les cellules somatiques adultes, nous avons émis l'hypothèse qu'elles pouvaient être reprogrammées directement en cardiomyocytes, sans passer par le stade pluripotent. Au cours du développement embryonnaire, les deux facteurs de transcription, Nkx2.5 et Gata-4, sont indispensables à la cardiomyogenèse. Habituellement, les CSM n'expriment pas ces deux facteurs, c'est pourquoi nous avons forcé leur expression par leur transfert dans les CSM murines. Nos résultats ont montré que l'expression de Nkx2.5 et Gata-4 dans les CSM modifiait l'expression de quelques facteurs de transcription cardiaques, mais n'était pas suffisante pour induire une réelle différenciation des CSM en cardiomyocytes fonctionnels. Malgré ces résultats, notre démarche est apparue intéressante. En effet, peu de temps après notre étude préliminaire, l'équipe de Ieda a publié des travaux montrant que l'expression de trois facteurs de transcription Gata-4, Mef2c et Tbx5 dans des fibroblastes cardiaques murins était capable d'induire leur différenciation en cardiomyocytes fonctionnels (Ieda *et al.*, 2010). A l'avenir, si nous voulons identifier les gènes permettant de reprogrammer les CSM en cardiomyocytes, il apparait nécessaire de développer des systèmes de sélection de gènes dans des modèles *in vitro*.

La Figure 10 résume notre approche d'ingénierie tissulaire et cellulaire.

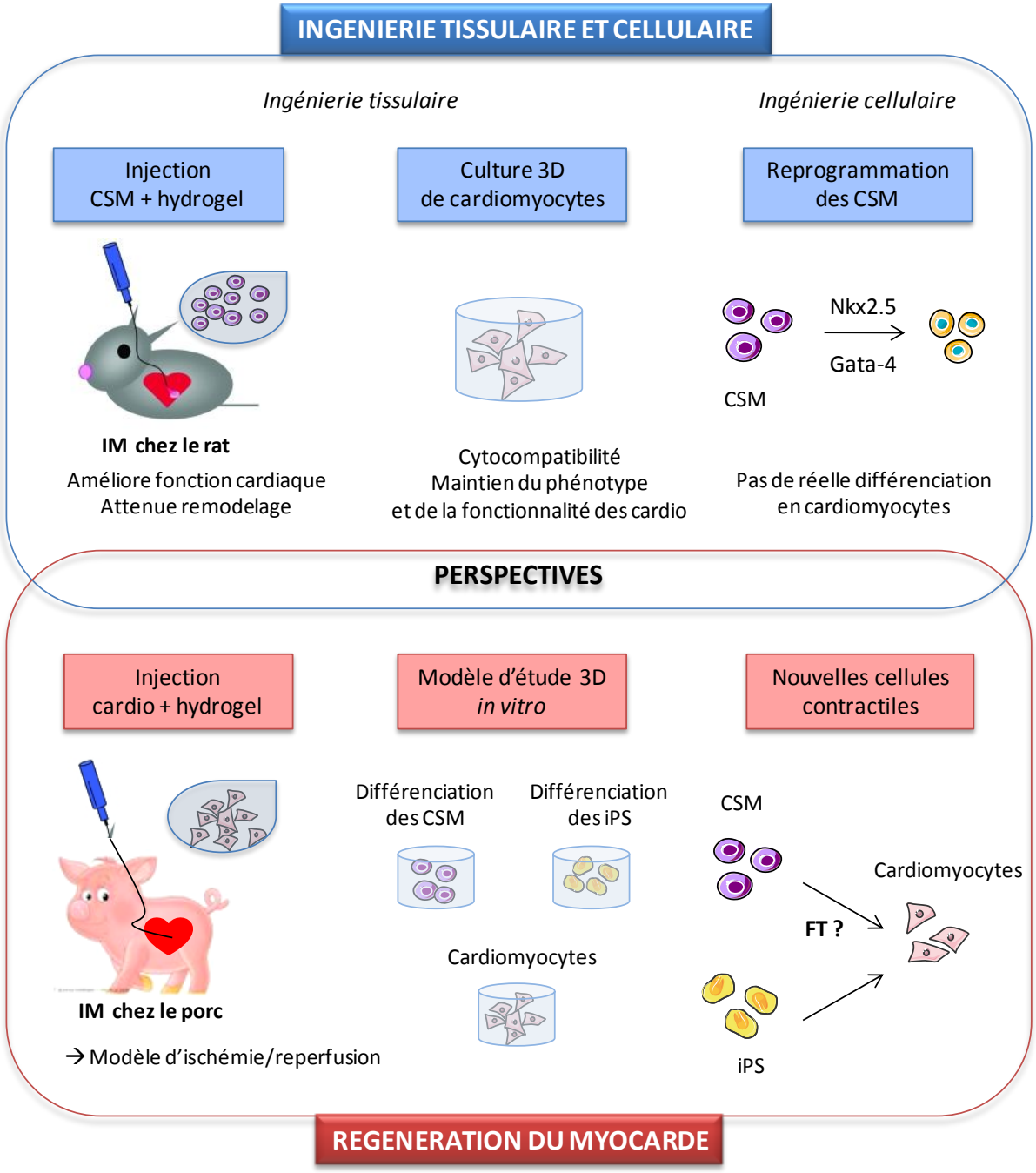

Figure 10: Nouvelles approches thérapeutiques de l'infarctus du myocarde : Cellules souches mésenchymateuses et ingénierie tissulaire et cellulaire.

Le cadre bleu présente les résultats de nos études et le cadre rouge, les perspectives de ce travail. cardio : cardiomyocytes ; CSM : cellules souches mésenchymateuses ; FT : facteurs de transcription; IM : infarctus du myocarde ; iPS : induced pluripotent stem cells ; 3D : trois dimensions.

2. Perspectives en ingénierie tissulaire cardiaque : la médecine régénératrice.

Le cœur était considéré, jusqu'à récemment, comme un organe possédant des cellules post-mitotiques dépourvu de capacités de régénération ou de réparation. Ce principe a été bousculé par une étude réalisée par l'équipe de Bergmann qui montre de manière originale et remarquable qu'environ 50% des cardiomyocytes sont renouvelés au cours de la vie (Bergmann *et al.*, 2009). Par la suite, plusieurs travaux ont décris la présence de niches de cellules souches cardiaques (CSC) endogènes (Laflamme and Murry, 2011). Ces cellules présentent des caractéristiques de cellules souches capables de se différencier dans tous les types cellulaires composant le cœur, à savoir des cardiomyocytes, des cellules musculaires et des cellules endothéliales. La capacité du cœur adulte humain à générer de nouveaux cardiomyocytes suggère qu'il peut être rationnel de développer des stratégies thérapeutiques visant à stimuler ce processus dans des pathologies cardiaques. Dans ce sens, l'ingénierie tissulaire peut contribuer au développement de biomatériaux capables de stimuler la prolifération des cardiomyocytes endogènes ou la différenciation des CSC en libérant divers facteurs, tels que des cytokines et des facteurs de croissance. Ces biomatériaux pourraient également favoriser la mobilisation des progéniteurs cardiaques et/ou endothéliaux afin de les attirer dans le cœur endommagé. Enfin, la capacité des biomatériaux à véhiculer des plasmides codant des facteurs de transcription capables de reprogrammer les cardio-fibroblastes endogènes en cardiomyocytes pourrait également permettre de régénérer un tissu cardiaque fonctionnel et contractile.

L'ingénierie tissulaire et cellulaire cardiaque est une nouvelle approche thérapeutique interdisciplinaire qui en s'efforçant de réunir les diverses compétences scientifiques, médicales et industrielles devrait permettre à la médecine régénératrice cardiaque de devenir une réalité clinique.

REFERENCES

Abarbanell AM, Coffey AC, Fehrenbacher JW, et al. (2009) Proinflammatory cytokine effects on mesenchymal stem cell therapy for the ischemic heart. Ann Thorac Surg, 88:1036-1043.

Aberg ND, Blomstrand F, Aberg MA, et al. (2003) Insulin-like growth factor-I increases astrocyte intercellular gap junctional communication and connexin43 expression in vitro. J Neurosci Res, 74:12-22.

Aggarwal S, Pittenger MF (2005) Human mesenchymal stem cells modulate allogeneic immune cell responses. Blood, 105:1815-1822.

Airey JA, Almeida-Porada G, Colletti EJ, et al. (2004) Human mesenchymal stem cells form Purkinje fibers in fetal sheep heart. Circulation, 109:1401-1407.

Amado LC, Saliaris AP, Schuleri KH, et al. (2005) Cardiac repair with intramyocardial injection of allogeneic mesenchymal stem cells after myocardial infarction. Proc Natl Acad Sci U S A, 102:11474-11479.

Angoulvant D, Ivanes F, Ferrera R, Matthews PG, Nataf S, Ovize M (2011) Mesenchymal stem cell conditioned media attenuates in vitro and ex vivo myocardial reperfusion injury. J Heart Lung Transplant, 30:95-102.

Arminan A, Gandia C, Bartual M, et al. (2009) Cardiac differentiation is driven by NKX2.5 and GATA4 nuclear translocation in tissue-specific mesenchymal stem cells. Stem Cells Dev, 18:907-918.

Askari AT, Unzek S, Popovic ZB, et al. (2003) Effect of stromal-cell-derived factor 1 on stem-cell homing and tissue regeneration in ischaemic cardiomyopathy. Lancet, 362:697-703.

Athias P, Vandroux D, Tissier C, Rochette L (2006) [Development of cardiac physiopathological models from cultured cardiomyocytes]. Ann Cardiol Angeiol (Paris), 55:90-99.

Bao C, Guo J, Lin G, Hu M, Hu Z (2008) TNFR gene-modified mesenchymal stem cells attenuate inflammation and cardiac dysfunction following MI. Scand Cardiovasc J, 42:56-62.

Baroli B (2007) Hydrogels for tissue engineering and delivery of tissue-inducing substances. J Pharm Sci, 96:2197-2223.

Bartholoma P, Gorjup E, Monz D, Reininger-Mack A, Thielecke H, Robitzki A (2005) Three-dimensional in vitro reaggregates of embryonic cardiomyocytes: a potential model system for monitoring effects of bioactive agents. J Biomol Screen, 10:814-822.

Bergmann O, Bhardwaj RD, Bernard S, et al. (2009) Evidence for cardiomyocyte renewal in humans. Science, 324:98-102.

Bimber B, Dettman RW, Simon HG (2007) Differential regulation of Tbx5 protein expression and sub-cellular localization during heart development. Dev Biol, 302:230-242.

Boor PJ, Ferrans VJ (1985) Ultrastructural alterations in allylamine cardiovascular toxicity. Late myocardial and vascular lesions. Am J Pathol, 121:39-54.

Bourges X, Weiss P, Coudreuse A, Daculsi G, Legeay G (2002a) General properties of silated hydroxyethylcellulose for potential biomedical applications. Biopolymers, 63:232-238.

Bourges X, Weiss P, Daculsi G, Legeay G (2002b) Synthesis and general properties of silated-hydroxypropyl methylcellulose in prospect of biomedical use. Adv Colloid Interface Sci, 99:215-228.

Boyle AJ, McNiece IK, Hare JM (2010) Mesenchymal stem cell therapy for cardiac repair. Methods Mol Biol, 660:65-84.

Bursac N, Papadaki M, Cohen RJ, et al. (1999) Cardiac muscle tissue engineering: toward an in vitro model for electrophysiological studies. Am J Physiol, 277:H433-444.

Cadee JA, van Luyn MJ, Brouwer LA, et al. (2000) In vivo biocompatibility of dextran-based hydrogels. J Biomed Mater Res, 50:397-404.

Cai Z, Manalo DJ, Wei G, et al. (2003) Hearts from rodents exposed to intermittent hypoxia or erythropoietin are protected against ischemia-reperfusion injury. Circulation, 108:79-85.

Cai Z, Zhong H, Bosch-Marce M, et al. (2008) Complete loss of ischaemic preconditioning-induced cardioprotection in mice with partial deficiency of HIF-1 alpha. Cardiovasc Res, 77:463-470.

Calverley DC, Roth GJ (1998) Antiplatelet therapy. Aspirin, ticlopidine/clopidogrel, and anti-integrin agents. Hematol Oncol Clin North Am, 12:1231-1249, vi.

Can A, Karahuseyinoglu S (2007) Concise review: human umbilical cord stroma with regard to the source of fetus-derived stem cells. Stem Cells, 25:2886-2895.

Chamberlain G, Fox J, Ashton B, Middleton J (2007) Concise review: mesenchymal stem cells: their phenotype, differentiation capacity, immunological features, and potential for homing. Stem Cells, 25:2739-2749.

Chan CW, Kwong YL, Kwong RY, Lau CP, Tse HF (2010) Improvement of myocardial perfusion reserve detected by cardiovascular magnetic resonance after direct endomyocardial implantation of autologous bone marrow cells in patients with severe coronary artery disease. J Cardiovasc Magn Reson, 12:6.

Charbord P (2010) Bone marrow mesenchymal stem cells: historical overview and concepts. Hum Gene Ther, 21:1045-1056.

Chaudhry PA, Mishima T, Sharov VG, et al. (2000) Passive epicardial containment prevents ventricular remodeling in heart failure. Ann Thorac Surg, 70:1275-1280.

Chavan V, Patil N, Karnik ND (2007) Study of leukocytic hydrolytic enzymes in patients with acute stage of coronary heart disease. Indian J Med Sci, 61:73-82.

Chen B, Han BH, Sun XH, Lim RW (1997) Inhibition of muscle-specific gene expression by Id3: requirement of the C-terminal region of the protein for stable expression and function. Nucleic Acids Res, 25:423-430.

Chen S, Liu Z, Tian N, et al. (2006) Intracoronary transplantation of autologous bone marrow mesenchymal stem cells for ischemic cardiomyopathy due to isolated chronic occluded left anterior descending artery. J Invasive Cardiol, 18:552-556.

Chen SL, Fang WW, Ye F, et al. (2004) Effect on left ventricular function of intracoronary transplantation of autologous bone marrow mesenchymal stem cell in patients with acute myocardial infarction. Am J Cardiol, 94:92-95.

Cheng Z, Ou L, Zhou X, et al. (2008) Targeted migration of mesenchymal stem cells modified with CXCR4 gene to infarcted myocardium improves cardiac performance. Mol Ther, 16:571-579.

Chlopcikova S, Psotova J, Miketova P (2001) Neonatal rat cardiomyocytes--a model for the study of morphological, biochemical and electrophysiological characteristics of the heart. Biomed Pap Med Fac Univ Palacky Olomouc Czech Repub, 145:49-55.

Christman KL, Fang Q, Yee MS, Johnson KR, Sievers RE, Lee RJ (2005) Enhanced neovasculature formation in ischemic myocardium following delivery of pleiotrophin plasmid in a biopolymer. Biomaterials, 26:1139-1144.

Christman KL, Fok HH, Sievers RE, Fang Q, Lee RJ (2004a) Fibrin glue alone and skeletal myoblasts in a fibrin scaffold preserve cardiac function after myocardial infarction. Tissue Eng, 10:403-409.

Christman KL, Lee RJ (2006) Biomaterials for the treatment of myocardial infarction. J Am Coll Cardiol, 48:907-913.

Christman KL, Vardanian AJ, Fang Q, Sievers RE, Fok HH, Lee RJ (2004b) Injectable fibrin scaffold improves cell transplant survival, reduces infarct expansion, and induces neovasculature formation in ischemic myocardium. J Am Coll Cardiol, 44:654-660.

Commeau P (2011) [Management of acute myocardial infarction. How improve primary angioplasty?]. Presse Med, 40:606-610.

Cortes-Morichetti M, Frati G, Schussler O, et al. (2007) Association between a cell-seeded collagen matrix and cellular cardiomyoplasty for myocardial support and regeneration. Tissue Eng, 13:2681-2687.

Curtis MW, Russell B (2009) Cardiac tissue engineering. J Cardiovasc Nurs, 24:87-92.

Curtis MW, Russell B (2011) Micromechanical regulation in cardiac myocytes and fibroblasts: implications for tissue remodeling. Pflugers Arch, 462:105-117.

d'Ayala GG, Malinconico M, Laurienzo P (2008) Marine derived polysaccharides for biomedical applications: chemical modification approaches. Molecules, 13:2069-2106.

Dai W, Wold LE, Dow JS, Kloner RA (2005) Thickening of the infarcted wall by collagen injection improves left ventricular function in rats: a novel approach to preserve cardiac function after myocardial infarction. J Am Coll Cardiol, 46:714-719.

Davis ME, Hsieh PC, Takahashi T, et al. (2006) Local myocardial insulin-like growth factor 1 (IGF-1) delivery with biotinylated peptide nanofibers improves cell therapy for myocardial infarction. Proc Natl Acad Sci U S A, 103:8155-8160.

Davis ME, Motion JP, Narmoneva DA, et al. (2005) Injectable self-assembling peptide nanofibers create intramyocardial microenvironments for endothelial cells. Circulation, 111:442-450.

de la Fuente R, Bernad A, Garcia-Castro J, Martin MC, Cigudosa JC (2010) Retraction: Spontaneous human adult stem cell transformation. Cancer Res, 70:6682.

Deng C, Zhang P, Vulesevic B, et al. (2010) A collagen-chitosan hydrogel for endothelial differentiation and angiogenesis. Tissue Eng Part A, 16:3099-3109.

Deuse T, Peter C, Fedak PW, et al. (2009) Hepatocyte growth factor or vascular endothelial growth factor gene transfer maximizes mesenchymal stem cell-based myocardial salvage after acute myocardial infarction. Circulation, 120:S247-254.

Di Nicola M, Carlo-Stella C, Magni M, et al. (2002) Human bone marrow stromal cells suppress T-lymphocyte proliferation induced by cellular or nonspecific mitogenic stimuli. Blood, 99:3838-3843.

Dobner S, Bezuidenhout D, Govender P, Zilla P, Davies N (2009) A synthetic non-degradable polyethylene glycol hydrogel retards adverse post-infarct left ventricular remodeling. J Card Fail, 15:629-636.

Dominici M, Le Blanc K, Mueller I, et al. (2006) Minimal criteria for defining multipotent mesenchymal stromal cells. The International Society for Cellular Therapy position statement. Cytotherapy, 8:315-317.

Dow J, Simkhovich BZ, Kedes L, Kloner RA (2005) Washout of transplanted cells from the heart: a potential new hurdle for cell transplantation therapy. Cardiovasc Res, 67:301-307.

Du YY, Zhou SH, Zhou T, et al. (2008) Immuno-inflammatory regulation effect of mesenchymal stem cell transplantation in a rat model of myocardial infarction. Cytotherapy, 10:469-478.

Dubois G, Segers VF, Bellamy V, et al. (2008) Self-assembling peptide nanofibers and skeletal myoblast transplantation in infarcted myocardium. J Biomed Mater Res B Appl Biomater, 87:222-228.

Engler AJ, Carag-Krieger C, Johnson CP, et al. (2008) Embryonic cardiomyocytes beat best on a matrix with heart-like elasticity: scar-like rigidity inhibits beating. J Cell Sci, 121:3794-3802.

Engler AJ, Sen S, Sweeney HL, Discher DE (2006) Matrix elasticity directs stem cell lineage specification. Cell, 126:677-689.

Enoki C, Otani H, Sato D, Okada T, Hattori R, Imamura H (2010) Enhanced mesenchymal cell engraftment by IGF-1 improves left ventricular function in rats undergoing myocardial infarction. Int J Cardiol, 138:9-18.

Enomoto Y, Gorman JH, 3rd, Moainie SL, et al. (2005) Early ventricular restraint after myocardial infarction: extent of the wrap determines the outcome of remodeling. Ann Thorac Surg, 79:881-887; discussion 881-887.

Eschenhagen T, Fink C, Remmers U, et al. (1997) Three-dimensional reconstitution of embryonic cardiomyocytes in a collagen matrix: a new heart muscle model system. FASEB J, 11:683-694.

Evans SM, Mummery C, Doevendans PA (2007) Progenitor cells for cardiac repair. Semin Cell Dev Biol, 18:153-160.

Fatimi A, Tassin JF, Quillard S, Axelos MA, Weiss P (2008) The rheological properties of silated hydroxypropylmethylcellulose tissue engineering matrices. Biomaterials, 29:533-543.

Faustino RS, Behfar A, Perez-Terzic C, Terzic A (2008) Genomic chart guiding embryonic stem cell cardiopoiesis. Genome Biol, 9:R6.

Fazel S, Chen L, Weisel RD, et al. (2005) Cell transplantation preserves cardiac function after infarction by infarct stabilization: augmentation by stem cell factor. J Thorac Cardiovasc Surg, 130:1310.

Feng C, Zhu J, Zhao L, et al. (2009) Suberoylanilide hydroxamic acid promotes cardiomyocyte differentiation of rat mesenchymal stem cells. Exp Cell Res, 315:3044-3051.

Fernandes S, Naumova AV, Zhu WZ, Laflamme MA, Gold J, Murry CE (2010) Human embryonic stem cell-derived cardiomyocytes engraft but do not alter cardiac remodeling after chronic infarction in rats. J Mol Cell Cardiol, 49:941-949.

Feygin J, Mansoor A, Eckman P, Swingen C, Zhang J (2007) Functional and bioenergetic modulations in the infarct border zone following autologous mesenchymal stem cell transplantation. Am J Physiol Heart Circ Physiol, 293:H1772-1780.

Flynn A, O'Brien T (2011) Stem cell therapy for cardiac disease. Expert Opin Biol Ther, 11:177-187.

Forest VF, Tirouvanziam AM, Perigaud C, et al. (2010) Cell distribution after intracoronary bone marrow stem cell delivery in damaged and undamaged myocardium: implications for clinical trials. Stem Cell Res Ther, 1:4.

Freestone NS, Ribaric S, Mason WT (1996) The effect of insulin-like growth factor-1 on adult rat cardiac contractility. Mol Cell Biochem, 163-164:223-229.

Freyman T, Polin G, Osman H, et al. (2006) A quantitative, randomized study evaluating three methods of mesenchymal stem cell delivery following myocardial infarction. Eur Heart J, 27:1114-1122.

Friedenstein AJ, Gorskaja JF, Kulagina NN (1976) Fibroblast precursors in normal and irradiated mouse hematopoietic organs. Exp Hematol, 4:267-274.

Friis T, Haack-Sorensen M, Mathiasen AB, et al. (2011) Mesenchymal stromal cell derived endothelial progenitor treatment in patients with refractory angina. Scand Cardiovasc J, 45:161-168.

Fujimoto KL, Ma Z, Nelson DM, et al. (2009) Synthesis, characterization and therapeutic efficacy of a biodegradable, thermoresponsive hydrogel designed for application in chronic infarcted myocardium. Biomaterials, 30:4357-4368.

Furlani D, Li W, Pittermann E, et al. (2009) A transformed cell population derived from cultured mesenchymal stem cells has no functional effect after transplantation into the injured heart. Cell Transplant, 18:319-331.

Garbern JC, Hoffman AS, Stayton PS (2010) Injectable pH- and temperature-responsive poly(N-isopropylacrylamide-co-propylacrylic acid) copolymers for delivery of angiogenic growth factors. Biomacromolecules, 11:1833-1839.

Ghosh TK, Packham EA, Bonser AJ, Robinson TE, Cross SJ, Brook JD (2001) Characterization of the TBX5 binding site and analysis of mutations that cause Holt-Oram syndrome. Hum Mol Genet, 10:1983-1994.

Gilbert DR, Schroeder M, van Helden J (2000) Interactive visualization and exploration of relationships between biological objects. Trends Biotechnol, 18:487-494.

Gnecchi M, He H, Liang OD, et al. (2005) Paracrine action accounts for marked protection of ischemic heart by Akt-modified mesenchymal stem cells. Nat Med, 11:367-368.

Gnecchi M, He H, Melo LG, et al. (2009) Early beneficial effects of bone marrow-derived mesenchymal stem cells overexpressing Akt on cardiac metabolism after myocardial infarction. Stem Cells, 27:971-979.

Gnecchi M, He H, Noiseux N, et al. (2006) Evidence supporting paracrine hypothesis for Akt-modified mesenchymal stem cell-mediated cardiac protection and functional improvement. FASEB J, 20:661-669.

Gnecchi M, Zhang Z, Ni A, Dzau VJ (2008) Paracrine mechanisms in adult stem cell signaling and therapy. Circ Res, 103:1204-1219.

Gorman RC, Jackson BM, Burdick JA, Gorman JH (2011) Infarct restraint to limit adverse ventricular remodeling. J Cardiovasc Transl Res, 4:73-81.

Griffith LG, Naughton G (2002) Tissue engineering--current challenges and expanding opportunities. Science, 295:1009-1014.

Grinnemo KH, Mansson A, Dellgren G, et al. (2004) Xenoreactivity and engraftment of human mesenchymal stem cells transplanted into infarcted rat myocardium. J Thorac Cardiovasc Surg, 127:1293-1300.

Hahn JY, Cho HJ, Kang HJ, et al. (2008) Pre-treatment of mesenchymal stem cells with a combination of growth factors enhances gap junction formation, cytoprotective effect on cardiomyocytes, and therapeutic efficacy for myocardial infarction. J Am Coll Cardiol, 51:933-943.

Hakuno D, Fukuda K, Makino S, et al. (2002) Bone marrow-derived regenerated cardiomyocytes (CMG Cells) express functional adrenergic and muscarinic receptors. Circulation, 105:380-386.

Halkos ME, Zhao ZQ, Kerendi F, et al. (2008) Intravenous infusion of mesenchymal stem cells enhances regional perfusion and improves ventricular function in a porcine model of myocardial infarction. Basic Res Cardiol, 103:525-536.

Hao X, Silva EA, Mansson-Broberg A, et al. (2007) Angiogenic effects of sequential release of VEGF-A165 and PDGF-BB with alginate hydrogels after myocardial infarction. Cardiovasc Res, 75:178-185.

Hardy ME, Lawrence CL, Standen NB, Rodrigo GC (2006) Can optical recordings of membrane potential be used to screen for drug-induced action potential prolongation in single cardiac myocytes? J Pharmacol Toxicol Methods, 54:173-182.

Hare JM, Traverse JH, Henry TD, et al. (2009) A randomized, double-blind, placebo-controlled, dose-escalation study of intravenous adult human mesenchymal stem cells (prochymal) after acute myocardial infarction. J Am Coll Cardiol, 54:2277-2286.

Hattan N, Kawaguchi H, Ando K, et al. (2005) Purified cardiomyocytes from bone marrow mesenchymal stem cells produce stable intracardiac grafts in mice. Cardiovasc Res, 65:334-344.

Hatzistergos KE, Blum A, Ince T, Grichnik JM, Hare JM (2011) What is the oncologic risk of stem cell treatment for heart disease? Circ Res, 108:1300-1303.

He XQ, Chen MS, Li SH, et al. (2010) Co-culture with cardiomyocytes enhanced the myogenic conversion of mesenchymal stromal cells in a dose-dependent manner. Mol Cell Biochem, 339:89-98.

Henning RJ, Burgos JD, Vasko M, et al. (2007) Human cord blood cells and myocardial infarction: effect of dose and route of administration on infarct size. Cell Transplant, 16:907-917.

Herrmann JL, Abarbanell AM, Weil BR, et al. (2011) Optimizing stem cell function for the treatment of ischemic heart disease. J Surg Res, 166:138-145.

Hiroi Y, Kudoh S, Monzen K, et al. (2001) Tbx5 associates with Nkx2-5 and synergistically promotes cardiomyocyte differentiation. Nat Genet, 28:276-280.

Hsieh PC, Davis ME, Gannon J, MacGillivray C, Lee RT (2006a) Controlled delivery of PDGF-BB for myocardial protection using injectable self-assembling peptide nanofibers. J Clin Invest, 116:237-248.

Hsieh PC, MacGillivray C, Gannon J, Cruz FU, Lee RT (2006b) Local controlled intramyocardial delivery of platelet-derived growth factor improves postinfarction ventricular function without pulmonary toxicity. Circulation, 114:637-644.

Hu X, Wang J, Chen J, et al. (2007) Optimal temporal delivery of bone marrow mesenchymal stem cells in rats with myocardial infarction. Eur J Cardiothorac Surg, 31:438-443.

Hu X, Yu SP, Fraser JL, et al. (2008) Transplantation of hypoxia-preconditioned mesenchymal stem cells improves infarcted heart function via enhanced survival of implanted cells and angiogenesis. J Thorac Cardiovasc Surg, 135:799-808.

Ieda M, Fu JD, Delgado-Olguin P, et al. (2010) Direct reprogramming of fibroblasts into functional cardiomyocytes by defined factors. Cell, 142:375-386.

Ifkovits JL, Tous E, Minakawa M, et al. (2010) Injectable hydrogel properties influence infarct expansion and extent of postinfarction left ventricular remodeling in an ovine model. Proc Natl Acad Sci U S A, 107:11507-11512.

Itano N (2008) Simple primary structure, complex turnover regulation and multiple roles of hyaluronan. J Biochem, 144:131-137.

Iwakura A, Fujita M, Kataoka K, et al. (2003) Intramyocardial sustained delivery of basic fibroblast growth factor improves angiogenesis and ventricular function in a rat infarct model. Heart Vessels, 18:93-99.

Jacot JG, McCulloch AD, Omens JH (2008) Substrate stiffness affects the functional maturation of neonatal rat ventricular myocytes. Biophys J, 95:3479-3487.

Janssens S (2010) Stem cells in the treatment of heart disease. Annu Rev Med, 61:287-300.

Jawad H, Ali NN, Lyon AR, Chen QZ, Harding SE, Boccaccini AR (2007) Myocardial tissue engineering: a review. J Tissue Eng Regen Med, 1:327-342.

Jiang W, Ma A, Wang T, et al. (2006) Homing and differentiation of mesenchymal stem cells delivered intravenously to ischemic myocardium in vivo: a time-series study. Pflugers Arch, 453:43-52.

Jiang XJ, Wang T, Li XY, et al. (2009) Injection of a novel synthetic hydrogel preserves left ventricle function after myocardial infarction. J Biomed Mater Res A, 90:472-477.

Johns TN, Olson BJ (1954) Experimental myocardial infarction. I. A method of coronary occlusion in small animals. Ann Surg, 140:675-682.

Kamihata H, Matsubara H, Nishiue T, et al. (2001) Implantation of bone marrow mononuclear cells into ischemic myocardium enhances collateral perfusion and regional function via side supply of angioblasts, angiogenic ligands, and cytokines. Circulation, 104:1046-1052.

Katritsis DG, Sotiropoulou P, Giazitzoglou E, Karvouni E, Papamichail M (2007) Electrophysiological effects of intracoronary transplantation of autologous mesenchymal and endothelial progenitor cells. Europace, 9:167-171.

Katritsis DG, Sotiropoulou PA, Karvouni E, et al. (2005) Transcoronary transplantation of autologous mesenchymal stem cells and endothelial progenitors into infarcted human myocardium. Catheter Cardiovasc Interv, 65:321-329.

Kellar RS, Shepherd BR, Larson DF, Naughton GK, Williams SK (2005) Cardiac patch constructed from human fibroblasts attenuates reduction in cardiac function after acute infarct. Tissue Eng, 11:1678-1687.

Kelley ST, Malekan R, Gorman JH, 3rd, et al. (1999) Restraining infarct expansion preserves left ventricular geometry and function after acute anteroapical infarction. Circulation, 99:135-142.

Khor E, Lim LY (2003) Implantable applications of chitin and chitosan. Biomaterials, 24:2339-2349.

Kim YS, Park HJ, Hong MH, et al. (2009) TNF-alpha enhances engraftment of mesenchymal stem cells into infarcted myocardium. Front Biosci, 14:2845-2856.

Kinnaird T, Stabile E, Burnett MS, et al. (2004) Marrow-derived stromal cells express genes encoding a broad spectrum of arteriogenic cytokines and promote in vitro and in vivo arteriogenesis through paracrine mechanisms. Circ Res, 94:678-685.

Kofidis T, Akhyari P, Boublik J, et al. (2002) In vitro engineering of heart muscle: artificial myocardial tissue. J Thorac Cardiovasc Surg, 124:63-69.

Kofidis T, de Bruin JL, Hoyt G, et al. (2005) Myocardial restoration with embryonic stem cell bioartificial tissue transplantation. J Heart Lung Transplant, 24:737-744.

Koninckx R, Hensen K, Daniels A, et al. (2009) Human bone marrow stem cells co-cultured with neonatal rat cardiomyocytes display limited cardiomyogenic plasticity. Cytotherapy:1-15.

Kretlow JD, Klouda L, Mikos AG (2007) Injectable matrices and scaffolds for drug delivery in tissue engineering. Adv Drug Deliv Rev, 59:263-273.

Krupnick AS, Kreisel D, Engels FH, et al. (2002) A novel small animal model of left ventricular tissue engineering. J Heart Lung Transplant, 21:233-243.

Kuraitis D, Suuronen EJ, Sellke FW, Ruel M (2010) The future of regenerating the myocardium. Curr Opin Cardiol, 25:575-582.

Kutschka I, Chen IY, Kofidis T, et al. (2006) Collagen matrices enhance survival of transplanted cardiomyoblasts and contribute to functional improvement of ischemic rat hearts. Circulation, 114:I167-173.

Labovsky V, Hofer EL, Feldman L, et al. (2010) Cardiomyogenic differentiation of human bone marrow mesenchymal cells: Role of cardiac extract from neonatal rat cardiomyocytes. Differentiation, 79:93-101.

Ladhoff J, Fleischer B, Hara Y, Volk HD, Seifert M (2010) Immune privilege of endothelial cells differentiated from endothelial progenitor cells. Cardiovasc Res, 88:121-129.

Laflamme MA, Murry CE (2011) Heart regeneration. Nature, 473:326-335.

Laham RJ, Sellke FW, Edelman ER, et al. (1999) Local perivascular delivery of basic fibroblast growth factor in patients undergoing coronary bypass surgery: results of a phase I randomized, double-blind, placebo-controlled trial. Circulation, 100:1865-1871.

Le Visage C, Gournay O, Benguirat N, et al. (2011) Mesenchymal Stem Cell Delivery into Rat Infarcted Myocardium Using a Porous Polysaccharide-Based Scaffold: A Quantitative Comparison with Endocardial Injection. Tissue Eng Part A.

Lee CH, Singla A, Lee Y (2001) Biomedical applications of collagen. Int J Pharm, 221:1-22.

Lehoczky-Mona J, McCandless EL (1964) Ischemic Induction of Chondrogenesis in Myocardium. Arch Pathol, 78:37-42.

Leor J, Aboulafia-Etzion S, Dar A, et al. (2000) Bioengineered cardiac grafts: A new approach to repair the infarcted myocardium? Circulation, 102:III56-61.

Leor J, Amsalem Y, Cohen S (2005) Cells, scaffolds, and molecules for myocardial tissue engineering. Pharmacol Ther, 105:151-163.

Leor J, Tuvia S, Guetta V, et al. (2009) Intracoronary injection of in situ forming alginate hydrogel reverses left ventricular remodeling after myocardial infarction in Swine. J Am Coll Cardiol, 54:1014-1023.

Li Q, Turdi S, Thomas DP, Zhou T, Ren J (2010a) Intra-myocardial delivery of mesenchymal stem cells ameliorates left ventricular and cardiomyocyte contractile dysfunction following myocardial infarction. Toxicol Lett, 195:119-126.

Li XY, Wang T, Jiang XJ, et al. (2010b) Injectable hydrogel helps bone marrow-derived mononuclear cells restore infarcted myocardium. Cardiology, 115:194-199.

Lickert H, Takeuchi JK, Von Both I, et al. (2004) Baf60c is essential for function of BAF chromatin remodelling complexes in heart development. Nature, 432:107-112.

Lim SY, Kim YS, Ahn Y, et al. (2006) The effects of mesenchymal stem cells transduced with Akt in a porcine myocardial infarction model. Cardiovasc Res, 70:530-542.

Liu W, Zhang B, Lu WW, et al. (2004) A rapid temperature-responsive sol-gel reversible poly(N-isopropylacrylamide)-g-methylcellulose copolymer hydrogel. Biomaterials, 25:3005-3012.

Livak KJ, Schmittgen TD (2001) Analysis of relative gene expression data using real-time quantitative PCR and the 2(-Delta Delta C(T)) Method. Methods, 25:402-408.

Loffredo FS, Steinhauser ML, Gannon J, Lee RT (2011) Bone marrow-derived cell therapy stimulates endogenous cardiomyocyte progenitors and promotes cardiac repair. Cell Stem Cell, 8:389-398.

Lopez JJ, Edelman ER, Stamler A, et al. (1997) Basic fibroblast growth factor in a porcine model of chronic myocardial ischemia: a comparison of angiographic, echocardiographic and coronary flow parameters. J Pharmacol Exp Ther, 282:385-390.

Lu WN, Lu SH, Wang HB, et al. (2009) Functional improvement of infarcted heart by co-injection of embryonic stem cells with temperature-responsive chitosan hydrogel. Tissue Eng Part A, 15:1437-1447.

Lutolf MP, Hubbell JA (2005) Synthetic biomaterials as instructive extracellular microenvironments for morphogenesis in tissue engineering. Nat Biotechnol, 23:47-55.

Madonna R, Geng YJ, De Caterina R (2009) Adipose tissue-derived stem cells: characterization and potential for cardiovascular repair. Arterioscler Thromb Vasc Biol, 29:1723-1729.

Makino S, Fukuda K, Miyoshi S, et al. (1999) Cardiomyocytes can be generated from marrow stromal cells in vitro. J Clin Invest, 103:697-705.

Markel TA, Wang Y, Herrmann JL, et al. (2008) VEGF is critical for stem cell-mediated cardioprotection and a crucial paracrine factor for defining the age threshold in adult and neonatal stem cell function. Am J Physiol Heart Circ Physiol, 295:H2308-2314.

Matsumoto R, Omura T, Yoshiyama M, et al. (2005) Vascular endothelial growth factor-expressing mesenchymal stem cell transplantation for the treatment of acute myocardial infarction. Arterioscler Thromb Vasc Biol, 25:1168-1173.

Maurel A, Azarnoush K, Sabbah L, et al. (2005) Can cold or heat shock improve skeletal myoblast engraftment in infarcted myocardium? Transplantation, 80:660-665.

Mazo M, Gavira JJ, Abizanda G, et al. (2010) Transplantation of mesenchymal stem cells exerts a greater long-term effect than bone marrow mononuclear cells in a chronic myocardial infarction model in rat. Cell Transplant, 19:313-328.

Melnikova IN, Christy BA (1996) Muscle cell differentiation is inhibited by the helix-loop-helix protein Id3. Cell Growth Differ, 7:1067-1079.

Merceron C, Portron S, Masson M, et al. (2010) Cartilage tissue engineering: From hydrogel to mesenchymal stem cells. Biomed Mater Eng, 20:159-166.

Merceron C, Portron S, Masson M, et al. (2011) The effect of two and three dimensional cell culture on the chondrogenic potential of human adipose-derived mesenchymal stem cells after subcutaneous transplantation with an injectable hydrogel. Cell Transplant.

Merceron C, Vinatier C, Clouet J, Colliec-Jouault S, Weiss P, Guicheux J (2008) Adipose-derived mesenchymal stem cells and biomaterials for cartilage tissue engineering. Joint Bone Spine, 75:672-674.

Mias C, Lairez O, Trouche E, et al. (2009) Mesenchymal stem cells promote matrix metalloproteinase secretion by cardiac fibroblasts and reduce cardiac ventricular fibrosis after myocardial infarction. Stem Cells, 27:2734-2743.

Mias C, Trouche E, Seguelas MH, et al. (2008) Ex vivo pretreatment with melatonin improves survival, proangiogenic/mitogenic activity, and efficiency of mesenchymal stem cells injected into ischemic kidney. Stem Cells, 26:1749-1757.

Min JJ, Ahn Y, Moon S, et al. (2006) In vivo bioluminescence imaging of cord blood derived mesenchymal stem cell transplantation into rat myocardium. Ann Nucl Med, 20:165-170.

Miyahara Y, Nagaya N, Kataoka M, et al. (2006) Monolayered mesenchymal stem cells repair scarred myocardium after myocardial infarction. Nat Med, 12:459-465.

Morkin E (2000) Control of cardiac myosin heavy chain gene expression. Microsc Res Tech, 50:522-531.

Morrison DA, Sacks J (2003) Balancing benefit against risk in the choice of therapy for coronary artery disease. Lesson from prospective, randomized, clinical trials of percutaneous coronary intervention and coronary artery bypass graft surgery. Minerva Cardioangiol, 51:585-597.

Morrison SJ, Spradling AC (2008) Stem cells and niches: mechanisms that promote stem cell maintenance throughout life. Cell, 132:598-611.

Mukherjee D (2011) Antithrombotics and stent type for primary PCI. Lancet, 377:2154-2156.

Naito M, Stirk CM, Smith EB, Thompson WD (2000) Smooth muscle cell outgrowth stimulated by fibrin degradation products. The potential role of fibrin fragment E in restenosis and atherogenesis. Thromb Res, 98:165-174.

Nemer G, Nemer M (2001) Regulation of heart development and function through combinatorial interactions of transcription factors. Ann Med, 33:604-610.

Neuman Y, Pereg D, Boyko V, Behar S, Mosseri M (2011) Primary angioplasty in patients following coronary artery bypass surgery: Trends in Application and Outcome. Results from the Acute Coronary Syndrome Israeli Survey (ACSIS) 2000-2008. Catheter Cardiovasc Interv.

Noiseux N, Gnecchi M, Lopez-Ilasaca M, et al. (2006) Mesenchymal stem cells overexpressing Akt dramatically repair infarcted myocardium and improve cardiac function despite infrequent cellular fusion or differentiation. Mol Ther, 14:840-850.

Ohnishi S, Sumiyoshi H, Kitamura S, Nagaya N (2007) Mesenchymal stem cells attenuate cardiac fibroblast proliferation and collagen synthesis through paracrine actions. FEBS Lett, 581:3961-3966.

Okamoto K, Miyoshi S, Toyoda M, et al. (2007) 'Working' cardiomyocytes exhibiting plateau action potentials from human placenta-derived extraembryonic mesodermal cells. Exp Cell Res, 313:2550-2562.

Okuyama H, Krishnamachary B, Zhou YF, Nagasawa H, Bosch-Marce M, Semenza GL (2006) Expression of vascular endothelial growth factor receptor 1 in bone marrow-derived mesenchymal cells is dependent on hypoxia-inducible factor 1. J Biol Chem, 281:15554-15563.

Olsson A, Bredin F, Franco-Cereceda A (2005) Echocardiographic findings using tissue velocity imaging following passive containment surgery with the Acorn CorCap cardiac support device. Eur J Cardiothorac Surg, 28:448-453.

Padin-Iruegas ME, Misao Y, Davis ME, et al. (2009) Cardiac progenitor cells and biotinylated insulin-like growth factor-1 nanofibers improve endogenous and exogenous myocardial regeneration after infarction. Circulation, 120:876-887.

Papadaki M, Bursac N, Langer R, Merok J, Vunjak-Novakovic G, Freed LE (2001) Tissue engineering of functional cardiac muscle: molecular, structural, and electrophysiological studies. Am J Physiol Heart Circ Physiol, 280:H168-178.

Parikh D, Juergens CP (2011) Abciximab as an adjunctive therapy for patients undergoing percutaneous coronary interventions. Expert Opin Biol Ther, 11:235-246.

Peran M, Marchal JA, Lopez E, et al. (2010) Human cardiac tissue induces transdifferentiation of adult stem cells towards cardiomyocytes. Cytotherapy, 12:332-337.

Perin EC, Dohmann HF, Borojevic R, et al. (2003) Transendocardial, autologous bone marrow cell transplantation for severe, chronic ischemic heart failure. Circulation, 107:2294-2302.

Perl L, Weissler A, Mekori YA, Mor A (2010) Cellular therapy in 2010: focus on autoimmune and cardiac diseases. Isr Med Assoc J, 12:110-115.

Peroni D, Scambi I, Pasini A, et al. (2008) Stem molecular signature of adipose-derived stromal cells. Exp Cell Res, 314:603-615.

Pfeffer MA, Braunwald E (1990) Ventricular remodeling after myocardial infarction. Experimental observations and clinical implications. Circulation, 81:1161-1172.

Pignier C, Ancey C, Fares N, Bescond J, Potreau D (2002) Reexpression of the nifedipine-resistant calcium channel during dedifferentiation of adult rat ventricular cardiomyocytes. J Cardiovasc Electrophysiol, 13:178-183.

Piro M, Della Bona R, Abbate A, Biasucci LM, Crea F (2010) Sex-related differences in myocardial remodeling. J Am Coll Cardiol, 55:1057-1065.

Pittenger MF, Mackay AM, Beck SC, et al. (1999) Multilineage potential of adult human mesenchymal stem cells. Science, 284:143-147.

Poncelet AJ, Hiel AL, Vercruysse J, Hermans D, Zech F, Gianello P (2010) Intracardiac allogeneic mesenchymal stem cell transplantation elicits neo-angiogenesis in a fully immunocompetent ischaemic swine model. Eur J Cardiothorac Surg, 38:781-787.

Prockop DJ, Olson SD (2007) Clinical trials with adult stem/progenitor cells for tissue repair: let's not overlook some essential precautions. Blood, 109:3147-3151.

Psaltis PJ, Zannettino AC, Worthley SG, Gronthos S (2008) Concise review: mesenchymal stromal cells: potential for cardiovascular repair. Stem Cells, 26:2201-2210.

Rane AA, Chuang JS, Shah A, et al. (2011) Increased infarct wall thickness by a bio-inert material is insufficient to prevent negative left ventricular remodeling after myocardial infarction. PLoS One, 6:e21571.

Renner P, Eggenhofer E, Rosenauer A, et al. (2009) Mesenchymal stem cells require a sufficient, ongoing immune response to exert their immunosuppressive function. Transplant Proc, 41:2607-2611.

Roncalli J, Mouquet F, Piot C, et al. (2010) Intracoronary autologous mononucleated bone marrow cell infusion for acute myocardial infarction: results of the randomized multicenter BONAMI trial. Eur Heart J.

Rosland GV, Svendsen A, Torsvik A, et al. (2009) Long-term cultures of bone marrow-derived human mesenchymal stem cells frequently undergo spontaneous malignant transformation. Cancer Res, 69:5331-5339.

Rosova I, Dao M, Capoccia B, Link D, Nolta JA (2008) Hypoxic preconditioning results in increased motility and improved therapeutic potential of human mesenchymal stem cells. Stem Cells, 26:2173-2182.

Roura S, Farre J, Hove-Madsen L, et al. (2010) Exposure to cardiomyogenic stimuli fails to transdifferentiate human umbilical cord blood-derived mesenchymal stem cells. Basic Res Cardiol, 105:419-430.

Rubio D, Garcia-Castro J, Martin MC, et al. (2005) Spontaneous human adult stem cell transformation. Cancer Res, 65:3035-3039.

Ruvinov E, Leor J, Cohen S (2010) The effects of controlled HGF delivery from an affinity-binding alginate biomaterial on angiogenesis and blood perfusion in a hindlimb ischemia model. Biomaterials, 31:4573-4582.

Sakakibara Y, Tambara K, Sakaguchi G, et al. (2003) Toward surgical angiogenesis using slow-released basic fibroblast growth factor. Eur J Cardiothorac Surg, 24:105-111; discussion 112.

Schuleri KH, Feigenbaum GS, Centola M, et al. (2009) Autologous mesenchymal stem cells produce reverse remodelling in chronic ischaemic cardiomyopathy. Eur Heart J, 30:2722-2732.

Schussler O, Chachques JC, Mesana TG, Suuronen EJ, Lecarpentier Y, Ruel M (2010) 3-dimensional structures to enhance cell therapy and engineer contractile tissue. Asian Cardiovasc Thorac Ann, 18:188-198.

Segers VF, Tokunou T, Higgins LJ, MacGillivray C, Gannon J, Lee RT (2007) Local delivery of protease-resistant stromal cell derived factor-1 for stem cell recruitment after myocardial infarction. Circulation, 116:1683-1692.

Sepulveda JL, Belaguli N, Nigam V, Chen CY, Nemer M, Schwartz RJ (1998) GATA-4 and Nkx-2.5 coactivate Nkx-2 DNA binding targets: role for regulating early cardiac gene expression. Mol Cell Biol, 18:3405-3415.

Shachar M, Tsur-Gang O, Dvir T, Leor J, Cohen S (2011) The effect of immobilized RGD peptide in alginate scaffolds on cardiac tissue engineering. Acta Biomater, 7:152-162.

Shao ZQ, Takaji K, Katayama Y, et al. (2006) Effects of intramyocardial administration of slow-release basic fibroblast growth factor on angiogenesis and ventricular remodeling in a rat infarct model. Circ J, 70:471-477.

Shapira-Schweitzer K, Seliktar D (2007) Matrix stiffness affects spontaneous contraction of cardiomyocytes cultured within a PEGylated fibrinogen biomaterial. Acta Biomater, 3:33-41.

Shimizu T, Yamato M, Isoi Y, et al. (2002) Fabrication of pulsatile cardiac tissue grafts using a novel 3-dimensional cell sheet manipulation technique and temperature-responsive cell culture surfaces. Circ Res, 90:e40.

Shiojima I, Komuro I, Oka T, et al. (1999) Context-dependent transcriptional cooperation mediated by cardiac transcription factors Csx/Nkx-2.5 and GATA-4. J Biol Chem, 274:8231-8239.

Sierra DH (1993) Fibrin sealant adhesive systems: a review of their chemistry, material properties and clinical applications. J Biomater Appl, 7:309-352.

Silva GV, Litovsky S, Assad JA, et al. (2005) Mesenchymal stem cells differentiate into an endothelial phenotype, enhance vascular density, and improve heart function in a canine chronic ischemia model. Circulation, 111:150-156.

Snyder M, Huang XY, Zhang JJ (2010) Stat3 directly controls the expression of Tbx5, Nkx2.5, and GATA4 and is essential for cardiomyocyte differentiation of P19CL6 cells. J Biol Chem, 285:23639-23646.

Spinale FG (2007) Myocardial matrix remodeling and the matrix metalloproteinases: influence on cardiac form and function. Physiol Rev, 87:1285-1342.

Sun L, Cui M, Wang Z, et al. (2007) Mesenchymal stem cells modified with angiopoietin-1 improve remodeling in a rat model of acute myocardial infarction. Biochem Biophys Res Commun, 357:779-784.

Takahashi K, Tanabe K, Ohnuki M, et al. (2007) Induction of pluripotent stem cells from adult human fibroblasts by defined factors. Cell, 131:861-872.

Takahashi K, Yamanaka S (2006) Induction of pluripotent stem cells from mouse embryonic and adult fibroblast cultures by defined factors. Cell, 126:663-676.

Takeuchi JK, Bruneau BG (2009) Directed transdifferentiation of mouse mesoderm to heart tissue by defined factors. Nature, 459:708-711.

Tang J, Wang J, Guo L, et al. (2010) Mesenchymal stem cells modified with stromal cell-derived factor 1 alpha improve cardiac remodeling via paracrine activation of hepatocyte growth factor in a rat model of myocardial infarction. Mol Cells, 29:9-19.

Tang J, Wang J, Yang J, et al. (2009) Mesenchymal stem cells over-expressing SDF-1 promote angiogenesis and improve heart function in experimental myocardial infarction in rats. Eur J Cardiothorac Surg, 36:644-650.

Tang J, Xie Q, Pan G, Wang J, Wang M (2006) Mesenchymal stem cells participate in angiogenesis and improve heart function in rat model of myocardial ischemia with reperfusion. Eur J Cardiothorac Surg, 30:353-361.

Tang JM, Wang JN, Zhang L, et al. (2011) VEGF/SDF-1 promotes cardiac stem cell mobilization and myocardial repair in the infarcted heart. Cardiovasc Res.

Tarte K, Gaillard J, Lataillade JJ, et al. (2010) Clinical-grade production of human mesenchymal stromal cells: occurrence of aneuploidy without transformation. Blood, 115:1549-1553.

Taylor PL, Barker RA, Blume KG, et al. (2010) Patients beware: commercialized stem cell treatments on the web. Cell Stem Cell, 7:43-49.

Thompson WD, Smith EB, Stirk CM, Marshall FI, Stout AJ, Kocchar A (1992) Angiogenic activity of fibrin degradation products is located in fibrin fragment E. J Pathol, 168:47-53.

Tian Q, Oberhofer M, Ruppenthal S, et al. (2011) Optical action potential screening on adult ventricular myocytes as an alternative QT-screen. Cell Physiol Biochem, 27:281-290.

Tolar J, Nauta AJ, Osborn MJ, et al. (2007) Sarcoma derived from cultured mesenchymal stem cells. Stem Cells, 25:371-379.

Toma C, Pittenger MF, Cahill KS, Byrne BJ, Kessler PD (2002) Human mesenchymal stem cells differentiate to a cardiomyocyte phenotype in the adult murine heart. Circulation, 105:93-98.

Tongers J, Losordo DW, Landmesser U (2011) Stem and progenitor cell-based therapy in ischaemic heart disease: promise, uncertainties, and challenges. Eur Heart J, 32:1197-1206.

Toole BP (2001) Hyaluronan in morphogenesis. Semin Cell Dev Biol, 12:79-87.

Trojani C, Weiss P, Michiels JF, et al. (2005) Three-dimensional culture and differentiation of human osteogenic cells in an injectable hydroxypropylmethylcellulose hydrogel. Biomaterials, 26:5509-5517.

Trouche E, Girod Fullana S, Mias C, et al. (2010) Evaluation of alginate microspheres for mesenchymal stem cell engraftment on solid organ. Cell Transplant, 19:1623-1633.

Tse JR, Engler AJ (2011) Stiffness gradients mimicking in vivo tissue variation regulate mesenchymal stem cell fate. PLoS One, 6:e15978.

Tsubokawa T, Yagi K, Nakanishi C, et al. (2010) Impact of anti-apoptotic and anti-oxidative effects of bone marrow mesenchymal stem cells with transient overexpression of heme oxygenase-1 on myocardial ischemia. Am J Physiol Heart Circ Physiol, 298:H1320-1329.

Tsur-Gang O, Ruvinov E, Landa N, et al. (2009) The effects of peptide-based modification of alginate on left ventricular remodeling and function after myocardial infarction. Biomaterials, 30:189-195.

Uccelli A, Moretta L, Pistoia V (2006) Immunoregulatory function of mesenchymal stem cells. Eur J Immunol, 36:2566-2573.

Urbanek K, Rota M, Cascapera S, et al. (2005) Cardiac stem cells possess growth factor-receptor systems that after activation regenerate the infarcted myocardium, improving ventricular function and long-term survival. Circ Res, 97:663-673.

van der Bogt KE, Schrepfer S, Yu J, et al. (2009) Comparison of transplantation of adipose tissue- and bone marrow-derived mesenchymal stem cells in the infarcted heart. Transplantation, 87:642-652.

Ventura C, Cantoni S, Bianchi F, et al. (2007) Hyaluronan mixed esters of butyric and retinoic Acid drive cardiac and endothelial fate in term placenta human mesenchymal stem cells and enhance cardiac repair in infarcted rat hearts. J Biol Chem, 282:14243-14252.

Vinatier C, Magne D, Moreau A, et al. (2007) Engineering cartilage with human nasal chondrocytes and a silanized hydroxypropyl methylcellulose hydrogel. J Biomed Mater Res A, 80:66-74.

Vinatier C, Magne D, Weiss P, et al. (2005) A silanized hydroxypropyl methylcellulose hydrogel for the three-dimensional culture of chondrocytes. Biomaterials, 26:6643-6651.

Vinatier C, Mrugala D, Jorgensen C, Guicheux J, Noel D (2009) Cartilage engineering: a crucial combination of cells, biomaterials and biofactors. Trends Biotechnol, 27:307-314.

Vunjak-Novakovic G, Tandon N, Godier A, et al. (2010) Challenges in cardiac tissue engineering. Tissue Eng Part B Rev, 16:169-187.

Wang H, Zhang X, Li Y, et al. (2010) Improved myocardial performance in infarcted rat heart by co-injection of basic fibroblast growth factor with temperature-responsive chitosan hydrogel. J Heart Lung Transplant, 29:881-887.

Wang T, Jiang XJ, Lin T, et al. (2009a) [Effect of a novel injectable hydrogel implant on ventricular remodeling in rabbits with experimental myocardial infarction]. Zhonghua Xin Xue Guan Bing Za Zhi, 37:174-177.

Wang T, Jiang XJ, Lin T, et al. (2009b) The inhibition of postinfarct ventricle remodeling without polycythaemia following local sustained intramyocardial delivery of erythropoietin within a supramolecular hydrogel. Biomaterials, 30:4161-4167.

Wang T, Jiang XJ, Tang QZ, et al. (2009c) Bone marrow stem cells implantation with alpha-cyclodextrin/MPEG-PCL-MPEG hydrogel improves cardiac function after myocardial infarction. Acta Biomater, 5:2939-2944.

Wang T, Wu DQ, Jiang XJ, et al. (2009d) Novel thermosensitive hydrogel injection inhibits post-infarct ventricle remodelling. Eur J Heart Fail, 11:14-19.

Wang YQ, Wang M, Zhang P, et al. (2008) Effect of transplanted mesenchymal stem cells from rats of different ages on the improvement of heart function after acute myocardial infarction. Chin Med J (Engl), 121:2290-2298.

Westrich J, Yaeger P, He C, et al. (2010) Factors affecting residence time of mesenchymal stromal cells (MSC) injected into the myocardium. Cell Transplant, 19:937-948.

Xu X, Xu Z, Xu Y, Cui G (2005) Effects of mesenchymal stem cell transplantation on extracellular matrix after myocardial infarction in rats. Coron Artery Dis, 16:245-255.

Yamada Y, Sakurada K, Takeda Y, Gojo S, Umezawa A (2007) Single-cell-derived mesenchymal stem cells overexpressing Csx/Nkx2.5 and GATA4 undergo the stochastic cardiomyogenic fate and behave like transient amplifying cells. Exp Cell Res, 313:698-706.

Yan C, Pochan DJ (2010) Rheological properties of peptide-based hydrogels for biomedical and other applications. Chem Soc Rev, 39:3528-3540.

Yang J, Zhou W, Zheng W, et al. (2007) Effects of myocardial transplantation of marrow mesenchymal stem cells transfected with vascular endothelial growth factor for the improvement of heart function and angiogenesis after myocardial infarction. Cardiology, 107:17-29.

Yang MC, Chi NH, Chou NK, et al. (2010a) The influence of rat mesenchymal stem cell CD44 surface markers on cell growth, fibronectin expression, and cardiomyogenic differentiation on silk fibroin - Hyaluronic acid cardiac patches. Biomaterials, 31:854-862.

Yang Z, Zhang F, Ma W, et al. (2010b) A novel approach to transplanting bone marrow stem cells to repair human myocardial infarction: delivery via a noninfarct-relative artery. Cardiovasc Ther, 28:380-385.

Ye Z, Zhou Y, Cai H, Tan W (2011) Myocardial regeneration: Roles of stem cells and hydrogels. Adv Drug Deliv Rev.

Yoon J, Min BG, Kim YH, Shim WJ, Ro YM, Lim DS (2005) Differentiation, engraftment and functional effects of pre-treated mesenchymal stem cells in a rat myocardial infarct model. Acta Cardiol, 60:277-284.

Yoon SJ, Fang YH, Lim CH, et al. (2009) Regeneration of ischemic heart using hyaluronic acid-based injectable hydrogel. J Biomed Mater Res B Appl Biomater, 91:163-171.

Yu J, Du KT, Fang Q, et al. (2010) The use of human mesenchymal stem cells encapsulated in RGD modified alginate microspheres in the repair of myocardial infarction in the rat. Biomaterials, 31:7012-7020.

Yu J, Gu Y, Du KT, Mihardja S, Sievers RE, Lee RJ (2009) The effect of injected RGD modified alginate on angiogenesis and left ventricular function in a chronic rat infarct model. Biomaterials, 30:751-756.

Yu J, Vodyanik MA, Smuga-Otto K, et al. (2007) Induced pluripotent stem cell lines derived from human somatic cells. Science, 318:1917-1920.

Zeng L, Hu Q, Wang X, et al. (2007) Bioenergetic and functional consequences of bone marrow-derived multipotent progenitor cell transplantation in hearts with postinfarction left ventricular remodeling. Circulation, 115:1866-1875.

Zhang C, Sun A, Zhang S, et al. (2010a) Efficacy and safety of intracoronary autologous bone marrow-derived cell transplantation in patients with acute myocardial infarction: insights from randomized controlled trials with 12 or more months follow-up. Clin Cardiol, 33:353-360.

Zhang G, Nakamura Y, Wang X, Hu Q, Suggs LJ, Zhang J (2007a) Controlled release of stromal cell-derived factor-1 alpha in situ increases c-kit+ cell homing to the infarcted heart. Tissue Eng, 13:2063-2071.

Zhang M, Mal N, Kiedrowski M, et al. (2007b) SDF-1 expression by mesenchymal stem cells results in trophic support of cardiac myocytes after myocardial infarction. FASEB J, 21:3197-3207.

Zhang M, Methot D, Poppa V, Fujio Y, Walsh K, Murry CE (2001) Cardiomyocyte grafting for cardiac repair: graft cell death and anti-death strategies. J Mol Cell Cardiol, 33:907-921.

Zhang X, Wang H, Ma X, et al. (2010b) Preservation of the cardiac function in infarcted rat hearts by the transplantation of adipose-derived stem cells with injectable fibrin scaffolds. Exp Biol Med (Maywood), 235:1505-1515.

Zhao T, Zhang D, Millard RW, Ashraf M, Wang Y (2009) Stem cell homing and angiomyogenesis in transplanted hearts are enhanced by combined intramyocardial SDF-1alpha delivery and endogenous cytokine signaling. Am J Physiol Heart Circ Physiol, 296:H976-986.

Zhou Y, Wang S, Yu Z, et al. (2009) Direct injection of autologous mesenchymal stromal cells improves myocardial function. Biochem Biophys Res Commun, 390:902-907.

Zimmermann WH, Didie M, Wasmeier GH, et al. (2002a) Cardiac grafting of engineered heart tissue in syngenic rats. Circulation, 106:I151-157.

Zimmermann WH, Eschenhagen T (2003) Cardiac tissue engineering for replacement therapy. Heart Fail Rev, 8:259-269.

Zimmermann WH, Melnychenko I, Wasmeier G, et al. (2006) Engineered heart tissue grafts improve systolic and diastolic function in infarcted rat hearts. Nat Med, 12:452-458.

Zimmermann WH, Schneiderbanger K, Schubert P, et al. (2002b) Tissue engineering of a differentiated cardiac muscle construct. Circ Res, 90:223-230.

Zisa D, Shabbir A, Suzuki G, Lee T (2009) Vascular endothelial growth factor (VEGF) as a key therapeutic trophic factor in bone marrow mesenchymal stem cell-mediated cardiac repair. Biochem Biophys Res Commun, 390:834-838.

ANNEXES

1. Communications orales.

Eva Mathieu, Emilie Rederstorff, Guillaume Lamirault, Virginie Forest, Claire Toquet, Pierre Weiss, Jérôme Guicheux and Patricia Lemarchand. Intramyocardial injection of mesenchymal stem cells loaded within a scaffolding biomaterial improves cardiac function after acute myocardial infarction.
The 24th Annual Conference of the European Society for Biomaterials (ESB), September 4-8, 2011, Dublin Ireland.

Mathieu E, Lamirault G, Toquet C, Rederstorff E, Weiss P, Guicheux J and Lemarchand P. Hydrogel loaded with mesenchymal stem cells preserves cardiac function and ventricular remodeling after myocardial infarction.
Le 6ème Colloque National des Cellules Souches de l'IFR26 6 juin 2011-Nantes.

E. Mathieu, E. Rederstorff, Guillaume Lamirault, V. Forest, K. Biteau, P. Hulin, C. Toquet, P. Weiss, J. Guicheux and P. Lemarchand. Hydrogel loaded with mesenchymal stem cell preserves cardiac function and ventricular remodeling after myocardial infarction.
Groupe de Réflexion en recherche cardiovasculaire (GRRC), 12-14 Mai 2011, Lyon, France.

2. Présentation affichées.

Eva Mathieu, Emilie Rederstorff, Guillaume Lamirault, Virginie Forest, Claire Toquet, Pierre Weiss, Jérôme Guicheux and Patricia Lemarchand. Intramyocardial injection of mesenchymal stem cells loaded within a scaffolding biomaterial improves cardiac function after acute myocardial infarction.
The American Heart Association's Scientific Sessions 2011, November 12-16, 2011, Orlando, Floride

Eva Mathieu, Emilie Rederstorff, Guillaume Lamirault, Virginie Forest, Claire Toquet, Pierre Weiss, Jérôme Guicheux and Patricia Lemarchand. Intramyocardial injection of mesenchymal stem cells loaded within a scaffolding biomaterial improves cardiac function after acute myocardial infarction.
Tissue Engineering and Regenerative Medical International Society (TERMIS) EU meeting. June 7-10, 2011, Grenada, Spain.

Eva Mathieu, Emilie Rederstorff, Guillaume Lamirault, Virginie Forest, Claire Toquet, Pierre Weiss, Jérôme Guicheux and Patricia Lemarchand. Intramyocardial injection of mesenchymal stem cells loaded within a scaffolding biomaterial improves cardiac function after acute myocardial infarction.
The 8th Edition of the International Symposium on Stem Cell Therapy and Cardiovascular Innovations. June 9th and 10th 2011, Madrid, Spain.

E. Mathieu, E. Rederstorff, Guillaume Lamirault, V. Forest, K. Biteau, P. Hulin, C. Toquet, P. Weiss, J. Guicheux and P. Lemarchand. An injectable biomaterial for mesenchymal stem cell-based myocardial tissue engineering: *in vitro* and *in vivo* bioassessment.
The First European Conference on Mesenchymal Stem Cells, November 18-20, 2010, Toulouse, France.

E. Mathieu, P. Naud, V. Forest, S. Demolombe, P. Lemarchand. Reprogramming of mesenchymal stem cells into cardiomyocytes.
Stem cell Therapy and Exploration of Monogenic diseases (STEM-pole).

3. Publications.

E. Mathieu, G. Lamirault, C. Toquet, E. Rederstorff, , V. Forest, K. Biteau, P. Hulin, , P. Weiss, J. Guicheux and P. Lemarchand. Intramyocardial delivery of mesenchymal stem cell-seeded hydrogel preserves cardiac function and attenuates ventricular remodeling after myocardial infarction. 2011. *Submitted in Biomaterials.*

E. Mathieu, E. Rederstorff, G. Lamirault, P. Hulin, V. Forest, P. Weiss, J. Guicheux and P. Lemarchand. Three-dimensional culture of functional cardiomyocytes in a cellulose derived-hydrogel: A useful tool for cardiac cell and tissue bioengineering. 2011. *in preparation*.

E. Rederstorff, P. Weiss, S. Sourice, M. Masson, **E. Mathieu**, Samia Laib, S. Colliec-Jouault, B.H. Fellah, J. Guicheux, C. Vinatier. A Self-setting Hydrogel Mechanically Reinforced with a marine Exopolysaccharide as a Scaffold for Cartilage. 2011. *Submitted in Tissue Engineering.*

A.L. Leblond, P. Naud, V. Forest, C. Gourden, C. Sagan, B. Romefort , **E. Mathieu**, B. Delorme, C. Collin, J.C. Pagès, L. Sensebé , B. Pitard, P. Lemarchand. Developing cell therapy techniques for respiratory disease: Intratracheal delivery of genetically engineered stem cells in a murine model of airway injury. Hum Gene Ther. 2009 Nov; 20(11):1329-43.

4. Brevet.

Silylated biomolecule-based hydrogel for culturing cardiomyocytes and stem cells, and use of the hydrogel thereof for treating heart failure.

Inventeurs : Eva Mathieu, Pierre Weiss, Jérôme Guicheux et Patricia Lemarchand

Numéro de référence : EP n° 11 305 683.2

Déposants : INSERM, Université de Nantes, CHU de Nantes

Année : 2011

HUMAN GENE THERAPY 20:1329–1343 (November 2009)

DOI: 10.1089/hum.2009.035

Scientific Article

Developing Cell Therapy Techniques for Respiratory Disease: Intratracheal Delivery of Genetically Engineered Stem Cells in a Murine Model of Airway Injury

Anne-Laure Leblond,[1,2] Patrice Naud,[1–3] Virginie Forest,[1,2] Clothilde Gourden,[4] Christine Sagan,[5] Bénédicte Romefort,[1,2,6] Eva Mathieu,[1,2] Bruno Delorme,[7,8] Christine Collin,[9,10] Jean-Christophe Pagès,[9,10] Luc Sensebé,[7,8,11] Bruno Pitard,[1,2] and Patricia Lemarchand[1,2,6]

Abstract

Interest has increased in the use of exogenous stem cells to optimize lung repair and serve as carriers of a therapeutic gene for genetic airway diseases such as cystic fibrosis. We investigated the survival and engraftment of exogenous stem cells after intratracheal injection, in a murine model of acute epithelial airway injury already used in gene therapy experiments on cystic fibrosis. Embryonic stem cells and mesenchymal stem cells were intratracheally injected 24 hr after 2% polidocanol administration, when epithelial airway injury was maximal. Stem cells were transfected with reporter genes immediately before administration. Reporter gene expression was analyzed in trachea–lungs and bronchoalveolar lavage, using nonfluorescence, quantitative, and sensitive methods. Enzyme-linked immunosorbent assay quantitative results showed that 0.4 to 5.5% of stem cells survived in the injured airway. Importantly, no stem cells survived in healthy airway or in the epithelial lining fluid. Using 5-bromo-4-chloro-3-indolyl-β-D-galactopyranoside staining, transduced mesenchymal stem cells were detected in injured trachea and bronchi lumen. When the epithelium was spontaneously regenerated, the *in vivo* amount of engrafted mesenchymal stem cells from cell lines decreased dramatically. No stem cells from primary culture were located within the lungs at 7 days. This study demonstrated the feasibility of intratracheal cell delivery for airway diseases with acute epithelial injury.

Introduction

Respiratory diseases remain one of the main causes of morbidity and mortality. Interest in optimizing repair of the lung by the use of stem cells (SCs) has increased. In particular, combining the ability of SCs to engraft into damaged lungs with their ability to serve as carriers of a therapeutic gene has great potential for the treatment of pulmonary fibrosis (Loebinger *et al.*, 2008b) and genetic airway diseases such as cystic fibrosis. This developing therapeutic approach has been stimulated by early reports demonstrating that both embryonic SCs and SCs derived from adult bone marrow, including mesenchymal stem cells, can differentiate into respiratory cells *in vitro*, thus acquiring phenotypic and functional markers of airway and alveolar epithelial cells (Coraux *et al.*, 2005; Wang *et al.*, 2005; Rippon *et al.*, 2006).

Systemic administration of adult SCs from the bone marrow of mice after total body irradiation (Pereira *et al.*, 1995; Loebinger *et al.*, 2008a; Sueblinvong *et al.*, 2008) and/or pollutant reagent treatment has been reported (Beckett *et al.*,

[1]INSERM, UMR915, Institut du Thorax, Nantes, F-44000 France.
[2]Université de Nantes, Faculté de Médecine, Institut Fédératif de Recherche Thérapeutique 26 (IFR26), Nantes, F-44000 France.
[3]CNRS, ERL3147, Nantes, F-44000 France.
[4]In-Cell-Art, Nantes, F-44000 France.
[5]CHU Nantes, Service d'Anatomo-Pathologie, Nantes, F-44000 France.
[6]CHU Nantes, Institut du Thorax, Nantes, F-44000 France.
[7]INSERM, EA 3855-ERI 5, Microenvironnement de l'Hématopoïèse et Cellules Souches, Tours, F-37000 France.
[8]Université de Tours, Faculté de Médecine, Institut Fédératif de Recherche Thérapeutique 135 (IFR135), Tours, F-37000 France.
[9]CHRU de Tours Laboratoire de Biochimie et Biologie Moléculaire, Tours, F-37000 France.
[10]INSERM ERI 19, Université François Rabelais de Tours, Tours, F-37000 France.
[11]Etablissement Français du Sang Centre-Atlantique, Service Recherche, Tours, F-37000 France.

2005; MacPherson *et al.*, 2006; Mei *et al.*, 2007; Serikov *et al.*, 2007; Xu *et al.*, 2007; Loebinger *et al.*, 2008) and showed that the administered SCs were engrafted mainly in alveolar spaces (Pereira *et al.*, 1995; Beckett *et al.*, 2005; Mei *et al.*, 2007; Serikov *et al.*, 2007; Xu *et al.*, 2007; Loebinger *et al.*, 2008a; Sueblinvong *et al.*, 2008) and sometimes in conducting airway (Pereira *et al.*, 1995; Krause *et al.*, 2001; MacPherson *et al.*, 2005, 2006; Loi *et al.*, 2006; Serikov *et al.*, 2007). The SC differentiation as pneumocytes (type I or II) or airway epithelial cells was evaluated mostly by various fluorescence techniques. Reported engraftment rates of adult bone marrow SC-derived cells ranged from 0% (Wagers *et al.*, 2002) up to 20% (Krause *et al.*, 2001) in the lungs, and from 0.025% (Loi *et al.*, 2006) up to 4% (Krause *et al.*, 2001) in conducting airway. These discrepancies have been partly attributed to the various fluorescence techniques used to detect the donor-derived epithelial cells, leading to significant artifacts (Loebinger *et al.*, 2008a). Importantly, lung SC engraftment is currently estimated to be between 0.01 and 0.1% (Krause, 2005; Bruscia *et al.*, 2006). Despite this low engraftment level, there is evidence that SCs transplanted postinjury have some therapeutic effects (Loebinger *et al.*, 2008a).

In most of these studies, systemic administration of SCs required total body irradiation of the recipient to promote SC bone marrow engraftment, a difficult condition to apply in the clinical setting, especially in patients suffering from airway disease associated with chronic infections such as cystic fibrosis. Alternatively, considering the advantages of the intratracheal route to target the airway and the respiratory epithelium, more recent studies reported the intratracheal administration of adult SCs in reagent-injured lungs (Gupta *et al.*, 2007; Wong *et al.*, 2007). Using fluorescence techniques, SC engraftment was enhanced by the intratracheal route as compared with the intravenous route (Wong *et al.*, 2007, 2009) but remained at 5–10% (Gupta *et al.*, 2007; Wong *et al.*, 2007, 2009). The intratracheal route was also used for the administration of differentiated cells and showed both positive (Serrano-Mollar *et al.*, 2007) and negative results (Kuang *et al.*, 2005; Gupta *et al.*, 2007). SC or differentiated cell engraftment levels in these studies were assessed mostly by fluorescence techniques, which could explain these conflicting results.

The aims of our study were to evaluate the survival and engraftment of various types of exogenous SCs and differentiated cells after intratracheal injection. We used a murine model presenting acute epithelial airway injury without total body irradiation. This model was developed for gene therapy experiments on cystic fibrosis and consisted of intranasal injection of polidocanol detergent (Parsons *et al.*, 1998). Quantification of cell survival rates and determination of cell location within lungs were performed by enzyme-linked immunosorbent assay (ELISA), biochemical assay, and polymerase chain reaction (PCR).

Materials and Methods

Animal model and intratracheal administration

Male, 8- to 10-week-old Swiss mice were obtained from Janvier Laboratories (Le Genest St Isle, France). Animal experiments were performed in accordance with the *Guide for the Care and Use of Laboratory Animals* (Institute of Laboratory Animal Research, 1996). Mice were anesthetized with an intraperitoneal injection of xylazine (15 mg/kg) and ketamine (70 mg/kg), and placed supine. Briefly, intratracheal administration was performed with a 22-gauge catheter placed within an intubation cannula (Harvard Apparatus, Holliston, MA) that was removed immediately before injection. Airway injury was induced after anesthesia by intratracheal administration of 25 μl of 2% polidocanol [PDOC: polyoxyethylene (9) lauryl ether; Sigma-Aldrich, St. Louis, MO] (Borthwick *et al.*, 2001; MacPherson *et al.*, 2005) in phosphate-buffered saline (PBS) through the 22-gauge catheter. Cells (10^6 cells/25 μl) or PBS was intratracheally injected 24 hr after PDOC administration, using the same protocol. Mice were killed by an intraperitoneal lethal injection of thiopental (Nesdonal) 24 hr or 7 days after intratracheal administration.

Bronchoalveolar lavages

Bronchoalveolar lavages (BALs) were performed 24 hr after chloramphenicol acetyltransferase (CAT)-transfected cell administration in healthy or injured airway. Mice were anesthetized and the thoracic cavity was opened by careful dissection. The trachea was exposed, and a small transverse incision was made just below the level of the larynx. BAL was then performed with one dose of 1 ml of PBS, ensuring that both lungs inflated during the lavage process and that there was no leakage of lavage fluid from the trachea. BAL fluid was centrifuged at 400×*g* for 5 min. The supernatant was removed and stored at −80°C until ELISA. Cell pellet was suspended in lysis buffer and stored at −80°C until ELISA.

Cell cultures

Undifferentiated mouse embryonic stem cells (ESCs, R1 cell line; Nagy *et al.*, 1993) were cultured in dishes coated with 0.1% gelatin (Sigma-Aldrich). The culture medium was composed of Dulbecco's minimum essential medium with glucose at 4.5 g/liter (DMEM; Invitrogen, Carlsbad, CA) supplemented with 15% fetal calf serum (FCS; Invitrogen), 0.1% nonessential amino acids (Invitrogen), 1 m*M* sodium pyruvate (Invitrogen), 2 m*M* L-glutamine (Invitrogen), 10^{-7} *M* 2-mercaptoethanol (Sigma-Aldrich), penicillin–streptomycin (100 U/ml and 100 μg/ml, respectively; Invitrogen), and leukemia inhibitory factor (LIF, 2000 U/ml; Sigma-Aldrich).

Undifferentiated murine mesenchymal stem cells (BMC9 cells; Dennis and Caplan, 1996) were cultured as previously described (Chateauvieux *et al.*, 2007) in α-MEM with nucleosides (Invitrogen) supplemented with 10% FCS (Invitrogen), 2 m*M* L-glutamine (Invitrogen), and penicillin–streptomycin (100 U/ml and 100 μg/ml, respectively; Invitrogen).

A human hepatocellular carcinoma cell line (Hep 3B2.1-7, ATCC no. HB-8064; American Type Culture Collection [ATCC], Manassas, VA), transformed African green monkey kidney fibroblast cell line (COS-7, ATCC no. CRL-1651; ATCC), and murine osteosarcoma cell line (mOS-J; Joliat *et al.*, 2002) were used for control experiments. Cells were cultured in DMEM with glucose at 4.5 g/liter and supplemented with 15% FCS, 2 m*M* L-glutamine, and penicillin–streptomycin (100 U/ml and 100 μg/ml, respectively).

Primary culture of adult mesenchymal stem cells

Total bone marrow was obtained from wild-type adult male Swiss mice and male Rosa26 *lacZ* mice (background C57BL/6J×129S2; kindly provided by M.F. Gardahaut,

Nantes, France) by flushing femurs and tibias with culture medium. Cells were plated at a density of 500,000 cells/cm^2 in medium composed of α-MEM with nucleosides supplemented with 10% FCS, 2 m*M* L-glutamine, penicillin–streptomycin (100 U/ml and 100 μg/ml, respectively), and human fibroblast growth factor (FGF)-2 at 2 ng/ml (AbCys, Paris, France). The culture medium was changed on day 3 to remove nonadherent cells and was subsequently replaced weekly. The cells were grown for 2–3 weeks until confluent. Adherent cells were then detached with 0.5% trypsin–EDTA and plated at a density of 10,000 cells/cm^2. Subsequent passages and seeding of the cells were performed at a density of 5000 cells/cm^2. From passage 8, mesenchymal stem cell (MSC) cultures were characterized by fluorescence-activated cell-sorting (FACS) analysis (FACSCalibur instrument with CellQuestPro software; BD Biosciences, San Jose, CA) after incubation with anti-CD45–phycoerythrin (PE), anti-CD90–PE, anti-CD29–CyChrome, anti-Sca1–PE, anti-CD106–CyChrome (BD Biosciences) (Dominici *et al.*, 2006).

In vitro *cell transfection with chloramphenicol acetyltransferase or green fluorescent protein reporter gene and evaluation of gene transfer system efficacy*

ESCs, BMC9 cells, and differentiated cells were transfected with pCIK-CAT (4.7 kb) and pEGFP-C1 (4.7 kb) plasmids encoding chloramphenicol acetyltransferase (CAT) protein and GFP, respectively, using synthetic vectors just before intratracheal administration (Pitard *et al.*, 2001). DNA plasmids were complexed with ICAfectin 441 according to the manufacturer's instructions (In-Cell-Art, Nantes, France). After 2 hr, transfection complexes were removed by changing growth medium and cells were lysed for dosages or kept in culture for 24 hr or 7 days, or injected intratracheally as indicated previously.

MSCs from Swiss mice were transfected with pCIK-CAT and pEGFP-C1 plasmids, using nucleofection (Nucleofector solution; Amaxa Biosystems, Cologne, Germany), just before intratracheal administration (Aluigi *et al.*, 2006). After 2 hr, growth medium was changed and cells were lysed for dosages or kept in culture for 24 hr or 7 days, or injected intratracheally as indicated previously. The percentage of GFP-expressing cells was evaluated 24 hr after GFP nucleofection, using FACS analysis.

The efficacy of gene transfer systems was evaluated by cytometry for GFP-expressing cells and by ELISA for CAT-expressing cells. The percentage of GFP-expressing cells was evaluated 24 hr after GFP transfection, using FACS analysis (FACSCalibur instrument with CellQuestPro software). CAT protein quantity per stem cell at 24 hr was then calculated on the basis of *in vitro* data: CAT protein quantity in cell lysis buffer was divided by the cell number and by the percentage of GFP-expressing cells (obtained by FACS analysis). Last, this value was used to determine the minimal number of CAT-expressing stem cells required to be detected by ELISA *in vitro* or *in vivo*, considering that the CAT ELISA detection threshold was 50 pg of CAT protein (see later).

In vitro *stem cell transduction with* nls-lacZ *reporter gene*

BMC9 cells were transduced with an amphotropic recombinant murine retroviral vector carrying the *nls-lacZ* reporter gene (*lacZ* gene encoding β-galactosidase [β-Gal]) coupled to a nuclear localization signal [*nls*]; kindly provided by N. Ferry, Nantes, France). This retroviral vector was obtained from the human producer cell line TELCeB6AF7 derived from the Te671 cell line as described by Aubert and colleagues (2002). Twenty-four-hour recombinant retroviral supernatant was harvested from the confluent producer cell line and filtered through a 0.45-μm (pore size) membrane. The titer of the β-Gal supernatant, determined by end-point dilution with Te671 target cells, was 2×10^8 transducing particles/ml. After BMC9 cell transduction, retroviral vector was removed by changing the growth medium and cells were lysed for dosages or kept in culture or injected intratracheally as indicated previously.

To evaluate the percentage of β-Gal-transduced BMC9 cells, cells were fixed in 4% paraformaldehyde, washed with PBS, and incubated for 2 hr at 37°C in 5 m*M* $K_4Fe(CN)_6$, 5 m*M* $K_3Fe_3(CN)_6$, and 2 m*M* $MgCl_2$ in PBS containing 5-bromo-4-chloro-3-indolyl-β-D-galactopyranoside (X-Gal [0.5 mg/ml] dissolved in *N*,*N*-dimethylformamide at 20 mg/ml before dilution into the reaction mixture; Sigma-Aldrich). Cells were identified as positive for β-Gal activity by blue nuclear staining after X-Gal reaction. The percentage of β-Gal-expressing cells *in vitro* was determined by counting the number of nuclear-blue cells in a total of 200 cells.

MSCs from Swiss mice were transduced with a lentiviral vector carrying the *nls-lacZ* reporter gene. The vector was derived from pHR′ LacZ (Zufferey *et al.*, 1997) in which an *nls* from the simian virus 40 (SV40) T antigen was cloned in frame 5′ to the *lacZ* cDNA. The lentiviral vector was produced in human embryonic kidney 293T cells as previously described (Selig *et al.*, 1999). After transduction with 50 multiplicities of infection (MOI), lentiviral vector was removed by changing the growth medium and cells were lysed for dosages or kept in culture or injected intratracheally as indicated previously. The percentage of β-Gal-transduced MSCs was evaluated by *in vitro* X-Gal staining and counting as described previously.

Reporter gene assay and estimation of survival rate

CAT-transfected cells, BAL cells and BAL fluid, or whole frozen trachea–lungs were homogenized in reporter lysis buffer (Roche Diagnostics, Indianapolis, IN) supplemented with protease inhibitors (Roche Diagnostics). After centrifugation at 10,000 rpm for 5 min, CAT quantity was measured in supernatant with a VICTOR^2 multilabel counter (Perkin-Elmer Life Sciences, Waltham, MA), using a CAT ELISA kit according to the instructions of the supplier (Roche Diagnostics). Each sample was analyzed in duplicate. The CAT detection threshold was 50 pg. Protein content was measured with a bicinchoninic acid (BCA) protein assay kit (Pierce Biotechnology, Rockford, IL).

To estimate cell survival rate 24 hr after intratracheal administration, we first calculated CAT protein quantity per CAT-expressing cell, using *in vitro* data: CAT quantity in cell lysis buffer was divided by the cell number and by the percentage of GFP-expressing cells (obtained by FACS analysis). Last, the total *in vivo* CAT protein quantity per animal was divided by this *in vitro* value, in order to estimate the number of CAT-expressing cells per animal and subsequently the cell survival rate.

BMC9 cells and Rosa26 MSCs or whole frozen murine trachea–lungs were homogenized in 1 ml of reporter lysis buffer (Roche Diagnostics) supplemented with a protease inhibitor cocktail (Roche Diagnostics). After centrifugation at 10,000 rpm for 5 min, β-Gal activity was determined by enzymatic fluorimetric assay using 4-methylumbelliferyl-β-D-galactoside (4-MUG; Sigma-Aldrich) as a fluorescent substrate. Each cell and trachea–lung sample was analyzed in duplicate. The β-Gal activity detection threshold was 230 pg. Protein content was measured with a BCA protein assay kit. Additional experiments were done with lysates of β-Gal-transduced BMC9 cells or Rosa26 MSCs after three cycles of freezing and thawing. Viability was ascertained by trypan blue exclusion.

Detection of β-galactosidase activity

Tissues were fixed in 4% paraformaldehyde (at room temperature, 20 min) and rinsed three times with PBS. Immediately after fixation, trachea–lungs were stained by intratracheal infusion (though a 19-gauge needle; total volume, 5 ml) and immersion for 6 hr at 30°C in 5 m*M* $K_4Fe(CN)_6$, 5 m*M* $K_3Fe_3(CN)_6$, and 2 m*M* $MgCl_2$ in PBS containing X-Gal at 0.5 mg/ml (as indicated previously) to avoid the detection of endogenous β-Gal activity (Weiss *et al.*, 1997). Tissues were again washed with PBS and immediately embedded in paraffin. Tissues were identified as positive for β-galactosidase activity by nuclear blue staining after X-Gal reaction. Sections (4 μm thick) were stained with nuclear fast red (Sigma-Aldrich).

Detection of nls-lacZ *reporter gene*

Total DNA from whole murine trachea–lungs was isolated for PCR analysis. Tissues were digested overnight with lysis buffer containing proteinase K (10 mg/ml; Sigma-Aldrich). Total DNA was extracted with phenol–chloroform–isoamyl alcohol (Sigma-Aldrich) and then precipitated in ethanol. Total DNA from 10^6 transduced MSCs was also extracted for PCR experiments. PCR were performed with primers that specifically bind the *nls* sequence and the *lacZ* gene encoded in the *nls-lacZ* lentiviral vector: 5′-GTA ACA ACT CCG CCC CAT-3′ and 5′-GAC AGT ATC GGC CTC AGG AA-3′.

Statistical analysis

Data are expressed as means ± SEM. Statistical significance was evaluated by analysis of variance (ANOVA) to compare control and treatment groups of three or more. Tukey's test was subsequently used for pair-wise comparisons. A non-parametric Mann–Whitney test was performed to compare two groups. Statistical significance was set at $p < 0.05$.

Results

Transient epithelial airway injury induced by intratracheal polidocanol administration

Intratracheal administration of 2% PDOC induced macroscopic lung injury at 24 hr with hemorrhage (Fig. 1b, k, and n). The major histological findings at 24 hr were acute injury of the murine airway epithelium with focal shedding areas observed at the epithelial surface, with only a remaining layer of basal cells or a total denudation of the basement membrane (Fig. 1e and h). However, in some regions, the lumenal layer of epithelial cells was just disrupted or sloughed whereas the basal cell layer and the basement membrane remained intact (data not shown), as already described after intratracheal or intranasal administration (Driscoll *et al.* [2000] and Southam *et al.* [2002], respectively). Inflammation was present in pulmonary parenchyma (Fig. 1k and n, arrowheads). Trachea–lung sections 7 days after PDOC administration demonstrated significant improvement of hemorrhage (Fig. 1c and l) and of airway injury, with epithelial surface again covered by cilia (Fig. 1f and i). The PDOC effect did not significantly alter animal survival (see Supplementary Table S1 at www.liebertonline.com/hum).

ESC and BMC9 cell survival in murine airway with acute epithelial airway injury

In a first set of experiments, embryonic stem cells (ESCs) and adult mesenchymal stem cells (BMC9 cells) from well-characterized cell lines were intratracheally injected. ESCs and BMC9 cells were injected 24 hr after PDOC administration, when epithelial airway injury induced by PDOC was acute (MacPherson *et al.*, 2005). Stem cell survival was evaluated 24 hr after stem cell administration. To calculate the survival rate, we used a quantitative method based on *in vivo* expression of reporter genes by transplanted cells. Stem cells were transfected 2 hr before intratracheal injection *in vitro* with plasmids encoding the CAT or GFP reporter gene. CAT-transfected stem cells were then intratracheally injected, at a time when they did not yet express the foreign genes (see later). We hypothesized that only surviving stem cells would express *in vivo* CAT protein in trachea–lungs 24 hr after intratracheal cell injection.

Two hours after the beginning of cell incubation with both plasmids and synthetic vectors, transfection complexes were removed and reporter gene expression was evaluated. Neither CAT protein nor cell fluorescence was detected in stem cells by ELISA (Fig. 2b) and microscopy (data not shown), demonstrating that stem cells did not express CAT or GFP protein at the time of *in vivo* injection. *In vitro* reporter gene expression was also evaluated 24 hr and 7 days after incubation with plasmids and synthetic vectors. As evaluated by

FIG. 1. Epithelial damage induced by intratracheal administration of polidocanol (PDOC). (**a**–**c**) Trachea–lungs from (**a**) a control animal and from (**b** and **c**) animals injected with PDOC: (**b**) 24 hr and (**c**) 7 days after PDOC administration. (**d**–**i**) Tracheal sections and (**j**–**o**) bronchial sections from (**d**, **g**, **j**, and **m**) control animals and from animals injected with PDOC: (**e**, **h**, **k**, and **n**) 24 hr and (**f**, **i**, **l**, and **o**) 7 days after PDOC administration. Original magnification: (**k**)×4; (**d**–**f**)×10; (**j** and **l**)×20; (**g**–**i** and **m**–**o**)×100. Hematoxylin counterstaining. Solid arrows, airway epithelial damage, open arrow, ciliated cells; solid arrowheads, areas of inflammation; open arrowheads, hemorrhagic areas. Areas marked with asterisks are magnified in the adjacent panels.

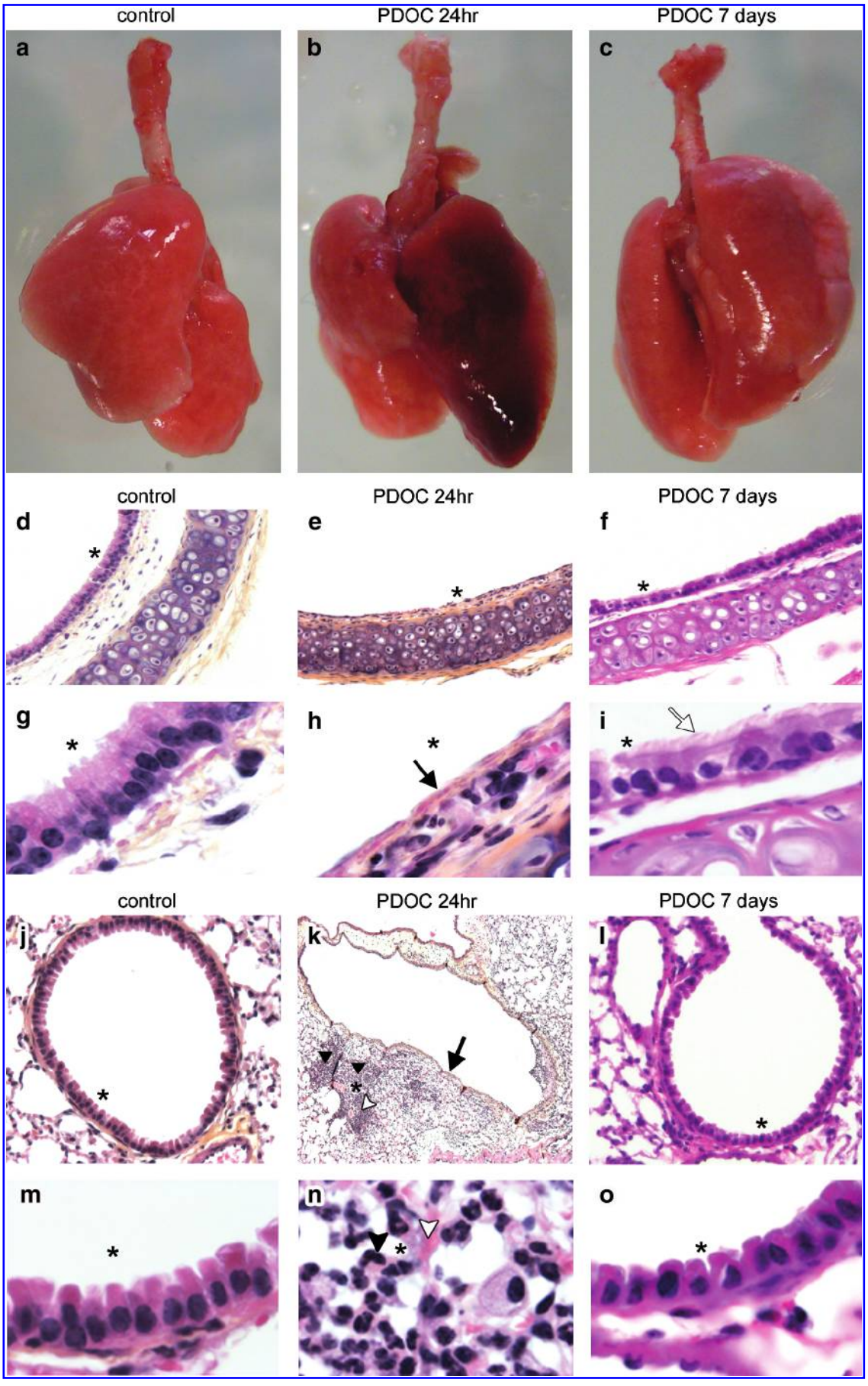
control
PDOC 24hr
PDOC 7 days
a
b
c
control
PDOC 24hr
PDOC 7 days
d
e
f
g
h
i
control
PDOC 24hr
PDOC 7 days
j
k
l
m
n
o

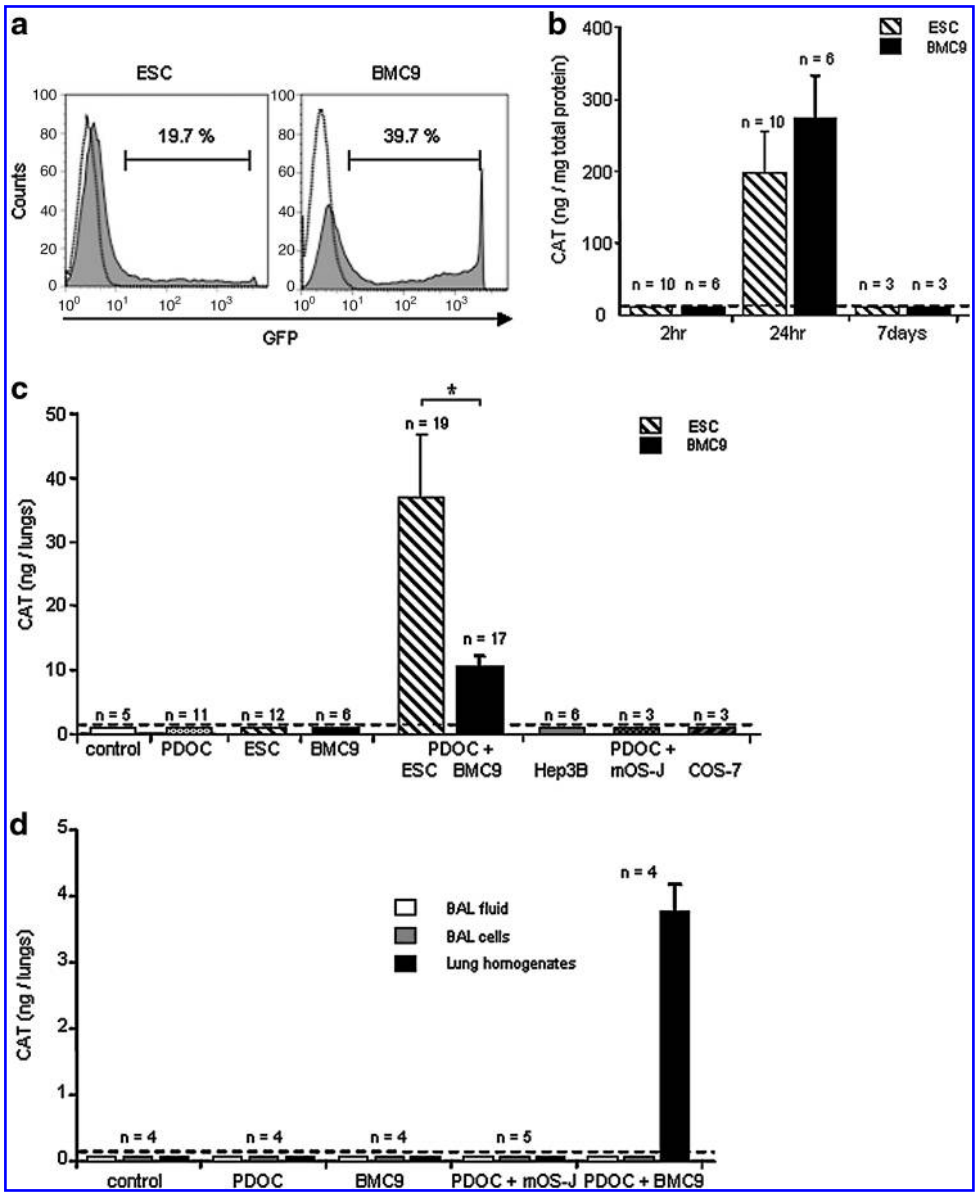

FIG. 2. *In vitro* cell transfection with reporter genes and *in vivo* chloramphenicol acetyltransferase (CAT) gene expression in injured airway 24 hr after intratracheal stem cell administration. To monitor stem cell survival *in vivo*, murine embryonic stem cells (ESCs) and adult mesenchymal stem cells (BMC9 cells) were transfected *in vitro* with plasmids encoding the CAT or GFP reporter gene just before intratracheal administration. (**a**) Representative histograms of FACS analysis of GFP-expressing ESCs or BMC9 cells 24 hr after *in vitro* transfection. (**b**) CAT protein quantification in ESC and BMC9 lysates by ELISA 2 hr, 24 hr, or 7 days after incubation with plasmids and synthetic vectors. (**c**) CAT protein quantification in whole trachea–lung homogenates by ELISA, 24 hr after ESC or BMC9 cell intratracheal injection. Evaluated groups included animals that were intratracheally injected with the following: no injection (control), PDOC only (PDOC), ESCs or BMC9 cells only (ESC, BMC9), PDOC and ESCs or BMC9 cells 24 hr later (PDOC + ESC, BMC9), PDOC and differentiated cells 24 hr later (PDOC + Hep 3B, mOS-J, COS-7). (**d**) CAT protein quantification in bronchoalveolar lavages and whole trachea–lung homogenates by ELISA 24 hr after BMC9 or murine differentiated cell (mOS-J) intratracheal injection. Evaluated groups included animals that were intratracheally injected with the following: no injection (control), PDOC only (PDOC), BMC9 cells only (BMC9), PDOC and mOS-J cells 24 hr later (PDOC + mOS-J), PDOC and BMC9 cells 24 hr later (PDOC + BMC9). Dashed line depicts control threshold. $*p < 0.05$.

FACS analysis, $19.4 \pm 0.2\%$ of ESCs ($n = 6$) and $37.0 \pm 4.4\%$ of BMC9 cells ($n = 6$) expressed GFP *in vitro* at 24 hr (Fig. 2a). However, CAT and GFP were not detected 7 days after transfection (Fig. 2b), suggesting that transgene expression was transient. Using quantitative CAT ELISA results and cellular rates of GFP expression, we calculated that CAT-expressing ESCs and CAT-expressing BMC9 cells contained, at 24 hr, 0.03 ± 0.01 pg of CAT per cell ($n = 10$) and 0.08 ± 0.02 pg of CAT per cell ($n = 6$), respectively. Cell values were further used to evaluate the number of *in vivo*-surviving cells after intratracheal injection.

For intratracheal administration, CAT-transfected ESCs and CAT-transfected BMC9 cells were harvested 2 hr after the beginning of transfection and injected intratracheally. Mice

were killed 24 hr after intratracheal administration; trachea–lungs were used *in toto* to quantify CAT protein by ELISA (Fig. 2c). No CAT protein was detected in control animals or animals injected with PDOC only. Importantly, CAT protein was detected in 19 of 31 animals (61%) intratracheally injected with PDOC and ESCs and in 17 of 21 animals (81%) intratracheally injected with PDOC and BMC9 cells, suggesting that ESCs and BMC9 cells survived within lungs and expressed reporter genes 24 hr after intratracheal injection. To estimate the number of surviving cells within the lungs at 24 hr, total CAT protein quantity per animal was divided by CAT quantity per cell *in vitro*. The survival rate of 10^6 injected stem cells was $3.69 \pm 0.86\%$ ($n = 19$), whereas this survival rate was significantly less with BMC9 cells ($0.43 \pm 0.12\%$, $n = 17$, Tukey's test; $p = 0.02$). CAT cell quantities were also used to calculate the *in vivo* cell detection threshold. A minimum of 10 (± 1.2)$\times 10^3$ ESCs and 4.3 (± 1.1)$\times 10^3$ BMC9 cells could be detected in one animal *in vivo*, corresponding to 0.4–1% of injected cells. These results suggest that even if the percentage of cells expressing reporter gene *in vitro* was low, this was still a sensitive method for *in vivo* detection of a small cell number.

Influence of differentiation state and airway environment on ESC and BMC9 cell survival

To determine whether cell survival ability in the injured murine airway was specific to stem cells, differentiated cells of various origins (Hep 3B, mOS-J, and COS-7 cells) were transfected *in vitro* with CAT plasmids under conditions similar to that of ESC and BMC9 cell transfection (data not shown). CAT-transfected differentiated cells were then intratracheally injected 2 hr after the beginning of incubation with CAT plasmid. No CAT protein was detected in any animal injected with PDOC and differentiated cells at 24 hr (Fig. 2c), suggesting that only stem cells survived after intratracheal injection into injured airway. CAT-transfected ESCs and BMC9 cells were injected into healthy control animals. No CAT protein was detected in any animal with a healthy airway 24 hr after stem cell injection (Fig. 2c), suggesting that stem cell survival was favored by airway injury.

Cell survival in epithelial lining fluid

To evaluate whether cells expressing CAT reporter protein were present within the epithelial lining fluid or after phagocytosis by alveolar macrophages, bronchoalveolar lavages (BALs) were performed at 24 hr under *in vivo* conditions, when phagocytosis was expected to be maximal (e.g., when CAT ELISA results were negative), using mesenchymal stem cells (BMC9 cells) in healthy airway and differentiated murine cells (mOS-J) in injured airway. As further controls, BALs were also performed in control and PDOC-treated animals and in animals intratracheally injected with PDOC and BMC9 cells. No CAT protein was detected in any BAL fluid or BAL cell sample from any animal (Fig. 2d), suggesting that if stem cells or differentiated cells were phagocytosed by alveolar macrophages, such phagocytosis did not alter CAT protein measurement or cell survival detection. Importantly, in animals intratracheally injected with PDOC and BMC9 cells, high levels of CAT protein were measured in trachea and lung homogenates whereas no CAT protein was detected in BAL fluid or BAL cell samples, suggesting that CAT-expressing cells were present mostly within the lungs and did not survive in the epithelial lining fluid (Fig. 2d).

BMC9 cell location at 24 hr and 7 days

We next investigated BMC9 cell location at 7 days, when the airway epithelium was known to be spontaneously regenerating (MacPherson *et al.*, 2005). As CAT expression using synthetic vectors was transient, we used integrative viral vectors allowing long-term foreign gene expression. BMC9 cells were transduced with a retroviral vector encoding the *nls-lacZ* gene. As evaluated by X-Gal staining, $57.2 \pm 0.1\%$ of BMC9 cells expressed nuclear β-galactosidase (β-Gal) when they were injected (Fig. 3a; $n = 6$). β-Gal activity in transduced BMC9 cells was significantly increased just before injection as compared with endogenous β-Gal activity in BMC9 cells (Fig. 3b; Mann–Whitney test, $p = 0.02$) and remained stable at 7 days (data not shown). Animals were assessed for β-Gal activity 24 hr and 7 days after intratracheal administration, using the 4-MUG method (Fig. 3c). In contrast to previous experiments, β-Gal-transduced BMC9 cells expressed the *nls-lacZ* gene at the time of intratracheal injection. Therefore, as a further control, we injected lysates of β-Gal-transduced BMC9 cells, and no significant increase in β-Gal activity was observed as compared with endogenous β-Gal activity (Tukey's test, $p = 0.98$). In animals intratracheally injected with PDOC and β-Gal-transduced BMC9 cells, 24 hr after injection β-Gal activity significantly increased as compared with that of control animals (Tukey's test, $p = 0.003$) and animals injected with PDOC and lysate of β-Gal-transduced BMC9 cells (Tukey's test, $p = 0.004$), confirming results with CAT gene transfer. However, 7 days after stem cell injection β-Gal activity was similar to that of control animals (Tukey's test, $p = 0.98$) and animals injected with PDOC and lysate of β-Gal-transduced BMC9 cells (Tukey's test, $p = 0.94$), suggesting that the number of surviving BMC9 cells in the airway epithelium decreased significantly between 24 hr and 7 days.

To locate BMC9 cells after intratracheal injection into injured airway, we performed X-Gal staining of *in toto* trachea–lungs at 24 hr and 7 days (Fig. 4). No blue staining was observed in trachea–lungs (Fig. 4a) and histological sections (Fig. 4b–d) from any control animal (Fig. 4a; $n = 3$), animal injected with PDOC (Fig. 4b; $n = 3$), or animal intratracheally injected with β-Gal-transduced BMC9 cells only (Fig. 4c; $n = 5$). No cell with nuclear blue staining was observed in any animal injected with PDOC and lysate of β-Gal-transduced BMC9 cells (Fig. 4d; $n = 5$), suggesting that cells with nuclear blue staining expressed the *nls-lacZ* gene *de novo.* In contrast, macroscopic and microscopic strong nuclear blue staining was observed in trachea and pulmonary lobes at 24 hr (Fig. 4e–m; $n = 16$) and 7 days (Fig. 4n–p; $n = 7$) in each animal intratracheally injected with PDOC and β-Gal-transduced BMC9 cells. At 24 hr, macroscopic analyses showed blue spots (≤ 5 spots) in trachea from 8 of 16 animals (Fig. 4e and f) and blue spots in one pulmonary lobe (15 of 16; Fig. 4g and h) or two pulmonary lobes (1 of 16; Fig. 4i and j). Blue spots were also observed in large bronchi from 5 of 16 animals (Fig. 4i and j). Histological analyses confirmed the macroscopic result for each sample, showing β-Gal-positive cells on histological sections where blue spots had been observed. Clusters of cells with blue nuclei were observed in the lumen

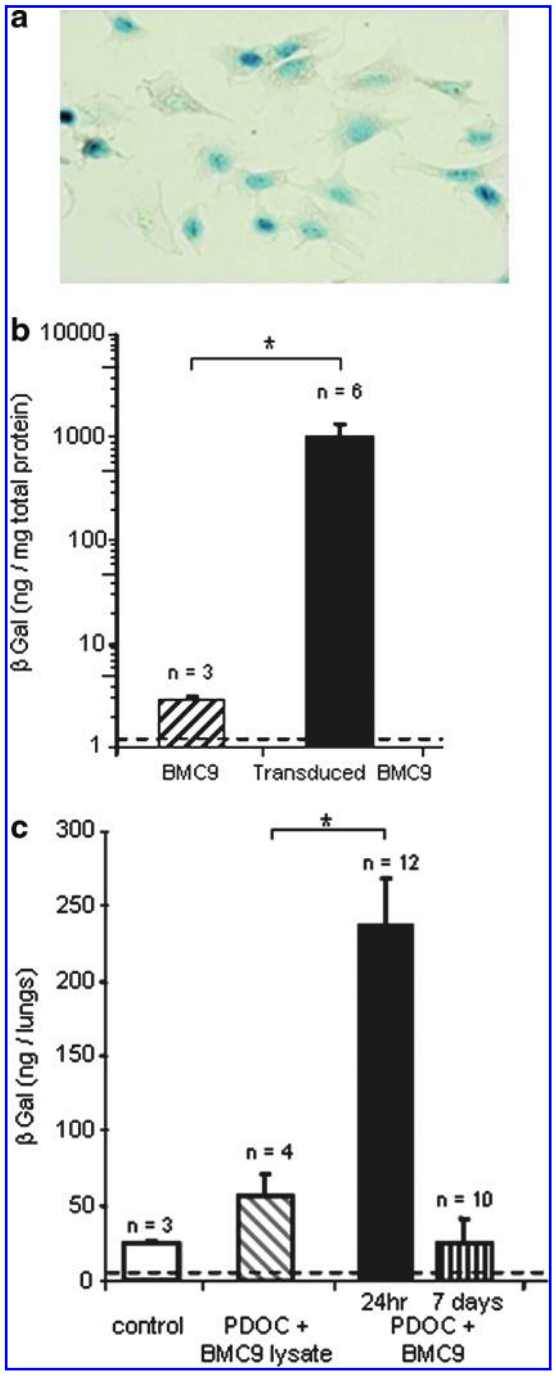

FIG. 3. *In vitro* and *in vivo* detection of β-Gal activity 24 hr or 7 days after β-Gal-transduced BMC9 intratracheal administration. BMC9 cells were transduced *in vitro* with a retroviral vector encoding the *nls-lacZ* gene before *in vivo* administration. (**a**) Representative example of β-Gal-transduced BMC9 cells just before injection, after X-Gal staining. Original magnification, ×20. (**b**) *In vitro* β-Gal activity in BMC9 cells and β-Gal-transduced BMC9 cells just before injection. (**c**) β-Gal activity in whole trachea–lung homogenates, 24 hr or 7 days after BMC9 cell intratracheal injection. Evaluated groups included animals that were intratracheally injected with the following: no injection (control), PDOC and lysate of β-Gal-transduced BMC9 cells (PDOC + BMC9 lysate), PDOC and β-Gal-transduced BMC9 cells (PDOC + BMC9). Dashed line depicts control threshold. $^*p < 0.05$. Color images available online at www.liebertonline.com/hum.

of injured trachea (Fig. 4k) and injured bronchi or bronchioles (Fig. 4l and m), but not in lung parenchyma (Fig. 4l). At 7 days, blue spots were observed in seven of seven animals, in the lumen of bronchioles (Fig. 4n–p). No blue cell was observed in trachea or in pulmonary parenchyma (data not shown). Clusters of blue cells were sometimes found in polyp-like structures, located in bronchioles and large bronchi. Polyp-like structures were not observed in any animal receiving PDOC only. Further quantitative and statistical analyses demonstrated that the development of polyp-like structures at 7 days was not due to stem cell administration but rather to a second intratracheal administration (PBS or BMC9 cells) 24 hr after PDOC injection (see Supplementary Table S2 at www.liebertonline.com/hum). Histological analyses at high magnification showed that β-Gal-expressing cells did not have a respiratory phenotype, with no cilia at 24 hr or 7 days (data not shown).

MSC survival in murine airway with acute epithelial airway injury

In a second set of experiments, to avoid *in vivo* cell survival linked to cell line transformation, we repeated previous experiments with the same experimental design, using murine MSCs from primary cultures. MSC cultures were characterized according to Dominici and colleagues (2006) and Chateauvieux and colleagues (2007). FACS analysis demonstrated that MSCs were $CD45^-$ (Fig. 5a; $0.4 \pm 0.1\%$, $n = 4$), $CD90^-$ ($0.43 \pm 0.2\%$, $n = 6$), $CD29^+Sca\text{-}1^+$ (Fig. 5a; 96.9 ± 1.3 and $98.1 \pm 0.7\%$, respectively, $n = 4$), and $CD106^+$ ($96 \pm 0.8\%$, $n = 4$).

MSCs were transiently transfected *in vitro* with plasmids encoding the CAT or GFP reporter gene. In contrast to ESCs and BMC9 cells, MSC transfection with synthetic vectors was ineffective (data not shown), and therefore nucleofection was used to obtain a significant gene transfer rate. As evaluated by FACS analysis, $56.8 \pm 2.9\%$ of MSCs expressed GFP *in vitro* at 24 hr (Fig. 5c; $n = 3$), but CAT and GFP were not detected 7 days after nucleofection (Fig. 5b), suggesting that foreign gene expression was again transient and that nucleofection could not be used for 7-day *in vivo* experiments. CAT-transfected MSCs contained 0.35 ± 0.02 pg of CAT per cell at 24 hr ($n = 6$). CAT-transfected MSCs were then intratracheally injected 2 hr after the beginning of incubation with CAT plasmid. In control mice and mice injected with PDOC only, no CAT protein was detected at 24 hr (Fig. 5d). Importantly, CAT protein was detected in each animal injected with PDOC and MSCs (Fig. 5d; $n = 8$; Tukey's test, $p < 0.001$), suggesting that MSCs from primary cultures survived in injured airway and expressed CAT protein after intratracheal administration. The MSC survival rate was $5.52 \pm 1.9\%$ ($n = 8$), and a minimum of 710 ± 45 CAT-expressing MSCs could be detected in one animal *in vivo*, corresponding to 0.07% of injected cells, confirming CAT ELISA sensitivity for *in vivo* experiments.

MSC location at 24 hr and 7 days

To investigate whether MSCs could be located into the airway epithelium 7 days after cell injection, we first used MSCs in primary cultures from $\beta\text{-Gal}^+$ transgenic (Rosa26) mice, thus continuously expressing cytoplasmic β-Gal (Fig. 6a). Using the 4-MUG method (Fig. 6c), *in vitro* β-Gal activity

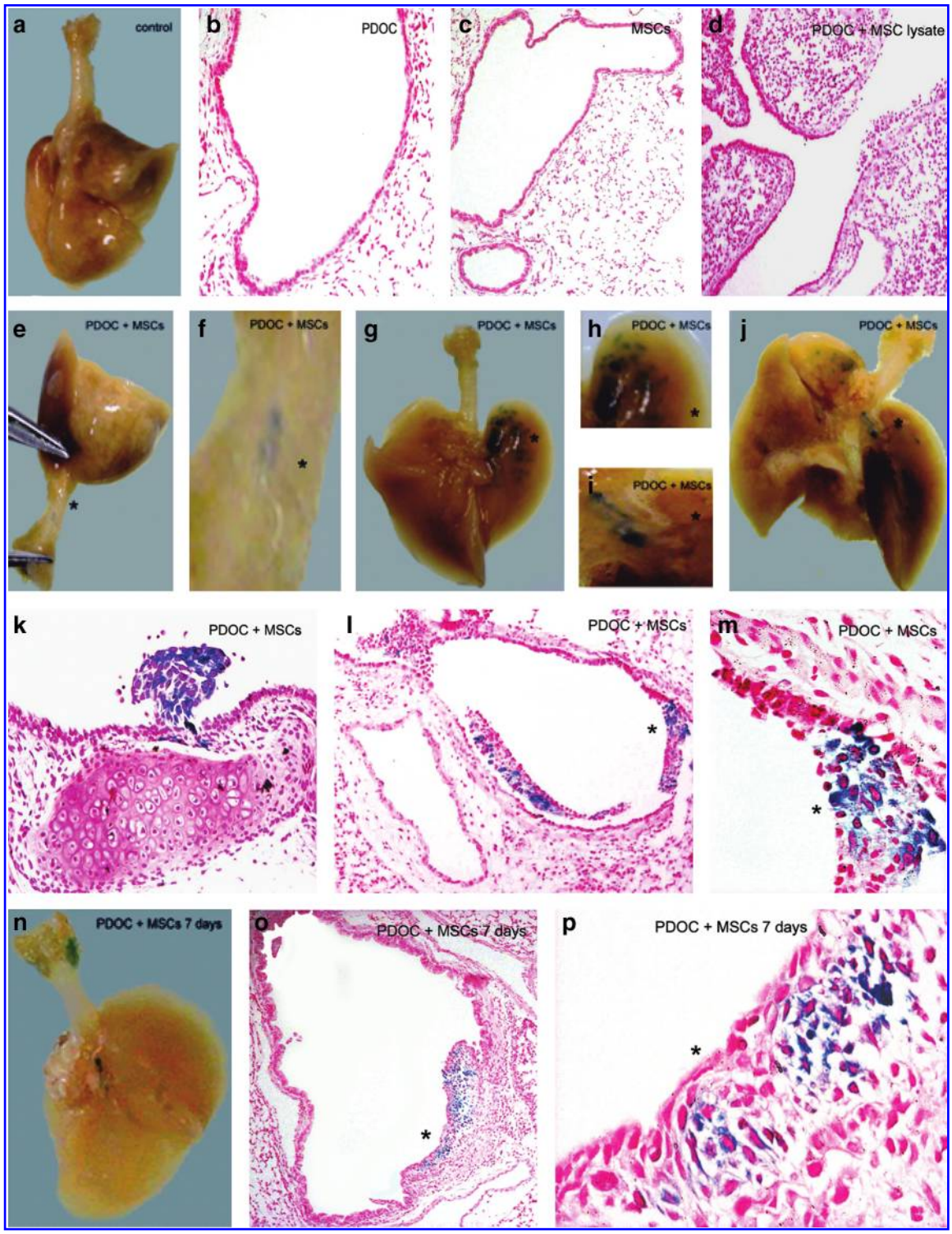

FIG. 4. BMC9 cell location 24 hr and 7 days after intratracheal injection, using X-Gal staining. (**a**–**d**) Trachea–lungs or histological sections 24 hr after X-Gal staining from (**a**) a control animal and from (**b**–**d**) animals intratracheally injected with PDOC (**b**), β-Gal-transduced BMC9 cells (**c**), or PDOC and, 24 hr later, β-Gal-transduced BMC9 lysate (**d**). No blue staining was observed in any control animal. (**e**–**j**) Trachea–lung, (**k**) tracheal, and (**l** and **m**) bronchial sections from animals intratracheally injected with PDOC and, 24 hr later, β-Gal-transduced BMC9 cells. Animals were killed 24 hr after BMC9 cell injection and stained with X-Gal. Blue spots were observed (**e** and **f**) in trachea and (**g**–**j**) in pulmonary lobes. (**f**, **h**, and **i**) Higher power views of the areas marked with asterisks in (**e**), (**g**), and (**j**), respectively. (**m**) Higher power view of the area marked with an asterisk in (**l**). (**n**–**p**) X-Gal-stained trachea–lung and histological sections from an animal intratracheally injected with PDOC and β-Gal-transduced BMC9 cells, and killed 7 days after BMC9 cell injection. Blue spots were observed in the lumen of bronchioles. (**p**) Higher power view of the area marked with an asterisk in (**o**). Original magnification: (**c**, **d**, and **o**)×4; (**b** and **l**)×10; (**k**)×20; (**m** and **p**)×40. Nuclear fast red counterstaining.

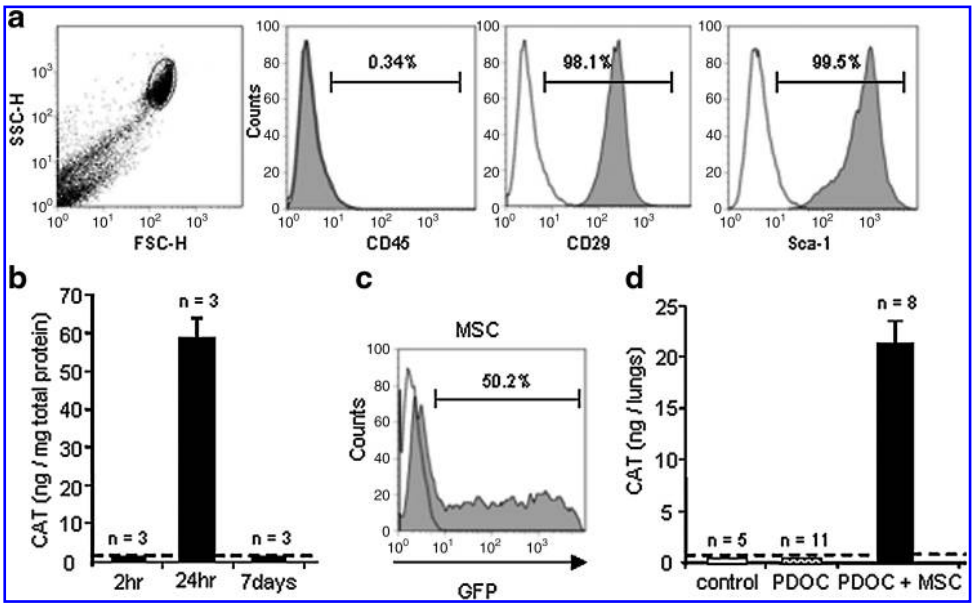

FIG. 5. *In vitro* cell transfection with reporter genes and *in vivo* CAT gene expression 24 hr after intratracheal administration into injured airway of murine adult mesenchymal stem cells (MSCs) from primary cultures. (**a**) MSC morphology and representative histograms of CD45, CD29, and Sca-1 labeling, using FACS analysis just before intratracheal injection. (**b**–**d**) To monitor MSC survival *in vivo*, MSCs were transfected *in vitro* with plasmids encoding the CAT or GFP reporter gene, using nucleofection, just before intratracheal injection. (**b**) CAT protein quantification in MSCs by ELISA, 2 hr, 24 hr, and 7 days after incubation with plasmid and nucleofection solution. (**c**) FACS analysis of GFP-expressing MSCs 24 hr after incubation with GFP plasmid and nucleofection solution. (**d**) CAT protein quantification in whole trachea–lung homogenates by ELISA, 24 hr after CAT-transduced MSC intratracheal injection. Evaluated groups included animals that were intratracheally injected with the following: no injection (control); PDOC only (PDOC); or PDOC and, 24 hr later, CAT-transduced MSCs (PDOC + MSC). Dashed line depicts control threshold.

was significantly increased in Rosa26 MSCs as compared with MSCs from Swiss mice (Fig. 6c; Mann–Whitney test, $p = 0.03$). Mice were assessed for β-Gal activity 24 hr and 7 days after intratracheal administration of Rosa26 MSCs or of a lysate of Rosa26 MSCs (Fig. 6d). As observed in previous experiments with β-Gal-transduced BMC9 cells, β-Gal activity was similar in murine airway from control animals and animals intratracheally injected with lysates of Rosa26 MSCs (Tukey's test, $p = 0.68$). In animals intratracheally injected with PDOC and Rosa26 MSCs, β-Gal activity was significantly increased as compared with that of both control groups (Tukey's test, $p = 0.01$). However, in contrast to previous experiments with β-Gal-transduced BMC9 cells, no blue staining was observed at 24 hr in trachea–lungs from animals injected intratracheally with PDOC and Rosa26 MSCs, and Rosa26 MSCs could not be located on histological slides (data not shown). Finally, β-Gal activity in murine injured airway returned to baseline 7 days after Rosa26 MSC intratracheal injection (Tukey's test, $p = 0.85$).

In a last set of experiments, as previously performed with BMC9 cells, we overexpressed the *nls-lacZ* gene in MSCs from wild-type Swiss mice, to locate them *in vivo* at 24 hr and 7 days. MSC transduction with the β-Gal retroviral vector remained ineffective. Therefore, MSCs from Swiss mice were transduced before intratracheal injection with a lentiviral vector encoding the *nls-lacZ* gene (Conrad *et al.*, 2007). After lentiviral transduction, $20.1 \pm 3.0\%$ of MSCs expressed β-Gal (Fig. 6b; $n = 4$). Nevertheless, no blue staining was observed in trachea–lungs from animals injected intratracheally with PDOC and β-Gal-transduced MSCs at 7 days (data not shown). Because rapid downregulation of foreign gene expression under the control of the cytomegalovirus promoter has been described in lungs (Pringle *et al.*, 2005), we used PCR concurrently to detect the presence of the *nls-lacZ* gene even without gene expression. PCR experiments using primers specific to the *nls-lacZ* gene were performed 24 hr and 7 days after β-Gal-transduced MSC injection (Fig. 6e). At 24 hr, PCR was positive in trachea–lungs from each animal injected with PDOC and β-Gal-transduced MSCs (Fig. 6e; $n = 7$), confirming that β-Gal-transduced MSCs were present 24 hr after injection into injured airway. However, no *nls-lacZ* gene was detected in animals 7 days after β-Gal-transduced MSC injection, suggesting that no β-Gal-transduced MSCs from primary culture survived at this time once the epithelium is regenerated (Fig. 6e; $n = 6$).

Discussion

Using independent methods based on reporter gene transfer, we demonstrated the short-term survival of various types of exogenous stem cells, including embryonic and adult mesenchymal stem cells, after intratracheal injection into murine airway presenting acute epithelial airway injury and without total body irradiation. In contrast to differentiated cells, 0.43 to 5.5% of stem cells were capable of surviving within the injured lungs at 24 hr. Importantly, no SCs survived in healthy airway or in the epithelial lining fluid. Biochemical staining showed that transduced MSCs were located in the lumen of conducting airway at 24 hr and at 7 days. However, the *in vivo* amount of engrafted MSCs

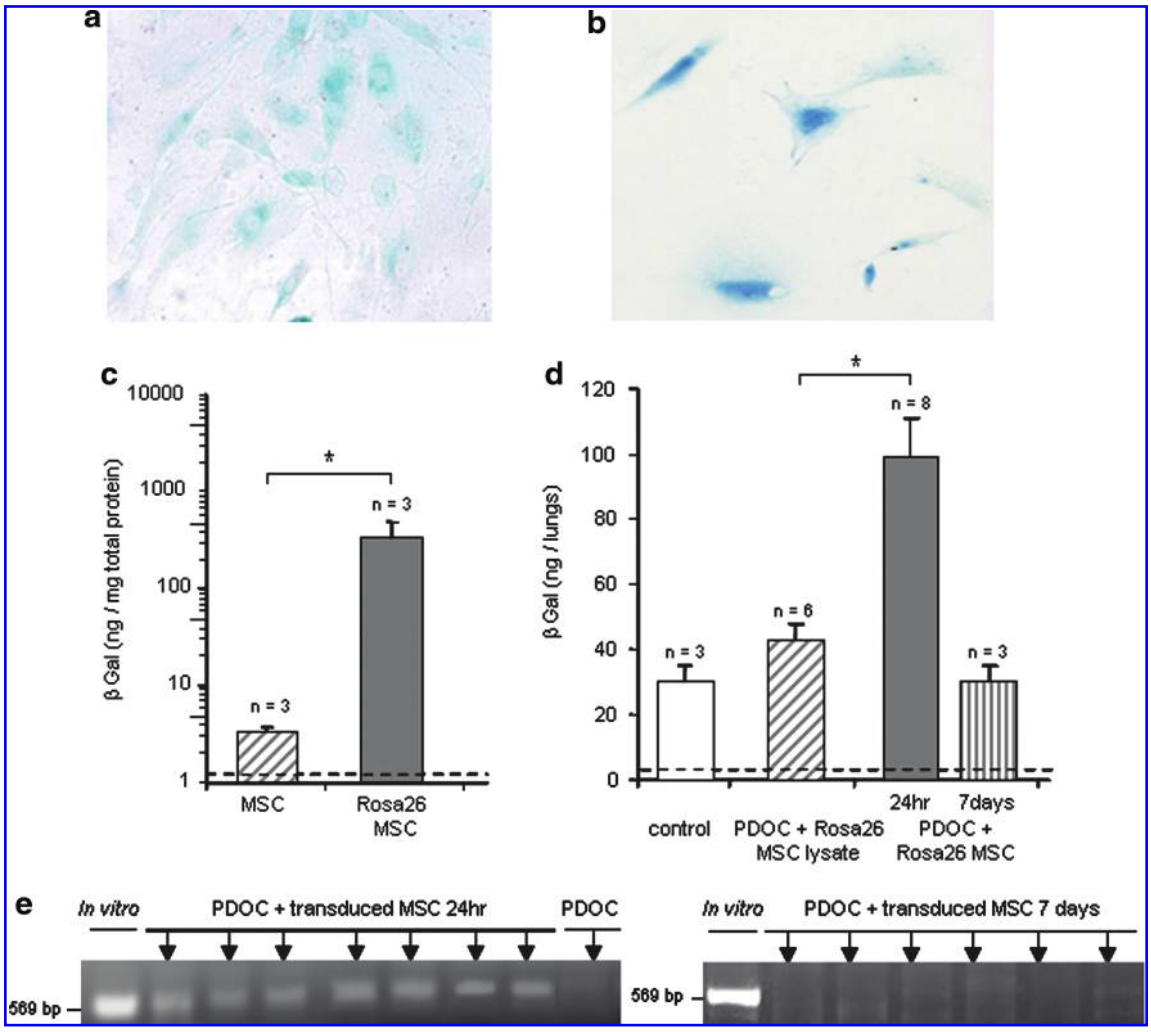

FIG. 6. *In vitro* and *in vivo* detection of Rosa26 MSCs and β-Gal-transduced MSCs 24 hr and 7 days after administration. MSCs from wild-type mice were transduced with a lentiviral vector encoding the *nls-lacZ* gene. (**a** and **b**) Representative example of (**a**) Rosa26 MSCs and (**b**) β-Gal-transduced MSCs after *in vitro* X-Gal staining just before intratracheal injection. Original magnification, ×20. (**c**) *In vitro* β-Gal activity in MSCs and Rosa26 MSCs just before intratracheal injection. (**d**) β-Gal activity in whole trachea–lung homogenates, 24 hr and 7 days after Rosa26 MSC intratracheal administration. Evaluated groups included animals that were intratracheally injected with the following: no injection (control), PDOC and lysate of Rosa26 MSCs (PDOC + Rosa26 MSC lysate), PDOC and Rosa26 MSCs (PDOC + Rosa26 MSC). Dashed line depicts control threshold. *$p < 0.05$. (**e**) *In vivo* detection of the *nls-lacZ* gene by PCR 24 hr and 7 days after intratracheal injection of β-Gal-transduced MSCs. Color images available online at www.liebertonline.com/hum.

decreased dramatically with time. No primary MSCs were located within lungs at 7 days.

In our study, several gene transfer systems were used, according to our aims and to cell types. Using careful timing, nonviral vectors were useful to allow expression of the foreign gene only after intratracheal cell injection. Gene delivery with viral vectors was used for *in vivo* studies at 7 days, but we had to use different viral vectors to transduce MSCs from cell lines and primary MSCs. Depending on the gene transfer system and the cell type, gene transfer efficacy was variable *in vitro*. Studies with retroviral vectors showed high efficacy and stable MSC transduction (up to 97%; Sales *et al.*, 2007) whereas studies with lentiviral vectors showed variable efficacy between murine MSCs (up to 50%) (Ricks *et al.*, 2008; Santoni de Sio *et al.*, 2008; Xu *et al.*, 2008) and human MSCs (up to 93%; Chan *et al.*, 2005). These data confirmed that primary murine MSCs are more difficult to transduce than human MSCs.

Engraftment of exogenous stem cells into the lungs has been reported in several *in vivo* studies, but the cell engraftment rate remains controversial (Loebinger *et al.*, 2008a). Our results highlight the main advantage of using ELISA and biochemical methods to detect and quantify a small number of administered cells in the whole organ. Although the *lacZ* gene is widely used to locate stem cells, some reports have shown that standard protocols for X-Gal staining can lead, especially in the lungs, both to false positive results as well as to failure to adequately detect β-Gal-expressing cells (Weiss *et al.*, 1997). In our study, although β-Gal activity significantly increased after intratracheal injection of MSCs from Rosa26 mice, surviving Rosa26 MSCs could not be located *in vivo* on histological slides, as already described in

another report (MacPherson *et al.*, 2005). The *lacZ* gene coupled with a nuclear localization signal had already been used in several studies from our group (Lemarchand *et al.*, 1994; Chapelier *et al.*, 1996) and others (Mastrangeli *et al.*, 1993) and was shown to allow easy distinction of endogenous from exogenous β-Gal activity. Using the *nls-lacZ* gene, we were able to detect and locate nuclear β-Gal-expressing cells, even when β-Gal activity in the whole lungs was not significantly different from baseline.

We investigated whether stem cells would be capable of locating specifically on the epithelial side of the airway after intratracheal administration. BAL experiments showed that stem cells expressing reporter protein did not survive in the epithelial lining fluid. X-Gal staining showed that stem cells were localized into the conducting airway *in vivo*. By injecting stem cells into healthy airway, we also confirmed the major role of the injured environment in the engraftment (MacPherson *et al.*, 2005). Stem cells may not engraft into healthy airway because of mucociliary clearance mechanisms that could impede access to airway epithelium, as described for *in vivo* gene transfer to the lungs (Weiss, 2002). We speculated that mucociliary clearance would be disrupted in polidocanol (PDOC)-treated airway and that the freshly denuded basement membrane may also specifically promote stem cell adherence and engraftment in the airway epithelium (Engelhardt *et al.*, 1992; Nikolova *et al.*, 2006). In the first set of experiments, murine ESCs were intratracheally injected and a significant survival cell rate was observed, although the *in vitro* ESC transfection rate was low. This confirms the great potential of ESC pluripotency for regenerative medicine and in particular airway injury. Nevertheless, ESCs for cell-based therapy have met with ethical, moral, and political challenges, and with inherent risks associated with immune rejection (Chidgey *et al.*, 2008). In further experiments, we focused our attention on MSCs because they are already used in the clinical setting (Uccelli *et al.*, 2008). Our ELISA data indicated that the MSC survival rate varied according to whether cultures were immortalized or primary, probably because of the different gene transfer systems we used. Survival rates (from 0.4 to 5.5%) 24 hr after intratracheal administration were higher than those described after intravenous administration (from 0.01 to 0.1%) and were in agreement with those usually described in stem cell therapy protocols, including cardiology (Robey *et al.*, 2008) and diabetology (Bottino *et al.*, 2003) protocols, and lung injury models (Gupta *et al.*, 2007; Wong *et al.*, 2007, 2009).

We hypothesized that MSC incorporation in the lungs at 7 days could be masked by downregulation of transgene expression in the lungs because of the common cytomegalovirus enhancer/promoter element in the viral vector constructs (Alton *et al.*, 1999; Pringle *et al.*, 2005). The negative results of PCR experiments on the *nls-lacZ* gene at 7 days demonstrated that this was not the case. Allogeneic rejection seems unlikely to be responsible for the lack of survival of differentiated cells at 24 hr because ESCs, although known to be targeted for rejection by the immune system (Chidgey *et al.*, 2008), survived at 24 hr. Nevertheless, allogeneic MSC rejection cannot be ruled out at 7 days.

Another hypothesis to explain negative MSC results at 7 days concerns the spontaneous regeneration of airway epithelium, which may have hampered MSC incorporation into the airway epithelium. At 24 hr, that is, when there is desquamation of the epithelial surface and a denuded basement membrane, the PDOC murine model is a good model to evaluate stem cell survival and presence in injured airway; but stem cell differentiation into airway epithelial cells is unlikely at this time. Seven days after PDOC administration, the epithelium was spontaneously regenerated, demonstrating that PDOC did not alter the lung's endogenous ability to regenerate. Therefore, the PDOC model may not be an adequate model to evaluate stem cell capability in regenerating lung epithelium, because the endogenous repair mechanisms may impede the MSC contribution to achieve structural lung regeneration. This limitation was described in the study by Wong and colleagues (2007), in which naphthalene-injured airway epithelium was still undergoing rapid cell turnover and regeneration and the number of administered stem cells also decreased with time. A more appropriate animal model to study stem cell contribution to structural lung regeneration would be a model with chronic epithelial airway injury and a recurrent loss of the epithelial surface, due to a lack, or exhaustion, of endogenous progenitor cells. This hypothesis was evaluated in animal models with permanent retinal epithelial degeneration such as the RCS rat model (D'Cruz *et al.*, 2000) and the rhodopsin knockout mouse (Humphries *et al.*, 1997). MSC engraftment and epithelial regeneration involving MSCs were observed in these animal models (Arnhold *et al.*, 2007; Inoue *et al.*, 2007). For lung tissue, a murine model overexpressing the β subunit of the epithelial Na^+ channel ($ENaC^{+/+}$) and showing epithelial degeneration in newborn animals (Mall *et al.*, 2008) may be more appropriate to evaluate the MSC contribution to lung regeneration.

Finally, an important limitation of our study was also the lack of phenotypic characterization of surviving cells. This characterization of stem cell-derived epithelial cells has been hampered by methodological problems, in the lungs as in many other organs such as the heart (Murry *et al.*, 2004) or the brain (Castro *et al.*, 2002), and remains difficult and controversial. In this regard, additional studies using complex transgenic models with reporter genes under the control of lung-specific promoters *in vivo* will be essential.

Acknowledgments

The authors thank Nicolas Ferry (Nantes, France) for providing the *nls-lacZ* retroviral vector and Marie-France Gardahaut (Nantes, France) for providing the Rosa26 mice. The authors are grateful to Beatrice Delasalle for statistical analyses. This work was supported in part by a grant from Vaincre la Mucoviscidose (Paris, France).

Author Disclosure Statement

No competing financial interests exist.

References

Alton, E.W., Stern, M., Farley, R., Jaffe, A., Chadwick, S.L., Phillips, J., Davies, J., Smith, S.N., Browning, J., Davies, M.G., Hodson, M.E., Durham, S.R., Li, D., Jeffery, P.K., Scallan, M., Balfour, R., Eastman, S.J., Cheng, S.H., Smith, A.E., Meeker, D., and Geddes, D.M. (1999). Cationic lipid-mediated CFTR gene transfer to the lungs and nose of patients with cystic fibrosis: A double-blind placebo-controlled trial. Lancet 353, 947–954.

Aluigi, M., Fogli, M., Curti, A., Isidori, A., Gruppioni, E., Chiodoni, C., Colombo, M.P., Versura, P., D'Errico-Grigioni, A., Ferri, E., Baccarani, M., and Lemoli, R.M. (2006). Nucleofection is an efficient nonviral transfection technique for human bone marrow-derived mesenchymal stem cells. Stem Cells 24, 454–461.

Arnhold, S., Absenger, Y., Klein, H., Addicks, K., and Schraermeyer, U. (2007). Transplantation of bone marrow-derived mesenchymal stem cells rescue photoreceptor cells in the dystrophic retina of the rhodopsin knockout mouse. Graefes Arch. Clin. Exp. Ophthalmol. 245, 414–422.

Aubert, D., Menoret, S., Chiari, E., Pichard, V., Durand, S., Tesson, L., Moullier, P., Anegon, I., and Ferry, N. (2002). Cytotoxic immune response blunts long-term transgene expression after efficient retroviral-mediated hepatic gene transfer in rat. Mol. Ther. 5, 388–396.

Beckett, T., Loi, R., Prenovitz, R., Poynter, M., Goncz, K.K., Suratt, B.T., and Weiss, D.J. (2005). Acute lung injury with endotoxin or NO_2 does not enhance development of airway epithelium from bone marrow. Mol. Ther. 12, 680–686.

Borthwick, D.W., Shahbazian, M., Krantz, Q.T., Dorin, J.R., and Randell, S.H. (2001). Evidence for stem-cell niches in the tracheal epithelium. Am. J. Respir. Cell Mol. Biol. 24, 662–670.

Bottino, R., Lemarchand, P., Trucco, M., and Giannoukakis, N. (2003). Gene- and cell-based therapeutics for type I diabetes mellitus. Gene Ther. 10, 875–889.

Bruscia, E.M., Ziegler, E.C., Price, J.E., Weiner, S., Egan, M.E., and Krause, D.S. (2006). Engraftment of donor-derived epithelial cells in multiple organs following bone marrow transplantation into newborn mice. Stem Cells 24, 2299–2308.

Castro, R.F., Jackson, K.A., Goodell, M.A., Robertson, C.S., Liu, H., and Shine, H.D. (2002). Failure of bone marrow cells to transdifferentiate into neural cells *in vivo*. Science 297, 1299.

Chan, J., O'Donoghue, K., de la Fuente, J., Roberts, I.A., Kumar, S., Morgan, J.E., and Fisk, N.M. (2005). Human fetal mesenchymal stem cells as vehicles for gene delivery. Stem Cells 23, 93–102.

Chapelier, A., Danel, C., Mazmanian, M., Bacha, E.A., Sellak, H., Gilbert, M.A., Herve, P., and Lemarchand, P. (1996). Gene therapy in lung transplantation: Feasibility of *ex vivo* adenovirus-mediated gene transfer to the graft. Hum. Gene Ther. 7, 1837–1845.

Chateauvieux, S., Ichante, J.L., Delorme, B., Frouin, V., Pietu, G., Langonne, A., Gallay, N., Sensebe, L., Martin, M.T., Moore K.A., and Charbord, P. (2007). Molecular profile of mouse stromal mesenchymal stem cells. Physiol. Genomics 29, 128–138.

Chidgey, A.P., Layton, D., Trounson, A., and Boyd, R.L. (2008). Tolerance strategies for stem-cell-based therapies. Nature 453, 330–337.

Conrad, C., Gupta, R., Mohan, H., Niess, H., Bruns, C.J., Kopp, R., von Luettichau, I., Guba, M., Heeschen, C., Jauch, K.W., Huss, R., and Nelson, P.J. (2007). Genetically engineered stem cells for therapeutic gene delivery. Curr. Gene Ther. 7, 249–260.

Coraux, C., Nawrocki-Raby, B., Hinnrasky, J., Kileztky, C., Gaillard, D., Dani C., and Puchelle, E. (2005). Embryonic stem cells generate airway epithelial tissue. Am. J. Respir. Cell Mol. Biol. 32, 87–92.

D'Cruz, P.M., Yasumura, D., Weir, J., Matthes, M.T., Abderrahim, H., LaVail, M.M., and Vollrath, D. (2000). Mutation of the receptor tyrosine kinase gene *Mertk* in the retinal dystrophic RCS rat. Hum. Mol. Genet. 9, 645–651.

Dennis, J.E., and Caplan, A.I. (1996). Differentiation potential of conditionally immortalized mesenchymal progenitor cells from adult marrow of a *H-2K^b*-tsA58 transgenic mouse. J. Cell Physiol. 167, 523–538.

Dominici, M., Le Blanc, K., Mueller, I., Slaper-Cortenbach, I., Marini, F., Krause, D., Deans, R., Keating, A., Prockop, D., and Horwitz, E. (2006). Minimal criteria for defining multipotent mesenchymal stromal cells: The International Society for Cellular Therapy position statement. Cytotherapy 8, 315–317.

Driscoll, K.E., Costa, D.L., Hatch, G., Henderson, R., Oberdorster, G., Salem, H., and Schlesinger, R.B. (2000). Intratracheal instillation as an exposure technique for the evaluation of respiratory tract toxicity: Uses and limitations. Toxicol. Sci. 55, 24–35.

Engelhardt, J.F., Yankaskas, J.R., and Wilson, J.M. (1992). *In vivo* retroviral gene transfer into human bronchial epithelia of xenografts. J. Clin. Invest. 90, 2598–2607.

Gupta, N., Su, X., Popov, B., Lee, J.W., Serikov, V., and Matthay, M.A. (2007). Intrapulmonary delivery of bone marrow-derived mesenchymal stem cells improves survival and attenuates endotoxin-induced acute lung injury in mice. J. Immunol. 179, 1855–1863.

Humphries, M.M., Rancourt, D., Farrar, G.J., Kenna, P., Hazel, M., Bush, R.A., Sieving, P.A., Sheils, D.M., McNally, N., Creighton, P., Erven, A., Boros, A., Gulya, K., Capecchi, M.R., and Humphries, P. (1997). Retinopathy induced in mice by targeted disruption of the rhodopsin gene. Nat. Genet. 15, 216–219.

Inoue, Y., Iriyama, A., Ueno, S., Takahashi, H., Kondo, M., Tamaki, Y., Araie, M., and Yanagi, Y. (2007). Subretinal transplantation of bone marrow mesenchymal stem cells delays retinal degeneration in the RCS rat model of retinal degeneration. Exp. Eye Res. 85, 234–241.

Institute of Laboratory Animal Research, Commission on Life Sciences, National Research Council. (1996). *Guide for the Care and Use of Laboratory Animals*. NIH Publication No. 85-23. (National Academies Press, Washington, D.C.).

Joliat, M.J., Umeda, S., Lyons, B.L., Lynes, M.A., and Shultz, L.D. (2002). Establishment and characterization of a new osteogenic cell line (MOS-J) from a spontaneous C57BL/6J mouse osteosarcoma. In Vivo 16, 223–228.

Krause, D.S. (2005). Engraftment of bone marrow-derived epithelial cells. Ann. N. Y. Acad. Sci. 1044, 117–124.

Krause, D.S., Theise, N.D., Collector, M.I., Henegariu, O., Hwang, S., Gardner, R., Neutzel, S., and Sharkis, S.J. (2001). Multi-organ, multi-lineage engraftment by a single bone marrow-derived stem cell. Cell 105, 369–377.

Kuang, P.P., Lucey, E., Rishikof, D.C., Humphries, D.E., Bronsnick, D., and Goldstein, R.H. (2005). Engraftment of neonatal lung fibroblasts into the normal and elastase-injured lung. Am. J. Respir. Cell Mol. Biol. 33, 371–377.

Lemarchand, P., Jones, M., Danel, C., Yamada, I., Mastrangeli, A., and Crystal, R.G. (1994). *In vivo* adenovirus-mediated gene transfer to lungs via pulmonary artery. J. Appl. Physiol. 76, 2840–2845.

Loebinger, M.R., Aguilar, S., and Janes, S.M. (2008a). Therapeutic potential of stem cells in lung disease: Progress and pitfalls. Clin. Sci. 114, 99–108.

Loebinger, M.R., Sage, E.K., and Janes, S.M. (2008b). Mesenchymal stem cells as vectors for lung disease. Proc. Am. Thorac. Soc. 5, 711–716.

Loi, R., Beckett, T., Goncz, K.K., Suratt, B.T., and Weiss, D.J. (2006). Limited restoration of cystic fibrosis lung epithelium

in vivo with adult bone marrow-derived cells. Am. J. Respir. Crit. Care Med. 173, 171–179.

MacPherson, H., Keir, P., Webb, S., Samuel, K., Boyle, S., Bickmore, W., Forrester, L., and Dorin, J. (2005). Bone marrow-derived SP cells can contribute to the respiratory tract of mice *in vivo*. J. Cell Sci. 118, 2441–2450.

MacPherson, H., Keir, P.A., Edwards, C.J., Webb, S., and Dorin, J.R. (2006). Following damage, the majority of bone marrow-derived airway cells express an epithelial marker. Respir. Res. 7, 145.

Mall, M.A., Harkema, J.R., Trojanek, J.B., Treis, D., Livraghi, A., Schubert, S., Zhou, Z., Kreda, S.M., Tilley, S.L., Hudson, E.J., O'Neal, W.K., and Boucher, R.C. (2008). Development of chronic bronchitis and emphysema in β-epithelial Na^+ channel-overexpressing mice. Am. J. Respir. Crit. Care Med. 177, 730–742.

Mastrangeli, A., Danel, C., Rosenfeld, M.A., Stratford-Perricaudet, L., Perricaudet, M., Pavirani, A., Lecocq, J.P., and Crystal, R.G. (1993). Diversity of airway epithelial cell targets for *in vivo* recombinant adenovirus-mediated gene transfer. J. Clin. Invest. 91, 225–234.

Mei, S.H., McCarter, S.D., Deng, Y., Parker, C.H., Liles, W.C., and Stewart, D.J. (2007). Prevention of LPS-induced acute lung injury in mice by mesenchymal stem cells overexpressing angiopoietin 1. PLoS Med. 4, e269.

Murry, C.E., Soonpaa, M.H., Reinecke, H., Nakajima, H., Nakajima, H.O., Rubart, M., Pasumarthi, K.B., Virag, J.I., Bartelmez, S.H., Poppa, V., Bradford, G., Dowell, J.D., Williams, D.A., and Field, L.J. (2004). Haematopoietic stem cells do not transdifferentiate into cardiac myocytes in myocardial infarcts. Nature 428, 664–668.

Nagy, A., Rossant, J., Nagy, R., Abramow-Newerly, W., and Roder, J.C. (1993). Derivation of completely cell culture-derived mice from early-passage embryonic stem cells. Proc. Natl. Acad. Sci. U.S.A. 90, 8424–8428.

Nikolova, G., Jabs, N., Konstantinova, I., Domogatskaya, A., Tryggvason, K., Sorokin, L., Fassler, R., Gu, G., Gerber, H.P., Ferrara, N., Melton, D.A., and Lammert, E. (2006). The vascular basement membrane: A niche for insulin gene expression and beta cell proliferation. Dev. Cell 10, 397–405.

Parsons, D.W., Grubb, B.R., Johnson, L.G., and Boucher, R.C. (1998). Enhanced *in vivo* airway gene transfer via transient modification of host barrier properties with a surface-active agent. Hum. Gene Ther. 9, 2661–2672.

Pereira, R.F., Halford, K.W., O'Hara, M.D., Leeper, D.B., Sokolov, B.P., Pollard, M.D., Bagasra, O., and Prockop, D.J. (1995). Cultured adherent cells from marrow can serve as long-lasting precursor cells for bone, cartilage, and lung in irradiated mice. Proc. Natl. Acad. Sci. U.S.A. 92, 4857–4861.

Pitard, B., Oudrhiri, N., Lambert, O., Vivien, E., Masson, C., Wetzer, B., Hauchecorne, M., Scherman, D., Rigaud, J.L., Vigneron, J.P., Lehn, J.M., and Lehn, P. (2001). Sterically stabilized BGTC-based lipoplexes: Structural features and gene transfection into the mouse airways *in vivo*. J. Gene Med. 3, 478–487.

Pringle, I.A., Raman, S., Sharp, W.W., Cheng, S.H., Hyde, S.C., and Gill, D.R. (2005). Detection of plasmid DNA vectors following gene transfer to the murine airways. Gene Ther. 12, 1206–1214.

Ricks, D.M., Kutner, R., Zhang, X.Y., Welsh, D.A., and Reiser, J. (2008). Optimized lentiviral transduction of mouse bone marrow-derived mesenchymal stem cells. Stem Cells Dev. 17, 441–450.

Rippon, H.J., Polak, J.M., Qin, M., and Bishop, A.E. (2006). Derivation of distal lung epithelial progenitors from murine embryonic stem cells using a novel three-step differentiation protocol. Stem Cells 24, 1389–1398.

Robey, T.E., Saiget, M.K., Reinecke, H., and Murry, C.E. (2008). Systems approaches to preventing transplanted cell death in cardiac repair. J. Mol. Cell. Cardiol. 45, 567–581.

Sales, V.L., Mettler, B.A., Lopez-Ilasaca, M., Johnson, J.A., Jr., and Mayer, J.E., Jr. (2007). Endothelial progenitor and mesenchymal stem cell-derived cells persist in tissue-engineered patch *in vivo*: Application of green and red fluorescent protein-expressing retroviral vector. Tissue Eng. 13, 525–535.

Santoni de Sio, F.R., Gritti, A., Cascio, P., Neri, M., Sampaolesi, M., Galli, C., Luban, J., and Naldini, L. (2008). Lentiviral vector gene transfer is limited by the proteasome at postentry steps in various types of stem cells. Stem Cells 26, 2142–2152.

Selig, L., Pages, J.C., Tanchou, V., Preveral, S., Berlioz-Torrent, C., Liu, L.X., Erdtmann, L., Darlix, J., Benarous, R., and Benichou, S. (1999). Interaction with the p6 domain of the Gag precursor mediates incorporation into virions of Vpr and Vpx proteins from primate lentiviruses. J. Virol. 73, 592–600.

Serikov, V.B., Popov, B., Mikhailov, V.M., Gupta, N., and Matthay, M.A. (2007). Evidence of temporary airway epithelial repopulation and rare clonal formation by BM-derived cells following naphthalene injury in mice. Anat. Rec. 290, 1033–1045.

Serrano-Mollar, A., Nacher, M., Gay-Jordi, G., Closa, D., Xaubet, A., and Bulbena, O. (2007). Intratracheal transplantation of alveolar type II cells reverses bleomycin-induced lung fibrosis. Am. J. Respir. Crit. Care Med. 176, 1261–1268.

Southam, D.S., Dolovich, M., O'Byrne, P.M., and Inman, M.D. (2002). Distribution of intranasal instillations in mice: Effects of volume, time, body position, and anesthesia. Am. J. Physiol. Lung Cell Mol. Physiol. 282, L833–L839.

Sueblinvong, V., Loi, R., Eisenhauer, P.L., Bernstein, I.M., Suratt, B.T., Spees, J.L., and Weiss, D.J. (2008). Derivation of lung epithelium from human cord blood-derived mesenchymal stem cells. Am. J. Respir. Crit. Care Med. 177, 701–711.

Uccelli, A., Moretta, L., and Pistoia, V. (2008). Mesenchymal stem cells in health and disease. Nat. Rev. Immunol. 8, 726–736.

Wagers, A.J., Sherwood, R.I., Christensen, J.L., and Weissman, I.L. (2002). Little evidence for developmental plasticity of adult hematopoietic stem cells. Science 297, 2256–2259.

Wang, G., Bunnell, B.A., Painter, R.G., Quiniones, B.C., Tom, S., Lanson, N.A., Jr., Spees, J.L., Bertucci, D., Peister, A., Weiss, D.J., Valentine, V.G., Prockop, D.J., and Kolls, J.K. (2005). Adult stem cells from bone marrow stroma differentiate into airway epithelial cells: Potential therapy for cystic fibrosis. Proc. Natl. Acad. Sci. U.S.A. 102, 186–191.

Weiss, D.J. (2002). Delivery of gene transfer vectors to lung: Obstacles and the role of adjunct techniques for airway administration. Mol. Ther. 6, 148–152.

Weiss, D.J., Liggitt, D., and Clark, J.G. (1997). *In situ* histochemical detection of β-galactosidase activity in lung: Assessment of X-Gal reagent in distinguishing *lacZ* gene expression and endogenous β-galactosidase activity. Hum. Gene Ther. 8, 1545–1554.

Wong, A.P., Dutly, A.E., Sacher, A., Lee, H., Hwang, D.M., Liu, M., Keshavjee, S., Hu, J., and Waddell, T.K. (2007). Targeted cell replacement with bone marrow cells for airway epithelial regeneration. Am. J. Physiol. Lung Cell Mol. Physiol. 293, L740–L752.

Wong, A.P., Keating, A., Lu, W.Y., Duchesneau, P., Wang, X., Sacher, A., Hu, J., and Waddell, T.K. (2009). Identification of a bone marrow-derived epithelial-like population capable of

repopulating injured mouse airway epithelium. J. Clin. Invest. 119, 336–348.

Xu, J., Woods, C.R., Mora, A.L., Joodi, R., Brigham, K.L., Iyer, S., and Rojas, M. (2007). Prevention of endotoxin-induced systemic response by bone marrow-derived mesenchymal stem cells in mice. Am. J. Physiol. Lung Cell Mol. Physiol. 293, L131–L141.

Xu, J., Qu, J., Cao, L., Sai, Y., Chen, C., He, L., and Yu, L. (2008). Mesenchymal stem cell-based angiopoietin-1 gene therapy for acute lung injury induced by lipopolysaccharide in mice. J. Pathol. 214, 472–481.

Zufferey, R., Nagy, D., Mandel, R.J., Naldini, L., and Trono, D. (1997). Multiply attenuated lentiviral vector achieves efficient gene delivery *in vivo*. Nat. Biotechnol. 15, 871–875.

Address correspondence to:
Dr. Patricia Lemarchand
INSERM, UMR915
Institut du Thorax
IRT-Université de Nantes
8 quai Moncousu, BP 70721
44007 Nantes cedex 1, France

E-mail: patricia.lemarchand@univ-nantes.fr

Received for publication March 11, 2009;
accepted after revision July 16, 2009.

Published online: October 7, 2009.

This article has been cited by:

1. Tillie-Louise Hackett, Stephanie Warner, Dorota Stefanowicz, Darryl KnightEpithelial Cells 139-148. [CrossRef]
2. Massimo Conese, Fiorentina Ascenzioni, A. Christopher Boyd, Charles Coutelle, Ida De Fino, Stefaan De Smedt, Joanna Rejman, Joseph Rosenecker, Dirk Schindelhauer, Bob J. Scholte. 2011. Gene and cell therapy for cystic fibrosis: From bench to bedside. *Journal of Cystic Fibrosis* **10**, S114-S128. [CrossRef]
3. Thorsten Walles. 2011. Tracheobronchial bio-engineering: Biotechnology fulfilling unmet medical needs. *Advanced Drug Delivery Reviews* **63**:4-5, 367-374. [CrossRef]
4. Uta Griesenbach, Eric W.F.W. Alton. 2011. Current Status and Future Directions of Gene and Cell Therapy for Cystic Fibrosis. *BioDrugs* **25**:2, 77-88. [CrossRef]
5. James B. Grotberg. 2011. Respiratory fluid mechanics. *Physics of Fluids* **23**:2, 021301. [CrossRef]
6. Darryl A Knight, Fabio M Rossi, Tillie-Louise Hackett. 2010. Mesenchymal stem cells for repair of the airway epithelium in asthma. *Expert Review of Respiratory Medicine* **4**:6, 747-758. [CrossRef]
7. Ahmed E. Hegab , Hiroshi Kubo , Naoya Fujino , Takaya Suzuki , Mei He , Hidemasa Kato , Mutsuo Yamaya . 2010. Isolation and Characterization of Murine Multipotent Lung Stem CellsIsolation and Characterization of Murine Multipotent Lung Stem Cells. *Stem Cells and Development* **19**:4, 523-536. [Abstract] [Full Text] [PDF] [PDF Plus]

Tissue Engineering

Tissue Engineering Manuscript Central: http://mc.manuscriptcentral.com/ten

A Self-setting hydrogel mechanically reinforced with a marine exopolysaccharide as a scaffold for cartilage tissue engineering

Journal:	*Tissue Engineering*
Manuscript ID:	Draft
Manuscript Type:	Original Article
Date Submitted by the Author:	n/a
Complete List of Authors:	Rederstorff, Emilie; INSERM U791-LIOAD, Group STEP Skeletal Tissue Engineering and Physiopathology Weiss, Pierre; INSERM U791-LIOAD, Group STEP Skeletal Tissue Engineering and Physiopathology Sourice, Sophie; INSERM U791-LIOAD, Group STEP Skeletal Tissue Engineering and Physiopathology Masson, Martial; INSERM U791-LIOAD, Group STEP Skeletal Tissue Engineering and Physiopathology Mathieu, Eva; institut du thorax INSERM U915, university of Nantes Laib, Samia; INSERM U791-LIOAD, Group STEP Skeletal Tissue Engineering and Physiopathology Colliec-Jouault, Sylvia; ifremer, french research institute for exploitation of the sea, Laboratory of biotechnology and marine molecules Fellah, Borhane; INSERM U791-LIOAD, Group STEP Skeletal Tissue Engineering and Physiopathology Guicheux, Jerome; INSERM U791-LIOAD, Group STEP Skeletal Tissue Engineering and Physiopathology Vinatier, Claire; INSERM U791-LIOAD, Group STEP Skeletal Tissue Engineering and Physiopathology
Keyword:	Cell Differentiation < Fundamentals of Tissue Engineering, 3-D Cell Culture < Enabling Technologies, Cartilage < Tissue Engineering Applications, Biodegradable Hydrogel
Abstract:	Polysaccharide-based hydrogels such as chitosan, alginate or glycosaminoglycan (GAG) derivatives have been widely used as three-dimensional (3D) scaffolds in cartilage tissue engineering. However none of them have shown adequate mechanical and biological properties. To develop a biomechanically and biologically competent hydrogel for cartilage tissue engineering, a cellulose-based hydrogel (Si-HPMC) was reinforced with a marine polysaccharide the GY785. In a previous work, we showed that GY785-doping improved the mechanical properties of the Si-HPMC. Therefore, the aims of the present work were (i) to investigate the ability of this Si-HPMC/GY785 to make possible the maintenance and recovery of a chondrocytic phenotype and (ii) to evaluate the potential of this Si-HPMC/GY785 associated with chondrocytes to form cartilaginous

	tissue in vivo. Primary rabbit articular chondrocytes (RAC) were either cultured in 3D within Si-HPMC/GY785 or transplanted with Si-HPMC/GY785 subcutaneously in nude mice for 3 weeks. RT-PCR analysis showed that primary chondrocytes 3D-cultured in Si-HPMC/GY785 expressed type II collagen and agrecan. In addition, these cells also produced an extracellular matrix (ECM) containing sulphated GAG and type II collagen. When dedifferentiated chondrocytes were replaced in 3D in Si-HPMC/GY785, expressions of type II collagen and agrecan were recovered and type I collagen expression decreased. Finally, histological analysis of hybrid constructs transplanted into nude mice revealed the production of a cartilage-like ECM containing sulphated GAG and type II collagen. These results indicate that mechanically GY785-reinforced Si-HPMC appears to be a promising hydrogel for cartilage tissue engineering.

A Self-setting hydrogel mechanically reinforced with a marine exopolysaccharide as a scaffold for cartilage tissue engineering

E. Rederstorff [1,2], P. Weiss[1], S. Sourice[1], M. Masson[1],E. Mathieu[3], Samia Laib[1], S. Colliec-Jouault[2], B. H. Fellah[1], J. Guicheux[1*], C. Vinatier[1,4].

[1] *INSERM UMRS 791 group STEP, University of Nantes, Laboratory of Osteo-Articular and Dental Tissue Engineering, School of Dental Surgery, 1 place Alexis Ricordeau, 44042 Nantes cedex 1, France*

[2] *Ifremer, French Research Institute for Exploitation of the Sea, Laboratory of Biotechnology and Marine Molecules, Rue de l'Ille d'Yeu BP 21105, 44311 Nantes Cedex 03, France*

[3] *Institut du thorax INSERM U915, University of Nantes*

[4] *GRAFTYS SA, Eiffel Park, Bâtiment D, 415 rue Claude Nicolas Ledoux, Pôle d'activités d'Aix en Provence, 13854 Aix en Provence Cedex 3, France.*

***Corresponding author:** Jerome Guicheux

INSERM U 791, Laboratoire d'ingénierie Ostéo-Articulaire et Dentaire (LIOAD).

Faculté de Chirurgie Dentaire, 1 Place Alexis Ricordeau, 44042 Nantes Cedex 1, France

Phone : +33 240412919 ; Fax : +33 240083712 ; e-mail : jerome.guicheux@inserm.fr

Keywords: Cartilage, Hydrogel, Glycosaminoglycan, Polysaccharides, Chondrocytes, Tissue engineering

Abstract

Polysaccharide-based hydrogels such as chitosan, alginate or glycosaminoglycan (GAG) derivatives have been widely used as three-dimensional (3D) scaffolds in cartilage tissue engineering. However none of them have shown adequate mechanical and biological properties. To develop a biomechanically and biologically competent hydrogel for cartilage tissue engineering, a cellulose-based hydrogel (Si-HPMC) was reinforced with a marine polysaccharide the GY785. In a previous work, we showed that GY785-doping improved the mechanical properties of the Si-HPMC. Therefore, the aims of the present work were (i) to investigate the ability of this Si-HPMC/GY785 to make possible the maintenance and recovery of a chondrocytic phenotype and (ii) to evaluate the potential of this Si-HPMC/GY785 associated with chondrocytes to form cartilaginous tissue *in vivo*. Primary rabbit articular chondrocytes (RAC) were either cultured in 3D within Si-HPMC/GY785 or transplanted with Si-HPMC/GY785 subcutaneously in nude mice for 3 weeks. RT-PCR analysis showed that primary chondrocytes 3D-cultured in Si-HPMC/GY785 expressed type II collagen and agrecan. In addition, these cells also produced an extracellular matrix (ECM) containing sulphated GAG and type II collagen. When dedifferentiated chondrocytes were replaced in 3D in Si-HPMC/GY785, expressions of type II collagen and agrecan were recovered and type I collagen expression decreased. Finally, histological analysis of hybrid constructs transplanted into *nude* mice revealed the production of a cartilage-like ECM containing sulphated GAG and type II collagen. These results indicate that mechanically GY785-reinforced Si-HPMC appears to be a promising hydrogel for cartilage tissue engineering.

Running title: Polysaccharide hydrogel for cartilage engineering

Introduction

Articular cartilage (AC) is an avascular connective tissue containing a cell type, the chondrocyte, which synthesizes an abundant extracellular matrix (ECM) (1) mainly composed of type II collagen and agrecan (2, 3). AC unfortunately has a poor capacity for self-repair (4, 5), and injuries to articular cartilage are thus irreversible and may lead to long-term joint degeneration (6).

In such circumstances, cell-based therapies for the regeneration of AC have been explored. Autologous chondrocyte transplantation (ACT) was used to treat full-thickness chondral defects(7). This technique, however, suffers from limitations such as low numbers of cells obtained through the biopsy, donor site morbidity and the dedifferentiation of chondrocytes towards a fibroblastic phenotype during the monolayer amplificative culture (8).

To overcome these limitations, tissue engineering has emerged as a new method involving the combination of cells, scaffolds and bioactive agents to build functional new tissue in order to replace damaged cartilage (9-12).

The ideal scaffold material for cartilage tissue engineering should be one which closely mimics the natural cartilage environment in a structural, mechanical and biofunctional way (13-16). Several studies have demonstrated that chondrocyte functions differ in 2D and 3D systems (17-21) with a progressive dedifferentiation of chondrocytes in 2D culture and a prevention of this phenomenon with a 3D culture (21, 22). Given that articular cartilage is a tissue subject to considerable stress, to mimic the environments of cartilage tissue in structural terms, the fundamental structure of a scaffold must therefore be a 3D system with adequate mechanical strength.

Due to their structure incorporating many of the cues needed by cells, a great number of different natural polymers have been studied and proposed for the preparation of scaffolds for cartilage. These polymers include collagen, fibrin, chitosan, hyaluronic acid, alginate and cellulose (23-25). Unfortunately, no scaffold made from these polymers or any combination of them has so far been the ideal material for cartilage tissue engineering, lacking the adequate combination of mechanical and biological properties. In this context, an injectable, self-setting silated hydroxypropyl methylcellulose (Si-HPMC) based hydrogel has been developed previously (26, 27) and described as a suitable matrix for the 3D culture of chondrocytes *in vitro* (28) and the repair of articular cartilage *in vivo* (29). However, in spite of good biological characteristics, this scaffold has weak mechanical properties. In order to develop a biomechanically and biologically competent hydrogel for cartilage tissue engineering this Si-HPMC scaffold was reinforced with 0.67% (w/v) of a marine polysaccharide, GY785. The aims of the present work were to investigate whether or not this new scaffold, Si-HPMC/GY785, could be used for engineering cartilage. In this attempt, we first assessed the cytocompatibility of Si-HPMC/GY785 with regard to articular chondrocytes. Secondly, we evaluated its ability to allow the maintenance and recovery of a chondrocytic phenotype. Finally, the potential of Si-HPMC/GY785 associated with chondrocytes to produce cartilaginous matrix *in vivo* was preliminary evaluated in subcutaneous pockets of *nude* mice.

Materials and Methods

Materials

Hydroxypropyl methylcellulose (HPMC) E4M® was purchased from Colorcon-Down chemical (Bougival, France). GY785 EPS was produced by Seadev-FermenSys SAS (Plouzané, France) and sterilized using ethylene oxide by IONISOS (Gien, France). Hyaluronidase, actinomycin-D, trypsin/EDTA, type II collagenase (290 units/mg), HEPES (4-(2-hydroxyethyl)-1-piperazineethanesulfonic) and isopropanol were purchased from Sigma-Aldrich (St-Louis, USA). Hank's Balanced sodium salt (HBSS), DMEM 4.5 G/l glucoe), penicillin/streptomycin, L-glutamine, Trizol®, DNase I and Taq DNA polymerase were obtained from Invitrogen corporation (Paisley, UK). Methyl Tetrazolium Salt (MTS) was purchased from promega (USA). A live and dead viability/cytotoxicity kit assay was obtained from Invitrogen. Fetal calf serum (FCS) was obtained from Dominique Dutscher (Brumath, France). Cell culture plastics were purchased from Corning (VWR, France). New Zealand rabbits were obtained from Grimaud frères (Roussay, France). Monoclonal antibody against collagen type II was purchased from Oncogene (San Diego, United States). All other chemicals were from standard laboratory suppliers and were of the highest purity available.

Synthesis of Si-HPMC/GY785 hydrogel

The Si-HPMC was synthesized by grafting 0.5% of silicium in weight on to HPMC (E4M®) in heterogeneous medium, as previously described (27). Si-HPMC powder (3%, w/v) was solubilized in 0.2M NaOH under constant stirring for 48h. The solution was then sterilized by steam (121°C, 30 min). For the production of Si-HPMC/GY785, sterile GY785 polysaccharide was mixed with the sterile Si-HPMC (3% w/v) basic solution at the concentration of 10 mg/mL (1% w/v) in Si-HPMC. The resulting Si-HPMC/GY785 (3%/1% w/v) mixture was left under mild rotatory stirring for 12h to dissolve the GY785. To allow the

formation of a reticulated hydrogel, 1 volume of Si-HPMC (3% w/v) or Si-HPMC/GY785 (3%/1% w/v) solution was mixed with 0.5 volume of 0.26 M HEPES buffer as previously described (28, 30). The final products consisted of hydrogels (pH=7.4) containing Si-HPMC (2%w/v) with or without GY785 (0.67% w/v) respectively named Si-HPMC and Si-HPMC/GY785. In the same manner, a hydrogel was produced with HPMC in order to obtain a Si-HPMC/HPMC (2/0.67) hydrogel used as a control of macromolecular incorporation of GY785 in the rheological experiments.

Rheological characteristics

One ml of Si-HPMC or Si-HPMC/GY785 or Si-HPMC/HPMC were allowed to reticulate in 12-well plates. Samples were incubated at 37°C for 1h before adding 2 ml of DMEM supplemented with 10% FCS, 1% penicillin/streptomycin and 1% L-glutamine (culture medium). The plates were maintained at 37°C in a humidified atmosphere and with medium change every 2 days. After 3 weeks, oscillatory measurements were performed at 25°C on Si-HPMC, Si-HPMC/GY785 or Si-HPMC/HPMC using the Haake MARS rheometer (ThermoHaake®, Germany) with titanium plate geometry (20 mm diameter (PP20 Ti), plate with 3mm gap) with a homemade device for direct measurement inside the 12-well plates. We applied a 0.2 N normal force on the hydrogels before the measurements. The complex viscosity (η^*) was determined as a function of stress under conditions of linear viscoelastic response in the 0.1 to 5 Pa range, at a constant oscillation frequency (ω) (1 Htz). The storage (G') and loss (G'') moduli were measured within the linear viscoelastic region.

Animals and surgical procedures

All animal handling and surgical procedures were conducted according to European Community guidelines for the care and use of laboratory animals (DE 86/609/CEE).

Experiments were performed according to Good Laboratory Practices (GLP) at the Experimental Therapeutics Unit at the University of Nantes.

Isolation of rabbit articular chondrocytes (RAC)

Rabbit articular cartilage was harvested from euthanized five-week old new zealand white rabbits and RAC were isolated by enzymatic digestion as described previously (31). The suspended RAC were plated (P0) at a density of 5.10^4 cells/cm^2 in a 75 cm^2 culture flask with culture medium. The cells were maintained at 37°C in a humidified atmosphere of 5% CO_2 and the culture medium was changed every 2-3 days. Cultured RAC were passaged up to four times. RAC from passages 1, 3 and 4 were frozen in Trizol® for subsequent real-time PCR analysis.

Cytocompatibility of Si-HPMC/GY785 hydrogel

Briefly, RAC were allowed to attach in 24-well plates at a final density of 1.10^4 cells/cm^2. After 24h, the culture medium was removed and 500µl of Si-HPMC/GY785 were added to each well. Samples were incubated at 37°C for 1h before adding 1 mL of culture medium. As a control, RAC were also cultured without Si-HPMC/GY785 and Si-HPMC (CT) or in the presence of actinomycin-D (5µg/mL), an inhibitor of RNA polymerase (29), which was used as a potent inducer of cell death. After 1, 2, and 3 days, the hydrogels and culture media were removed and Cell viability was measured using an MTS assay as described elsewhere (28). Results were expressed as relative MTS activity as compared to control conditions (cells cultured without Si-HPMC/GY785 and Si/HPMC).

Cell proliferation was evaluated by Trypan blue exclusion dye experiments in conditions as described above. After each indicated time, the hydrogel and culture medium were removed and the cells were detached by adding trypsin/EDTA for 2 min. The suspended cells were

transferred into fresh culture medium and counted after Trypan blue staining. Results were expressed as the total number of living cells per well.

Three-dimensional culture of rabbit articular chondrocytes (RAC)

RAC (freshly isolated or dedifferentiated (P2)) were gently mixed with Si-HPMC/GY785 or Si-HPMC hydrogel (prepared as described previously), at a density of 1.10^6 cells/mL. Hybrid constructs were then seeded in 12-well plates (1.5 mL/well) and incubated at 37°C and 5% CO2. After 1h incubation, 2 mL of culture medium was added to each well and changed every 2-3 days. After 3 weeks, cell viability, RAC phenotype and the production of sulphated glycosaminoglycans (GAG) and type II collagen were evaluated.

Cell viability in the three-dimensional cultures was visualized using a live and dead cytotoxic assay as previously described (30). The RAC imaging was performed using a confocal laser-scanning microscope (Nikon D-eclipse C1).

Hybrid constructs associating RAC and hydrogels at 3 and 5 weeks were fixed in formol over 1h and embedded into 2% agarose solution before embedding in paraffin. Serial sections of each paraffin block (5µm thickness) were made and processed for histological staining with alcian blue and immunostained for type II collagen (anti-rabbit type II collagen 1:100) as described elsewhere (32). Immunopositive cells showed brown staining with type II collagen antibody.

For the real-time PCR analysis, total RNA was extracted using trizol® reagent in accordance with the manufacturer's instructions. After DNase I digestion, RNA was quantified using a UV-spectrophotometer (Nanodrop NND-1000, Labtech, France). One microgram of RNA per sample was reverse-transcribed using the superscript III kit in a total volume of 20µL. Complementary DNA (cDNA) was amplified in a total volume of 25µL

PCR reaction mix containing 12.5µL of Brillant® SYBR® Green Master Mix (1X) and 30nM of SYBR green reference dye. The sequence and concentration of each primer set are shown in Table 1. The real time polymerase chain reaction was carried out in a MX3000P® real-time PCR system (Stratagene) under the following conditions: 10 min at 95°C followed by 40 cycles of 30 s at 60°C and 30 s at 72°C as previously described (33). The efficiency and specificity of each primer set was confirmed with standard curves of cycle threshold (Ct) values *versus* serial dilution of total RNA and melting profile evaluation. Cycle thresholds were normalized to GAPDH to control for cDNA differences. The results are reported as fold change in gene expression relative to control conditions.

In vivo tissue formation

Implantation: To investigate whether constructs associating RAC with Si-HPMC/GY785 or Si-HPMC allow the *in vivo* formation of cartilaginous tissue, constructs were implanted into subcutaneous pockets of 4-week-old nude mice (Swiss *nude* mice, Janvier, France). 5.10^5 freshly isolated RAC were gently mixed with 250µL of Si-HPMC/GY785 or Si-HPMC hydrogel prior to reticulation and implanted subcutaneously into nude mice as previously described (29). Si-HPMC/GY785 and Si-HPMC without cells were also implanted and used as negative controls. Each condition was tested in quadruplicate and 12 animals were implanted (2 implants per animal). After 3 weeks, the mice were sacrificed and the implants were recovered and processed histologically as described earlier.

Statistical analysis

Results are expressed as mean ± SEM of triplicate determinations. The comparative studies of means were performed by using one-way ANOVA followed by a *post hoc* test with statistical significance set at $p<0.001$.

Results

Rheological characteristics

To evaluate the effect on the viscoelastic properties of Si-HPMC of adding GY785, an oscillatory measurement making it possible to evaluate the elastic modulus (G') and viscous modulus (G'') was performed. The Si-HPMC/GY785 had a G' of about 723 +/-171 Pa and a G" of about 96 +/- 37 Pa. Si-HPMC and Si-HPMC/HPMC exhibited the same G' with values of about 398 +/- 65 Pa and 324 +/- 52 Pa and G" of about 28+/-6 Pa and 22+/-5 Pa respectively.

These results indicate that Si-HPMC/GY785 hydrogel has higher rigidity than Si-HPMC and Si-HPMC/HPMC whereas Si-HPMC and Si-HPMC/HPMC have similar rigidity.

Cytocompatibilty of Si-HPMC/GY785 hydrogels

To determine whether the Si-HPMC/GY785 hydrogel was cytotoxic or not, the viability and proliferation of primary rabbit articular chondrocytes (RAC) cultured in contact with Si-HPMC/GY785 was examined through measurement of MTS activity and cell counting after 24, 48 and 72h of culture. Si-HPMC hydrogel was used as a positive control. The results (Fig. 2 A) show that Si-HPMC and Si-HPMC/GY785 did not affect the MTS activity of RAC at 24h. After 48h of culture, the presence of Si-HPMC and Si-HPMC/GY785 slightly reduced the MTS activity of RAC by respectively 20 and 30%. However, after 72h there was no significant difference between the MTS activity of RAC cultured in the presence or in the absence of the two different hydrogels. On the contrary, actinomycin-D treatment reduced the MTS activity of RAC by nearly 70% as after just 24h of treatment.

Cell counting experiments (Fig 2 B) produced similar results. After 72h, no significant difference in cell number was observed between cells cultured in contact with Si-HPMC/GY785 and cells cultured in control conditions or in contact with Si-HPMC alone.

Taken together, these results indicate that Si-HPMC/GY785 has no adverse effects on RAC viability and proliferation.

To investigate the 3-dimensional cytocompatibility of Si-HPMC/GY785, the viability of RAC in three-dimensional culture in an Si-HPMC/GY785 hydrogel was visualized using confocal microscopy after 3 weeks of culture (Fig 2 C). Cells were stained with calcein AM and “EthD-1" which respectively label living cells green and dead cells red. As shown in Fig 2C, RAC 3-dimensionally (3D) cultured in Si-HPMC/GY785 were green and organized in nodular structures as observed with RAC cultured in Si-HPMC alone. The absence of red fluorescence indicates the absence of dead cells in the Si-HHPMC/GY785. These results show that RAC retained their viability and organized into nodular structures when three-dimensionally cultured in Si-HPMC/GY785 hydrogel indicating that GY785 incorporation failed to affect the 3D cytocompatibility of Si-HPMC.

Maintenance of chondrocyte phenotype in three-dimensional cultures

To assess whether Si-HPMC/GY785 made it possible to maintain a chondrocytic phenotype in a three-dimensional culture, RAC were cultured for 3 weeks either in two dimensions (2D) without hydrogels or in three dimensions (3D) in Si-HPMC/GY785 hydrogel or Si-HPMC alone as a control. The expression of transcripts coding for type I collagen (dedifferentiation marker) and type II collagen and agrecan were evaluated with real time PCR (Fig. 3 A). 2D cultured RAC showed lower expression of type II collagen and agrecan 10- and 14.3 times lower than primary RAC (P0) respectively. In contrast to RAC cultured in 2D, RAC cultured in 3D in Si-HPMC/GY785 expressed levels of type II collagen

and agrecan transcripts that were significantly higher, approximately 5 and 19 times respectively. Likewise, RAC cultured in 3D in Si-HPMC alone exhibited an expression of type II collagen and agrecan 2 and 7 times higher than primary RAC. Whereas the expression of type I collagen in 2D RAC (fig 3A) was more than 3 times higher than that of RAC (P0), 3D cultured RAC in Si-HPMC/GY785 exhibited a barely detectable increase in type I collagen expression. RAC cultured in 3D in Si-HPMC did not show increased expression of type I collagen as compared to primary RAC (P0).

These results taken as a whole suggest that Si-HPMC/GY785 made it possible to maintain a differentiated chondrocyte-like phenotype in RAC.

To further investigate the ability of Si-HPMC/GY785 to maintain a differentiated chondrocytic phenotype, the effect of 3D culture in Si-HPMC/GY785 on sulphated GAG and type II collagen production was investigated. In this attempt, Alcian blue staining and immunostaining for type II collagen were performed on RAC cultured in 3D in Si-HPMC/GY785 or Si-HPMC for 3 weeks. Under these conditions (Figure 3 B), samples exhibited positive Alcian blue staining and type II collagen immunostaining. These results show an accumulation of sulphated GAG and type II collagen in the extracellular matrix surrounding the RAC nodules formed in 3D culture in Si-HPMC/GY785 hydrogels as observed with Si-HPMC alone. Taken together, these results indicate that Si-HPMC/GY785 hydrogel made possible the 3D culture of functionally-competent RAC able to produce type II collagen and sulphated GAG.

Dedifferentiation of RAC in 2D cultures and redifferentiation in 3D cultures

It is well known that dedifferentiated articular chondrocytes are able to retrieve a chondrocytic phenotype when replaced in a three-dimensional environment (29, 34, 35). We therefore sought to evaluate whether this phenomenon also occurs with RAC initially cultured

in 2D and thereafter placed in 3D in Si-HPMC/GY785 hydrogels. For this experiment, freshly isolated RAC were first dedifferentiated into monolayer in four passages. Expressions of transcripts coding for type I and II collagen as well as agrecan were evaluated using real time PCR (Fig. 4A). When the RAC were passaged, they showed an approximately 4-fold decrease in type II collagen expression at passage 2 (P2) and 16-fold at P4 as compared to the primary RAC (P0). Likewise, agrecan expression exhibited a 3-fold and 4.5-fold decrease after passages 2 and 4 respectively (Fig. 4A, P2, P4). On the contrary, the expression of type I collagen transcript increased dramatically about 7 times and 10 times after respectively 2 and 4 passages in monolayer cultures (Fig. 4A). These results show that the RAC underwent a dedifferentiation process as early as passage 2 (P2).

Therefore, to investigate whether Si-HPMC/GY785 allows the recovery of a chondrocytic phenotype, dedifferentiated RAC P2 were placed for an 4 additional weeks either in 3D culture in Si-HPMC/GY785 or Si-HPMC or in a 2D culture. Real-time PCR analysis revealed that after 4 weeks, the RAC cultured in 3D in Si-HPMC/GY785 exhibited a 28-fold increase in type II collagen expression and a 75-fold increase in agrecan expression as compared to the RAC P2 (Figure 4B). On the contrary, the RAC cultured in 2D for the same additional duration failed to exhibit any significant increase in type II collagen and agrecan transcripts. Interestingly, expression of the dedifferentiation marker type I collagen after 4 weeks in 3D culture in Si-HPMC/GY785 was 3.4 times less than that measured in the RAC P2 (Fig. 4B). 2D RAC exhibited a 2-fold increase in type I collagen expression as compared to RAC P2. When compared to the control hydrogel (Si-HPMC), the RAC cultured in Si-HPMC/GY785 exhibited a 2-fold increase in expression of the transcript coding for type II collagen and agrecan. These results suggest that Si-HPMC/GY785 makes it possible to recover a chondrocyte-like phenotype in previously dedifferentiated RAC.

In vivo tissue formation

To investigate whether Si-HPMC/GY785 hydrogel makes possible the formation of cartilaginous tissue *in vivo*, constructs associating freshly isolated RAC with Si-HPMC/GY785 or Si-HPMC hydrogels were implanted subcutaneously into *nude* mice. After 3 weeks, histological examinations (Fig. 5) showed the formation of chondroid nodules with RAC associated with Si-HPMC/GY785 as well as with the control hydrogel (Si-HPMC). These nodules were positively stained with Alcian blue (Fig. 5), suggesting the production of an extracellular matrix containing GAG. In addition, these nodules were positively stained for type II collagen. As a control, Si-HPMC and Si-HPMC/GY785 alone showed neither the formation of nodular structure nor the presence of an extracellular matrix (data not shown).

These results indicate that Si-HPMC/GY785 makes possible the formation of cartilaginous tissue *in vivo* with freshly isolated RAC.

Discussion

Today, regenerative medicine is moving towards the development of less and less invasive surgical techniques with the aim of reducing morbidity and hospitalisation time. From this point of view, injectable hydrogels appear to be promising (36). The main challenge in developing new hydrogels is to allow the viability, proliferation and differentiation of cells inside the hydrogel whilst also providing suitable mechanical strength. In an attempt to propose a three-dimensional scaffolding hydrogel capable of supporting regeneration of functional cartilage mechanically and biologically, we doped a self-setting hydrogel based on cellulosic derivatives (Si-HPMC) with a marine polysaccharide of high molecular weight, GY785(30). With rheological oscillatory measurement, we demonstrated that incorporating GY785 into the Si-HPMC hydrogel increased the mechanical properties of the Si-HPMC(30). Marine-based polysaccharides (37) which have structural analogies with glycosaminoglycans (GAGs), are well acknowledged as molecules influencing cell proliferation, differentiation and adhesion (38). Moreover, their structural organization confers both hydration and mechanical properties on the extracellular matrix like agrecan in articular cartilage tissue.

Determining the rheological properties of Si-HPMC/GY785, Si-HPMC and Si-HPMC/HPMC hydrogels indicates that G' was higher than G" (Fig. 1) for the three hydrogels, thereby confirming that these hydrogels are solid after 3 weeks. The G' of Si-HPMC/GY785 is approximately 2 times higher than that of Si-HPMC or Si-HPMC/HPMC, showing that doping Si-HPMC with GY785 increased its rigidity. The storage modulus G' was also linked to the network density in polysaccharide hydrogels (39). In our study, the G' value revealed a higher network density with the adjunction of GY785 polysaccharides (Fig. 1).

In order to propose a Si-HPMC/GY785 hydrogel for cartilage tissue engineering, various *in vitro* characteristics must be explored as a prerequisite to *in vivo* experiments such as cytotoxicity, capacity to support a chondrocytic phenotype (40) and the production of a cartilaginous matrix by chondrocytes.

We were therefore first interested in examining the *in vitro* cytotoxicity of Si-HPC/GY78 with rabbit primary articular chondrocytes (RAC). In this attempt, we focused on a cytotoxicity test with direct contact with RAC (ISO 10993-5: Biological evaluation of medical devices-Part 5: test for *in vitro* cytotoxicity). As previously observed with the chondrocytic cell line C28/I2 (30), our data indicate that the Si-HPMC/ GY785 hydrogel is cytocompatible with respect to RAC as evidenced by estimation of mitochondrial dehydrogenase activity (MTS assay) and cell counting (Fig. 2). In addition, the dual fluorescent staining using, calcein AM and EthD-1 reagent, revealed that RAC three-dimensionally cultured in Si-HPMC/GY785 hydrogel retained their viability and formed nodules (Fig. 3). These results indicate that the Si-HPMC/GY785 hydrogel makes possible the three-dimensional culture of RAC without altering their viability and proliferation.

It is well known that maintaining or recovering a chondrocytic phenotype in a scaffolding hydrogel is a key point for cartilage tissue engineering strategies. Dedifferentiation of chondrocytes, evidenced by a concomitant decrease in type II collagen and agrecan expression and an increase in type I collagen expression, effectively occurs during *in vitro* 2D expansion into a monolayer (20, 41). In our hands and according to this dedifferentiation process (42), type II collagen and agrecan expressions were down-regulated along with passages in RAC, whereas that of type I collagen increased. However, culturing chondrocytes in three-dimensional scaffolds has been shown to not only prevent, but even to reverse, this phenomenon, allowing dedifferentiated chondrocytes to recover their phenotype (19). Accordingly, the expressions of type II collagen and agrecan are maintained in 3D cultures in

Si-HPMC/GY785, highlighting the ability of Si-HPMC/GY785 to maintain a chondrocyte-like phenotype *in vitro*. These results were further confirmed by the production of GAG and collagen type II by three-dimensionally cultured RAC in the Si-HPMC/GY785 hydrogel. In addition, the Si-HPMC/GY785 hydrogel could also induce the recovery of a chondrocytic phenotype of previously dedifferentiated RAC (P2) as evidenced by the increased expression of type II collagen and agrecan while expression of type I collagen remained stable. It therefore seems reasonable to speculate that Si-HPMC/GY785 make possible the three-dimensional culture and recovery of phenotypically stable chondrocytes.

To address the *in vivo* potential of Si-HPCM/GY785 as a new hydrogel for cartilage engineering, we finally embarked on preliminary animal experiment in a well-documented model of tissue engineering, the subcutis of nude mice. Hybrid systems associating chondrocytes (RAC) with Si-HPMC/GY785 were implanted into subcutaneous sites in the backs of *nude* mice. Si-HPMC associated with RAC was used as a control. After 3 weeks of implantation, constructs associating RAC with Si-HPMC/GY785 showed the formation of nodules with an extracellular matrix containing sulphated GAG and type II collagen. Moreover, no significant difference was observed in relation to hydrogel composition.

Conclusions

In conclusion, our results show that Si-HPMC doped with a marine polysaccharide has increased mechanical properties and is a convenient scaffold for the three-dimensional culture of chondrocytes. This mechanically-reinforced hydrogel makes it possible to grow phenotypically stable chondrocytes, capable of synthesizing cartilage-like ECM *in vitro* and *in vivo*. Our results as a whole strongly suggest that GY785-doped Si-HPMC may be a promising scaffold for cartilage tissue engineering. Whether this new scaffolding hydrogel is

clinically relevant for the treatment of articular cartilage will be given further attention in adapted animal models of full thickness cartilage defects.

Acknowledgements

E.R. received a fellowship from the "Region *Pays de la Loire"*, through the Bioregos grant. This study was supported by grants from the ANR TecSan "chondrograft", the Arthritis Fondation Courtin and the "Société Française de Rhumatologie". The authors would also like to thank C. Colombeix, C. Sinquin and J. Ratiskol.

References:

1. Steinert, A.F., S.C. Ghivizzani, A. Rethwilm, R.S. Tuan, C.H. Evans, and U. Noth, Major biological obstacles for persistent cell-based regeneration of articular cartilage, Arthritis Res Ther, 9, 213, 2007.
2. Hardingham, T.E. and A.J. Fosang, The structure of aggrecan and its turnover in cartilage, J Rheumatol Suppl, 43, 86, 1995.
3. Aigner, T. and J. Stove, Collagens--major component of the physiological cartilage matrix, major target of cartilage degeneration, major tool in cartilage repair, Adv Drug Deliv Rev, 55, 1569, 2003.
4. Caplan, A.I., M. Elyaderani, Y. Mochizuki, S. Wakitani, and V.M. Goldberg, Principles of cartilage repair and regeneration, Clin Orthop Relat Res, 254, 1997.
5. Lindahl, A., M. Brittberg, and L. Peterson, Cartilage repair with chondrocytes: clinical and cellular aspects, Novartis Found Symp, 249, 175, 2003.
6. Buckwalter, J.A., Articular cartilage: injuries and potential for healing, J Orthop Sports Phys Ther, 28, 192, 1998.
7. Brittberg, M., A. Lindahl, A. Nilsson, C. Ohlsson, O. Isaksson, and L. Peterson, Treatment of deep cartilage defects in the knee with autologous chondrocyte transplantation, N Engl J Med, 331, 889, 1994.
8. Bonaventure, J., N. Kadhom, L. Cohen-Solal, K.H. Ng, J. Bourguignon, C. Lasselin, and P. Freisinger, Reexpression of cartilage-specific genes by dedifferentiated human articular chondrocytes cultured in alginate beads, Exp Cell Res, 212, 97, 1994.
9. Getgood, A., R. Brooks, L. Fortier, and N. Rushton, Articular cartilage tissue engineering: today's research, tomorrow's practice?, J Bone Joint Surg Br, 91, 565, 2009.
10. van Osch, G.J., M. Brittberg, J.E. Dennis, Y.M. Bastiaansen-Jenniskens, R.G. Erben, Y.T. Konttinen, and F.P. Luyten, Cartilage repair: past and future--lessons for regenerative medicine, J Cell Mol Med, 13, 792, 2009.

11. Vinatier, C., C. Bouffi, C. Merceron, J. Gordeladze, J.M. Brondello, C. Jorgensen, P. Weiss, J. Guicheux, and D. Noel, Cartilage tissue engineering: towards a biomaterial-assisted mesenchymal stem cell therapy, Curr Stem Cell Res Ther, 4, 318, 2009.
12. Chung, C. and J.A. Burdick, Engineering cartilage tissue, Adv Drug Deliv Rev, 60, 243, 2008.
13. Lynn, A.K., R.A. Brooks, W. Bonfield, and N. Rushton, Repair of defects in articular joints. Prospects for material-based solutions in tissue engineering, J Bone Joint Surg Br, 86, 1093, 2004.
14. Stoop, R., Smart biomaterials for tissue engineering of cartilage, Injury, 39 Suppl 1, S77, 2008.
15. Bonzani, I.C., J.H. George, and M.M. Stevens, Novel materials for bone and cartilage regeneration, Curr Opin Chem Biol, 10, 568, 2006.
16. Griffith, L.G. and G. Naughton, Tissue engineering--current challenges and expanding opportunities, Science, 295, 1009, 2002.
17. Hauselmann, H.J., R.J. Fernandes, S.S. Mok, T.M. Schmid, J.A. Block, M.B. Aydelotte, K.E. Kuettner, and E.J. Thonar, Phenotypic stability of bovine articular chondrocytes after long-term culture in alginate beads, J Cell Sci, 107 (Pt 1), 17, 1994.
18. Kimura, T., N. Yasui, S. Ohsawa, and K. Ono, Chondrocytes embedded in collagen gels maintain cartilage phenotype during long-term cultures, Clin Orthop Relat Res, 231, 1984.
19. Benya, P.D. and J.D. Shaffer, Dedifferentiated chondrocytes reexpress the differentiated collagen phenotype when cultured in agarose gels, Cell, 30, 215, 1982.
20. Brodkin, K.R., A.J. Garcia, and M.E. Levenston, Chondrocyte phenotypes on different extracellular matrix monolayers, Biomaterials, 25, 5929, 2004.
21. Mukaida, T., K. Urabe, K. Naruse, J. Aikawa, M. Katano, S.H. Hyon, and M. Itoman, Influence of three-dimensional culture in a type II collagen sponge on primary cultured and dedifferentiated chondrocytes, J Orthop Sci, 10, 521, 2005.

22. Dehne, T., R. Schenk, C. Perka, L. Morawietz, A. Pruss, M. Sittinger, C. Kaps, and J. Ringe, Gene expression profiling of primary human articular chondrocytes in high-density micromasses reveals patterns of recovery, maintenance, re- and dedifferentiation, Gene, 462, 8, 2010.

23. Puppi, D., F. Chiellini, A.M. Piras, and E. Chiellini, Polymeric materials for bone and cartilage repair, Progress in Polymer Science, 35, 403, 2010.

24. Mano, J.F., G.A. Silva, H.S. Azevedo, P.B. Malafaya, R.A. Sousa, S.S. Silva, L.F. Boesel, J.M. Oliveira, T.C. Santos, A.P. Marques, N.M. Neves, and R.L. Reis, Natural origin biodegradable systems in tissue engineering and regenerative medicine: present status and some moving trends, J R Soc Interface, 4, 999, 2007.

25. Hubbell, J.A., Materials as morphogenetic guides in tissue engineering, Curr Opin Biotechnol, 14, 551, 2003.

26. Bourges, X., P. Weiss, A. Coudreuse, G. Daculsi, and G. Legeay, General properties of silated hydroxyethylcellulose for potential biomedical applications, Biopolymers, 63, 232, 2002.

27. Bourges, X., P. Weiss, G. Daculsi, and G. Legeay, Synthesis and general properties of silated-hydroxypropyl methylcellulose in prospect of biomedical use, Advances in Colloid and Interface Science, 99, 215, 2002.

28. Vinatier, C., D. Magne, P. Weiss, C. Trojani, N. Rochet, G.F. Carle, C. Vignes-Colombeix, C. Chadjichristos, P. Galera, G. Daculsi, and J. Guicheux, A silanized hydroxypropyl methylcellulose hydrogel for the three-dimensional culture of chondrocytes, Biomaterials, 26, 6643, 2005.

29. Vinatier, C., D. Magne, A. Moreau, O. Gauthier, O. Malard, C. Vignes-Colombeix, G. Daculsi, P. Weiss, and J. Guicheux, Engineering cartilage with human nasal chondrocytes and a silanized hydroxypropyl methylcellulose hydrogel, J Biomed Mater Res A, 80, 66, 2007.

30. Rederstorff, E., P. Weiss, S. Sourice, P. Pilet, F. Xie, C. Sinquin, S. Colliec-Jouault, J. Guicheux, and S. Laib, An in vitro study of two GAG-like marine polysaccharides incorporated into injectable hydrogels for bone and cartilage tissue engineering, Acta Biomater, 7, 2119, 2011.

31. Ghayor, C., J.F. Herrouin, C. Chadjichristos, L. Ala-Kokko, M. Takigawa, J.P. Pujol, and P. Galera, Regulation of human COL2A1 gene expression in chondrocytes. Identification of C-Krox-responsive elements and modulation by phenotype alteration, J Biol Chem, 275, 27421, 2000.

32. Merceron, C., S. Portron, M. Masson, J. Lesoeur, B.H. Fellah, O. Gauthier, O. Geffroy, P. Weiss, J. Guicheux, and C. Vinatier, Chondrogenic potential of differentially cultured human adiposed-derived stem cells after transplantation with a cellulose hydrogel, Cell Transplant, in press, 2011.

33. Merceron, C., C. Vinatier, S. Portron, M. Masson, J. Amiaud, L. Guigand, Y. Cherel, P. Weiss, and J. Guicheux, Differential effects of hypoxia on osteochondrogenic potential of human adipose-derived stem cells, Am J Physiol Cell Physiol, 298, C355, 2010.

34. Chen, G., T. Sato, T. Ushida, R. Hirochika, and T. Tateishi, Redifferentiation of dedifferentiated bovine chondrocytes when cultured in vitro in a PLGA-collagen hybrid mesh, FEBS Lett, 542, 95, 2003.

35. Miot, S., T. Woodfield, A.U. Daniels, R. Suetterlin, I. Peterschmitt, M. Heberer, C.A. van Blitterswijk, J. Riesle, and I. Martin, Effects of scaffold composition and architecture on human nasal chondrocyte redifferentiation and cartilaginous matrix deposition, Biomaterials, 26, 2479, 2005.

36. Cushing, M.C. and K.S. Anseth, Materials science. Hydrogel cell cultures, Science, 316, 1133, 2007.

37. Colliec-Jouault, S., P. Zanchetta, D. Helley, J. Ratiskol, C. Sinquin, A.M. Fischer, and J. Guezennec, Les polysaccharides microbiens d'origine marine et leur potentiel en thérapeutique humaine, Pathologie Biologie, 52, 127, 2004.

38. Chiu, L.H., S.C. Chen, K.C. Wu, C.B. Yang, C.L. Fang, W.F. Lai, and Y.H. Tsai, Differential effect of ECM molecules on re-expression of cartilaginous markers in near quiescent human chondrocytes, J Cell Physiol, 226, 1981, 2011.

39. Moe, S.T., K.I. Draget, G. Skjåk-Bræk, and O. Simdsrød, Temperature dependence of the elastic modulus of alginate gels, Carbohydrate Polymers, 19, 279, 1992.

40. Pereira, R.C., C. Gentili, R. Cancedda, H.S. Azevedo, and R.L. Reis, Encapsulation of human articular chondrocytes into 3D hydrogel: phenotype and genotype characterization, Methods Mol Biol, 695, 167, 2010.

41. Schnabel, M., S. Marlovits, G. Eckhoff, I. Fichtel, L. Gotzen, V. Vecsei, and J. Schlegel, Dedifferentiation-associated changes in morphology and gene expression in primary human articular chondrocytes in cell culture, Osteoarthritis Cartilage, 10, 62, 2002.

42. Mandl, E.W., S.W. van der Veen, J.A. Verhaar, and G.J. van Osch, Multiplication of human chondrocytes with low seeding densities accelerates cell yield without losing redifferentiation capacity, Tissue Eng, 10, 109, 2004.

Figure legends:

Table 1: Sequences of primer pairs, gene bank accession numbers used for real time RT-PCR analysis and size of PCR products

Figure 1: Oscillatory measurements. Oscillatory measurements of the different hydrogels (Si-HPMC, Si-HPMC/HPMC (2/0.67) and Si-HPMC/GY785 (2/0.67)) after 3 weeks of storage at 37°C in a humid environment. Measurements (n=3) were made directly in 12 multi-well culture plates using a ThermoHaake®, (Germany, Mars™, Titanium plate PP20Ti) with the following parameters: gap ≈3mm, normal force 0.2N, 1 Htz, from 0.1 to 5 Pa, at 25°C. The conservative modulus G' and loss modulus G" are shown in Pa. *p<0.001 compared with the respective controls Si-HPMC and Si-HPMC/HPMC.

Figure 2: Cytocompatibility of Si-HPMC/GY785 with RAC in two-dimensional culture (2D) and three-dimensional culture (3D). Rabbit articular chondrocytes (RAC) were cultured in 2D on culture plates over 72h without hydrogel (positive control) or with actinomycin-D (5µg/ml) (negative control) or with Si-HPMC (2/0) or Si-HPMC/GY785 (2/0.67). **A**) Viability was assessed by MTS activity as indicated in the materials and methods. Results are expressed as relative MTS activity compared with the respective controls. *p<0.001 as compared to control conditions. **B**) Proliferation was assessed by scoring the cells after trypan blue staining. Results are expressed as the total number of cells per well. *p <0.001 compared with the respective controls. **C)** RAC were cultured in 3D for 3 weeks in Si-HPMC/GY785 (2/0.67) or Si-HPMC (2/0) prior to staining with calcein AM and EthD-1. Viability was visualized using confocal microscopy as indicated in the materials and methods. Scale length: 50 µm.

Figure 3: **A) maintenance of chondrocyte phenotype in three-dimensional culture.** Total RNA was purified from freshly isolated RAC (P0), from RAC cultured in two dimensions (2D) and RAC cultured in 3D for 3 weeks (3D) in Si-HPMC/GY785 or Si-HPMC. Expression of the chondrocytic markers (type II collagen and agrecan) as well as the dedifferentiation marker (Type I collagen) were investigated using real-time PCR as indicated in the materials and methods. Results are expressed as relative expression levels compared to the control conditions (P0). **B) Cartilaginous matrix production by RAC in three-dimensional culture.** Rabbit articular chondrocytes were cultured for 3 and 5 weeks in three dimensions (3D) in Si-HPMC/GY785 (2/0.67) and Si-HPMC (2/0). Alcian blue and immunohistochemical type II collagen stainings were carried out as detailed in the materials and methods. Samples were observed with a light microscope. Scale length: 50µm.

Figure 4: **A) Dedifferentiation of RAC in monolayer culture.** Total RNA was purified from freshly isolated RAC (P0), from RAC cultured in two dimensions for 2 (P2) and 4 (P4) passages. Real time PCR analysis for type II collagen and agrecan as well as type I collagen transcripts were performed using the primers and conditions detailed in the experimental procedures. Results are expressed as relative expression levels compared to the control conditions P0. * $p<0.001$ compared to RAC (P0). **B) Redifferentiation of RAC in three-dimensional culture.** Total RNA was purified from dedifferentiated RAC at passage 2 (P2) and from dedifferentiated RAC cultured for an additional time of 4 weeks (P2 4w) in Si-HPMC/GY785 (2/0.67) and Si-HPMC (2/0). Real time PCR analysis for type II and I collagen transcripts, as well as agrecan, were carried out using the primers and conditions detailed in the experimental procedures. Results are expressed as relative expression levels compared to the control conditions (P2). * $p<0.001$ compared to P2.

Figure 5: Histochemical analysis of tissue engineered cartilage. RAC associated with GY785/Si-HPMC or Si-HPMC were implanted subcutaneously into nude mice and analyzed 3 weeks later. Histological sections were stained, as described in the materials and methods, for the presence of GAG (Alcian blue) and type II collagen (Immunostaining). Samples were observed with a light microscope. Scale length: 50µm.

Gene	GeneBank	Forward primer	Reverse primer	Amplicon size
Glyceraldehyde 3 phosphate deshydrogenase (Gapdh)	NM_001082253	5′-agaacgggaagctggtcat-3′	5′-ttgatgttggcgggatct-3′	70 bp
Agrecan (Acan)	L38480.	5′-gaggatggcttccaccagt-3′	5′-tggggtacctgacagtctga-3′	61 bp
Type I collagen, chain α1 (Col1a1)	D49399.	5′-agcgatggtcctccaggt-3′	5′-gccagggtaaccacgttct-3′	63 bp
Type II collagen chain α1 (Col2a1)	D83228	5′-acagcaggttcacctataccg-3′	5′-cccacttaccggtgtgtttc-3′	60 bp

Table 1: Sequences of primer pairs, gene bank accession numbers used for real time RT-PCR analysis and size of PCR products
202x61mm (300 x 300 DPI)

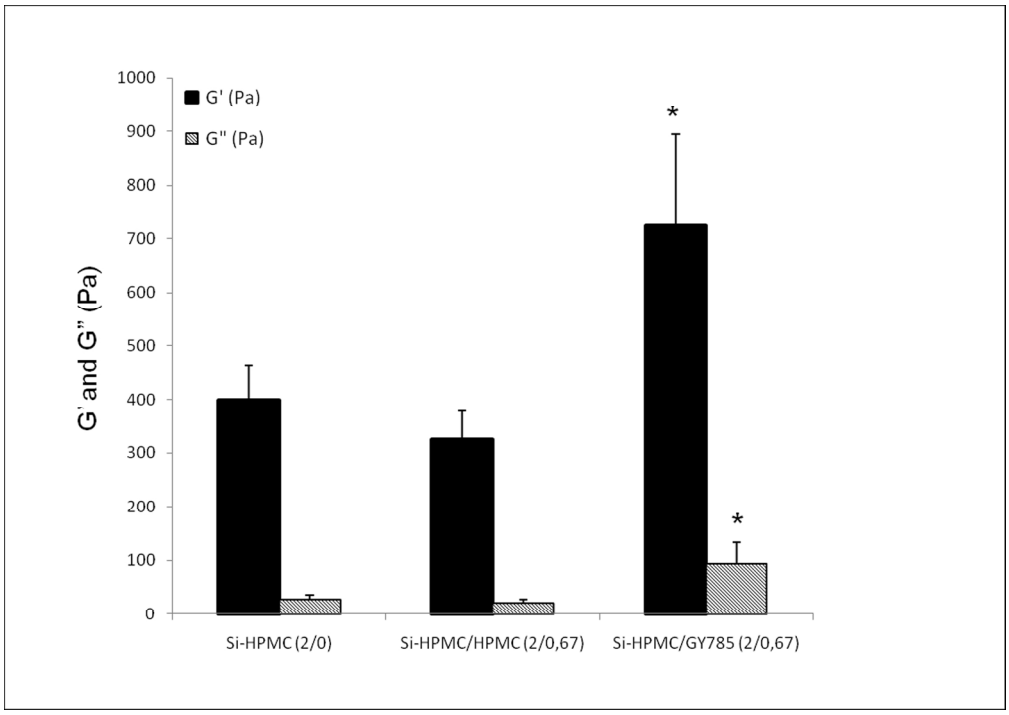

Figure 1: Oscillatory measurements. Oscillatory measurements of the different hydrogels (Si-HPMC, Si-HPMC/HPMC (2/0.67) and Si-HPMC/GY785 (2/0.67)) after 3 weeks of storage at 37°C in a humid environment. Measurements (n=3) were made directly in 12 multi-well culture plates using a ThermoHaake®, (Germany, Mars™, Titanium plate PP20Ti) with the following parameters: gap ≈3mm, normal force 0.2N, 1 Htz, from 0.1 to 5 Pa, at 25°C. The conservative modulus G' and loss modulus G" are shown in Pa. *p<0.001 compared with the respective controls Si-HPMC and Si-HPMC/HPMC.
190x134mm (300 x 300 DPI)

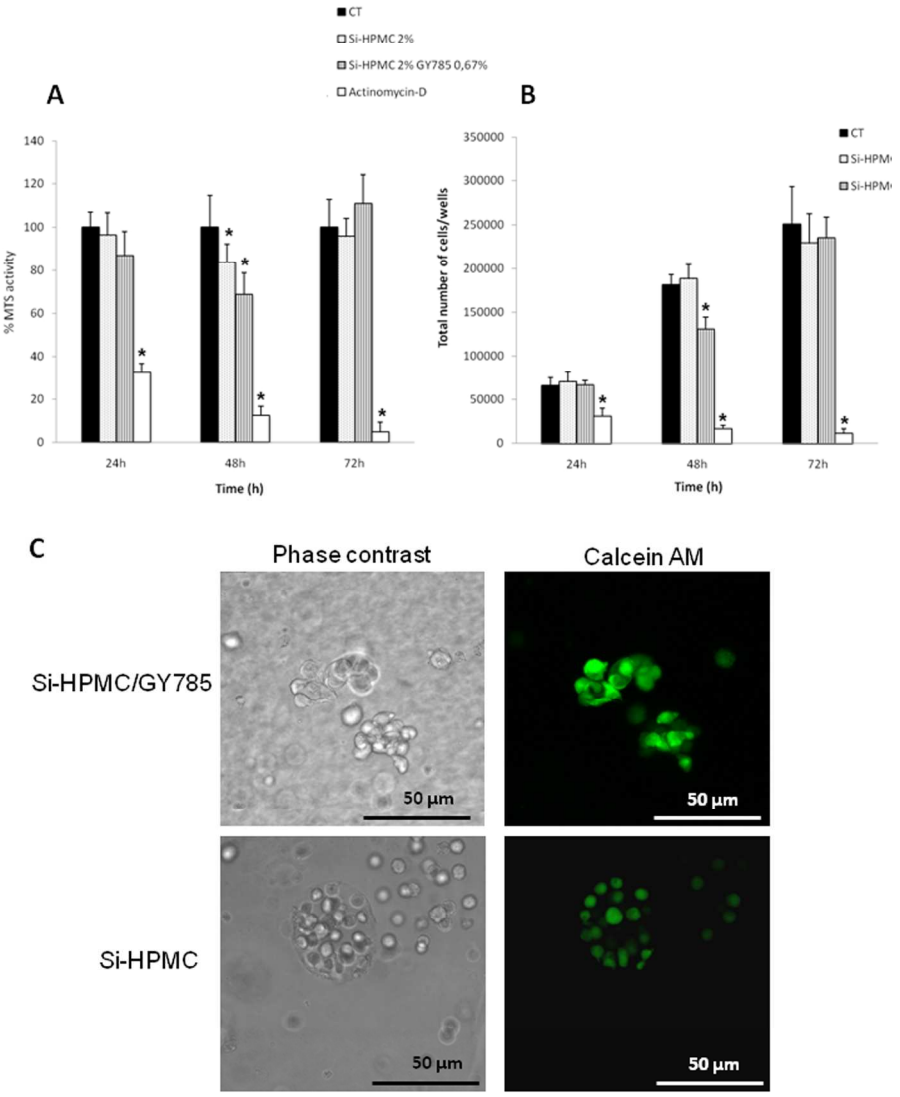

Figure 2: Cytocompatibility of Si-HPMC/GY785 with RAC in two-dimensional culture (2D) and three-dimensional culture (3D). Rabbit articular chondrocytes (RAC) were cultured in 2D on culture plates over 72h without hydrogel (positive control) or with actinomycin-D (5µg/ml) (negative control) or with Si-HPMC (2/0) or Si-HPMC/GY785 (2/0.67). A) Viability was assessed by MTS activity as indicated in the materials and methods. Results are expressed as relative MTS activity compared with the respective controls. *p<0.001 as compared to control conditions. B) Proliferation was assessed by scoring the cells after trypan blue staining. Results are expressed as the total number of cells per well. *p <0.001 compared with the respective controls. C) RAC were cultured in 3D for 3 weeks in Si-HPMC/GY785 (2/0.67) or Si-HPMC (2/0) prior to staining with calcein AM and EthD-1. Viability was visualized using confocal microscopy as indicated in the materials and methods. Scale length: 50 µm.
190x254mm (300 x 300 DPI)

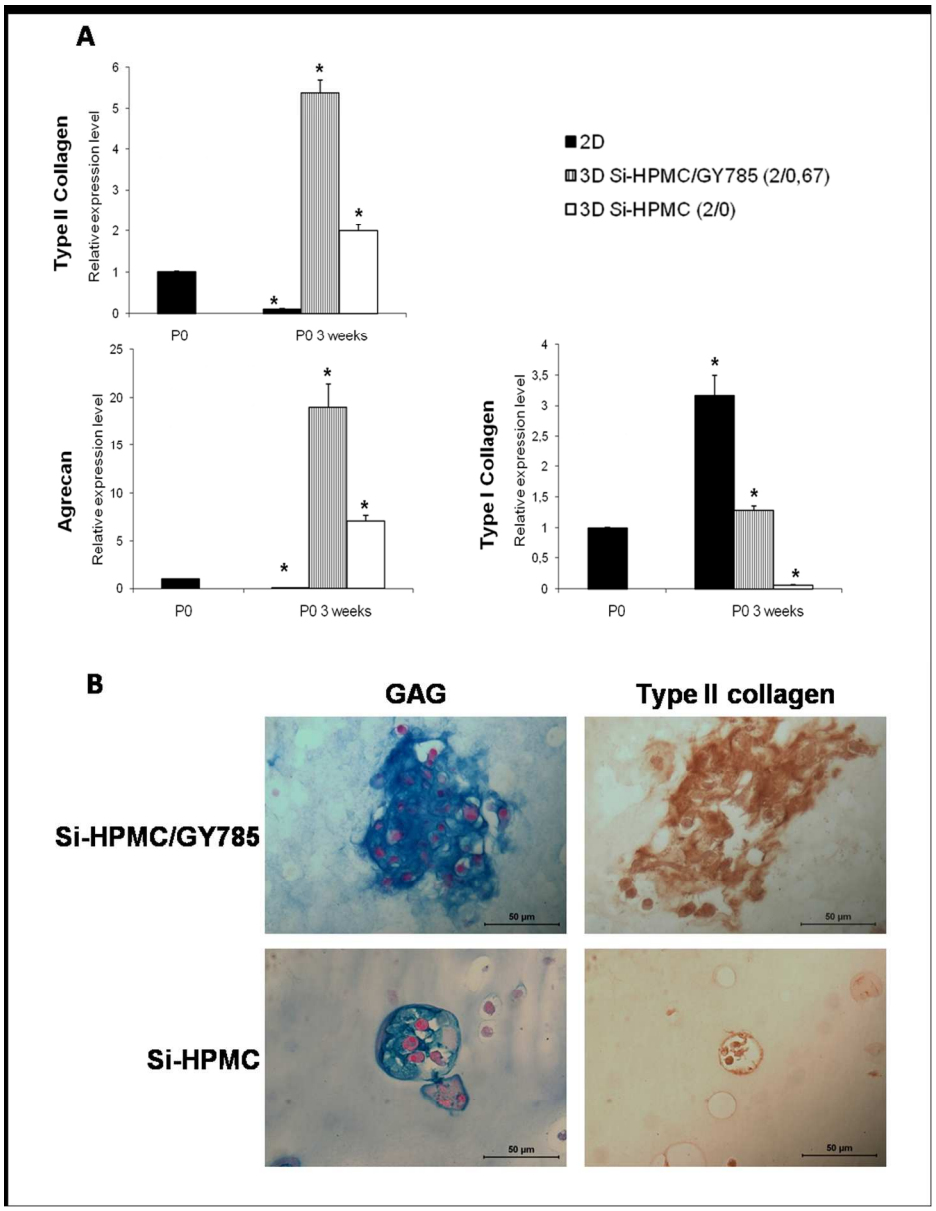

Figure 3: A) maintenance of chondrocyte phenotype in three-dimensional culture. Total RNA was purified from freshly isolated RAC (P0), from RAC cultured in two dimensions (2D) and RAC cultured in 3D for 3 weeks (3D) in Si-HPMC/GY785 or Si-HPMC. Expression of the chondrocytic markers (type II collagen and agrecan) as well as the dedifferentiation marker (Type I collagen) were investigated using real-time PCR as indicated in the materials and methods. Results are expressed as relative expression levels compared to the control conditions (P0). B) Cartilaginous matrix production by RAC in three-dimensional culture. Rabbit articular chondrocytes were cultured for 3 and 5 weeks in three dimensions (3D) in Si-HPMC/GY785 (2/0.67) and Si-HPMC (2/0). Alcian blue and immunohistochemical type II collagen stainings were carried out as detailed in the materials and methods. Samples were observed with a light microscope. Scale length: 50µm.
191x248mm (300 x 300 DPI)

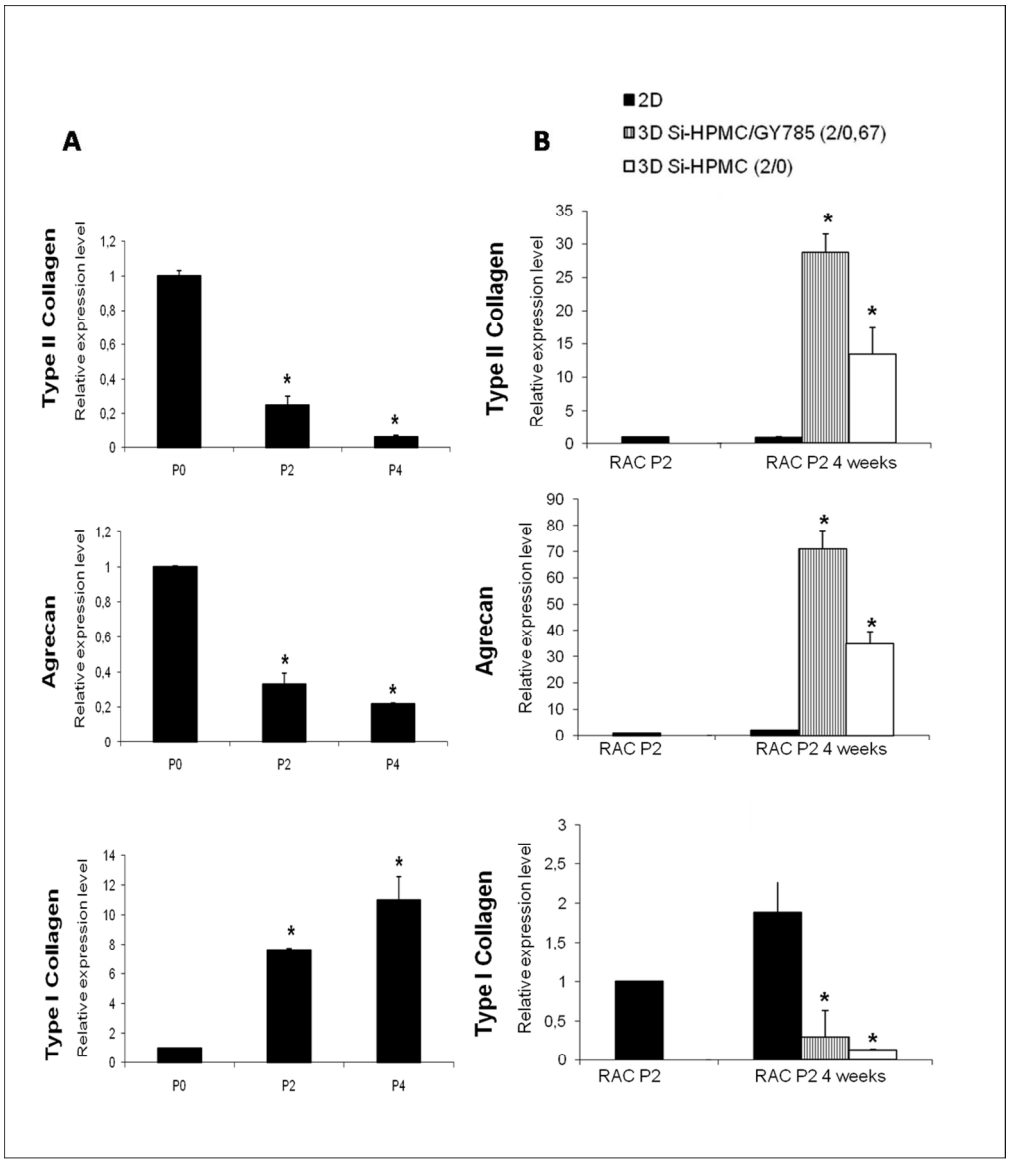

Figure 4: A) Dedifferentiation of RAC in monolayer culture. Total RNA was purified from freshly isolated RAC (P0), from RAC cultured in two dimensions for 2 (P2) and 4 (P4) passages. Real time PCR analysis for type II collagen and agrecan as well as type I collagen transcripts were performed using the primers and conditions detailed in the experimental procedures. Results are expressed as relative expression levels compared to the control conditions P0. * $p<0.001$ compared to RAC (P0). B) Redifferentiation of RAC in three-dimensional culture. Total RNA was purified from dedifferentiated RAC at passage 2 (P2) and from dedifferentiated RAC cultured for an additional time of 4 weeks (P2 4w) in Si-HPMC/GY785 (2/0.67) and Si-HPMC (2/0). Real time PCR analysis for type II and I collagen transcripts, as well as agrecan, were carried out using the primers and conditions detailed in the experimental procedures. Results are expressed as relative expression levels compared to the control conditions (P2). * $p<0.001$ compared to P2.
208x240mm (300 x 300 DPI)

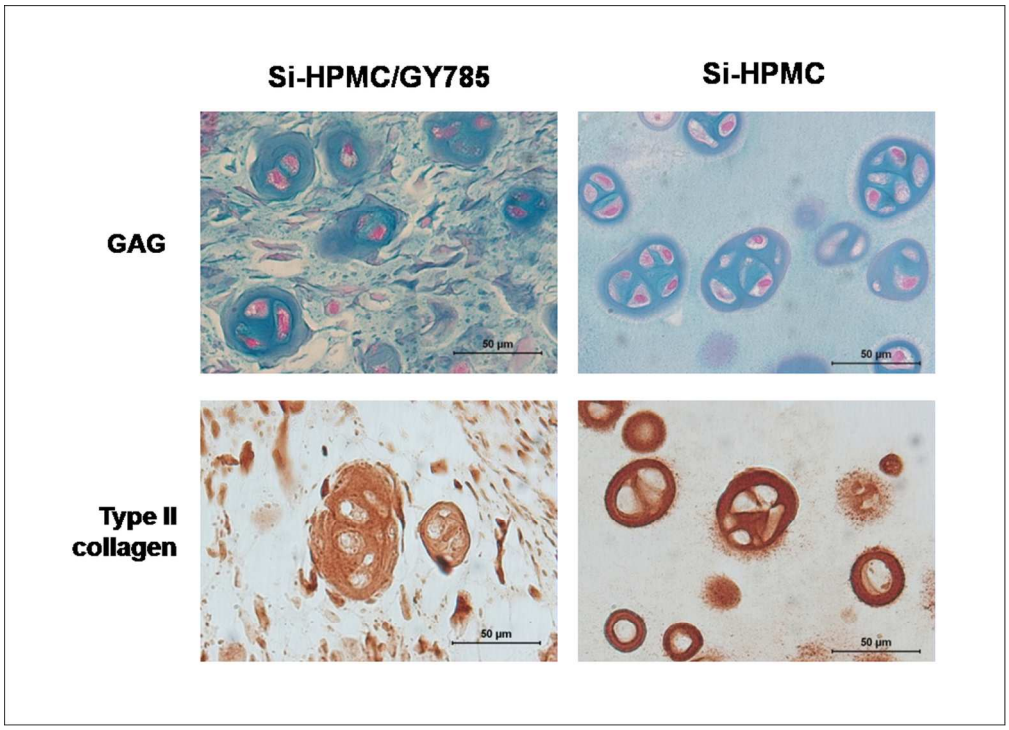

Figure 5: Histochemical analysis of tissue engineered cartilage. RAC associated with GY785/Si-HPMC or Si-HPMC were implanted subcutaneously into nude mice and analyzed 3 weeks later. Histological sections were stained, as described in the materials and methods, for the presence of GAG (Alcian blue) and type II collagen (Immunostaining). Samples were observed with a light microscope. Scale length: 50µm.
190x137mm (300 x 300 DPI)

SILYLATED BIOMOLECULE-BASED HYDROGEL FOR CULTURING CARDIOMYOCYTES AND STEM CELLS, AND USE OF THE HYDROGEL THEREOF FOR TREATING HEART FAILURE

The present invention relates to the use of an hydrogel comprising silylated biomolecule for the three-dimensional culture of cardiomyocytes or stem cells which are able to differentiate into cardiomyocytes, and to an aqueous composition comprising i) cardiomyocytes or stem cells which are able to differentiate into cardiomyocytes, and ii) a hydrogel comprising silylated biomolecule, for use for treating heat failure, in particular heart failure following myocardial infarction.

BACKGROUND OF THE INVENTION

Heart disease, especially myocardial infarction, is a leading cause of morbidity and mortality worldwide. Myocardial infarction is an absolute medical emergency whose incidence remains high with 120,000 cases per year in France. According to WHO data, on 50 million annual deaths worldwide, ischemic heart disease are the leading cause of death with 7.2 million deaths from coronary heart diseases. In France, MI prognosis remains poor, (10 to 12% of total annual mortality in adults). In addition, a significant morbidity and socio-economic should be also considered. Following MI, left ventricular remodeling includes early and progressive extracellular matrix degradation, infarct zone expansion, scar thinning, and eventually transition to heart failure (Cohn, et al., 2000; Jugdutt, 2003).

Current antiremodeling therapies are clearly limited, because many ventricles continue to enlarge (Bolognese et al., 2007; Savoye et al., 2006) and morbidity and mortality remain high (Verma et al., 2008). Pharmacological treatments currently available can only delay the progression to end-stage heart failure.

Heart transplantation remains the most effective management of the most severely affected patients, but the shortage of donor organs and complications associated with this intervention limits this approach. Further, lifelong immune suppression often causes serious complications.

Because the dominant cause of heart failure is loss of myocardium as a result of infarction and the limited regeneration potential of cardiomyocytes in mammals, cell therapy may provide a novel therapeutic option to modify left ventricular remodeling processes and prevent post-infarction heart failure. Thus, in recent years, the possibility of using cell transplantation for cardiac repairs has become the focus of intense research. Multiple cell types have been considered for such therapies, including skeletal myoblasts,

bone marrow-derived haematopoietic stem cells, mesenchymal stem cells, intrinsic cardiac stem cells (CSCs), embryonic stem cells (ESCs) and induced pluripotent stem (iPS) cells.

Conventional administration techniques use intramyocardial injections of suspended cells in culture medium. However, this technique is plagued by limited cell retention and survival. Several studies showed that more than 80%–90% of grafted cells die within 72 hours after injection into myocardium (Toma *et al*., Circulation, 105: 93-98, 2002; Maurel *et al*., Transplantation, 80: 660-665, 2005). Further, it was reported that approximately 90% of the cells delivered through a needle were lost to the circulation or leaked out of the injection site (Leor *et al*., Circulation, 102: 11156-61, 2000).

In addition, cell-seeded grafts have been proposed for *in vitro* cardiac tissue growth and subsequent in vivo transplantation. These grafts can consist of embryonic or neonatal cardiomyocytes seeded in three-dimensional scaffolds; the cardiac myocytes cultured in these scaffolds can spatially organize and differentiate into myocardium-like 3-dimensional tissue. These results suggest that cell therapy and tissue engineering of myocardium have potential for myocardial regeneration or replacement. However, current approaches to cardiac regeneration face important challenges. Recipient ischemic tissue may be inadequate for donor cell retention in sufficient quantity to allow for the desired effect, because the survival of cells from any source implanted in the myocardium varies between 1% and 10%. Also, nonspecific delivery of donor cells to other body sites constitutes an unwanted potential side effect.

A particularly useful approach to cardiac regeneration would be a method that could employ injection into the injured area in a manner similar to cell injection therapy (rather than surgical implantation of myocardium-like volume) and that would provide a suitable growth environment for cardiomyocytes.

In recent years, several types of biomaterials, mainly natural proteins, were used in the injectable cardiac tissue engineering, such as fibrin, alginate, matrigel, collagen and chitosan (see for review Wang *et al*., J. Cell. Mol. Med., 14(5): 1044-1055, 2010).

However, use of natural materials extracted from biological samples is associated with a major risk of microbial transmission, essentially virus transmission. Drawbacks associated with natural materials have prompted the inventors to develop synthetic materials for injectable cardiac tissue engineering.

The inventors had previously developed a silylated hydrogel as a culture matrix for three-dimensional culture of chondrocytes for use for regenerating *in vivo* cartilaginous tissues (application US 2007/0212389).

However, in view of the great difference between cartilaginous tissue and cardiac tissue, respectively hard and soft tissues, and of the physiological differences between chondrocytes and cardiomyocytes, the latter needing to retain contractile ability to be functional, it was not expected that silylated hydrogel is also usable for culturing functional cardiomyocytes.

DESCRIPTION OF THE INVENTION

The inventors have now found that a reticulated hydrogel comprising a silylated biomolecule able to form a pH-dependent self-reticulating hydrogel can be used for the three-dimensional culture of cardiomyocytes, or of stem cells which are able to differentiate into cardiomyocytes.

The inventors have also shown that this hydrogel comprising stem cells, in particular mesenchymal stem cells, once injected into the heart, in particular into left ventricle, has a cardioprotective effect.

The inventors have also shown the tolerability and cytocompatibility of silylated biomolecule hydrogel, in particluar Si-HPMC hydrogel, with cardiomyocytes, and its ability to maintain a cardiomyocyte phenotype and to allow physiological cardiomyocyte contractility. Results *in vivo* also showed that cells maintained their viability and that hydrogel of the invention had no adverse effect on cardiac tissue.

The inventors have also demonstrated that use of hydrogel comprising a silylated biomolecule comprising stem cells able to differentiate into cardiomyocytes, or mesenchymal stem cells, rapidly improves cardidac function and preserves long term cardiac function. Further, transplantation of hydrogel comprising a silylated biomolecule comprising stem cells decreases the infarct expansion, which indicates that this combination is capable of preventing negative left ventricular remodeling after myocardial infarction.

Therefore, a first aspect of the present invention relates to the use of a hydrogel comprising silylated biomolecules, for the three-dimensional culture of cardiomyocytes or stem cells which are able to differentiate into cardiomyocytes.

In a preferred embodiment, the cultured cells are cardiomyocytes.

Preferably, the hydrogel comprising silylated biomolecules is able to form a pH-dependent self-reticulating hydrogel at physiological pH (i.e. with a pH value from about 7.2 to about 7.6).

A second aspect of the invention is a method of culturing cardiomyocytes or stem cells which are able to differentiate into cardiomyocytes, comprising the *ex vivo* mixing of said cells with a hydrogel comprising silylated biomolecules at an appropriate pH for forming the hydrogel. Preferably, the pH of the hydrogel comprising silylated biomolecules is a physiological pH (pH from about 7.2 to about 7.6). In a preferred embodiment, the cultured cells are cardiomyocytes.

A third aspect of the invention relates to a method of treating heat failure, in particular heart failure following myocardial infarction, including administration by injection into myocardium of an aqueous composition, preferably at a physiological pH (pH from about 7.2 to about 7.6), said composition comprising:

i) cardiomyocytes or stem cells which are able to differentiate into cardiomyocytes; and

ii) a hydrogel solution, preferably at physiological pH (pH from about 7.2 to about 7.6), comprising silylated biomolecule.

A fourth aspect of the invention concerns an aqueous composition, preferably at a physiological pH (pH from about 7.2 to about 7.6) which comprises:

i) cardiomyocytes or stem cells which are able to differentiate into cardiomyocytes; and

ii) a hydrogel solution, preferably at physiological pH (pH from about 7.2 to about 7.6), comprising silylated biomolecule;

for use for treating heat failure, in particular heart failure following myocardial infarction.

To carry out the method of treating heat failure and medical application according to the third and fourth aspects of the invention, the aqueous composition will preferably be injectable (i.e. liquid or at least semi-liquid form, and not totally gelified). The man skilled in the art can easily determine the appropriate moment when said aqueous composition is suitable for being administrated (or used for treating).

Preferably, the aqueous composition is administered (or used for treating) from a few seconds to 15 minutes after the aqueous solution comprising silylated biomolecule is mixed with a buffering solution. The pH of the final aqueous solution which is administered preferably has a physiological value (i.e. pH from about 7.2 to about 7.6). Preferably, cardiomyocytes or stem cells are added when the aqueous solution of point (ii) above reaches a pH from 7.2 to 7.6.

Once injected into myocardium, viscosity of the aqueous composition gradually increases until formation of a hydrogel into which cardiomyocytes or stem cells which are able to differentiate into cardiomyocytes are present.

The aqueous composition is injected into myocardium, in particular into the left ventricle, and preferably into the sites along the infarcted area. The infarcted area can be identified by the surface scar and wall motion akinesis as described by Takagawa et al. (J. Appl. Physiol., 102(6): 2104-11, 2007, PMID: 17347379).

The injection may be carried out using a system comprising sterilizable syringe and needle, and connection pieces provided with single-use plungers.

In a preferred embodiment of the method of treating heart failure and medical application according to the third and fourth aspects of the invention, stem cells of the aqueous composition are mesenchymal stem cells. The beneficial effects of mesenchymal stem cell grafts are known to be related in part to their paracrine activity. Mesenchymal stem cells secrete angiogenic, antiapoptotic, and anti-inflammatory cytokines that contribute to the recovery of cardiac function and significantly decrease fibrosis in the heart (Aggarwal S and Pittenger MF., Blood, 105: 1815-1822, 2005; Tse WT *et al*., Transplantation, 75: 389-397, 2003; Nagaya N. *et al*., Circulation, 112: 1128-1135, 2005; and Li L, Zhang Y, Li Y, Yu B, Xu Y, *et al*., Transpl. Int., 21: 1181-1189, 2008).

A fifth aspect of the invention relates to a kit for obtaining an aqueous composition that is usable in a method of treating heat failure, in particular heart failure following myocardial infarction, and in the medical application of the invention described above.

The Kit of the fifth aspect of the invention may comprise i) cardiomyocytes or stem cells which are able to differentiate into cardiomyocytes, and ii) a hydrogel solution which comprises silylated biomolecule. Preferably, the kit comprises Mesenchymal stem cells.

The kit of the fifth aspect of the invention may also comprise instructions for the use of said kit in preparing a composition at physiological pH (pH from about 7.2 to about 7.6) comprising:

i) cardiomyocytes or stem cells which are able to differentiate into cardiomyocytes; and

ii) a hydrogel solution comprising silylated biomolecule;

said composition being intended to be injected into myocardium, in particular left ventricle.

A sixth aspect of the invention relates to a kit for the three-dimensional culture of cardiomyocytes or stem cells which are able to differentiate into cardiomyocytes.

The Kit of the sixth aspect of the invention may comprise i) cardiomyocytes or stem cells which are able to differentiate into cardiomyocytes, and ii) a hydrogel solution which comprises silylated biomolecule. Preferably, the kit comprises cardiomyocytes or Mesenchymal stem cells, more preferably cardiomyocytes.

The kit of the sixth aspect of the invention may also comprise instructions for the use of said kit in culturing cardiomyocytes or stem cells which are able to differentiate into cardiomyocytes in three-dimensional culture

Preferably, the hydrogel solution (ii) of the kits of the fifth and sixth aspects of the invention has a pH higher than 12, and hence is in liquid form (the silylated biomolecule comprised in the hydrogel solution is stable in aqueous solution at a pH greater than or equal to approximately 12.4).

Cardiomyocytes or stem cells can be provided in both kits in a culture medium. The culture media suitable for culturing such cells are well known to a person skilled in the art, for instance Dulbecco' S modified Eagle medium (DMEM), alpha Modified Eagle medium (α-MEM). Alternatively, the cells can be provided as frozen cells.

Both kits may further comprise a buffering solution which may be used to produce a hydrogel solution ii) with a physiological pH. A suitable buffering solution may be any solution of pH 4 or below which once mixed with the hydrogel solution in aqueous solution allow to obtain a final aqueous solution at physiological pH (i.e. with a pH value from 7.2 to 7.6, preferably 7.4) and at physiological osmotic pressure (i.e. about 300 mOsm/L). Examples of such a buffering solution are HCl, HEPES and TRIS.

In a preferred embodiment of the first, second and sixth aspects of the invention, the hydrogel has the following rheological characteristics at a pH value of 7.4 (after 3 weeks of reticulation):

- a compressive modulus at 5% stress from 220 to 15 000 Pa;
- a storage modulus (G') from 235 to 10 000 Pa;
- a loss modulus (G'') from 29 to 1000 Pa;
- a gel point from 5 to 45 minutes.

More preferably, the hydrogel of the first, second and sixth aspects of the invention contains 1 to 3% w/v of si-HPMC (before addition of cells).

Advantageously, the hydrogel contains 2% w/v of si-HPMC and has the following rheological characteristics at a pH value of 7.4 (after 3 weeks of reticulation):

- a compressive modulus at 5% stress from 1600 to 2600 Pa;
- a storage modulus (G') from 800 to 2500 Pa;

- a loss modulus (G'') from 30 to 110 Pa;
- a gel point from 20 to 30 minutes.

The inventors have found that a hydrogel with the above recited rheological characteristics is particularly adapted to cardyomyocyte culture since such a hydrogel allows maintenance of cardiomyocyte contractile activity in three-dimensional culture.

In a preferred embodiment of the third, fourth and fifth aspects of the invention, the hydrogel has the following rheological characteristics at a pH value of 7.4 (after 3 weeks of reticulation):

- a compressive modulus at 5% stress from 220 to 430 Pa;
- a storage modulus (G') from 235 to 450 Pa;
- a loss modulus (G'') from 29 to 60 Pa;
- a gel point from 23.8 to 30.6 minutes.

When the hydrogel is made of si-HPMC, such rheological characteristics are obtained when the final aqueous solution (i.e. after addition of the buffering solution) contains 1.5% w/v of si-HPMC (before addition of cells).

Preferably, the hydrogel contains 0.8 to 1.5% w/v of si-HPMC (before addition of cells)

The inventors have found that a hydrogel with the above recited rheological characteristics does not alter MSC viability or activity, and that injection such a hydrogel load with MSCs in the heart directly after MI leads to cardiac function and LV remodeling preservation.

The rheological measurements are carried out after 3 weeks of reticulation, at 25°C, on a rotational rheometer (Rheostress 300, ThermoHaake®, Germany) using a coni-cylindrical geometry with a diameter of 60 mm and a cone angle of 1°. A multiwave procedure with 3 frequencies 1, 3.2 and 10 Htz is used, and the imposed stress is 1 Pa. Oscillation tests measuring storage modulus (G') and loss modulus (G'') are performed to study the self-setting process and gel point. The gel points are given as the time taken for the liquid (G''>G') to turn into a solid (G'>G''). They are determined according to a derived percolation theory as disclosed by Fatimi *et al*. (Acta Biomater, 5: 3423-3432). Compressive modulus of scaffold is measured using a TA HD-Plus (Stable Micro Systems). The compressive modulus is calculated on the basis of strain change from 0 to 5%. Shear strain measurements are performed with a Haake mars. Frequencies are applied at a fixed total shear stress (1Pa) and 0,21N. Oscillation tests are performed to measure G' and G'' after 3 weeks of gelation.

Preferably, the hydrogel and hydrogen solution comprising silylated biomolecules used in the different aspects of the invention are able to form a self-reticulating hydrogel at a pH between 7 and 12.

As used herein, the terms « hydrogel » and « hydrogel solution » which are used indifferently mean a network of polymer chains that are water-insoluble, in which water is the dispersion medium.

As used herein, the term “silylated biomolecules” means any organic or synthetic molecules onto which are grafted a silyl function, preferably an alkoxysylane. Silylation allows the formation of covalent bonds between the biomolecules constituting the hydrogel as a function of pH. The silylated biomolecules are thus able to form a pH-dependent self-reticulating hydrogel.

The term “organic molecule” is intended to mean any molecule that is produced by a living organism or that is a derivative thereof, including large polymeric molecules such as proteins, polysaccharides, and nucleic acids as well as small molecules such as primary metabolites, secondary metabolites, and natural products.

The term “synthetic molecule” is intended to mean any molecule that is produced by chemical methods, such as proteins, polysaccharides, nucleic acids and a mix thereof.

As examples of biomolecules, mention may be made of:

- lipid derivatives such as phospholipids, glycolipids and sterols,
- chemical messengers such as hormones and neurotransmitters,
- vitamins,
- sugar derivatives such as carbohydrate, disaccharide, oligosaccharides, polysaccharides (including cellulose),
- amino acid derivatives such as amino acids (natural and/or non-standard), peptides, oligopeptides, polypeptides, proteins (said peptides, oligopeptides, polypeptides and proteins containing natural and/or non-standard aminoacid),
- nucleotides derivatives such as nucleotides, and biological polymers such as deoxyribonucleic acid (DNA), ribonucleic acid (RNA),
- biopolymers such as lignin, proteins, DNA, RNA, oligosaccharides, polysaccharides.

Preferably, the biomolecule is a polysaccharide, a protein, or a peptide.

As used herein, the term “polysaccharide” means a polymer made up of many monosaccharides joined together by glycosidic bonds. Natural and synthetic polysaccharides are included. Examples of polysaccharide are cellulose and derives

thereof, for instance hydroxypropylmethylcellulose (HPMC), hydroxyethylcellulose (HEC), and carboxymethylcellulose (CMC), pectin, chitosan and hyaluronic acid.

As used herein, the term “protein” means a polymer made of amino acids arranged in a linear chain and joined together by peptide bonds between the carboxyl and amino groups of adjacent amino acid residues. Glycoprotein as well as proteins containing natural and/or non-standard aminoacid are included. Albumin, laminin, gelatin, fibronectin, vitronectin and collagen are examples of protein.

The hydrogel may contain either only one kind of silylated biomolecule (i.e. all the biomolecules forming the polymer are the same), or silylated biomolecules of different nature, preferably two different silylated biomolecules, more preferably one silylated polysaccharide and one silylated protein or peptide.

In a preferred embodiment, the hydrogel contains a silylated HPMC, a silylated HEC or a silylated CMC polymer.

In a particularly preferred embodiment, the hydrogel contains only silylated HPMC.

In another preferred embodiment, the hydrogel is formed with:

- silylated collagen and silylated HPMC (leading to a hydrogel containing HPMC and collagen),
- silylated hyaluronic acid and silylated HPMC (leading to a hydrogel containing HPMC and hyaluronic acid),
- silylated tetrapeptide Arg-Gly-Asp-Ser (hereafter abbreviated “RGDS”) and silylated HPMC (leading to a hydrogel containing HPMC and RGDS), or
- silylated pectin and silylated hyaluronic acid (leading to a hydrogel containing pectin and hyaluronic acid).

The silylated biomolecules used to carry out the invention are preferably stable in aqueous solution at a pH greater than or equal to approximately 12.4.

Thus, the aqueous solution comprising silylated biomolecules of the invention are preferably liquid at a pH of about 12.4 or above.

As used herein, the expression “aqueous solution” means a solution wherein water is the major solvent.

Acidification of the solution causes a gradual increase in viscosity, due to the condensation of the silylated biomolecules via the formation of –Si-O-Si- covalent bond, and the formation of hydrogel. Because highly basic pH is detrimental for cells, even when cells are exposed to it for a short period, the silylated biomolecules is contacted with an acid in an aqueous solution to obtain a final aqueous solution at physiological pH (i.e. with a pH value from 7.2 to 7.6, preferably 7.4), before cardiomyocytes or stem cells are

added. The hydrogels and the aqueous solution comprising silylated biomolecules of the invention are preferably capable of gelation at physiological pH.

Addition of cells must occur before the total gelation of the final solution to hydrogel, preferably from a few seconds to 15 minutes after having contacted the silylated biomolecules with an acid and having obtained a final aqueous solution of pH from 7.2 to 7.6.

Processes for preparing silylated biomolecules and hydrogels according to the invention are well known by one skilled in the art. For instance, processes for the preparation of silylated HPMC and silylated HEC and for the preparation of hydrogel therefrom are described in US application 2007/0212389.

Methods for preparing silylated biomolecules are also described in application PCT/EP2011/050981. PCT/EP2011/050981 also disclosed the preparation of hydrogel comprising two different kinds of silylated biomolecules, in particular a silylated polysaccharide and a silylated protein or peptid.

Depending on whether the biomolecule used as starting material is carrying an amine or an alcohol function, or a carboxylic acid function, the two processes described below (and disclosed in application PCT/EP2011/050981) may be used to prepare silylated biomolecules.

For preparing a silylated biomolecule using a biomolecule carrying an alcohol or amine function, preferably chosen from a peptide, an oligopeptide, a protein, a deoxyribonucleic acid, a ribonucleic acid, pectin, chitosan, hyaluronic acid, a glycolipid as a starting material, the process (hereafter called “process 1”) comprises a step of reacting said biomolecule with a silylation agent having the following formula (II) or (IIbis):

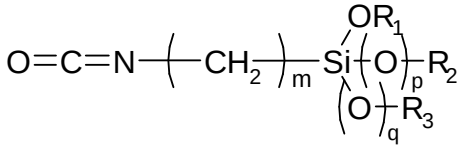

(II)

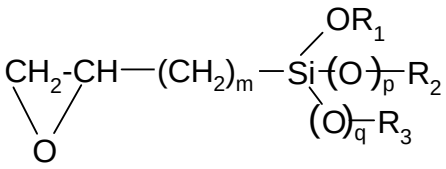

(IIbis)

wherein :

- m is an integer ranging from 1 to 6,
- p and q are independently 0 or 1, and
- R_1, R_2 and R_3 each independently represent a C_1-C_6 alkyl group.

Silylated biomolecules of formula (I):

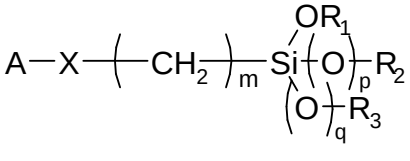

(I)

wherein:

- A is a biomolecule chosen from a peptide, an oligopeptide, a protein, a deoxyribonucleic acid, a ribonucleic acid, pectin, chitosan, hyaluronic acid, a glycolipid, and a polysaccharide
- m is an integer ranging from 1 to 6,
- p and q are independently 0 or 1,
- X is a –NHCONH- or a -OCONH- moiety, and
- R_1, R_2 and R_3 each independently represent a C_1-C_6 alkyl group.

are obtained by process 1.

During the process, the amine or the alcohol function of the biomolecule reacts with the isocyanate function of the silylation agent of formula (II), leading to the formation of an urea bond (–NHCONH-) (if the biomolecule is carrying an amine function) or a carbamate bond (-OCONH-)(if the biomolecule is carrying an alcohol function) according to the following scheme :

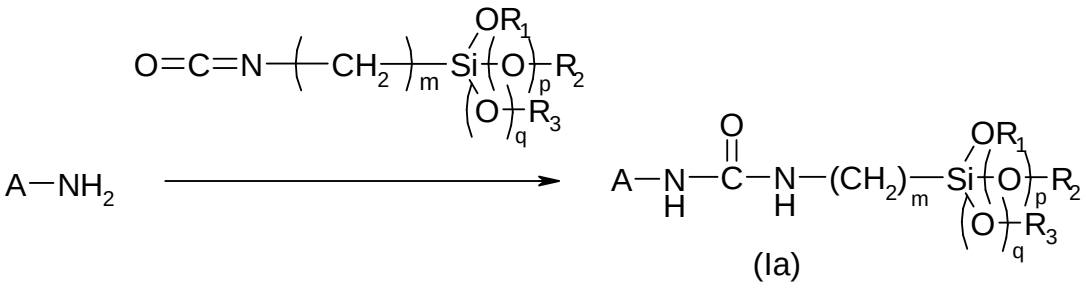

(Ia)

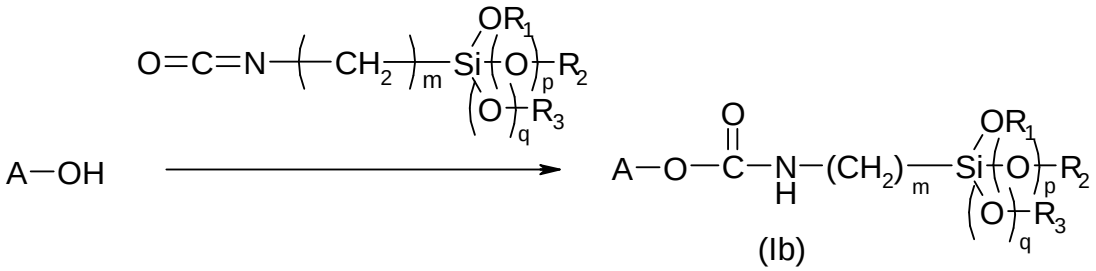

(Ib)

In one embodiment of process 1, the biomolecule is carrying an alcohol function and is preferably chosen from a deoxyribonucleic acid, a ribonucleic acid, pectin, chitosan, hyaluronic acid, a glycolipid and optionally from a peptide, an oligopeptide, a protein, when said peptide, oligopeptide, or protein comprise a moiety (an amino acid for example) carrying an alcohol function, for example the RGDS.

In one other embodiment of process 1, the biomolecule is carrying an amine function and is preferably chosen from a peptide, an oligopeptide, a protein, a deoxyribonucleic acid, a ribonucleic acid and chitosan. The biomolecule used in the process can also carry both an alcohol function and an amine function, for example when the biomolecule is chitosan.

In a preferred embodiment of process 1, the silylation agent used in the process is 3-isocyanatopropyltriethoxysilane.

Preferably, when the biomolecule is carrying amine functions, part of said amine functions are not protonated in the reaction medium. The lone pair of the amine has indeed to be available to attack the isocyanate function.

The temperature of the reaction of process 1 is not critical and may vary in wide range. The reaction is generally carried out at a temperature from -15℃ to 40℃, preferably 0℃ to 30℃, more preferably from 15℃ t o 25℃, which is advantageous as no denaturation of biomolecule occurs. Preferably, process 1 is carried out under inert atmosphere, for example under argon or nitrogen.

The reaction time is usually lasts from one hour to one week, preferably from twelve hours to five days, more preferably from one to three days.

Process 1 is generally carried out in a solvent. There is no particular restriction on the nature of the solvent to be used, provided that it has no adverse effect on the reaction or on the reagents involved. Organic solvents or mixture of organic solvent with an aqueous solution, typically water, are preferred. Examples of suitable organic solvents include acetonitrile, acetone, dimethylformamide and dimethylsulfoxide.

In one embodiment, process 1 is carried out in an anhydrous solvent, such as anhydrous acetonitrile, anhydrous acetone, anhydrous dimethylformamide or anhydrous dimethylsulfoxide, and in the presence of a base, preferably an organic base, usually an organic base containing a nitrogen atom which can be protonated, for example triethylamine, pyridine or trimethylamine.

In one other embodiment, process 1 is carried out in a mixture comprising an aqueous solution and a solvent miscible in water, such as acetonitrile, acetone, dimethylformamide and dimethylsulfoxide. The mixture is preferably a mixture of water and of dimethylsulfoxide. No base is required for this embodiment.

For preparing a silylated biomolecule using as starting material a biomolecule carrying a carboxylic acid or a carboxylate function, a process is described therein (hereafter called “process 2”). This process for the preparation of a silylated biomolecule of formula (I) as defined above, comprising the steps consisting of:

a) reacting a biomolecule carrying a carboxylic acid or a carboxylate function, preferably chosen from a peptide, an oligopeptide, a protein, pectin, hyaluronic acid, with 1-ethyl-3-(3-dimethylaminopropyl)carbodiimide hydrochloride (EDC.HCl) or with 1,1'-carbonyldiimidazole (CDI), then

b) adding to the reaction medium obtained in step a) a silylation agent having the following formula (III):

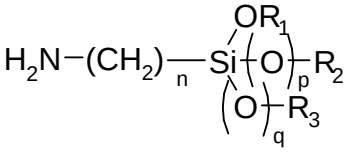

(III)

wherein,

- n is an integer ranging from 1 to 6
- p and q are independently 0 or 1, and
- R_1, R_2 and R_3 each independently represent a C_1-C_6 alkyl group.

Silylated biomolecules of formula (I), wherein X is a -CONH- moiety, are obtained by process 2. During process 2, the carboxylic function of the biomolecule is activated with EDC.HCl in step a) and then reacts with the amine function of the silylation agent of formula (III), leading to the formation of an amide bond (–CONH-) according to the following scheme :

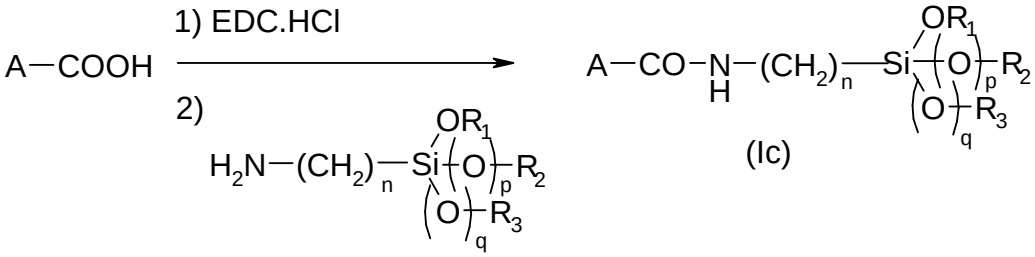

(Ic)

Prefered biomolecule used as starting material in step a) of process 2 are a peptide, an oligopeptide, a protein, pectin, and hyaluronic acid.

Step a) of process 2 can be carried out in the presence of a catalyst, such as N-hydroxysuccinimide.

The silylation agent used in step b) of process 2 is preferably (3-aminopropyl)triethoxysilane.

When EDC.HCl is used, steps a) and b) of process 2 are generally carried out in an aqueous solution, the pH of which is preferably from 4 to 6, most preferably from 4.7 to 5.3, preferably in water. When CDI is used, steps a) and b) of process 2 are generally carried out in dichloromethane or acetonitrile.

Steps a) and b) of process 2 are generally carried out at a temperature from -15℃ to 40℃, preferably 0℃ to 30℃, more preferably fr om 15℃ to 25℃, which is advantageous as no denaturation of biomolecule occurs.

Step a) of process 2 usually lasts from 4 h to 24h, preferably from 12 h to 18 h, and step b) of process 2 usually lasts from 4 h to 24h, preferably from 12 h to 18 h.

Both processes 1 and 2 lead to the formation of a strong covalent bond between the silylation agent and the biomolecule.

The weight concentration of the biomolecule used as starting material in the solvent in processes 1 and 2 is generally from 0,01 to 30%, preferably from 0,1 to 20%, more preferably from 0,5 to 15%.

Advantageously, processes 1 and 2 are carried out without any metal catalyst, more particularly tin based catalyst.

When process 2 wherein EDC. HCl is used is carried out, the reaction medium is generally homogeneous. When process 1 or process 2 wherein CDI is used are carried out, the reaction medium is generally heterogeneous. A suspension of the biomolecule in the solvent is generally observed, which can be isolated easily from the reaction mixture, for example by sedimentation or centrifugation.

The cardiomyocytes and the stem cells which are able to differentiate into cardiomyocytes used in the different aspects of the invention may be, for example, human, non human primate, rat, dog, mouse, or cat cells, more preferably human cells.

The stem cells may be, for example, embryonic stem cells, or adult stem cells such as skeletal myoblasts (stem cells from muscle), bone-marrow-derived stem cells (in particular mesenchymal stem cells), cardiac stem cells (disclosed by Beltrami *et al*., Cell, 114: 763-776, 2003).

In a preferred embodiment, stem cells are mesenchymal stem cells.

Methods for isolating embryonic and adult stem cells are well known by the person skilled in the art, and are for example disclosed in Pittenger *et al*. (Circ Res., 95(1): 9-20, 2004, PMID : 15242981), and in Blin *et al*. (J. Clin. Invest., 1;120(4) :1125-39, 2010 doi: 10.1172/JCI40120. Epub 2010 Mar 24. PMID 20335662).

The stem cells may also be induced pluripotent stem cells (hereafter abbreviated “iPS”), that is population of cells with characteristics reminiscent of embryonic stem cells which is generated from somatic tissues through nuclear reprogramming via the ectopic expression of genes related to pluripotency. Processes for generating iPS cells are for instance described by Takahashi *et al*. (Cell, 131: 861-872, 2007), Yu *et al*. (Science, 318: 1917-1920, 2007) and Okita *et al*. (Nature, 448: 313-317, 2007).

In embodiments where cardiomyocytes are cultured, said cardiomyocytes may be derived from stem cells or iPS cells.

Further, in embodiments where stem cells able to differentiate into cardiomyocytes are cultured, the hydrogel may comprise agents which allow induction of cardiomyocyte differentiation, so that the final cells obtained are cardiomyocytes.

Buffering solutions which may be used to produce a final aqueous solution with a physiological pH are well known to one of ordinary skill in the art. Examples of such a buffering solution are 4-(2-hydroxyethyl)-1-piperazineethanesulfonic acid (HEPES, HCl)

The present invention will be further illustrated by the additional description and drawings which follow, which refer to examples illustrating the characterization of the properties of a hydrogel according to the invention comprising cardiomyocytes or stem cells, and its use to preserve cardiac function and left ventricular remodeling in acute stage following myocardial infarction. It should be understood however that these examples are given only by way of illustration of the invention and do not constitute in anyway a limitation thereof.

BRIEF DESCRIPTION OF THE FIGURES

- Figure 1 illustrates viability of cardiomyocytes cultured with or without Si-HPMC.

Cardiomyocytes were cultured in 2D with or without Si-HPMC (control) or in the presence of actinomycin-D (5µg/ml) during the indicated times. Viability was assessed by MTS activity. Results are expressed as relative MTS activity compared with the respective control. **P*<0.001 as compared to control conditions.

- Figure 2 illustrates a real-time RT-PCR analysis of cardiomyocyte phenotype in culture in 2D with the Si-HPMC hydrogel. mRNA was harvested from cardiomyocytes after 1, 2 and 3 days of culture with or without Si-HPMC (control). Real-time RT-PCR was performed by using nkx2.5, gata4, cardiac sarcomeric α-actin and connexin43 and corrected by HPRT gene expression levels. *P<0.001.

- Figure 3 illustrates the quantification of cardiomyocyte contractility in 2D culture. The contractility was quantified manually by counting the cardiomyocytes beats for one minute. This frequency was measured after 24 and 48 hours of culture in 2D of cardiomyocytes with or without (control) Si-HPMC. Results are expressed as beat number / minute. **P*<0.01.

- Figure 4 illustrates the three-dimensional cellular viability of MSCs in Si-HPMC hydrogel. MSCs were cultured in 3D into Si-HPMC hydrogel during the indicated times. Cells were stained with calcein-AM and EthD-1, which label living cells in green and dead cells in red, respectively. MSC viability was assessed by the intensity of green fluorescence, as a consequence of incorporation of the calcein fluorescent probe into cell cytoplasm. Percentages of living and dead MSCs cultured in 3D within hydrogel over 7 days (p= NS as compared between groups).

- Figure 5 illustrates measurements of VEGF protein concentrations by ELISA assay. VEGF concentrations in **(A)** control supernatants of MSCs cultured without hydrogel (p<0.001 for all comparaisons) and in **(B)** supernatants of MSCs cultured in 3D within hydrogel (p<0.001, for all comparaisons). VEGF concentrations were expressed as $pg.ml^{-1}$ for 10^4 cells.

- Figure 6 illustrates the evaluation of cardiac function by echocardiography in rats after myocardial infarction (MI). Measurements were performed at baseline before MI and 1, 7, 28 and 56 days after MI. **(A)** LV end-diastolic diameter (LVEDD), **(B)** LV end-systolic diameter (LVESD). **(C)** The fraction shorting (FS) and **(D)** Ejection fraction (EF). $^{¥}p$<0.05 compared to day 1 post-infarction in the same group, *p<0.001 compared to the PBS group at the same time-point, $^{\$}$p<0.05 compared to the Hydrogel group at the same time-point and ^{+}p<0.05 compared to the MSCs at the same time-point.

- Figure 7 illustrates the effects on Myocardial Infarction and fibrosis of injection of PBS (control group), Hydrogel, MSC, or MSC+hydrogel into myocardium of rats suffering from myocardial infarction. **(A)** Representative histologic sections of Masson trichrome staining for infarct size measurement (collagen-rich areas in blue and healthy myocardium in red; original magnifications: x40). **(B)** Circumferential infarct size (MI size) to total LV tissue and **(C)** percentage of fibrosis to LV tissue. For (B) and (C): *p<0.05 and **p<0.001 compared to the PBS group and $^{\$}p$<0.05 and $^{\$\$}p$<0.001 compared to Hydrogel group.

- Figure 8 illustrates the effects on scar thickness and infarct expansion of injection of PBS (control group), Hydrogel, MSC, or MSC+hydrogel into myocardium of rats suffering from myocardial infarction. **(A)** Representative photomicrographs of Masson trichrome staining of the scar area (collagen-rich areas in blue and healthy myocardium in red; Original magnifications: X100). **(B)** Relative scar thickness (average scar thickness/average wall thickness). (*p<0.05 and **p<0.001, two-way ANOVA). **(C)** Infarct

expansion index ([LV cavity area/whole LV area]/relative scar thickness). For (B) and (C): *p<0.05 and **p<0.001.

EXAMPLES

Example 1: Preparation of hydrogel

Materials

- HPMC E4M TM (Colorcon- Dow Chemical, France)
- Glycidoxypropyltriméthoxysilane (GPTMS) (Acros, Belgium)
- HEPES and HCl (Sigma-Aldrich, St Louis, the USA)
- NaOH and NaCl (International VWR, Fontenay-under-Wood, France)

Synthesis of Si-HPMC hydrogel

As previously described (Bourges *et al*., Adv. Colloid Interface Sci., 99: 215-228, 2002), the synthesis of Si-HPMC was performed by grafting 14, 24% of 3-GPTMS on E4M®in heterogeneous medium. Aqueous solution of Si-HPMC was prepared at 3% w/w concentration. The powder was dissolved in sodium hydroxide solution (0.2M NaOH) at 25℃ for 48h. Si-HPMC solution was then dialyzed in a dialysis bag against 3.8l of NaOH solution (0.09M) for 12h and with 4L of NaOH solution (0.09M) for 2h. The solution was then sterilized by steam (121℃, 30mn). To allow the formation of a reticulated hydrogel, 1 volume of the solution was finally mixed with 1 volume of a 0,13 M HEPES buffer.

Rheological measurements

Dynamic rheological measurements were performed on a Haake Rheometer (rheostress 300) using a coni-cylindrical geometry with a diameter of 60 mm and a cone angle of 1°. We used a multiwave procedure with 3 frequencies 1, 3.2 and 10 Hz, and the imposed stress was 1 Pa. Oscillation tests measuring storage modulus (G') and loss modulus (G'') were performed to study the self-setting process and gel point. Compressive modulus of scaffold was measured using a TA HD-Plus (Stable Micro Systems). Six specimens were tested after three weeks of reticulation and the compressive modulus was calculated on the basis of strain change from 0 to 5%. Shear strain measurements were performed with a Haake mars. Frequencies were applied at a fixed total shear stress (1Pa) and 0,21N. Oscillation tests were performed to measure G' and G'' after 3 weeks of gelation. Nine specimens were tested.

Results:

Rheological properties of Si-HPMC hydrogel mixed with one volume of a 0,13M buffer (1v1) were measured. The compressive modulus at 5% stress and the storage modulus (G') and loss modulus (G'') of Si-HPMC were performed after three weeks of reticulation.

The final product (Si-HPMC) consisted of a reticulated hydrogel after 27.2 ± 3.4 min with a pH value of 7.4. Dynamic rheological measurements were performed to characterize this hydrogel. Shear strain measurements were performed to determine de storage modulus (G'), which characterized the hard component and the loss modulus (G''), which characterized the liquid component. The compressive modulus reflects the capacity of a material to resist to strengths. When the limit of the compressive strength is reached, the hydrogel is destroyed. In the case of our Si-HPMC hydrogel, compressive modulus was about 328.56± 96,97 Pa. After three weeks of reticulation and a finished self-setting process, we observed a value of 343.17 ± 106.5 Pa for the storage modulus (G') and a value of 44.48 ± 15.43 the loss modulus (G'').

Example 2: Preparation and cell culture

Materials

- Dulbecco' S modified Eagle medium (DMEM), alpha Modified Eagle medium (α-MEM)

- Hank's Balanced sodium salt (HBSS), horse serum, Penicillin/streptomycine, L-glutamine, collagenase II (284,00 unit/mg), Trypsine/EDTA (Invitrogen corporation, Paisley, the U.K.)

- pancreatin (0.1mg/ml), laminin (Sigma-Aldrich, St-Louis, USA)

- Fetal Calf Serum (FCS) (Hyclone Perbio, Thermo Fisher scientific)

- Animals: neonatal C57Bl/6j mice and Lewis female rats (Janvier, France)

Isolation and culture Cardiomyocytes:

Primary cardiomyocytes were isolated from 1 or 2-day-old neonatal C57Bl/6j mice hearts. Briefly, neonatal mice were sacrificed and hearts were rapidly removed and placed into dishes on ice. After atria and great vessels were removed, hearts were minced and digested repeatedly (10min x 8) in HBSS solution supplemented with collagenase II (284,00 unit/mg) and pancreatin (0.1mg/ml) at 37℃ and 5% CO2. After centrifugation, cells were resuspended in culture media (DMEM with 10% horse serum, 5% SVF, 1% penicilline/streptomycine).

For two dimensional culture with the Si-HPMC hydrogel, cardiomyocytes were plated in 24-well plates (coated with laminin 10µg/ml) at the density of 55 000 cells/cm² and maintained at 37℃ in a humidified atmosphere a nd 5% CO2. After 48 hr, culture medium was removed and 500 µl of Si-HPMC were added in each well. Samples were incubated at 37 ℃ for 1 h before adding 500 µl of culture medium. For 3D-culture of suspended cardiomyocytes in Si-HPMC hydrogel, 10 µl of culture medium containing 9 x 10^6 cardiomyocytes were mixed with 1 ml of Si-HPMC. 500 µl of cells/Si-HPMC mixture were seeded in 12-well plates and incubated at 37℃ and 5% CO2. After 1 hr incubation, 1 ml of culture medium was added in each well and plates were incubated. For cardiomyocyte 3D-culture in a micro-drop of Si-HPMC hydrogel, 5 µl of culture medium containing 2 x 10^4 cardiomyocytes were directly injected in a micro-drop of Si-HPMC after 2 hours of polymerization.

Isolation and culture of MSC:

Bone marrow (BM) was obtained from Lewis female rats weighing 180–200 g. BM from femurs cavity was flushed with α-MEM medium containing 10% FBS and 1% penicillin/streptomycin, and the cell suspension was centrifuged (1200 rpm, 7 min). Cells were then plated in culture flasks (200 000 cells/cm2). Non adherent cells were removed after 72 hours, and MSCs were recovered by their capacity to strongly adhere to plastic culture dishes. MSCs were then routinely cultured and were used for experiments after the third passage.

Example 3: Study of the cytotoxicity of hydrogel

Materials

- Plate culture 24 wells Corning-Costar (Corning BV, Schiphol-Rijk, The Netherlands).

- Actinomycin D and Dyméthylsulfoxyde (DMSO) (Sigma-Aldrich)

- Methyl Tetrazolium Salt (MTS) (Titer Concealment 96 MTS, Promega corporation, Madison, WI).

- Buffered salt phosphates (PBS, Invitrogen corporation)

A. Cardiomyocyte viability:

Cardiomyocyte viability in 2D culture was measured using an **MTS assay** as previously described (Relic et al., 2001; Magne et al., 2003). As a control, cells were also cultured in the absence of Si-HPMC or in the presence of actinomycin-D (5 mg/ml), an inhibitor of RNA polymerase (Kimura et al., 2002) used as a potent inducer of cell death.

After 24 and 48 hours, hydrogels and culture media were removed and MTS solution was added in each well for 1–3 h according to the manufacturer's instructions. Finally, colorimetric measurement was performed on a spectrophotometer at an optical density of 490 nm. Results were expressed as relative MTS activity compared to control condition (cells cultured in the absence of Si-HPMC).

Results:

Cardiomyocyte viability was evaluated using MTS activity at 24 and 48 hours of 2D culture in presence of Si-HPMC hydrogel. No significant difference was observed between control cultures and the cultures carried out in contact with hydrogel (see Figure 1). On the other hand, the actinomycin-D, inhibitor of the transcription, used here as cytotoxicity positive control induced a significant reduction in MTS activity of cardiomyocytes after 24 hours of culture. In the presence of actinomycin D MTS activity decreased by nearly 55% after a 24h treatment and by 90% after a 48h treatment. Therefore, the Si-HPMC hydrogel maintains cardiomyocyte viability.

B. Cardiomyocyte phenotype

- **Transcripts analyses:**

Materials:

- RNeasy Mini Kit (Qiagen S.A., France)

- High-capacity cDNA Archive kit (Applied Biosystems, life technologies corporation, USA)

- Taqman gene expression (Applied Biosystems, life technologies corporation, USA)

In order to analyze cardiomyocyte phenotype, expression of mRNA coding for cardiomyocyte markers was quantified by RT-PCR. RT-PCR analysis of transcripts was performed on cardiomyocytes in 2D culture in the absence or presence of Si-HPMC.

Total RNA extraction and DNAse treatment Total RNAs from each cardiac sample were isolated and DNase-treated with the RNeasy Fibrous Tissue Mini Kit following manufacturer's instructions.

Reverse transcription: First-stand cDNA was synthesized from 200 ng of total RNAs using the High-capacity cDNA Archive kit.

Reaction of polymerase in chain (PCR) On-line PCR was performed using the following primers: nkx2.5 (nkx2.5, Mm00657783_m1), gata4 (gata4, Mm00484689_m1), actin alpha cardiac muscle 1 (actc1, Mm01333821_m1), gap junction protein alpha 1

(gja1, Mm00439105_m1). Fluorescence signals were normalized to the hypoxanthine guanine phosphoribosyl transferase 1 (hprt1, Mm03024075_m1), used as reference gene. Data were averaged and then used for the $2^{-\Delta CT}$ calculation. $2^{-\Delta CT}$ corresponded to the ratio of each gene expression versus hprt.

Results:

The ability of Si-HPMC to maintain cardiomyocyte phenotype after 1 day, 2 and 5 days of 2D culture was evaluated by relative quantification of cardiogenic marker (nkx2.5, gata-4, cardiac sarcomeric α-actin and connexin 43) mRNAs, using TaqMan real-time PCR (see Figure 2). Expression levels of these cardiomyocyte markers were maintained during the 5 days of culture in presence or absence d'HPMC. Importantly, the presence of the Si-HPMC hydrogel did not alter expression levels of these genes in cardiomyocytes.

- **Immunostaining:**

Materials:

- Formaldehyde solution 37% (Sigma-Aldrich)
- Triton X-100 (Sigma-Aldrich)
- Bovine serum albumin (Sigma-Aldrich)
- Polyclonal antibodies: anti-nkx2.5 and anti-gata4 (Santa Cruz Biotechnology, USA).
- Monoclonal anti-connexin 43(Millipore)
- Secondary antibodies Alexa fluor (Molecular Probes, Leiden, The Netherlands)
- Vectaschield® medium with DAPI nuclear (vector laboratories, US. Headquaters)

Cardiomyocytes were fixed in 4% formaldehyde for 30 min at room temperature and permeabilized with 0.2% Triton X-100, bovine serum albumin, and phosphate-buffered saline (BSA-PBS). then, cells were incubated for 1h at room temperature with primary antibodies: polyclonal anti-nkx2.5 (1:500), polyclonal anti-gata4 (1:500), monoclonal anti-connexin 43 (1:100) and monoclonal anti-sarcomeric alpha actin (1:1000). Cells were washed and incubated for 45 min at room temperature with fluorescence-conjugated secondary antibodies at a 1:1000 dilution: Alexa fluor 568 mouse anti goat IgG, Alexa Fluor 488 goat anti-mouse IgG and Alexa fluor 594 goat anti-mouse IgG. Cells were washed carefully with PBS and the samples were mounted with Vectaschield® medium with DAPI nuclear. Cardiomyocytes were observed using fluorescence microscopy, and pictures were taken using a Zeiss Axioskop2 with equal exposure times. The extent of fluorescence was measured by using MetaMorpho microscope image analysis software (version 6.3).

Results:

The expression and localization of proteins nkx2.5, gata4, cardiac sarcomeric α-actin and connexin 43 were observed by immunofluorescence staining after 48 hours of culture (data not shown). The expression of both transcription factors nkx2.5 and gata-4 were maintained in the nuclei of cardiomyocytes cultured with Si-HPMC, as well as membrane expression of connexin 43. Staining for sarcomeric α-actin revealed typical sarcomeric striations in cardiomyocytes cultured in presence or absence of Si-HPMC. These results suggest Si-HPMC hydrogel maintained cardiomyocyte phenotype.

C. Cardiomyocyte contractility

After 24 and 48 hours of culture in the presence or absence Si-HPMC, cardiomyocytes were observed by videoscopy using a Nikon eclipse TE200E microscope. Spontaneous contractions were quantified over one minute. Functional activity of 3D cultured cardiomyocytes was visualized using videoscopy after 48 hours of culture.

Results:

Cardiomyocyte contractility was qualitatively and quantitatively characterized by image analysis of the contraction videos. After 24 hours of 2D culture, cardiomyocytes began to display spontaneous contractions and after 48 hours their contractile activity was synchronous. Contraction rate was almost similar when cardiomyocytes were cultured in the absence or presence of the Si-HPMC hydrogel (see Figure 3) (140 beats/ min at 24 hrs and 80 beats/ min at 48 hrs). The seeded cardiomyocytes suspended in Si-HPMC hydrogel showed a round morphology since these cells could not adhere to matrix. In addition, cells had very few intercellular contacts which prevented evaluation of electromechanical coupling. However after 48 hours of culture, several cardiomyocytes showed spontaneous contractile activity, cells had migrated and created contacts with neighboring cells favoring contraction. To promote electromechanical coupling between cells, cardiomyocytes were seeded into micro-droplets in the hydrogel. After 48 hours of culture, clusters of cells with synchronous contractility were observed. These results suggest that Si-HPMC hydrogel allows maintenance of cardiomyocyte contractile activity in 2D and 3D culture.

Example 4: Injection of Si-HPMC hydrogel with MSC in myocardium

Materials and Methods

Isolation and culture of BM-MSC

Bone marrow (BM) was obtained from Lewis female rats weighing 180–200 g (Janvier France, http://www.janvier-europe.com). BM from femur cavity was flushed with α-MEM medium (Invitrogen corporation, Paisley, the U.K) containing 10% FCS (Hyclone Perbio, Thermo Fisher scientific), 1% L-Glutamin, 1% penicillin/streptomycin (Invitrogen) and 2ng/ml of human FGF2 (AbCys P100-18B).The cell suspension was centrifuged (1200 rpm, 7 min). Cells were then plated in culture flasks (200 000 cells/cm2). Non adherent cells were removed after 72 hours, and mesenchymal stem cells (MSCs) were recovered by their capacity to strongly adhere to plastic culture dishes. MSCs were then routinely cultured and were used for experiments after verification of their phenotype by flow cytometric analysis for surface markers (CD29, CD45, CD90 and Sca1) at passage 3.

Silanized hydroxypropyl methylcellulose-based hydrogel preparation

- Synthesis of Si-HPMC hydrogel

Hydroxypropyl methylcellulose (HPMC) E4M® was purchased from Colorcon-Down chemical (Bougival, France). The synthesis of Si-HPMC was performed by grafting 0.5% of silicium in weight on HPMC (E4M®) heterogeneous medium, as previously described by Boor PJ, and Ferrans VJ. (Am. J. Pathol., 121: 39-54, 1985) (Si-HPMC powder 3%) was solubilized in 0.2M NaOH under constant stirring for 48h. The solution was dialyzed against 0.09 M NaOH using 6–8 kDa dialysis tubes (SpectraPor 1, Fisher Scientific, France). The resulting viscous solution (pH 12.6) and a 4-(2-hydroxyethyl)-1-piperazineethanesulfonic acid buffer (HEPES, pH 3.6; Sigma-Aldrich, St Louis, the USA) were separately steam sterilized by steam (121℃, 3 0 min) and then mixed using luer-lock syringes at a volume ratio of 1/1 as previously described by Bourges *et al*. (Adv. Colloid Interface Sci., 99: 215-228, 2002). Final product consists in hydrogel (pH=7.4) containing Si-HPMC concentration of 1.5%.

- Rheological measurements

Reticulation of 1 ml Si-HPMC was induced in 12-well plates. Dynamic rheological measurements were performed on a rotational rheometer (Rheostress 300, ThermoHaake®, Germany) using a coni-cylindrical geometry with a diameter of 60 mm and a cone angle of 1°. We used a multiwave procedu re with 3 frequencies 1, 3.2 and 10 Htz, and the imposed stress was 1 Pa. Oscillation tests measuring storage modulus (G') and loss modulus (G'') were performed to study the self-setting process and gel point. The

gel points are given as the time taken for the liquid (G''>G') to turn into a solid (G'>G''). They were determined according to a derived percolation theory (Fatimi *et al*., Acta Biomater., 5: 3423-3432, 2009). Compressive modulus of scaffold was measured using a TA HD-Plus (Stable Micro Systems). Six specimens were tested after three weeks of reticulation and the compressive modulus was calculated on the basis of strain change from 0 to 5%. Shear strain measurements were performed with a Haake mars. Frequencies were applied at a fixed total shear stress (1Pa) and 0,21N. Oscillation tests were performed to measure G' and G'' after 3 weeks of gelation. Nine specimens were tested.

Cytocompatibility of Si-HPMC hydrogel

- Cellular viability in 3D culture

For 3D culture, MSC viability was quantitatively assessed by Live & Dead assays (Kit, Invitrogen, France) along with confocal image analysis. Briefly, MSCs were dispersed into the hydrogels within the 5 minutes following their preparation at a final concentration of 1.10^6 cells/ml of hydrogel. 250 µl of mixture was molded into ultra-low attachment 24-well plates and incubated at 37°C for 1h to allow the hydrogels to crosslink. Afterwards, 500 µl of culture medium was added per well and the samples were incubated for 24h, 48h and 7 days before Live & Dead assays were performed. In each well, the culture medium was replaced by 200µl of a solution containing 2.5 ml of culture medium supplemented with 0.25µl of calcein-AM (5 mM) and 5µL of ethidium homodimer-1(EthD-1; 2mM).

After 5 to 10 minutes, the dye mixture was removed and the hydrogels were intensively rinsed with some phosphate buffered saline, before being observed on a confocal laser-scanning microscope Nikon A1R (Nikon France) equipped with an argon laser (488nm) and a laser diode (561nm).

Images were recorded in 512 x 512 pixels with an objective CFI Plan Fluor ELWD 40Xx40 LD NA:0.6. Resonant mode was used in bidirectionnel scanning with average 16. For each sample, 6 random positions (x,y,z) were chosen within the hydrogel, and a stack of 100 planes were taken from these 6 positions along the z axis with 10 µm step size.

Images obtained per sample were analyzed and the percentages of living cells (in green) and dead cells (in red) were determined by using ImageJ (NIH) version 1.43u for Windows with the plugin "colour deconvolution". Each condition was tested in triplicate, and each experiment was repeated three times.

- Secretion of VEGF of MSCs in 3D culture

Secretion of vascular endothelium growth factor (VEGF) in supernatants from MSCs was quantified by specific enzyme-linked immunosorbent assay (ELISA) using a VEGF ELISA kit according to the manufacturer's protocol (R&D Systems, Minneapolis, MN). Briefly, MSCs were cultivated in 3 dimensional into Si-HMPC hydrogel (10^6cells/ml of Si-HPMC hydrogel) and cell culture supernatant samples were collected from wells after 1, 2 and 7 days of culture. MSCs cultivated in 2 dimensions without hydrogel were used as control. Each condition was tested in triplicate, and each experiment was repeated three times.

Induction of MI in Rats and implantation

Animal studies were performed in accordance with the regional Ethical Committee CREEA (Comités régionaux d'éthique en matière expérimentation animale). Female Lewis congenic rats (180-190g) (Janvier France,) were anesthetized with a mix of isoflurane/oxygen inhalation (3%/97%), incubated and ventilated (Harvard Rodent Ventilator, Harvard Apparatus). A left lateral thoracotomy in the fourth intercostals space was performed to expose the anterior surface of the heart. The proximal left ascending coronary artery was identified and ligatured with a 6.0 polypropylene snare (Ethicon). The infarcted area was identified by the surface scar and wall motion akinesis. Immediately after coronary artery ligation, a total of 150 µl of Si-HPMC hydrogel alone (hydrogel), MSCs alone (3.10^6 cells) or in combination with the Si-HPMC hydrogel (MSC+hydrogel), or PBS (used as control), were delivered into the myocardium with a 26-gauge needle into 3 sites along the infarcted area. Sham-operated animals were subjected to the same surgical procedure without coronary artery ligation and injection. In all experiments, we at least 10 rats were used in each group.

Echocardiographic measurements

Echocardiographic measurements were obtained at 1 day before MI (baseline), and 1 day and 7, 28 and 56 days after MI. Echocardiographic assessments were performed in-anesthetized rats (2% isoflurane inhalation) using a General Electric Vivid 7VR (GE Medical System; Milwaukee, WI, http://www.gehealthcare.com) equipped with a 13-MHz transducer. Cardiac dimensions: Left ventricular end-diastolic diameter (LVEDD), end-systolic diameter (LVESD), and fraction shortening (LVFS) were recorded from M-mode images using averaged measurements from three to five consecutive cardiac cycles according to the American Society of Echocardiography. Left ventricular end-diastolic and end-systolic volumes (LVEDV and LVESV, respectively) were calculated from

bidimensional long-axis parasternal views taken through the infarcted area by means of the single-plane area-length method ($V = (8 \times A^2)/(3 \times \pi \times L)$). LV ejection fraction (LVEF) was calculated as follows: LVEF=((LVEDV-LVESV)/LVEDV)x100. All measurements were averaged on three consecutive cardiac cycles and analyzed by a single observer who was blinded to the treatment status of the animals.

Histopathology

Rat hearts were harvested, washed in PBS (pH 7.4) and fixed in 10% formalin for histology. Hearts were embedded in paraffin and 6µm sections were cut from the apex to the level just below ligation. Three evenly spaced sections were stained with Masson trichrome and observed with a Nikon TE2000-E inverted microscope.

Circumferential extent of scar to total LV tissue (Kanashiro-Takeuchi RM *et al*., Proc. Natl. Acad. Sci. USA., 107: 2604-2609, 2010), relative scar thickness, and infarct expansion index (Ruvinov et al., Biomaterials, 32: 565-578, 2011) were quantified using ImageJ (NIH) version 1.43u for Windows.

Average of epicardial and endocardial infarct ratios were calculated for each section based on measurement of epicardial and endocardial infarct lengths and epicardial and endocardial LV circumference. For each heart,infarct size was calculated as the average of the value obtained for the 3 analyzed sections. . Relative scar thickness was calculated as average scar thickness divided by average wall thickness, averaged from 3 measurements of scar and septum thickness, respectively.average, Infarct expansion index was calculated as follows: [LV cavity area/whole LV area]/relative scar thickness. Percentage area of fibrosis in the remote left ventricle was quantified using an in-house image analysis program base on the following formula: %fibrosis=fibrotic area / (fibrotic area + healthy area).

Statistical Analysis

All values are shown as mean±SEM. Comparative studies of means were performed by using one-way ANOVA followed by post-hoc test when appropriate (Fisher's projected least significant difference) with $p<0.05$ as threshold for statistical significance. Echocardiographic parameters during 8-week follow-up were compared within groups and between groups using one-way ANOVA for repeated measurements followed by post hoc tests, respectively. For a given parameter, $p<0.05$ was considered significant. All tests were carried out using SigmaStat for Windows 3.5.

Results

Rheological characteristics of Si-HPMC hydrogel

Rheological properties of Si-HPMC solution mixed with acid buffer (1/1) were measured. The compressive modulus at 5% stress and the storage modulus (G') and loss modulus (G'') of Si-HPMC were performed after three weeks of reticulation. The final product (Si-HPMC) consisted of a reticulated hydrogel with a pH value of 7.4 after 27.2±3.4 min. Dynamic rheological measurements were performed to characterize this hydrogel including shear strain measurements to evaluate the storage modulus (G'), which characterizes the hard component, and the loss modulus (G''), which characterizes the liquid component. Compressive modulus, which reflects the stiffness of the material in compressive experiment, was 328.6±97.0Pa. After three weeks of reticulation and a finished self-setting process, a value of 343.2±106.5Pa for the G' and a value of 44.5±15.4Pa for the G'' were observed.

MSC viability and activity in three dimensional culture within Si-HPMC hydrogel

To evaluate whether Si-HPMC hydrogel was cytotoxic, MSC viability was quantified in 3D culture in Si-HPMC by conventional fluorescent microscopy (data not shown). MSC viability was maintained during the whole culture period, from day 1 to day 7 (85.1±3.9% at day 1; 80.0±3.0% at day 2 and 74.3±3.9% at day 7; p=0.10 one-way ANOVA between groups) (Fig.4).

To assess whether VEGF secretion was maintained in MSC 3D-cultured within Si-HPMC hydrogel for 7 days, VEGF concentrations were measured (ELISA) in supernatants at different time-points. Whereas VEGF concentrations in the control supernatants (MSCs cultured without hydrogel) were much higher (Fig.5.A), VEGF concentration in supernatants from 3D-cultured MSCs within hydrogel increased overtime from 29.5±1.7pg.ml^{-1} at day 1 to 91.0±5.1pg.ml-1 at day 2 to 181.2±6.4pg.ml^{-1} at day 7; p<0.001 for all comparisons) (Fig.5.B).

Comparative effects of hydrogel, MSC, and MSC+hydrogel on cardiac function and LV remodeling

MI was induced in 62 rats by ligation of the left anterior descending coronary artery. After MI induction, rats were randomised into 4 treatment groups to receive intramyocardial injections of (1) PBS as control, (2) Si-HPMC hydrogel alone (hydrogel), (3) MSCs alone (MSC) and (4) Si-HPMC hydrogel loaded with MSCs (MSC+hydrogel). Overall mortality at 24 hours after surgery was 30.7±7.7% (19/62 rats) with no significant

differences between treatment groups (see below Table 1A). Echocardiography was performed 1 day after coronary ligation, to select rats with a significant myocardial infarction so as to maximize possible treatment effects (defined as animals with LVEF≤70%; table 1B). The number of selected rats was not significantly different between treatment groups (see below Table 1B). Importantly, parameters of left ventricular (LV) dimensions and function measured at day 1 were not different between the 4 treatment groups in the animals entering the echocardiography follow-up study (See below Table 2).

	Animals number at baseline	Living animals at day 1
PBS	11	10
hydrogel	14	11
MSC	15	9
MSC+hydrogel	22	13
Total	62	43

Table 1A

	Animals number with LVEF>70% at day 1	Animals number with LVEF<70% at day 1
PBS	4	6
hydrogel	4	7
MSC	1	8
MSC+hydrogel	4	9
Total	13	30

Table 1B

Parameter	PBS (n = 6)	hydrogel (n = 7)	MSCs (n = 8)	MSC+hydrogel(n = 9)
LVEDD (mm)				
Bsl	5.4 ± 0.2	5.2 ± 0.2	5.6 ± 0.1	5.6 ± 0.2
d1	5.9 ± 0.1	5.8 ± 0.3	6.2 ± 0.2	6.0 ± 0.1
d7	6.6 ± 0.1	6.1 ± 0.3	6.3 ± 0.1	6.1 ± 0.2
d28	7.2 ± 0.2¥	6.9 ± 0.3¥	7.0 ± 0.3	6.6 ± 0.3
d56	7.4 ± 0.3¥	7.3 ± 0.5¥	7.0 ± 0.4	6.8 ± 0.2
LVESD (mm)				
Bsl	2.4 ± 0.1	2.6 ± 0.2	2.8 ± 0.1	3.0 ± 0.2
d1	4.0 ± 0.1	4.1 ± 0.3	4.3 ± 0.1	4.3 ± 0.2
d7	5.0 ± 0.1¥	4.0 ± 0.3 *	4.3 ± 0.2 *	3.9 ± 0.2 *
d28	5.7 ± 0.3¥	5.0 ± 0.3 *	5.2 ± 0.4 *	4.3 ± 0.3 *
d56	6.0 ± 0.3¥	5.5 ± 0.5 *	4.9 ± 0.3 *	4.8 ± 0.1 * $
FS (%)				
Bsl	56.6 ± 1.7	49.4 ± 2.0	49.5 ± 1.0	47.1 ± 2.2
d1	29.0 ± 2.4	29.9 ± 2.8	30.4 ± 1.8	27.9 ± 1.9
d7	24.1 ± 0.9	34.1 ± 2.0 *	31.2 ± 2.5	36.9 ± 1.7 ¥ * +
d28	20.2 ± 2.3	28.0 ± 1.2*	26.7 ± 3.3 *	34.4 ± 1.9 ¥ * + $
d56	19.6 ± 1.5	25.6 ± 2.9 *	30.8 ± 2.4 *	29.4 ± 1.5 * $
EF (%)				
Bsl	87.4 ± 1.5	86.0 ± 1.2	86.8 ± 1.9	88.2 ± 1.5
d1	61.3 ± 4.0	64.6 ± 2.6	64.6 ± 1.8	61.2 ± 2.9
d7	55.7 ± 2.4	68.0 ± 2.3	63.5 ± 3.2	76.0 ± 1.6 ¥ * +
d28	49.0 ± 2.5	71.7 ± 2.6 *	72.4 ± 1.5 *	76.4 ± 1.5 ¥ *
d56	47.4 ± 2.4	56.9 ± 4.6	65.4 ± 3.3 *	68.5 ± 2.0 ¥ $

Table 2

As expected in the PBS group, MI led to a time-dependent increase in LV chamber dimensions (LVEDD: 5.9±0.1mm at day 1 vs 7.4±0.3mm at day 56; p<0.05. LVESD: 4.0±0.1mm at day 1 *vs* 6.0±0.3mm at day 56; *p*<0.05.) (Figures 6.A and 6.B) and reduction in EF (61.3±1.5% at day 1 *vs* 47.4±2.4% at day 56; *p*<0.05) (Fig. 6.D) and fraction shortening (FS) (29.0±2.4% at day 1 *vs* 19.6±1.5% at day 56; *p*<0.001) (Fig.6.C). As compared to PBS group injections of hydrogel, MSC or MSC+hydrogel significantly attenuated the MI-induced increase of LV end-systolic diameter (LVESD) (Fig.6.B) and reduction of FS (Fig.6.C) and EF (Fig.6.D). Interestingly, significant differences were observed between these 3 groups:

(1) In the hydrogel groups, LVEF was significantly increased at 28 days after injection as compared to PBS group (71.7±2.6% *vs* 49.0±2.5%; p<0.001) but not at day 7 and day 56. In addition, the LVESD was reduced during the whole study as compared to PBS group but not the LVEDD. The LVESD, the LVFS and the LVEF were not significantly altered during the whole study as compared to day 1 but the LVEDD was increased at day 28 and 56 as compared to day 1 (7.3±0.5mm at day 56 *vs* 5.8±0.3mm at day 1; *p*<0.001).

(2) In the MSC group, LVEF was significantly increased at 28 and 56 days after injection as compared to PBS group (at day 56: 65.4±3.3% *vs* 47.4±2.4%; p<0.001), but not at day 7. In addition, the LVESD was reduced during the whole study as compared to PBS group but not the LVEDD. The LVESD, the LVEDD, the LVFS and the LVEF were not significantly altered during the whole study as compared to day 1.

(3) In the MSC+hydrogel group LVEF was significantly increased at day 7 up to day 56 after injection as compared to PBS group (at day 7: 76.0±1.6% *vs* 55.7±2.4%; *p*<0.001). In addition, the LVESD was reduced during the whole study as compared to PBS group but not the LVEDD. The LVFS and the LVEF were significantly increased compared to day 1 (61.2±2.9%) at 28 days (76.4±1.5%; p<0.001) then maintained at 56 days (68.5±2.0%; p=0.05).

Interestingly the LVEF was higher at day 7 as compared to LVEF in MSC group (76.0±1.6% *vs* 63.5±3.2%; *p*<0.05) and at day 56 in compared to hydrogel group (68.5±2.0% *vs* 56.9±4.6%; *p*<0.05). Similar results were observed for LVFS (Fig.6C).

Comparative effects of hydrogel, MSC or MSC+hydrogel on infarct expansion and ventricular fibrosis.

Morphometric analysis of heart sections was performed to analyse LV remodeling. For all animals, Infarct area was located in the anterior region of the left ventricle (Fig.7A).

The MI size had been reduce as compared to the PBS group (53.8±2.5%) in the hydrogel group (43.0±4.2%; $p<0.05$), in the MSC group (35.2±1.5%; $p<0.001$) and in the MSC+hydrogel group (28.2±1.2%; $p<0.001$) (Fig.7.B). In addition the MI size was reduced in MSC and MSC+hydrogel groups as compared to the hydrogel group.

The percentage of ventricular fibrosis (Fig.7.C) was significantly reduced as compared to the PBS group (27.8±1.6%) in the hydrogel group (19.0±2.5%; $p<0.05$), MSC group (7.9±0.6%; $p<0.001$) and MSC+hydrogel group (6.7±0.6%; $p<0.001$).

Relative scar thickness (Fig.8.B) was significantly increased as compared to PBS group (0.36±0.05) in hydrogel group (0.53±0.04; $p<0.05$), MSC group (0.59±0.04; $p<0.05$), and MSC+hydrogel group (0.63±0.04; $p<0.001$).

Infarct expansion index (Fig.8.C) was significantly decreased as compared to PBS group (1.73±0.24) in hydrogel group (0.97±0.09; $p<0.001$), MSC group (0.81±0.04, $p<0.001$), and MSC+hydrogel (0.66±0.04; $p<0.001$).

Interestingly, chondroid metaplasia of the endocardium was observed in 83% rats in PBS group (Fig.8.A) whereas this feature was visible in 67% rats in the hydrogel goup, 60% rats in the MSC group, and only in 14% in rats in hydrogel+MSC groups.

Taken together, these results shows that (1) hydrogel neither altered MSC viability nor activity and (2) injection of Si-HPMC hydrogel load with MSCs in the heart directly after MI leads to cardiac function and LV remodeling preservation as compared to hydrogel or MSCs alone.

CLAIMS

1. Use of a hydrogel comprising silylated biomolecules, for the three-dimensional culture of cardiomyocytes or stem cells which are able to differentiate into cardiomyocytes.

2. The use according to claim 1, wherein the silylated biomolecule is selected from the group consisting of a silylated polysaccharide, a silylated peptide or a silylated protein, or a biomolecule consisting of association of two silylated biomolecules thereof of different nature.

3. The use according to claim 1 or 2, wherein the silylated polysaccharide is selected from the group consisting of: silylated cellulose, silylated hydroxypropylmethylcellulose (HPMC), silylated hydroxyethylcellulose (HEC), silylated carboxymethylcellulose (CMC), silylated pectin, silylated chitosan and silylated hyaluronic acid.

4. The use according to claim 3, wherein the silylated polysaccharide is silylated hydroxypropylmethylcellulose (HPMC), and the cultured cells are cardiomyocytes.

5. The use according to any one of claims 1 to 4, wherein the hydrogel comprising silylated biomolecules has the following rheological characteristics at a pH value of 7.4 (after 3 weeks of reticulation):

- a compressive modulus at 5% stress from 220 to 15 000 Pa;
- a storage modulus (G') from 235 to 10 000 Pa;
- a loss modulus (G'') from 29 to 1000 Pa;
- a gel point from 5 to 45 minutes.

6. A method of culturing cardiomyocytes or stem cells which are able to differentiate into cardiomyocytes, comprising the *ex vivo* mixing of said cells with a hydrogel solution comprising silylated biomolecules at an appropriate pH for forming the hydrogel.

7. The method of culturing according to claim 6, wherein the hydrogel solution comprising silylated biomolecules has a pH from about 7.2 to about 7.6.

8. The method of culturing according to claim 6 or 7, wherein the hydrogel solution has the following rheological characteristics at a pH value of 7.4 (after 3 weeks of reticulation):

- a compressive modulus at 5% stress from 220 to 15 000 Pa;
- a storage modulus (G') from 235 to 10 000 Pa;
- a loss modulus (G'') from 29 to 1000 Pa;
- a gel point from 5 to 45 minutes.

9. An aqueous composition which comprises:

i) cardiomyocytes or stem cells which are able to differentiate into cardiomyocytes; and

ii) a hydrogel solution comprising silylated biomolecule;

for use for treating heat failure, in particular heart failure following myocardial infarction.

10. The aqueous composition according to claim 9, wherein said aqueous composition has a physiological pH.

11. The aqueous composition according to claim 9 or 10, wherein cells (i) are stem cells.

12. The aqueous composition according to claim 11, wherein the stem cells are mesenchymal stem cells.

13. The aqueous composition according to any one of claims 9 to 12, wherein the hydrogel solution (ii) has the following rheological characteristics at a pH value of 7.4 (after 3 weeks of reticulation):

- a compressive modulus at 5% stress from 220 to 430 Pa;
- a storage modulus (G') from 235 to 450 Pa;
- a loss modulus (G'') from 29 to 60 Pa;
- a gel point from 23.8 to 30.6 minutes.

14. A kit for obtaining an aqueous composition that is usable in a method of treating heat failure, said kit comprising i) cardiomyocytes or stem cells which are able to differentiate into cardiomyocytes, and ii) a hydrogel solution which comprises silylated biomolecule.

15. The kit according to claim 14, further comprising instructions for the use of said kit in preparing a composition comprising:

i) cardiomyocytes or stem cells which are able to differentiate into cardiomyocytes; and

ii) a hydrogel solution comprising silylated biomolecule;

said composition being intended to be injected into myocardium.

16. The kit according to claim 14 or 15, wherein the cells of (i) are stem cells which are able to differentiate into cardiomyocytes.

17. The kit according to any of claims 14 to 16, wherein the stem cells which are able to differentiate into cardiomyocytes are mesenchymal stem cells.

18. The kit according to any of claims 14 to 17, wherein the hydrogel solution of (ii) has the following rheological characteristics at a pH value of 7.4 (after 3 weeks of reticulation):

- a compressive modulus at 5% stress from 220 to 430 Pa;
- a storage modulus (G') from 235 to 450 Pa;
- a loss modulus (G'') from 29 to 60 Pa;
- a gel point from 23.8 to 30.6 minutes.

19. A kit for the three-dimensional culture of cardiomyocytes or stem cells which are able to differentiate into cardiomyocytes, said kit comprising i) cardiomyocytes or stem cells which are able to differentiate into cardiomyocytes, and ii) a hydrogel solution which comprises silylated biomolecule.

20. The kit according to claim 19, wherein the hydrogel solution (ii) has the following rheological characteristics at a pH value of 7.4 (after 3 weeks of reticulation):

- a compressive modulus at 5% stress from 220 to 15 000 Pa;
- a storage modulus (G') from 235 to 10 000 Pa;
- a loss modulus (G'') from 29 to 1000 Pa;
- a gel point from 5 to 45 minutes.

SILYLATED BIOMOLECULE-BASED HYDROGEL FOR CULTURING CARDIOMYOCYTES AND STEM CELLS, AND USE OF THE HYDROGEL THEREOF FOR TREATING HEART FAILURE

The present invention relates to the use of an hydrogel comprising silylated biomolecule for the three-dimensional culture of cardiomyocytes or stem cells which are able to differentiate into cardiomyocytes, and to an aqueous composition comprising i) cardiomyocytes or stem cells which are able to differentiate into cardiomyocytes, and ii) a hydrogel comprising silylated biomolecule, for use for treating heat failure, in particular heart failure following myocardial infarction.

Figure< None>

Nouvelles approches thérapeutiques de l'infarctus du myocarde : Cellules souches mésenchymateuses et ingénierie tissulaire et cellulaire.

Résumé :

L'objectif de ce travail a été de développer des stratégies d'ingénierie tissulaire et cellulaire visant à optimiser la thérapie cellulaire de l'infarctus du myocarde (IDM) en utilisant des cellules souches mésenchymateuses (CSM) issues de la moelle osseuse. Dans un modèle d'IDM chez le rat, nous avons montré que l'injection intramyocardique de CSM à l'aide d'un hydrogel d'hydroxylpropyl méthylcellulose silanisée (HPMC-Si), préservait la fonction cardiaque et atténuait l'intensité du remodelage ventriculaire gauche. Dans la perspective d'améliorer nos connaissances de base concernant les événements moléculaires physiopathologiques cardiaques, nous avons développé un modèle d'étude cardiaque à partir de cultures en trois dimensions (3D) de cardiomyocytes (CM) néonataux murins dans l'HPMC-Si. Nous avons montré que l'HPMC-Si était cytocompatible avec des CM et qu'il permettait la culture des CM battants en 3D. Finalement, afin d'obtenir des CM fonctionnels, nous nous sommes intéressés à la reprogrammation directe des CSM en CM. Nous avons montré, *in vitro*, que l'expression des deux facteurs de transcription (FT) cardiogéniques, Nkx2.5 et Gata-4, modifiait l'expression de quelques autres FT cardiaques, mais n'était pas suffisante pour induire une différenciation des CSM en CM. Ces travaux montrent l'intérêt d'utiliser l'ingénierie tissulaire et cellulaire pour améliorer l'efficacité de la régénération cardiaque. Le développement de cette nouvelle approche prometteuse doit permettre à l'avenir d'améliorer la survie, la différenciation et l'intégration des cellules dans le tissu cardiaque afin de permettre une régénération du myocarde après un infarctus.

Mots clés :
Régénération cardiaque, infarctus du myocarde, cellules souches mésenchymateuses, hydrogel.

New therapeutic approaches for myocardial infarction: Mesenchymal stem cells and tissue and cell engineering.

Abstract

The objective of this study was to develop strategies of tissue and cell engineering to optmize the effects of stem cell therapy for myocardial infarction (MI).We demonstrated that the intramyocardial injection of a self-setting silanized hydroxypropyl methylcellulose (Si-HPMC) hydrogel seeded with mesenchymal stem cells (MSC) preserve cardiac function and attenuate left ventricular (LV) remodeling during an 8-week follow-up study in a rat model of myocardial infarction (MI). To improve our understanding of the molecular events involved in cardiac physiopathology, we have developed a 3D model of cultured neonatal murine cardiomyocytes within Si-HPMC. We showed that the Si-HPMC hydrogel was cytocompatible with neonatal murine CM and the Si-HPMC allowed the three dimensional culture of functional beating CM. Finally, to obtain functional beating CM we were interested in deciphering whether the direct reprogramming of MSC by gene transfer could give rise to CM. We showed *in vitro* that the expression of two cardiogenic transcription factors (TF), Nkx2.5 and Gata-4, induced a change in the expression of some other cardiac TF, but was not sufficient to induce a differentiation of MSC in CM. Our works highlight the interest of using tissue and cell engineering to IDMprove the efficiency of cardiac regeneration. The development of this promising new approach should allow improving survival, differentiation and integration of cells in cardiac tissue to allow a myocardial regeneration after MI.

Key words:
Cardiac regeneration, myocardial infarction, mesenchymal stem cell, hydrogel